PROCESSES IN ALKALINE PEROXIDE BLEACHING OF PINUS RADIATA TMP

Yos Adiguna Ginting, B.Sc. (Hons.)

Submitted in fulfilment of the requirements

for the degree of

Doctor of Philosophy

University of Tasmania / Dept of Chemistry

May, 1996

DECLARATION

To the best of my knowledge, this thesis contains no material previously published or written by another person, except where due reference is made in the text of the thesis.

Y. A. Ginting

May 1996

Yos Ginting
12/2/1997

ABSTRACT

The response of *Pinus radiata* thermomechanical pulp to alkaline peroxide has been studied. Factors influencing the maximum brightness attained for various bleaching conditions have also been examined and the concepts of 'reagent limited' and 'pulp limited' have been related to the observation of limiting brightness on repeated bleaching.

Further observations were carried out on the kinetic behaviour during constant reagent concentration. Several previously reported kinetic models have been tested and found to be inadequate to describe the observed kinetic behaviour in terms of a minimum of chemically meaningful parameters.

From the experimental evidence, a new kinetic model which is defined in terms of first order processes has been proposed. This model assumes the existence of a single class of chromophores which reacts to give colourless products and potential chromophores. The process of the elimination of chromophores is opposed by a colour formation process from the conversion of potential chromophores to chromophores in an equilibrium type reaction.

The 'equilibrium' model was found not only to be able to describe the observed light absorption coefficients - time (K-t) relationship under constant reagent concentration, but also to explain the response of the pulp when reagent concentrations are changed part way through the bleaching process.

Previously reported results on the reactions between alkaline peroxide and the model lignin chromophore cinnamaldehyde have been studied by means of computational methods. From these calculations, it was found that the epoxidation of cinnamaldehyde is exothermic with an overall activation energy close to zero. The experimental presence of two epoxide isomers with the *trans* isomer as the preferred product agrees with the results of our calculations.

Good agreement between the results of the less sophisticated PM3 calculations and the more sophisticated *ab initio* calculations at RHF/6-31G(d) suggest that PM3 can be used for further studies without sacrificing significant accuracy of the results. PM3 is also computationally preferred since it generally requires less computation time to perform.

The research presented in this thesis is an extension of the work performed by the author during his study at an undergraduate level. As such, some of the results which were obtained from the previous study are included in parts of this thesis.

ACKNOWLEDGMENTS

I would firstly like to express thanks to my supervisors Dr. Brian Yates and Dr. Adrian Wallis for their guidance, insight and eagerness to see this work progress. Their advice were always worthwhile and without them this work would not have been possible.

Without the support and encouragement of Dr. Karen Stack and Dr. Phillip Wright, this would not have been possible, both in terms of providing motivation and advice which were essential for the completion of this work. I am indebted to Dr. John Abbot for the guidance and support during the early stage of this work. I am also appreciative of the help provided by Dr. Michael Whitbeck of the Desert Research Institute at Reno, Nevada USA in helping with the computer programming. I am also grateful to Ms. Catherine Rowland and Ms. Katrina Frankcombe for their proof reading of sections of this thesis.

Funding of a Postgraduate Award by the Indonesian Institute of Sciences and the Australian Newsprint Mills is gratefully acknowledged. I also thank the University of Tasmania Supercomputing Facility for access to their facilities.

I would like to thank Prof. Allan Canty, Prof. Paul Haddad and the entire staff of the Chemistry Department for ensuring the adequacy of facilities and supports. To my fellow students, Rhitu Rao, Vicky Barnett, Daniel Finnegan, Damien Blackwell and George Heard, who provided a terrific atmosphere for both work and play, I offer my thanks.

Finally, I would like to thank my parents and Christina Novitha for the constant love, care and support throughout the entire course of this degree.

TABLE OF CONTENTS

CHAPTER 1

Pulp and Paper: An Overview

1.1 Introduction

The use of paper is always on the increase. The current development in the use of electronic media and computer technology does not even slow down the demand of paper. In fact, it is predicted that the demand of paper will increase dramatically. In the past decade, an increase of 20% in the total world production of paper was observed[1], and with many developing countries emerging, the increase in demand will almost be a certainty.

In Australia, the pulp and paper industry is one of its largest manufacturing sectors. Australia is a major exporter of unprocessed wood chips and there exists considerable scope for expansion in this sector with the availability of large scale forest resources. Even so, Australia remains a net importer of paper products as well as pulp for conversion to finished products and it appears that this will continue in the foreseeable future.

The Australian pulp and paper industry, led by several major companies, including Australian Newsprint Mills (ANM) and Australia Paper, has proved to be an expanding one. Both these companies have expanded and developed their original plants in recent years[2].

The current growing concern in the forestry and environmental protection areas, together with the fact that Australia is still a paper importer, makes the development of technology for low pollutant levels and high efficient usage of fibre resources a very important subject. The objective of this study was to develop a suitable kinetic model for the alkaline peroxide bleaching of *Pinus radiata* thermomechanical pulp and having done so, to use the model to partially unravel the underlying chemical processes which occur during the bleaching process. The alkaline peroxide bleaching of *Pinus radiata* thermomechanical pulp was selected for the following reasons.

Firstly, thermomechanical pulping is one of the most efficient processes for the utilisation of fibre. Using this process, lignin and other non-cellulosic materials in the original wood are almost entirely retained. In contrast to this, chemical pulping removes almost all of the lignin. On a dry basis, mechanical pulping yields approximately 95% of the weight of wood as pulp, while the yield of bleached kraft pulp (a chemical pulp) is 45-50% of the weight of wood used[2]. Secondly, *Pinus radiata* used for pulp production is easily obtainable from plantation forests. The relatively short period of harvesting (15 years) makes *Pinus radiata* a practically inexhaustible source of fibres which can be utilised without the destruction of native forests. Lastly, peroxide is an environmentally sound reagent for bleaching in comparison with chlorine-based reagents, since its decomposition products are water and oxygen.

There have been numerous studies on bleaching of mechanical pulps with alkaline hydrogen peroxide in which the resulting brightness of pulps are reported as a function of time and reagent concentration[3-7]. Most investigations have been carried out under conditions where the concentrations of hydrogen peroxide and hydroxide ion fall significantly during the course of the bleaching process. Although such conditions simulate industrial practice, the results are difficult to interpret in terms of kinetic phenomena associated with individual reaction processes. Over the past decade there have been some kinetic investigations reported under conditions where the total peroxide concentration and pH have been maintained at constant levels[8-11], to facilitate interpretation of rate processes. These studies have usually been carried out at relatively low pulp consistencies, so that the rate of consumption of reagents is reduced to low levels, allowing monitoring and continuous readjustment to initial concentration values, as the bleaching process continues under isothermal conditions.

Recently a kinetic model based on the assumption of two distinct chromophore types was reported from the study of the bleaching of a *Eucalyptus* stone groundwood (SGW)[11]. In that study, Wright and Abbot[11] have examined changes in the light absorption coefficient (K) under constant conditions of pH and peroxide concentration, as K is found to show a better correlation with chromophore concentration than the more standard measurement of brightness[9]. The objective of this study was to construct a kinetic formulation which relates to

concentrations of reacting species (both chromophores and reagents), rather than formulate models which are limited to empirical formulation[12, 13]. For the purpose of kinetic model development carried out in this study, several previously reported studies on alkaline peroxide bleaching of *Pinus radiata* TMP have been examined[10, 12, 13] in the context of various kinetic models. Brightness has been used as an indicator of chromophore content as they are concerned with trends which reflect the validity of proposed kinetic models, rather than accurate determination of exact kinetic parameters. It has been shown, however, that the general behaviour of brightness gain with time closely parallels changes in K for peroxide bleaching of *Pinus radiata* TMP[14].

Several studies in kinetic phenomena during alkaline peroxide bleaching of mechanical and chemimechanical pulps have been reported[8-11, 15-20]. Kinetic expressions have been formulated to describe brightness gain under normal process conditions, where the concentration of peroxide and pH fall continuously[15-18]. Experiments at low consistency with constant concentrations of peroxide and alkali have also been undertaken and these studies can lead to kinetic formulations which can help to elucidate mechanisms of chemical processes involved[8-11, 19, 20]. There have also been attempts to relate the two approaches[9, 15]. Recent studies have suggested that peroxide bleaching should be regarded as a reversible process, in which chromophore formation as well as chromophore elimination should be considered simultaneously[20]. Photochemical reversibility of brightness gain is a well known

phenomenon when bleached pulps are exposed to light, particularly at wavelengths in the ultra-violet region[21]. It is also known that bleached mechanical pulps and lignin model compounds can undergo darkening processes when exposed to alkaline hydrogen peroxide under certain conditions[12, 22, 23].

As mentioned previously, the objectives of this study were to develop a suitable kinetic model for alkaline peroxide bleaching of *Pinus radiata* thermomechanical pulp and to investigate the bleaching reaction mechanism of a chromophore computationally. To facilitate the achievement of these objectives, the study has been divided into several stages. In the first stage (Chapter 4), our goal was to attempt to differentiate between various possible models using a more quantitative approach than has been previously reported. In the second stage (Chapter 5), the most favoured model obtained from the first stage was tested against experimental observations along with a discussion of the possible chemical reaction mechanisms related to the proposed model. In Chapter 6, the mechanism of epoxidation of cinnamaldehyde model chromophore was investigated using computational methods.

1.2 Structure of Wood and Wood Pulping Processes

1.2.1 The Structure of Wood

The raw material required to make paper is wood. It is a complex matrix of fibres composed of several constituents as follows :

The first component of wood is cellulose. It is the main constituent of any woody plant and comprises approximately 40-45% of the dry substance in most wood species[3]. Cellulose is a linear homopolysaccharide with a degree of polymerisation of about 10,000 glucose units. In wood, individual cellulose molecules undergo intra and intermolecular hydrogen bonding to form bundles of cellulose molecules called micro fibrils[24]. In turn, micro fibrils aggregate to form fibrils and finally cellulose fibres[3]. As a result of its fibrous structure, cellulose has a high tensile strength and is insoluble in most solvents[24].

The second component of wood are the hemicelluloses which are a group of heterogeneous polysaccharides which, like cellulose, provide physical support for the plant. In contrast with cellulose, hemicelluloses have a much smaller degree of polymerisation of about 200 units and are extensively branched. Hemicelluloses generally comprise between 20 and 30% of the dry weight of wood[24].

The third component is lignin which imparts rigidity to the cell walls and, in woody parts, acts as a permanent bonding agent between cells generating a composite structure outstandingly resistant towards impact,

compression and bending[25]. During the pulping process, this bonding effect is broken and the wood is disintegrated into individual fibres. Such disintegration can be achieved either by mechanically rupturing the lignin-bonded structure, or by chemically removing the lignin[2].

Softwoods generally contain between 26-32% lignin while hardwoods have a slightly lower lignin content of 20-28%[26]. Lignins have been found to consist of polymers of phenyl propane (C_6 - C_3) which are divided into two classes according to their main structural elements. Softwood lignin is often referred to as 'guaiacyl lignin' since lignin of this type is largely a polymerisation product of guaiacyl monomers such as coniferyl alcohol[24] (Figure 1.1).

Hardwood lignins are co-polymers of syringyl and guaiacyl units which vary in ratios from 4 : 1 to 2 : 1. Despite steady progress in lignin characterisation over the last fifty years, the exact nature of lignin still remains unclear as a result of its great structural complexity. This complexity is a result of the elaborate manner in which the phenyl propane units in lignin are linked, and is further complicated by the fact that the phenyl propane units are not structurally identical[27]. Nevertheless, detailed studies on isolated lignin preparations have clarified the main structural features of lignin, including the major functional groups and types of linkages, and this work has been comprehensively reviewed in previous publications[26, 27].

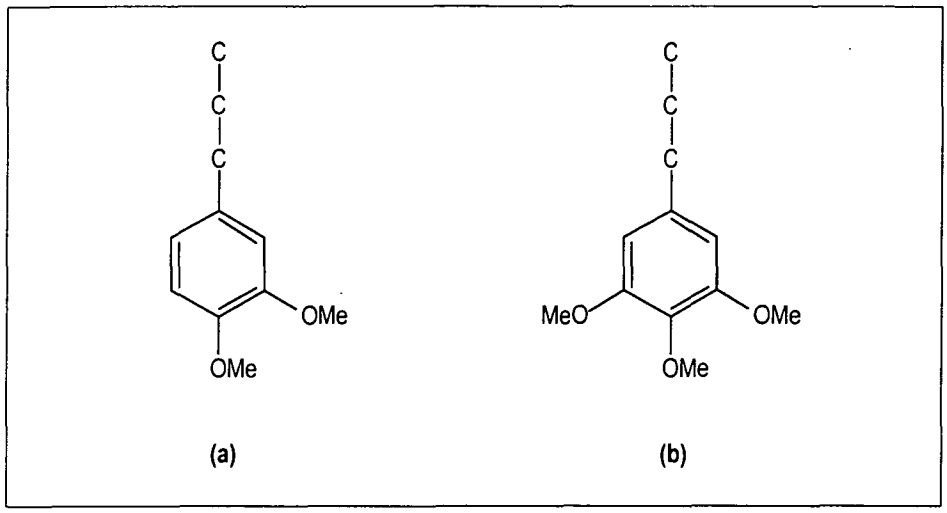

Figure 1.1 The basic building blocks of lignin: (a) the guaiacyl monomer and (b) the syringyl monomer.[24]

Extractives, a mixture of lower molecular weight compounds, are the least abundant component of wood and may be divided into three sub-groups comprising aliphatic compounds (fats and waxes), terpenes and terpenoids, and phenolic compounds[24, 26]. The content and composition of extractives varies considerably among wood species and also within different parts of the same tree[24, 26]. Extractives are characterised by their ready extractability in organic solvents such as ethanol, acetone and dichloromethane, although a smaller proportion of extractives (eg. tannins) may be extracted with water[24].

1.2.2 Thermomechanical Pulping

As it is known today, thermomechanical pulping is a process involving two separate steps. The first step involves preheating of the chips for a

short period at relatively low pressure with the purpose of softening the lignin. This is followed by refining after the lignin has softened.

The chips are heated to a temperature that does not exceed the glass transition point of the lignin so that the lignin remains in the glassy state[28]. This preheating softens the lignin and makes the chips less brittle. This in turns allows easier fibre separation without fibre breakage or splintering, creating more long fibres, less debris and fewer shives[28]. If this chip reduction is carried out without presteaming as in ordinary refiner mechanical pulping, the chips are brittle and tend to break under the impact, thus resulting in a large percentage of fines and debris in the pulp[28]. A simplified representation of thermomechanical pulping is shown in Figure 1.2.

The colour of mechanical pulp is primarily introduced in the defibration stage. Figure 1.3 shows how the colour of mechanical pulp changes after pulping and bleaching. This colour has been reported to depend on several factors such as wood quality, wood storage, barking efficiency and also the chemical reactions taking place during the defibration[29].

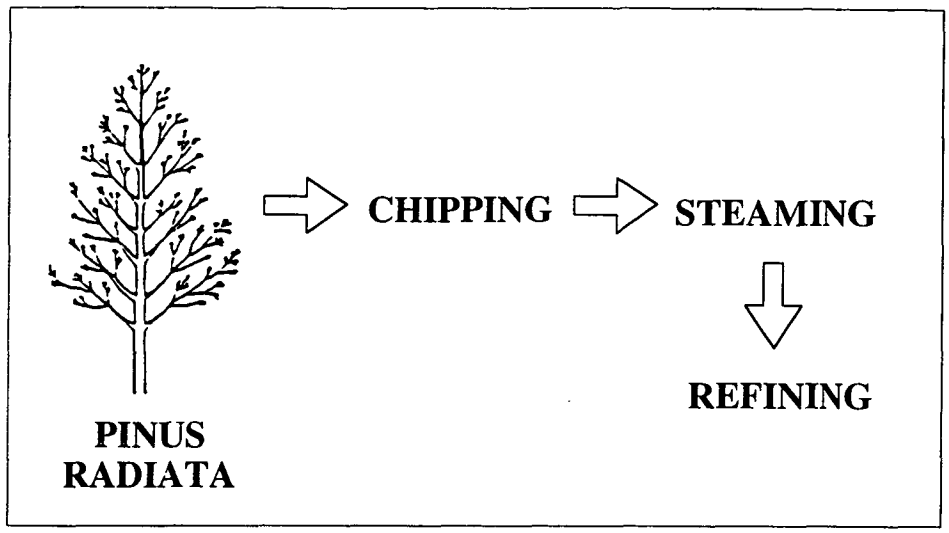

Figure 1.2. Thermomechanical pulping process of *Pinus radiata.*

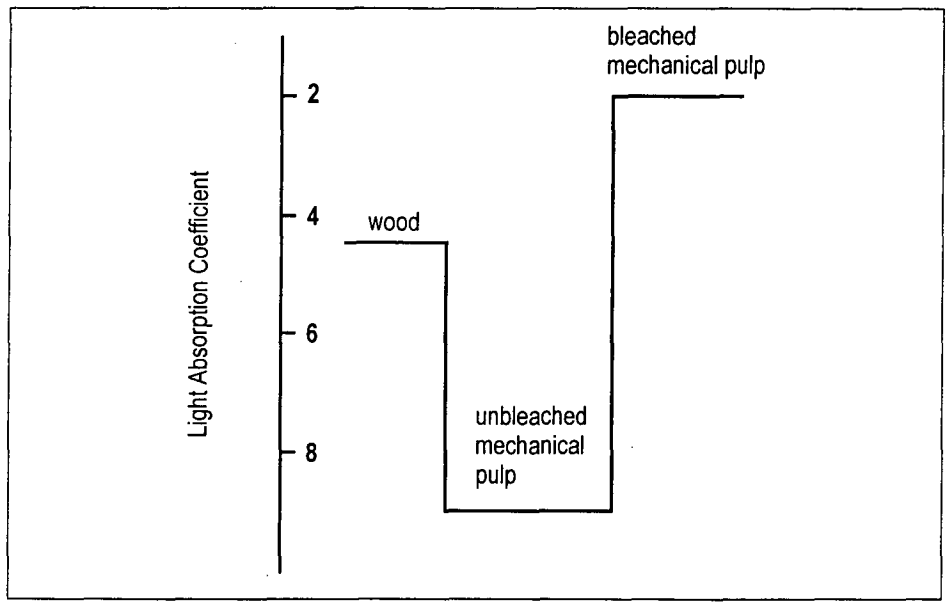

Figure 1.3 Changes in the colour of pulp made from spruce wood (as represented by the light absorption coefficient) after pulping and bleaching with 4% hydrogen peroxide.[29]

1.2.3 Kraft Pulping Process

The kraft process is one of the most common chemical pulping methods. It involves cooking the wood chips at 170°C-180°C in a solution of sodium hydroxide and sodium sulfide to solubilize the lignin. The dissolved lignin is removed by washing with water. This 'unwanted' lignin is normally collected by evaporation and burnt to provide process energy and to recover the sodium based cooking chemicals[2].

During cooking, the lignin content of the solid material is reduced from around 50% to 3-4%, and this residual lignin is the material that gives the characteristic brown colour to kraft pulp. This residual lignin cannot simply be removed by continuing the cooking process, because the remaining lignin is unreactive and the cellulose fibres become prone to significant damage. This residual lignin may also become more highly coloured[2].

1.3 Newsprint and Mechanical Pulp

The major components of newsprint are high yield mechanical or chemi-mechanical pulps. These pulps are distinct from the chemical pulps used to produce fine papers.

Chemical pulps are almost invariably bleached with chlorine-based chemicals, such as chlorine, chlorine dioxide and hypochlorite, to

achieve the high brightness levels required for these grades[28]. The objective in bleaching chemical pulps is to remove traces of residual lignin in the pulp which remain after pulping. These are processes which can give rise to highly toxic organo-chlorine compounds[2, 28].

In contrast, mechanical pulps, which are produced through physical separation of the wood fibres (or after mild chemical treatment as for chemimechanical pulps), as used in paper grades that do not require the same high levels of brightness, can use bleaching agents which are environmentally not so harmful. The objective in bleaching (or brightening) these high yield pulps is to chemically change the structure of the coloured materials or chromophores present in the pulp so that colourless substances are produced. For thermomechanical pulp, the bleaching reagents can be divided into two classes, reducing agents (sulfite, dithionite, and borohydride) and oxidising agents (peroxide). Among these classes dithionite and peroxide are the most commonly used commercially[26]. Their reactions during bleaching process will be described in section 1.4.

It is forecast that bleached mechanical pulps will find greater acceptance as a suitable substitute for expensive bleached chemical pulps in paper grades such as liquid packaging board, fine writing papers, tissues and fluff[1]. With today's stricter pollution control regulations, hydrogen peroxide has gained its popularity as the bleaching agent for brightening mechanical pulps. More recent developments have found application for

hydrogen peroxide in bleaching of deinked waste papers and as a partial replacement for chlorine and chlorine dioxide in the bleaching of chemical pulps in the first and second extraction stages[29]. However peroxide is a relatively expensive chemical which tends to decompose during the bleaching process into products with little or no bleaching effect[29]. The actual mechanisms of peroxide reactions during bleaching are also not well understood. As a result, research in this area is of considerable interest for both the industrial and scientific communities.

1.4 Bleaching of Pulp

The main purpose of bleaching is to improve the optical properties of paper. First and foremost among these properties is its brightness or whiteness, however, other properties such as opacity and receptivity to printing inks are normally also affected by bleaching[2].

In the production of chemical pulps, bleaching involves the almost complete removal of residual lignin. In contrast to this, bleaching of mechanical pulps such as TMP is lignin retaining, that is, the lignin is modified to reduce the colour but not removed from the fibre[30]. In this way the high yield of mechanical pulps is maintained while the optical properties are improved[30].

The residual lignin in fibres can affect their surface properties, their stiffness and that of the paper from which they are made[2]. Furthermore,

the residual lignin is largely responsible for 'ageing' of paper, that is, deterioration of colour on storage, especially on exposure to light[2]. For this reason, it is virtually impossible to use unbleached paper for archival material or even for record-keeping over periods of years.

Bleaching to a high brightness is an expensive task and there is no incentive for pulp and paper manufacturers to undertake this if the market does not require it. However, the market demand for higher brightness paper products has increased significantly in recent years, due partly to the enormous increase in consumption of various kinds of printing papers. This market growth no doubt reflects rising living standards and increasing literacy and communication facilities.

It is known that quite a number of structures present in lignin are responsible for the absorption of visible light. Such chromophores and potential chromophores (leucochromophores) include phenols and catechols in combination with unsaturated systems of styrene, stilbene, diphenyl methane, and butadiene structures[26]. Structural units such as α–β unsaturated aldehydes, α-carbonyl and o-quinones in lignin have also been reported[31] to be responsible for the colour of lignin in pulp (Figure 1.4).

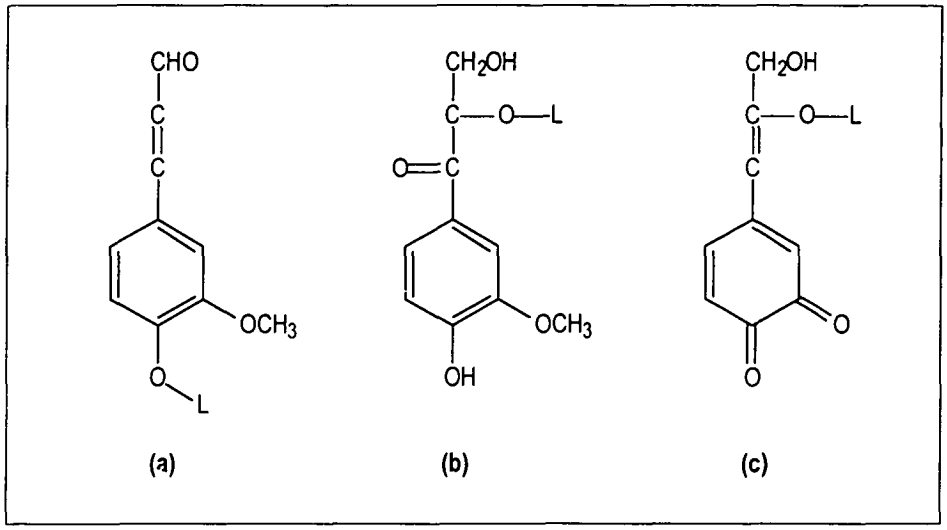

Figure 1.4 Some structural groups representative of chromophores in lignin. (a) α–β unsaturated aldehydes, (b) α- carbonyl structures, (c) ortho quinones. L = Lignin.[31]

1.4.1 Dithionite Bleaching

For some quinone structures, the standard redox potentials are probably of the order E^0 = 0.7- 0.9 V[28]. The standard reduction potential for dithionite is given in Equation 1.1.

$$2\ SO_3^{2-} + 2\ H_2O + 2\ e^- \rightleftharpoons S_2O_4^{2-} + 4\ HO^- \ (E^0 = -1.12V) \quad (1.1)$$

From the standard potential value shown in Equation 1.1, it can be seen that dithionite is capable of reducing quinone structures, thereby decreasing the colour of lignin in pulp and producing a bleaching effect. In addition to its decomposition through oxidation into hydrogen sulfite or sulfite as in Equation (1.1), dithionite may also disproportionate into thiosulfate and hydrogen sulfite as in Equation 1. 2[26].

$$2\ S_2O_4^{2-} + H_2O \longrightarrow S_2O_3^{2-} + 2\ HSO_3^- \quad (1.2)$$

It is also known that dithionite is oxidised in the presence of air (Equation 1.3).

$$S_2O_4^{2-} + H_2O + O_2 \longrightarrow HSO_3^- + HSO_4^- \quad (1.3)$$

In theory the maximum bleaching effects for dithionite will be reached at pH 8 - 9 and at a temperature of 20^0 C - 60^0 C, however a pH in the region of 5-6 is normally used in practice to avoid the oxidation of dithionite by any oxygen which cannot be excluded from the system[26].

1.4.2. Hydrogen Peroxide Bleaching

Hydrogen peroxide bleaching is carried out under conditions where concentrations of both hydrogen peroxide and hydroxyl ions are significant, however it is probably only the perhydroxyl anion (HO_2^-) which is active in bleaching.

In order to understand and mathematically describe peroxide bleaching processes in terms of the active bleaching reagent (HO_2^-), it is essential to know the equilibrium constant for the equilibrium between hydrogen peroxide (H_2O_2) and the perhydroxyl anion (HO_2^-). The hydrogen peroxide equilibrium can be written as

$$H_2O_2 \rightleftharpoons H^+ + OOH^- \quad (1.4)$$

or

$$H_2O + OOH^- \rightleftharpoons OH^- + H_2O_2 \quad (1.5)$$

Consequently, two equilibrium constants may be derived:

$$K_a = \frac{[H^+][OOH^-]}{[H_2O_2]} \quad (1.6)$$

and

$$K_b = \frac{[OH^-][H_2O_2]}{[OOH^-]} \quad (1.7)$$

These two equilibrium constants are related to each other via the ionic product of water.

$$K_a = \frac{K_w}{K_b} \quad (1.8)$$

where

$$K_w = [H^+][OH^-] \quad (1.9)$$

All these equilibrium constants can be expected to be dependent on temperature and ionic strength. Since peroxide bleaching is carried out under alkaline conditions and hydroxide ions can take part in other reactions of importance, the hydroxide ion form of the equilibrium, i.e. the constant K_b, is more relevant in studies of peroxide bleaching[32].

Studies by Teder and Tormund[32] showed that the temperature dependence of K_b for hydrogen peroxide can be described by the expression

$$pK_b = \frac{1330}{T} - 2.13 \qquad T = \text{absolute temperature (K)} \qquad (1.10)$$

It should be noted that alkaline peroxide is also susceptible to a decomposition reaction under strong alkaline conditions to give oxygen (Equation 1.11).

$$2\ HO_2^- \longrightarrow O_2 + 2\ HO^- \qquad (1.11)$$

A base-catalysed decomposition mechanism (Figure 1.5) involving hydroxyl and superoxide anion radicals has also been reported[33].

$$H_2O_2 + HO^- \rightarrow HO_2^- + H_2O$$
$$H_2O_2 + HO_2^- \rightarrow HO\cdot + O_2^{\cdot-} + H_2O$$
$$HO\cdot + O_2^{\cdot-} \rightarrow O_2 + HO^-$$
$$H_2O_2 + HO_2^- \rightarrow O_2 + HO^- + H_2O$$

Figure 1.5 Base-catalysed free radical mechanism of peroxide decomposition.[33]

This implies that under bleaching conditions, peroxide is unstable and decomposes into products with little or no bleaching activity. The presence of metal ions such as iron and manganese is known to catalyse this decomposition. The mechanism of this decomposition (Figure 1.6) has been reported by Isbell *et al.*[34].

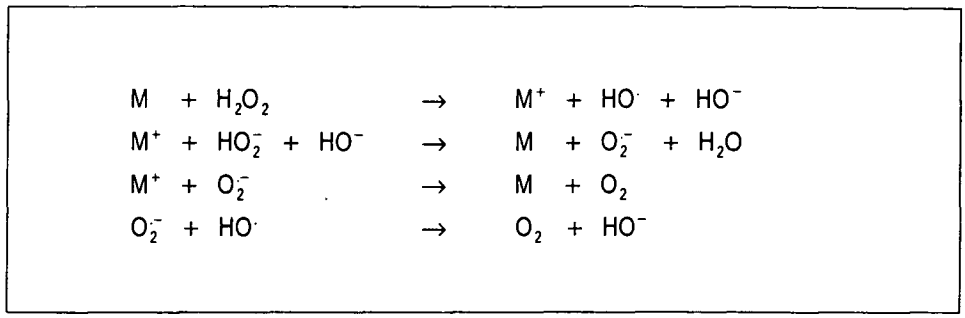

Figure 1.6. Transition metal ion-catalysed free radical mechanism of peroxide decomposition. M = transition metal ion.[34]

To minimise the decomposition reaction, two types of additives are normally employed during peroxide bleaching. The first additive type is used to stabilise peroxide bleaching liquor. Sodium silicate is one such additive which has been found to give considerable improvements in the bleaching response of mechanical pulps[35]. Magnesium sulfate has a similar effect and is especially useful when the hardness of the water is low[28]. The second additive type reduces peroxide decomposition through the removal of trace levels of transition metal ion catalysts. Chelating agents such as DTPA (diethylenetriaminepentaacetic acid) and DTMPA (diethylenetriaminepenta-monophosphonic acid) fall into this category. The structures of DTPA and DTMPA are shown in Figure 1.7.

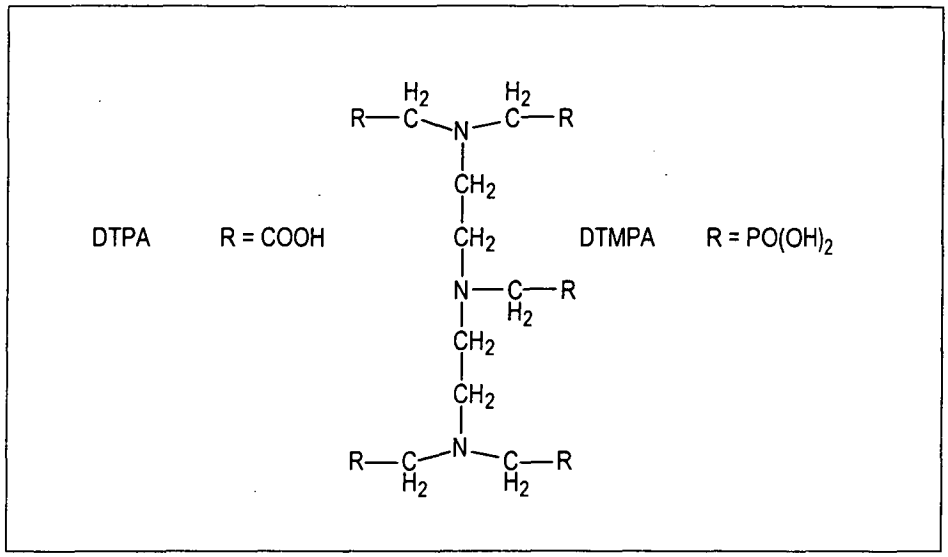

Figure 1.7 Structures of chelating agents DTPA and DTMPA. Additives used to reduce the decomposition of peroxide by chelating trace metal ions present in the pulp.

It is also known that peroxide oxidation is not selective, i.e. some of the peroxide is used in reactions with non-chromophoric compounds[26]. The peroxide bleaching reaction is believed to result in decolouration of para and ortho quinones and cinnamaldehyde like structures[26] although the actual overall reaction is not known exactly since many chromophoric compounds are present in the pulp. Figure 1.8 summarises the reaction of hydrogen peroxide during the bleaching of pulp.

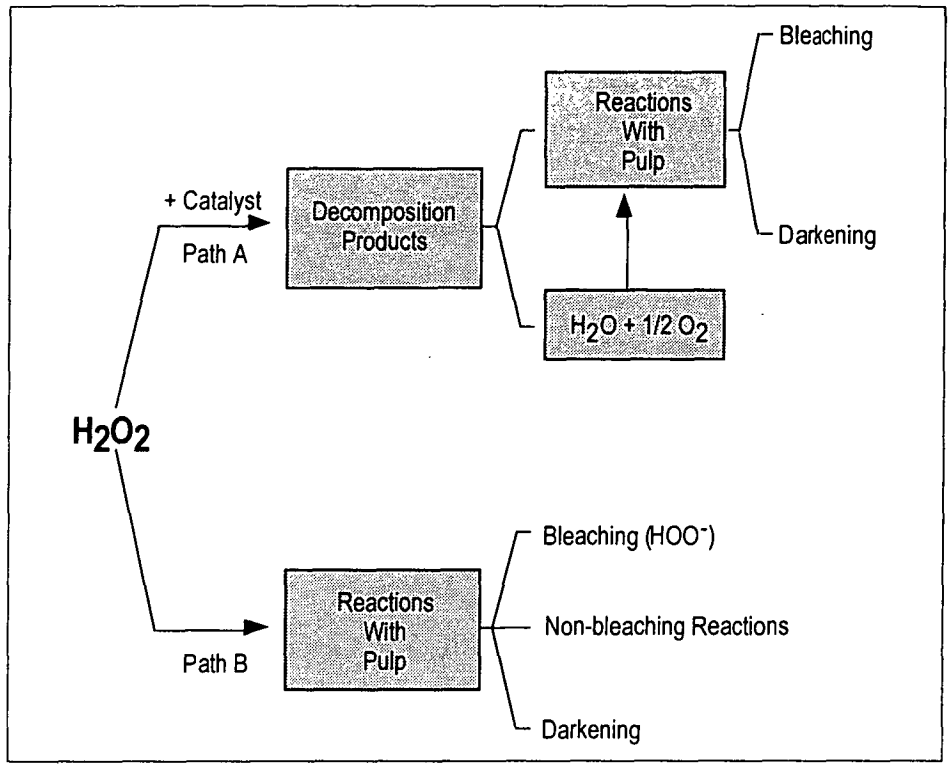

Figure 1.8 Reactions of hydrogen peroxide.

1.5 Colour of Pulps, Brightness and Light Absorption Coefficient

1.5.1 Measurement of Colour in Lignin Rich Pulps

Bleaching is concerned with the removal of colour from pulps. For chemical pulps, the bleaching process results in the removal of residual lignin, hence the decolouration of bleached chemical pulp is reflected by measuring the decrease in the concentration of lignin in the pulp (the so called Kappa number determination). For high yield mechanical pulps such as TMP, decolouration is achieved without delignification, therefore the degree of colour is measured by determining the

concentration of chromophores contained in the pulp using optical techniques. To estimate the chromophore concentration in the fibres, the light absorption coefficient (denoted k_{457} or K) is normally used since this quantity is directly proportional to the concentration of light absorbing groups in lignin at any wavelength[36].

In the pulp and paper industry, a more common measure of the concentration of coloured material in paper is the brightness. Its popularity is due to the simplicity of the measurement itself, but it suffers from the drawback of being dependent not only on the chromophoric content but also on the physical structure of the pulp (i.e. the light scattering properties). Since light scattering properties of pulp may be affected by bleaching, the more fundamental property of light absorption coefficient (K) is generally preferred to brightness as a method for monitoring changes in pulp colour.

The term brightness (R_∞) refers to the reflectance of a thick pile of identical sheets. This quantity is dependent on the wavelength of the light used. The whiteness of the paper as observed by the human eye is most sensitive in the blue region of the visible spectrum of a wavelength near 457 nm, hence this wavelength is the one used in the brightness measurement. The %ISO scale of brightness ranges from zero to one hundred. Zero and one hundred on the %ISO scale are defined by a standard black cavity and a magnesium oxide plate respectively. Newsprint generally has a brightness value of about 60 %ISO.

1.5.2. Kubelka - Munk Theory

Although brightness is a useful parameter for specifying the end use properties of paper, it is not a fundamental quantity but rather a complicated function of two more basic phenomena, light scattering and light absorption. Light scattering occurs when incident light strikes an internal or external fibre surface in paper while light absorption arises from the absorption of light by chromophoric substances.

When studying the chemistry of bleaching, the primary phenomenon of interest is light absorption because changes in this property are directly related to the removal of chromophoric structures[8, 36, 37]. For this reason, brightness is an unsuitable quantity for studying bleaching chemistry since it contains an additional component which describes the scattering properties of a paper sheet.

In 1931, Kubelka and Munk derived a cumbersome and incomplete set of equations to describe the relative contributions of light scattering and light absorption to brightness measurements. Kubelka[38, 39] (1948) was later able to provide simplified and more practical forms of the so-called Kubelka-Munk equations, allowing light absorption and light scattering effects to be easily calculated from brightness measurements. Although initially employed in the textile industry, the Kubelka-Munk equations were recognised as particularly useful in studying the bleaching of pulp

and paper, since they provided a direct method for monitoring absorption of light by chromophoric structures.

Derivation of the Kubelka-Munk equations is based on the scattering and absorption of light in successive thin layers of homogeneous material[36, 38-40], (Figure 1.9). The material is assumed to have a mass per unit area (or 'grammage') of W kg/m^2 and each thin layer has a grammage of dW kg/m^2. Two quantities, S and K, representing light scattering and light absorption phenomena respectively are defined so that if the surface layer of material is exposed to light of intensity i, a fraction of light i.S.dW is scattered while the amount i.K.dW is absorbed in the layer. The so-called light scattering (S) and light absorption (K) coefficients are both expressed in units of $(grammage)^{-1}$ ie. m^2/kg. The remaining light not absorbed or scattered in the surface layer continues through to the next layer where the absorption and scattering processes are repeated.

The complete derivation of the Kubelka-Munk equations from first principles is complex and results in many forms of equations, however only a few have practical applications. An excellent summary of the Kubelka-Munk equations as applied to the optical properties of paper has been presented by Robinson[41]. The most practical forms of the equations are presented in Equations (1.12-1.14).

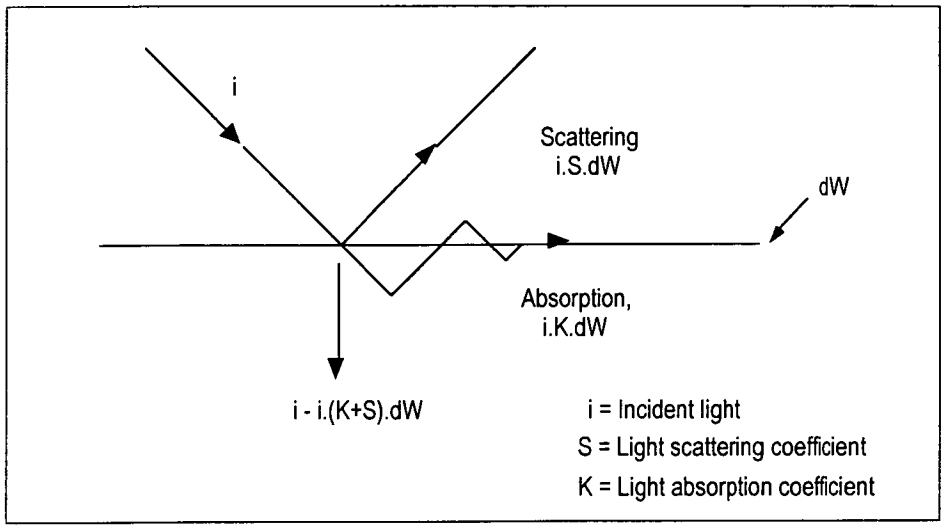

Figure 1.9 Diagram showing the physical basis for derivation of the Kubelka-Munk equations. K and S represent light absorption and scattering coefficients respectively (units m^2/kg) and W represents the mass/unit area of the surface (units kg/m^2).

1.5.3 Kubelka-Munk Equations

$$SW = \frac{R_\infty}{1-R_\infty^2} \ln\left(\frac{1-\Omega R_\infty^2}{1-\Omega}\right) \tag{1.12}$$

$$1+\frac{K}{S} = \frac{1}{2}\left(\frac{1}{R_\infty}+R_\infty\right) = a \tag{1.13}$$

$$\frac{1}{2}\left(\frac{1}{R_\infty}-R_\infty\right) = \sqrt{a^2-1} \tag{1.14}$$

where
- R_∞ = reflectance of an infinitely thick pile of sheets
- R_0 = reflectance of a single sheet on a black background
- Ω = opacity = R_0/R_∞
- W = grammage = mass/unit area (kg/m^2)
- K = absorption coefficient (m^2/kg)
- S = scattering coefficient (m^2/kg)

When measuring the light absorption coefficients of paper sheets using the Kubelka-Munk equations, care must be taken to ensure that the

sheets conform to three 'rules' arising from theoretical considerations during derivation of the equations[38-40] . The three rules are:

- that the optical density of the sheet must not be too low (eg. a thin specimen or poorly scattering material)
- that light must not be substantially absorbed before scattering (eg. a very dark material)
- that light scattering must not dominate over light absorption (eg. a very light material)

These three rules define the boundaries of an 'allowed region' in which all absorption coefficient measurements should fall[40]. When absorption coefficients fall outside these limits, the Kubelka-Munk equations cease to be exact and more approximate equations must be used[38, 39]. The position of the different boundary limits are somewhat ill-defined and depend on factors such as instrument geometry and levels of acceptable error. Figure 1.10 shows limits of the Kubelka-Munk equations as proposed by Teder and Tormund[40].

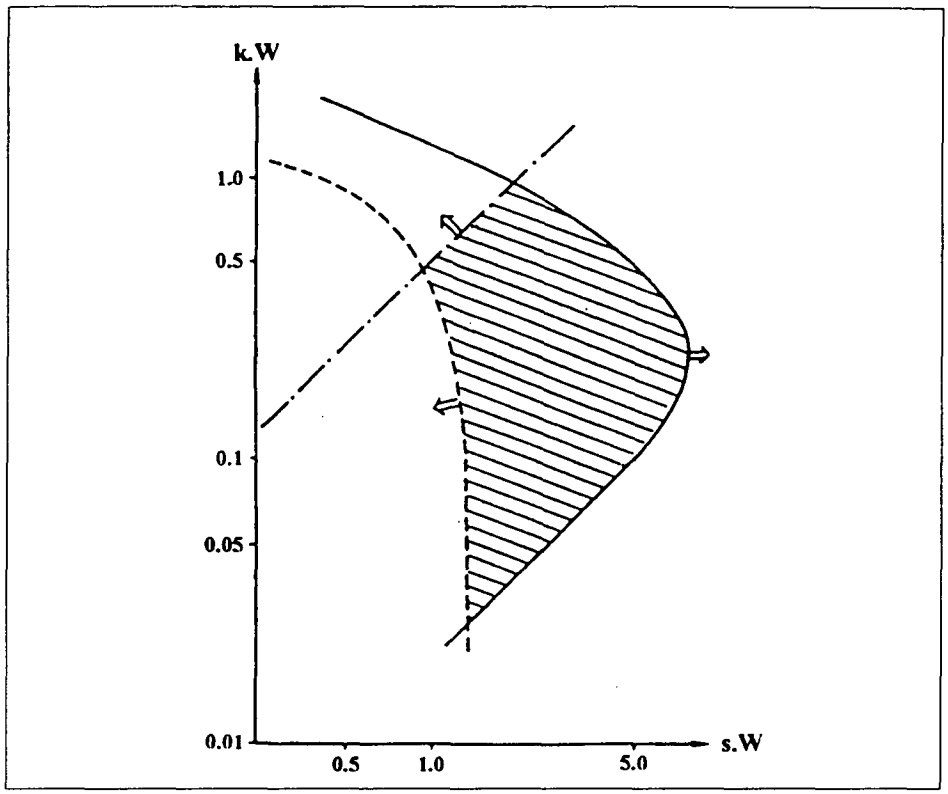

Figure 1.10 The limits of applicability of the Kubelka-Munk equations as calculated by Teder and Tormund.[40]

1.6 Methods for Studying Kinetic and Reaction Mechanisms

Kinetic studies of alkaline peroxide bleaching can be carried out by two methods, the constant conditions method and the differential method[9]. In the constant conditions method, the concentration of active bleaching chemicals, peroxide and alkali are held constant throughout bleaching. This condition is maintained by adding chemicals (alkali and peroxide) to a very low consistency pulp slurry as they are consumed.

The advantage of this method is that it is easy to isolate the effect of each variable. The condition also resembles the technique commonly used for bleaching chromophore model compounds. This makes a comparison between bleaching of pulp and bleaching of chromophore model compounds easier. It is also an established technique for kinetic investigation of pulp bleaching and thus facilitates comparison with the kinetics of other processes. The disadvantage of this method is the divergence from mill conditions. This is especially pronounced in the case of pulp consistency and the chemical concentration profile during the bleaching[9].

The differential method on the other hand resembles mill bleaching conditions. That is, the bleaching chemicals are charged to the pulp at the start, and the concentration of peroxide and alkali then decrease as the bleaching proceeds. The advantages and disadvantages of the differential method are exactly the opposite to those of the constant conditions method[9].

1.7 Parameters That Affect Bleaching

The bleaching effect is the result of many simultaneous reactions, including the removal of some chromophores and the creation of others due to the presence of alkali[42]. The course of bleaching with time is

characterised by a rapid initial phase and a slower final phase as shown in Figure 1.11.

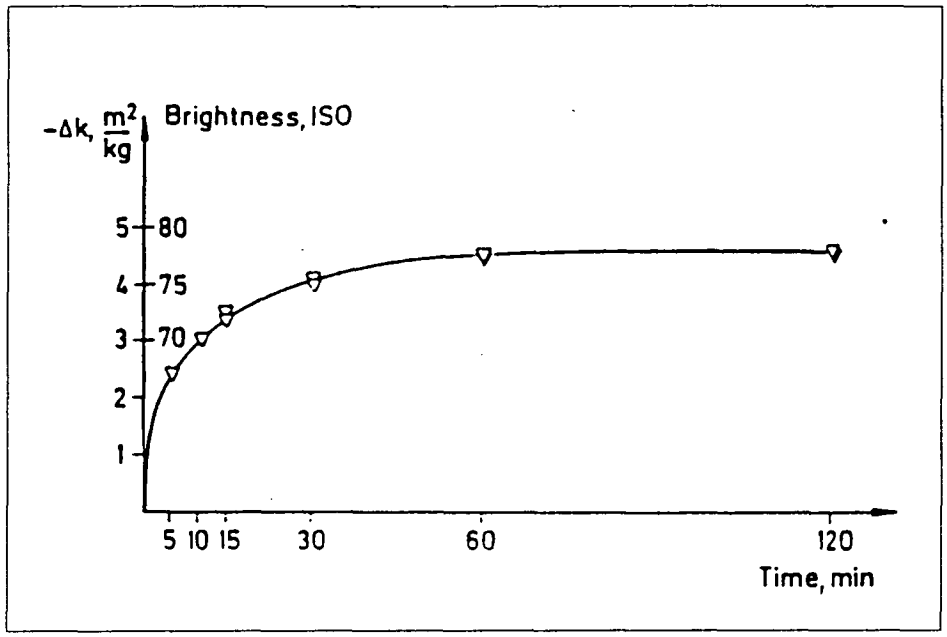

Figure 1.11 Decrease in light absorption coefficient (-ΔK) and increase in brightness versus bleaching time for a typical conventional (differential) bleaching. The bleaching response is characterised by a rapid initial phase and a slower final phase.[42]
Bleaching conditions:

peroxide charge	=	4% on o.d. pulp
initial pH	=	11.1
pulp consistency	=	15 %
temperature	=	50°C

Peroxide bleaching is carried out in alkaline media, where the OH^- ion dominates. The concentration of H^+ ions, measured as pH, is thus of little importance. For that reason pOH is frequently used in kinetic studies in place of pH.

1.7.1 Effect of Peroxide and Alkali Concentration

Under constant conditions, the bleaching rate is increased as the alkali concentration is increased as shown in Figure 1.12. It has also been reported that there is a maximum in the bleaching rate corresponding to increase in alkali which varies with temperature[9]. A more detailed study has indicated that increasing alkalinity increases the bleaching rate up to pOH = 2.5 (pH = 11.5 at 24°C and 10.5 at 60°C) where the rate passes through a maximum. A further increase leads to a decreased bleaching rate[42]. At pOH =2 (pH=12 at 24°C) the bleaching rate is of the same order as at pOH 3.5 (pH 10.5 at 24°C and 9.5 at 60°C). This is shown in Figure 1.13.

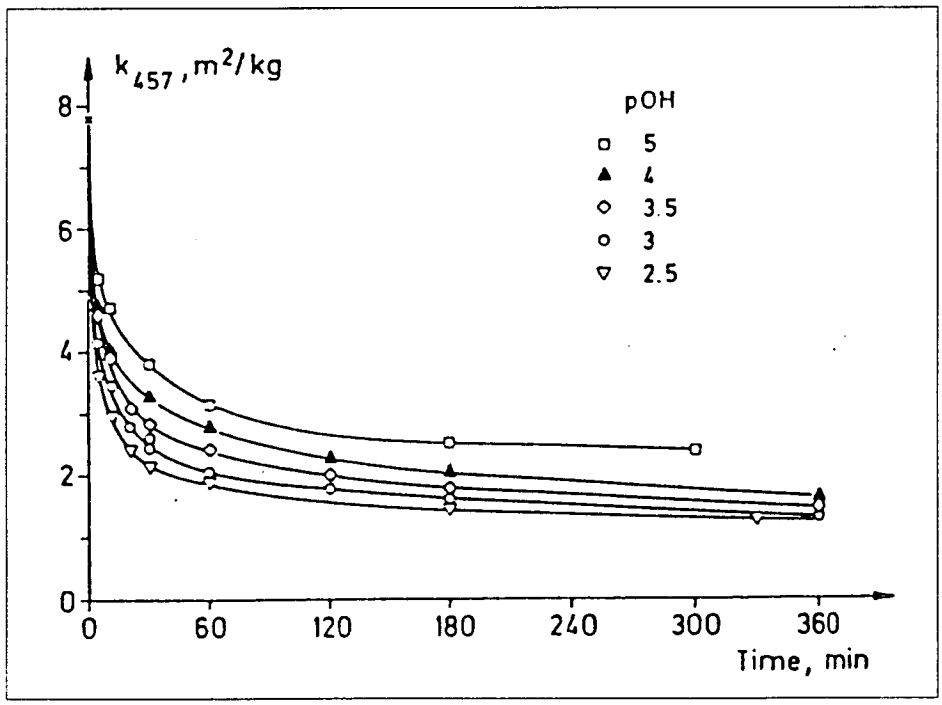

Figure 1.12 Light absorption coefficient versus bleaching time at different pOH levels under constant conditions. Increased alkali concentration increases the bleaching rate. Bleaching conditions: $[H_2O_2]_{total}$= 0.176 mol/l, temperature = 60°C.[42]

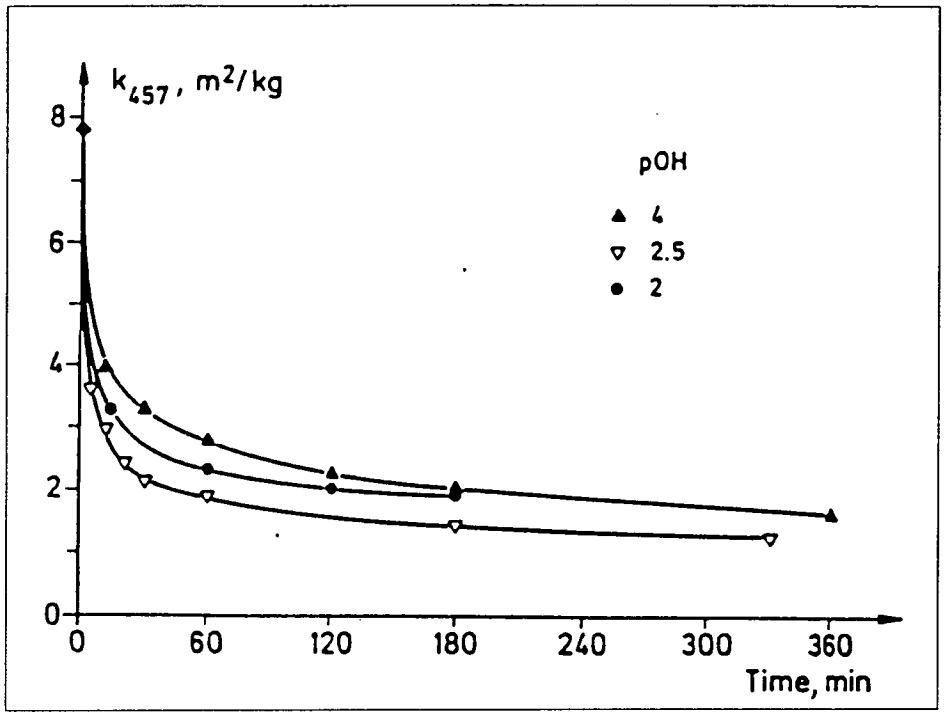

Figure 1.13 The light absorption coefficient versus bleaching time at different pOH levels under constant conditions. Alkali concentrations higher than pOH =2.5 (pH 11.5 measured at 24°C) results in decreased bleaching rate.[42]
Bleaching conditions: $[H_2O_2]$total = 0.176 mol/l, temperature = 60°C

According to Sjögren *et al.*[42] the observation of a maximum bleaching rate with pH is due to the presence of two counteracting reactions, one the bleaching itself and the other one involving colouring reactions. It is known that addition of pure alkali to mechanical pulp decreases the pulp brightness. The addition of alkali to the bleaching liquid therefore can give :

1. Accelerated formation of chromophores.
2. Increased peroxide anion concentration resulting in an accelerated destruction of chromophores.

Another possible explanation of the maximum in the bleaching rate with respect to the alkali concentration might be based on the peroxide

equilibrium. Figure 1.14 shows the degree of peroxide dissociation versus the alkalinity.

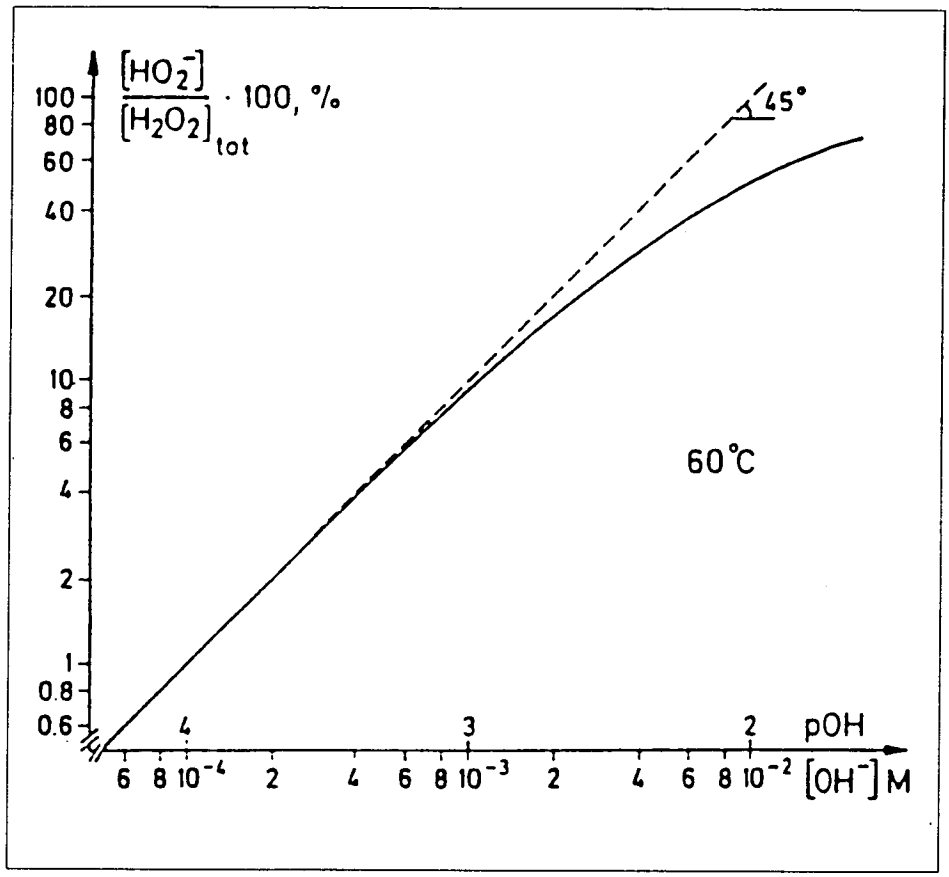

Figure 1.14 The degree of peroxide dissociation versus hydroxyl anion concentration. Temperature 60°C. At pOH > 2.5 perhydroxyl anion produced is less than required to counteract chromophore formation caused by the increase in alkali concentration.[42]

This equilibrium indicates that an increase in the alkali concentration above about pOH 2.5 (pH 11.5 at 24°C) does not give a proportional increase in the perhydroxyl anion concentration, i.e. the increase in the peroxide anion concentration is probably not enough to counteract the colour formation reactions caused by the increased alkali concentration.

The assumption that alkali creates chromophores and perhydroxyl anions eliminate chromophores has been confirmed by showing that the bleaching rate is decreased by increased alkalinity at a given peroxide anion concentration[42]. The concentration of the peroxide anion may be increased either by adding more alkali or by adding more hydrogen peroxide. The effects on the reaction rate of these two methods are compared in Figure 1.15.

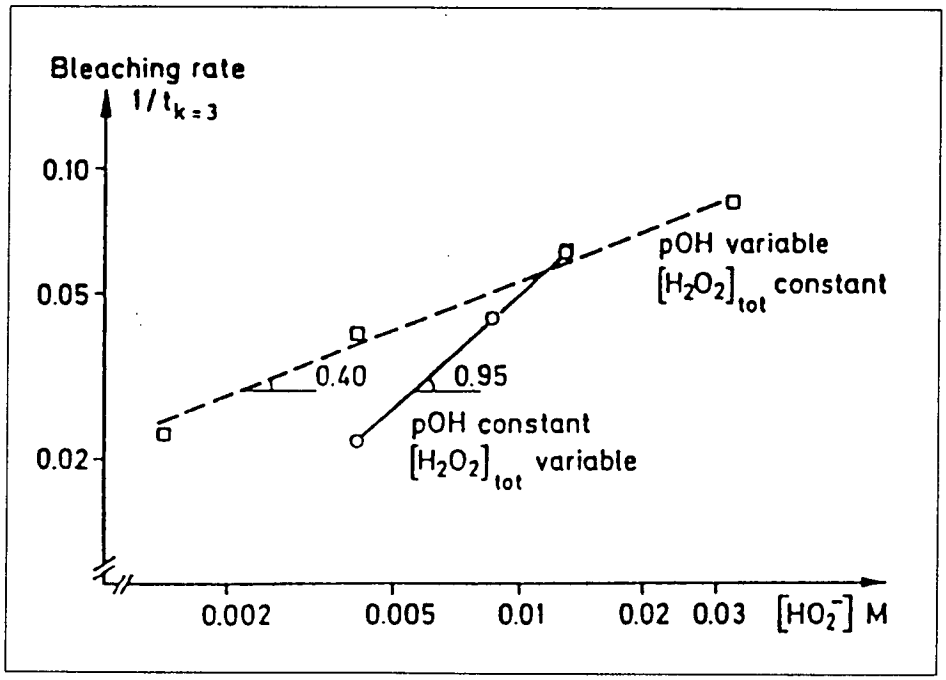

Figure 1.15 The bleaching rate versus peroxide anion concentration. The bleaching rate is of first order with respect to the peroxide anion if pOH is constant (continuous line). The reaction order is lower (about 0.4), if the peroxide concentration is increased by means of alkali, showing the counteracting, colouring action of added alkali (broken line).[42]

Both methods of increasing the peroxide anion concentration lead to an increase in the bleaching rate. If more peroxide is added while the alkalinity is kept constant the bleaching rate is first order with respect to

the peroxide anion. This is also in agreement with results obtained from the bleaching of model compounds[29]. If more alkali is added while the total concentration of hydrogen peroxide is kept constant a lower reaction order is observed showing the counteracting alkali induced reaction. The conclusion is that the bleaching rate is affected by both peroxide anion and alkali concentrations.

In a recent study, Garver *et al.*[43] published the first results from an investigation of the molecular weight distribution of the soluble products in the alkaline hydrogen peroxide liquor by size-exclusion chromatography. They concluded that maximum bleaching efficiency, in terms of the highest brightness gained for peroxide consumed, occurs at low alkaline pH, low temperature, low peroxide charge and with multistage bleaching and produces fewest soluble products

1.7.2 Effect of Pulp Consistency

High pulp consistencies have been shown by many workers to be favourable for peroxide bleaching[5, 44, 45]. This effect has been attributed to increases in the bleaching ability of the peroxide[9]. At high consistencies the peroxide concentration is greater for a given peroxide charge and a higher proportion of the peroxide is expected to be inside the fibre wall and thus available for bleaching[5, 6, 18]. An alternative explanation for the increased bleaching response at higher consistencies is the reduction of unfavourable peroxide consuming reactions[46, 47]. Ali

et al. suggest that the effect is due to the effective chelation of metal ion decomposition catalysts by the pulp at high consistencies[46], while Hagglund and Lindstrom suggest that the increased dewatering necessary to produce high consistency pulps results in less carry over of dissolved substances and heavy metals into the bleaching process[47]. Recently, it was suggested that the production of hydroxyl radical which is partly responsible for the pulp darkening reactions is reduced at higher consistency and thus result in a brighter pulp[48].

1.8 Formation and Removal of Chromophores

In the defibration of wood, fairly high temperatures are created in the defibration zone. It can also be assumed that small amounts of oxygen are present, which together with a high humidity favours auto-oxidative processes. Under such conditions, hydroquinone and catechol structures are easily converted into the corresponding quinones via phenoxy radicals with reaction rates which rapidly increase with increasing pH of the surrounding liquor[29]. Even under mild neutral conditions the quinones formed are able to undergo further reaction. Thus hydroxylation and subsequent oxidation by oxygen can give rise to deeply coloured hydroxylated quinones. In the presence of other reactive phenols, such as bark constituents, various quinoid coupling products may also be created[29]. These reactions are summarised in Figure 1.16.

It can thus be concluded that, in addition to the native wood chromophores, new quinones of various types are created during defibration due to the auto-oxidation of phenolic compounds in lignin. The presence of transition metal ions may further increase the colour by catalysing the reactions and forming complexes with the products.

Up to this time, due to the inherent chemical complexity of pulp, almost all chromophore studies have been performed on chromophore model compounds. One possible reaction mechanism during peroxide bleaching of mechanical pulps[49] is shown in Figure 1.17.

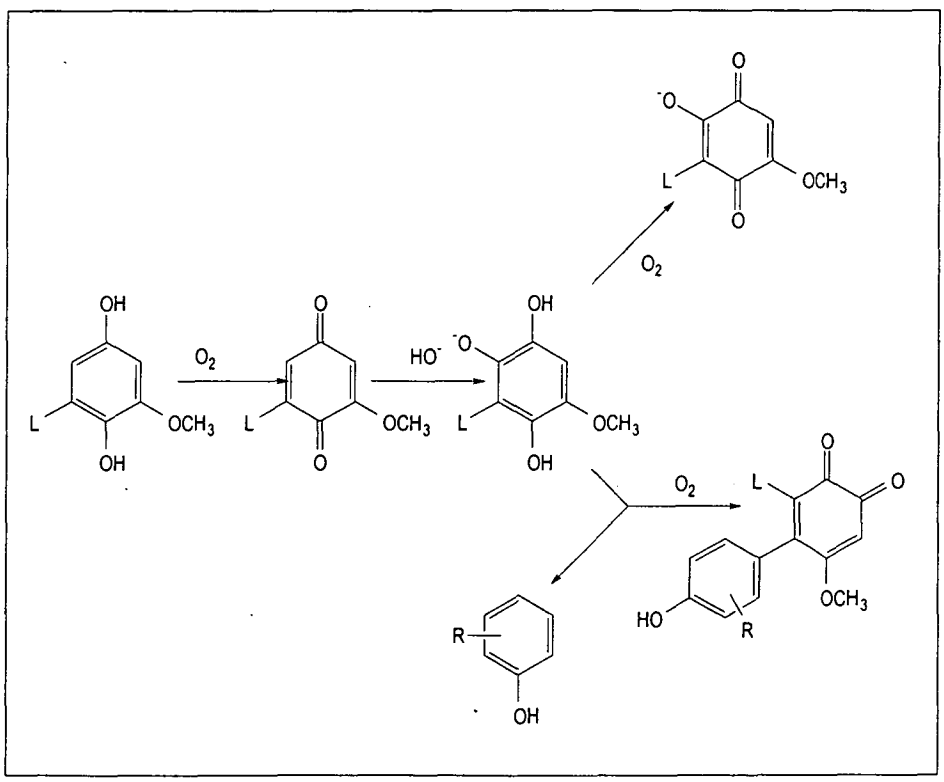

Figure 1.16 Examples of auto-oxidative processes leading to the formation of quinone structures in lignin.[29]

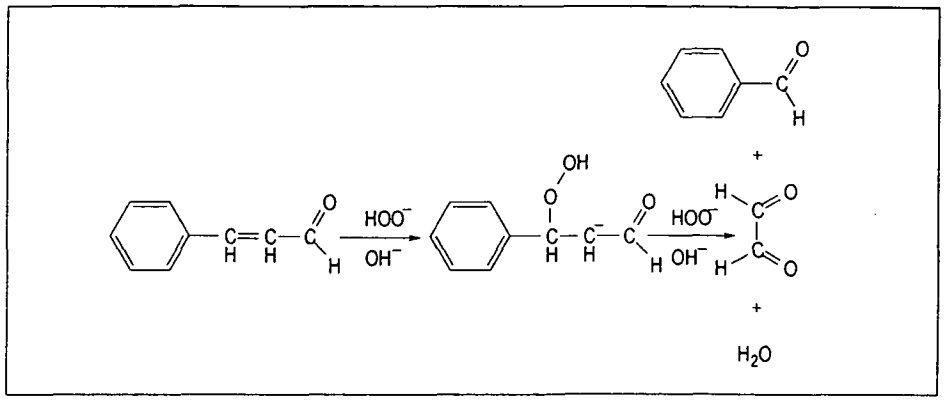

Figure 1.17 Possible mechanism in peroxide bleaching of mechanical pulp.[49]

As can be seen in Figure 1.17, the mechanism for decolouration is achieved by the disruption of the highly coloured conjugated system. The aldehyde groups formed are subsequently oxidised to carboxyl groups in the alkaline medium. Investigation using chromophore model compounds carried out by Gellerstedt[29] indicated that cinnamaldehyde like structures are rapidly oxidised by alkaline hydrogen peroxide giving rise to the corresponding aromatic aldehyde and formic acid as shown in Figure 1.18. In Figure 1.19, the cinnamaldehyde-like structure is oxidised via the formation of an epoxide[31]. For the mechanism shown in Figure 1.19, the reported first order rate constant for the disappearance of cinnamaldehyde like structure is a factor of 20 larger than the appearance of the product 3,4-dimethoxybenzaldehyde like structure, which suggests that the reaction is inhibited by alkali. This correlates with the observed behaviour for alkaline peroxide bleaching of pulp.

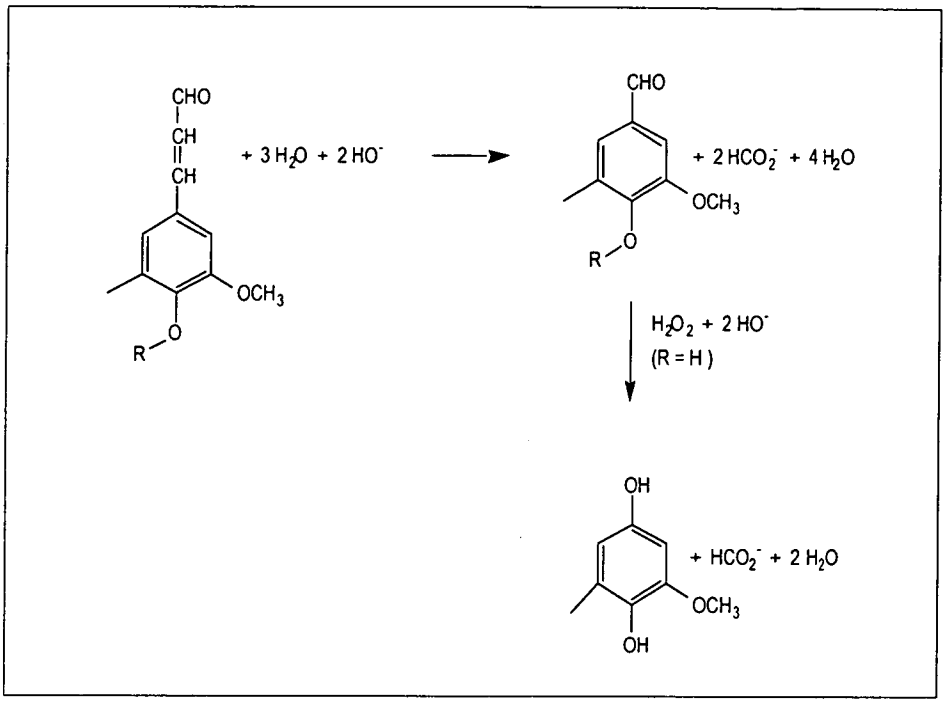

Figure 1.18 Reactions between alkaline hydrogen peroxide and cinnamaldehyde like structures.[29]

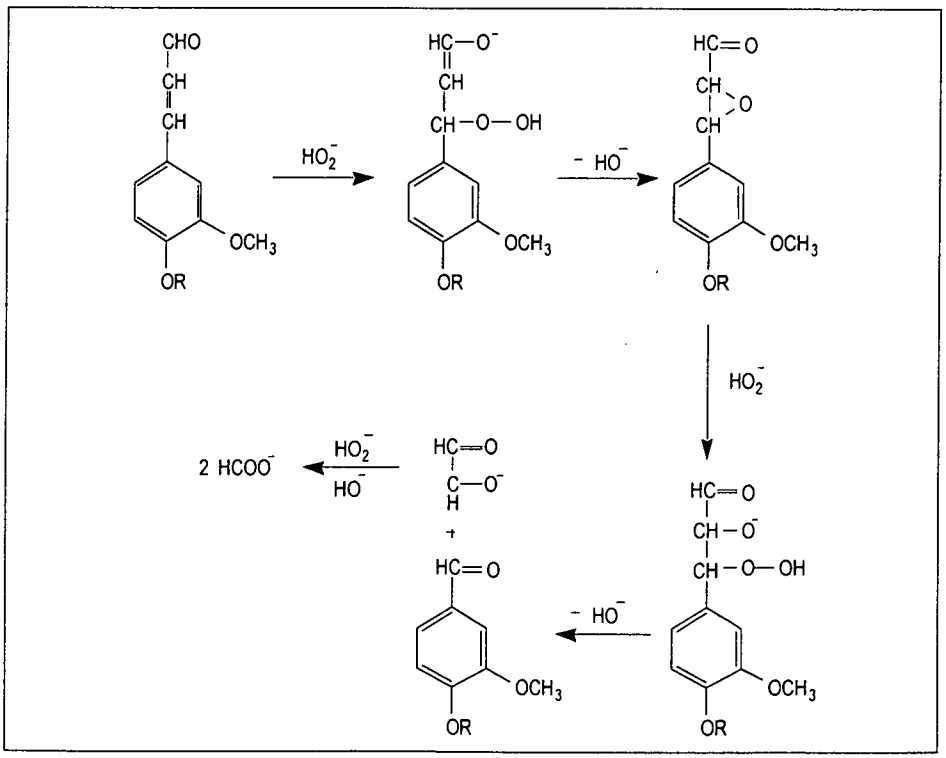

Figure 1.19 Mechanism for the cleavage of cinnamaldehyde like structures by alkaline hydrogen peroxide.[31]

1.9 Kinetic Models and Reaction Mechanisms

There has been recent interest in developing kinetic models which describe the response of mechanical pulps to alkaline peroxide under mill conditions[15-18]. Various complex polynomial expressions have been formulated to represent relationships between the brightness of a pulp and process variables including the consistency of the pulp, and applied dosages of peroxide and alkali. For example, a 5-parameter model has been suggested[16] as a kinetic representation for conventional one-stage alkaline peroxide bleaching.

$$\text{Brightness} = A_0 + A_1 * p + A_2 * p^2 + A_3 * (c) + A_4 * (c)^2 + A_5 * (c) * p \quad (1.15)$$

where $p = [H_2O_2]$ and c = consistency

Even more complex expressions, with up to 12 parameters have been reported for the description of a two-stage peroxide bleaching sequence[17]. These types of expressions relate pulp brightness to a chosen set of controllable process variables such as initial pulp consistency and reagent concentration. The values of the parameters are varied to provide an adequate fitting between experimental and calculated brightness values. The adequacy of the fitting can be improved, by introducing additional terms in the expression, each with an associated coefficient. These types of expression can be regarded as a series of arbitrary terms in which the variables have no specific chemical

meaning. For example, there may be no fundamental significance in finding a term dependent on the square of consistency in the above expression. The term is included with its associated coefficient, A_4, because this combination results in the calculated brightnesses lying closer to the experimental values. Because these types of expression are not based on a series of terms which have individual significance, they cannot be expected to yield fundamental information concerning chemical processes which occur during bleaching processes.

Another approach in describing kinetic phenomena during peroxide bleaching is based on the assumption that even complex phenomena can be described and understood using the same approaches as applied to simpler chemical processes. This approach assumes that the rate of loss or formation of a particular chemical species depends on its concentration in the system, as well as the concentration of other species with which it reacts. Analysis of kinetic phenomena is greatly simplified by reducing the number of variables in a particular experiment. For alkaline peroxide bleaching this can be achieved by maintaining the pH and peroxide concentration at constant levels[8-11, 19].

In the development of kinetic models for alkaline peroxide bleaching under constant reagent concentrations, the light absorption coefficient (K) is normally used as a measure of changes in the pulp[8-11, 19]. The light absorption coefficient provides a better measure of chromophore concentration in the pulp than brightness which, as previously stated,

depends on light scattering properties as well as light absorption. Results relating changes in absorption coefficient with time under constant conditions have been reported for spruce SGW pulp[9], *Pinus radiata* TMP[10] and *Eucalyptus regnans* SGW[11, 19]. Despite the differences in the species being studied, the general form of these K-time profiles under constant reagent conditions is the same in all cases, with initial rapid decline in K, followed by a much slower rate of chromophore reduction at long bleaching times.

1.10 Computational Models and Model Chemistries

Models are inseparable from chemists. For example, the use of plastic models is inarguably one of the best ways in helping to understand and visualise the structure of molecules for both beginning chemistry students and researchers. With the wide acceptance and availability of computers, these students and researchers have also begun to use computer visualisation programs to obtain the same information[50, 51].

Computational chemistry, like other model chemistry, uses a set of predefined objects and rules to approximate real chemical entities and processes. In more detail, computational chemistry simulates chemical structures and reactions numerically, based in full or in part on the fundamental laws of physics. Using computational chemistry, chemical

phenomena can be studied by running calculations on computers rather than by examining reactions and compounds experimentally. In fact some of the reactions which are difficult to be studied experimentally such as short-lived molecules and molecules which have unstable intermediates can be studied computationally like stable molecules. The capability of computational chemistry however does not end here. Information about transition states which are nearly impossible to obtain experimentally can also be collected by using appropriate methods of computational chemistry. Because of these reasons, computational chemistry is therefore both an independent research area as well as a vital adjunct to experimental studies[51].

Despite all the advantages mentioned above, there has been very little application of computational methods by researchers concerned with the chemical analyses of wood and its components. One of the earliest reports on research of this type was the examination of the physical chemistry of lignin precursor using the Hückel, the Pariser-Parr-Pople and complete neglect of diatomic overlap (CNDO) molecular orbital theories[52]. Other studies have involved a systematic examination of hydrogen bond strengths in lignin model compounds[53-55] and study of spin densities[56].

In 1984, Elder and Worley[57] applied molecular orbital calculations to wood chemistry. The semi-empirical, self consistent field method of modified neglect of diatomic overlap (MNDO) was used to study the

dehydrogenation of coniferyl alcohol and the electronic structure of the reactive free radicals which form the lignin polymer. The technique was applied to study the first steps of the polymerisation of coniferyl alcohol to form softwood lignin which forms a reactive free radical. There are two possible mechanisms by which this reaction may proceed: by the loss of neutral hydrogen to form the free radical directly, or via the loss of a charged proton, thus forming a phenolate ion which loses a single electron to give a free radical as shown in Figure 1.20[58].

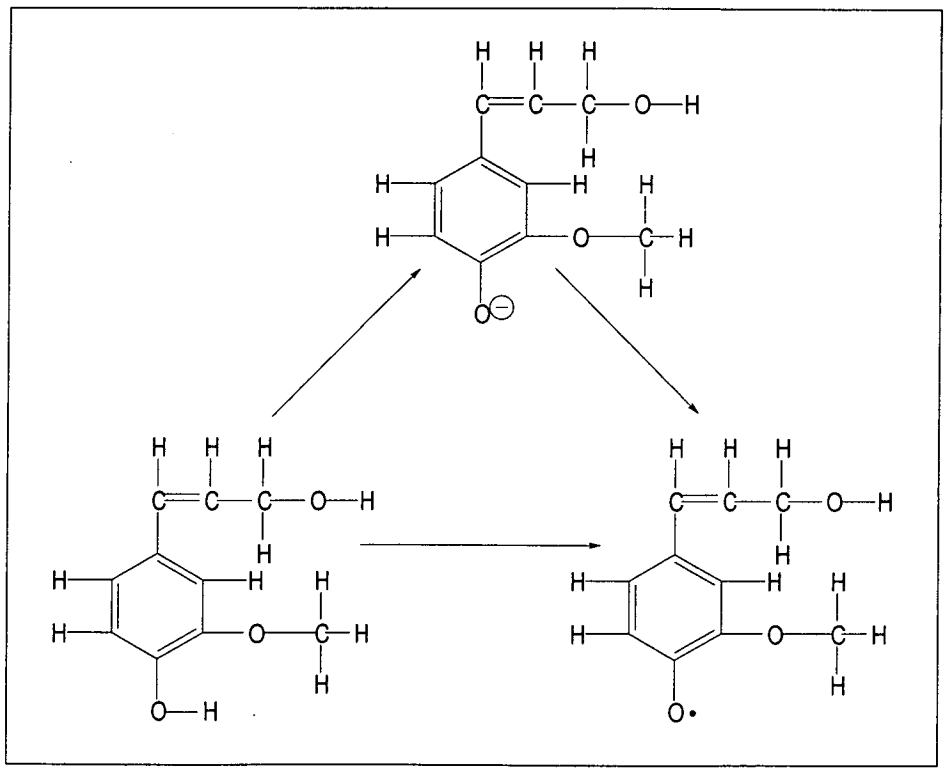

Figure 1.20 Possible routes for the formation of coniferaldehyde radical.[58]

The two potential mechanisms have been examined by calculation of energy levels for the structures shown in Figure 1.20 where it was found that the energy of the ion and radical are both higher than that of the

coniferyl alcohol ground state as expected. Although the energy of the ion was subsequently found to be 62.5 kcal mol^{-1} lower than the radical, a definitive conclusion about the favoured path was unable to be obtained due to the unavailability of the experimental value of electron affinity for the coniferyl radical. Nevertheless, the value of electron affinity of the coniferyl radical obtained from the calculation (2.71 eV), was in good accord with a previous study undertaken by Dewar and Rzepa on phenoxy radical[59].

Later in the same series, Elder, McKee and Worley[60] investigated guaiacylglycocerol-β-coniferyl ether, the corresponding phenolate anion, and quinone methide (Figure 1.21).

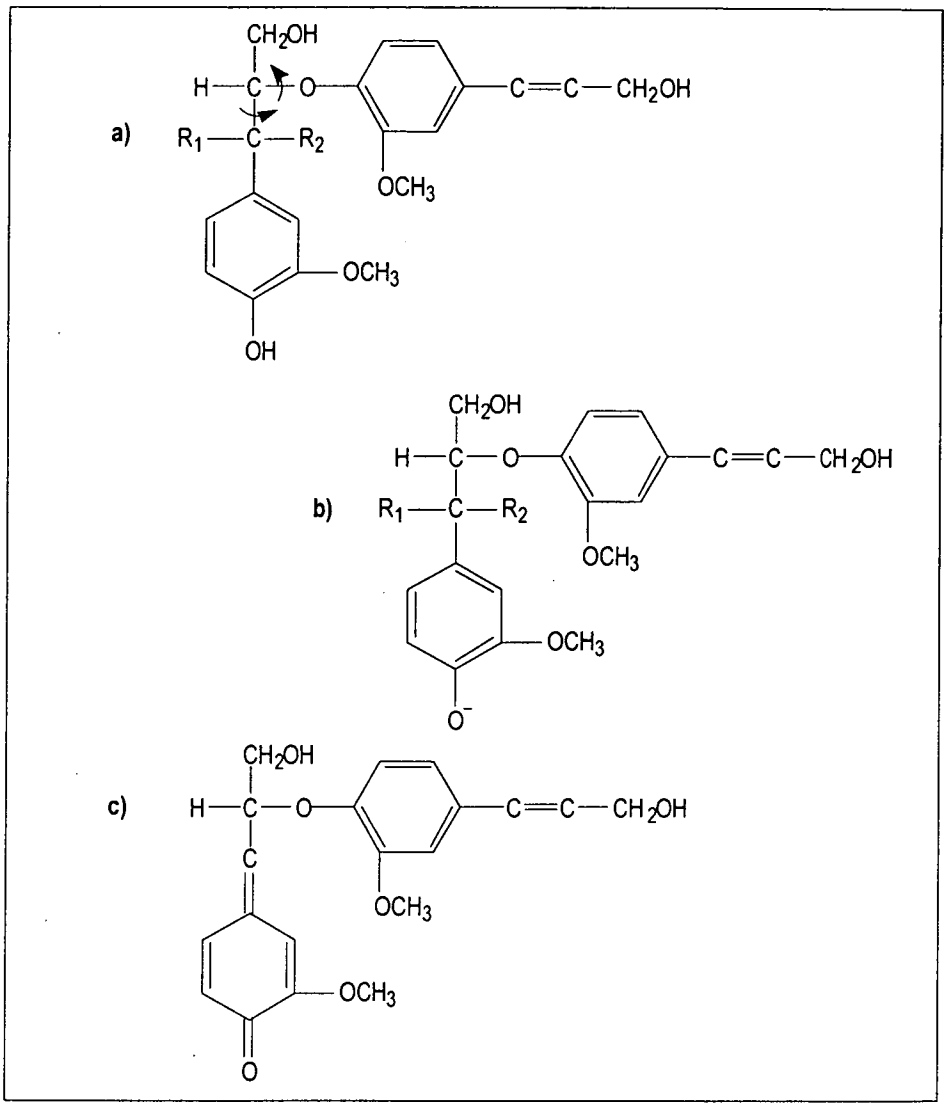

Figure 1.21 Structures for a) free phenol, b) phenolate anion, c) quinone methide intermediates of guaiacylglycocerol-b-coniferyl alcohol as studied by Elder[60]. The arrows indicate the bonds about which rotations were performed. Where: R_1 = H, R_2 = OH is the *erythro* isomer, and R_1 = OH and R_2 = H for the *threo* isomer.

The structural determination was carried out using Assisted Model Building with Energy Refinement (AMBER)[61] while the molecular orbital calculations were accomplished with the semi-empirical, self-consistent field method of modified of diatomic overlap (MNDO). The

results from this study were reported to be in support of the mechanism proposed by experimental work.

A more recent application of molecular orbital theory to bleaching reactions was reported by Garver[62] where semi-empirical methods were used to calculate electron populations, frontier orbital properties, and geometries and energies of molecules to define lignin reactivity in terms of bleaching reactions. Peroxide and chlorine substitution have been used as examples of nucleophilic and electrophilic reactions respectively.

From this study, it was indicated that chlorination and methoxyl substitution reduce the energy of arenium intermediates which, together with the highest occupied molecular orbitals on the lignin structures, control the substitution reaction. The rate of chlorine bleaching of hardwoods is higher because of the greater frequency of methoxyl oxygen sites for oxidation.

In the reaction of peroxide with acetoguaicone, it was concluded that the rate limiting step is the formation of the epoxide intermediate and that increasing the nucleophilicity of the hydrogen peroxide may have little effect on the reaction rate.

Recently, Shevchenko[63] presented a critical review of the applications of theoretical methods to the studies of the structure and chemical reactivity of lignin which included simulation of macromolecular properties, conformational calculations, quantum chemical analyses of electronic

structure, spectra and chemical reactivity. The review also discussed modern concepts of spatial organisation and chemical reactivity of lignins.

The accuracy of the theoretical calculations have also generated a new dimension in the relationship between material scientists and quantum chemists with several papers in the literature[64, 65] addressing the subject of the profitable liaison between them. This may seem fairly improbable since one group is highly applied while the other is highly theoretical. However, if we assume that macroscopic properties are ultimately governed by molecular structure, the connection becomes more plausible.

1.11 References

1. Coleman, M. J., *Cooperative Editorial Feature from Tappi Journal and Pulp and Paper Journal* 10 (1990).

2. Barker, G. J. and Cullinan, H. T., *Search* 20 (6) :195 (1989).

3. Andrews, D. H. and Singh, R. P., In *The Bleaching of Pulp*, "Chapter 8 : Peroxide Bleaching", Singh, R. P. (Eds.), Tappi Press, Atlanta, 1979.

4. Strunk, W. G., *Pulp and Paper* 54 (16) :156 (1980).

5. Dence, C. W. and Omori, S., *Tappi J.* 71 (10) :120 (1986).

6. Moldenius, S., *Svensk Papperstidning* 85 (15) :R116 (1982).

7. Colodette, J. L. and Dence, C. W., *J. Pulp Paper Sci.* 15 (3) :J79 (1989).

8. Lundqvist, M., *Svensk Papperstidning* 82 (1) :16 (1979).

9. Moldenius, S. and Sjögren, B., *J. Wood Chem. Technol.* 2 (4) :447 (1982).

10. Allison, R. W. and Graham, K. L., *J. Pulp Paper Sci.* 15 (4) :J145 (1989).

11. Wright, P. J. and Abbot, J., *J. Wood Chem. Technol.* 11 (3) :349 (1991).

12. Allison, R. W., *Appita* 36 (5) :362 (1983).

13. Flowers, A. G. and Banham, P. W., *Appita* 38 (2) :127 (1988).

14. Abbot, J., Brown, D. G., Hobbs, G., Jewell, I. and Wright, P., *Appita Conf. Proceedings*, 1 :223 (1991).

15. Bergman, E. K. and Edwards, L. L., *Pulp and Paper* (1986).

16. Braller, P., Kappel, J. and Resch, F., *Tappi Pulp. Conf. Proceedings*, 299 (1990).

17. Meyer, K. A., Kappel, J. and Petschaller, F., *Tappi Pulp. Conf. Proceedings*, 291 (1990).

18. Meyrant, P. and Dodson, M., *Tappi Pulp. Conf. Proceedings*, 669 (1989).

19. Wright, P. J., Ginting, Y. A. and Abbot, J., *J. Wood Chem. Technol.* 12 (1) :111 (1992).

20. Abbot, J. and Ginting, Y. A., *J. Pulp Paper Sci.* 18 (3) :J85 (1992).

21. Heitner, C. and Schmidt, J. A., *Int. Symp. Wood Pulp. Chem.*, 1 :131 (1991).

22. Pero, R. W. and Dence, C. W., *J. Pulp Paper Sci.* 12 (6) :J192 (1986).

23. Kutney, G. W. and Evans, T. D., *Svensk Papperstidning* 88 (9) :R84 (1985).

24. Wright, P. J., *PhD Thesis*, Department of Chemistry, University of Tasmania (1993).

25. Sarkanen, K. V., In *Lignins - Occurrence, Formation, Structure and Reactions.*, "Chapter 1: Definition and Nomenclature", Sarkanen, K. V. and Ludwig, C. H. (Eds.), Wiley-Interscience, New York, 1971.

26. Sjöstrom, E., In *Wood Chemistry*, Academic Press, New York, 1984.

27. Wardrop, A. B., In *Lignins - Occurrence, Formation, Structure and Reactions.*, "Chapter 2: Occurence and Formation in Plants", Sarkanen, K. V. and Ludwig, C. H. (Eds.), Wiley-Interscience, New York, 1971.

28. Casey, J. P., In *Chemistry and Chemical Technology, Volume 1: Pulp and Paper*, Wiley-Interscience, New York, 1980.

29. Gellerstedt, G., Petterson, I. and Sundin, S., *1st Int. Symp. Wood and Pulp. Chem.*, II :120 (1981).

30. Smook, G. A., In *Handbook for Pulp and Paper Technologist*, "Overview of Pulping Methodology", Kocurek, M. J. (Eds.), Joint Textbook Committee of the paper Industry, Canada, 1988.

31. Gellerstedt, G. and Agnemo, R., *Acta Chem. Scand.* B34 (4) :275 (1980).

32. Teder, A. and Tormund, D., *Svensk Papperstidning* 83 (4) :106 (1980).

33. Roberts, J. L., Morrison, M. M. and Sawyer, D. T., *J. Am. Chem. Soc.* 100 (1) :329 (1978).

34. Isabell, H. S., Parks, E. and Naves, R. G., *Carbohydr. Res.* 45 197 (1975).

35. Burton, J. T., *J. Pulp Paper Sci.* 14 (4) :J95 (1986).

36. Robertson, G. J., In *Fundamentals of Paper Performance*, "Chapter 9: General and Theoretical Concepts of the Optical Properties of Paper.", APPITA Technical Association, 1985.

37. Axegård, P., Moldenius, S. and Olm, L., *Svensk Papperstidning* 82 (5) :131 (1979).

38. Kubelka, P., *J. Opt. Soc. Am.* 38 (5) :448 (1948).

39. Kubelka, P., *J. Opt. Soc. Am.* 38 (12) :1067 (1948).

40. Teder, A. and Tormund, D., *Trans. Tech. Assoc. CPPA* 3 (2) :TR41 (1977).

41. Robinson, J. V., *Tappi* 58 (10) :152 (1975).

42. Sjögren, B. and Moldenius, S., *1st Int. Symp. Wood and Pulp. Chem.*, 2 :125 (1981).

43. Garver Jr., T. M., Maa, K. J., Xu, E. C. and Holah, D. G., *Res. Chem. Intermed.* 21 (3-5) :503 (1995).

44. Reichert, J. S. and Pete, R. H., *Tappi* 32 (2) :97 (1949).

45. Strunk, W. G., *Pulp and Paper* 54 (6) :156 (1980).

46. Ali, T., McArthur, D., Stott, D., Fairbank, M. and Whiting, P., *J. Pulp Paper Sci.* 12 (6) :J166 (1986).

47. Hagglund, T. and Lindstrom, L., *Int. Pulp Bleaching Conf. Proceedings*, 163 (1985).

48. Been, J., *Tappi J.* 78 (8) :144 (1995).

49. Reeves, R. H. and Pearl, I. A., *Tappi* 48 (2) :121 (1965).

50. Clark, T., In *A Handbook of Computational Chemistry*, John Wiley and Sons, New York, 1985.

51. Foresman, J. B. and Frisch, Æ., In *Exploring Chemistry with Electronic Structure Methods: A Guide to Using Gaussian*, Gaussian Inc., Pittsburgh, PA 15213, 1993.

52. Lindberg, J., Henriksson, J. and Heriksson, A., *Fin. Kemists. Medd.* 79 (2) :30 (1970).

53. Remko, M. and Polcin, J., *Chem. Zvesti* (30) :170 (1976).

54. Remko, M. and Polcin, J., *Z. Phys. Chem.* (258) :219 (1977).

55. Remko, M., *Adv. Molec. Relax. Interact.* (14) :315 (1979).

56. Martensson, O. and Karlsson, G., *Arkiv Kemi* 31 (2) :5 (1968).

57. Elder, T. J. and Worley, S. D., *Wood Sci. Technol.* 18 (4) :307 (1984).

58. Sarkanen, K. V., In *Lignins - Occurrence, Formation, Structure and Reactions.*, "Chapter 4: Precursors and Their Polymerization", Sarkanen, K. V. and Ludwig, C. H. (Eds.), Wiley-Interscience, New York, 1971.

59. Dewar, M. J. S. and Rzepa, H. S., *J. Am. Chem. Soc.* 100 784 (1978).

60. Elder, T. J., McKee, M. L. and Worley, S. D., *Holzforschung* 42 (4) :233 (1988).

61. Weiner, P. K. and Kollman, P. A., *J. Comput. Chem.* 2 (3) :287 (1981).

62. Garver Jr., T. M., *Int. Pulp Bleaching Conf. Proceedings*, 5 (1994).

63. Shevchenko, S. M., *Croatica Chemica Acta* 67 (1) :95 (1994).

64. Hayns, M. R., *Int. J. Quantum Chem.* (21) :217 (1982).

65. Calais, J. L., *Int. J. Quantum Chem.* (21) :231 (1982).

CHAPTER 2

Experimental Methods

2.1 Pulp Samples

The *Pinus radiata* thermomechanical pulp was provided by Australian Newsprint Mills from TMP unit 2 at their Boyer mill. The pulp was stored at 8% consistency and 4^0C until used.

2.2 Chemicals Used

Hydrogen peroxide (30%) and sulphuric acid (98%) were supplied by Ajax Chemicals. Semi-conductor grade sodium hydroxide (99.99%) obtained from Aldrich Chemicals was used as the alkali source to minimise the introduction of transition metal impurities. Diethylenetriamine-pentaacetic acid (DTPA) (97%) was also obtained from Aldrich Chemicals.

For the pulp digestion prior to metal content analysis, concentrated nitric acid (AR grade), concentrated sulphuric acid (AR grade) and perchloric acid (70% AR Grade) were all supplied by Aldrich Chemicals.

Potassium iodide (laboratory grade), sodium thiosulfate (Aldrich, 99%), dilute sulfuric acid, saturated ammonium molybdate and 1% starch solution were used for iodometric determination of hydrogen peroxide[1].

2.3 Chelation of Pulps

In some cases pulps were pretreated with DTPA prior to bleaching. The required amount of pulp, generally 5 or 10 gram oven dried (g.o.d.), was added to Milli-Q water to give a pulp slurry of 2.5% consistency, and maintained at 20^0C. To this slurry, 0.5% on o.d. pulp of DTPA was added and the mixture stirred occasionally during 15 to 30 minutes treatment time. The slurry was then filtered to approximately 20% consistency and washed with two 200 mL portions of Milli-Q water. Atomic absorption results show that metal ion concentrations, particularly copper and manganese are reduced using this treatment.

2.4 Determination of Transition Metal Contents[2]

Three samples, weighing of about 5 gram oven dried (g.o.d.) were oven dried in 500 mL conical flasks in a dust free area for about 24 hours. To each of the samples, 50 mL concentrated nitric acid and 5 mL concentrated sulphuric acid were added. The mixture was then warmed

gently after the initial violent reaction had subsided. The reaction was continued until no pulp was visible. Perchloric acid (5 mL) and boiling beads were then added. The mixture was then heated on the hotplate until a clear solution was obtained. On occasions, when the solution darkened, more concentrated nitric acid was added. The final solution obtained was colourless or straw coloured. The solution was then cooled and transferred to a 100 mL volumetric flask and diluted up to the mark using Milli-Q deionised water.

The manganese (Mn), copper (Cu) and iron (Fe) contents were then determined on a Varian spectrAA-10 spectrophotometer with an acetylene-air flame. Solutions of manganese, iron and copper were prepared by standard methods and used for calibrating the spectrophotometer prior to sample analysis. Typical values of metal ion contents for unchelated pulp are listed in Table 2.1.

Table 2.1 Transition metal contents of the unchelated *Pinus radiata* thermomechanical pulp taken from Australian Newsprint Mills at Boyer as used in this study.

Metal Ion	Content (ppm)
Iron	5.99
Manganese	32.1
Copper	4.20

2.5 Differential Method Bleaching

Bleaching studies were carried out using polyethylene or Teflon vessels maintained at either 50°C or 95°C in a constant temperature water bath (Figure 2.1). The vessel was tightly capped, however, oxygen was not purged. The pulp suspensions were rapidly stirred during the course of the bleaching reactions. The bleaching experiments were performed by mixing the appropriate amounts of pulp, hydrogen peroxide and sodium hydroxide with the required volume of Milli-Q water to give a consistency of 4%. Sodium silicate was reported to have small influence on the reaction rates[3] and therefore it was not introduced in the bleaching experiments. The pulp was not pre-treated by chelation. The pulp and dilution water were heated to reaction temperature before addition of reagents.

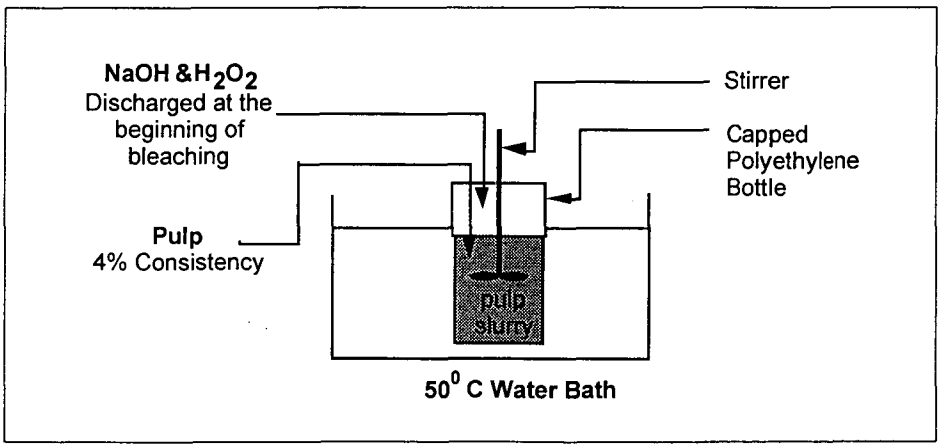

Figure 2.1 Experimental setup for the differential bleaching experiments.

For the repeated cycle experiments, the pulp suspensions and residual liquor was rapidly cooled to room temperature by addition to cold water,

at the end of each cycle. The pulp was then filtered and washed with Milli-Q water, before addition of fresh hydrogen peroxide and sodium hydroxide (at the required reaction temperature) to begin the next cycle.

Residual peroxide concentrations were determined on filtrates by iodometric titration with standard sodium thiosulfate, after acidification and addition of potassium iodide and a few drops of saturated ammonium molybdate solution[1].

Pulp samples were withdrawn at intervals to determine the brightness of the pulp and consumption of hydrogen peroxide. All pulp samples were thoroughly washed with deionised water.

2.6 Constant Conditions Bleaching

Bleaching experiments were performed by adding sufficient *Pinus radiata* TMP Pulp to 8 L of Milli-Q water such that a pulp slurry of 0.3% consistency[4-6] was achieved. Sodium silicate was reported to have small influence on the reaction rates[3] and therefore it was not introduced in the bleaching experiments. The pulp was not pre-treated by chelation. The slurry was vigorously stirred in a polyethylene reaction vessel maintained at 50^{0}C in a constant temperature water bath (Figure 2.2). The vessel was tightly capped, however, oxygen was not purged. Before each bleaching run, an aliquot of pulp was removed to make blank handsheets so that changes in pulp, due to storage, could be monitored.

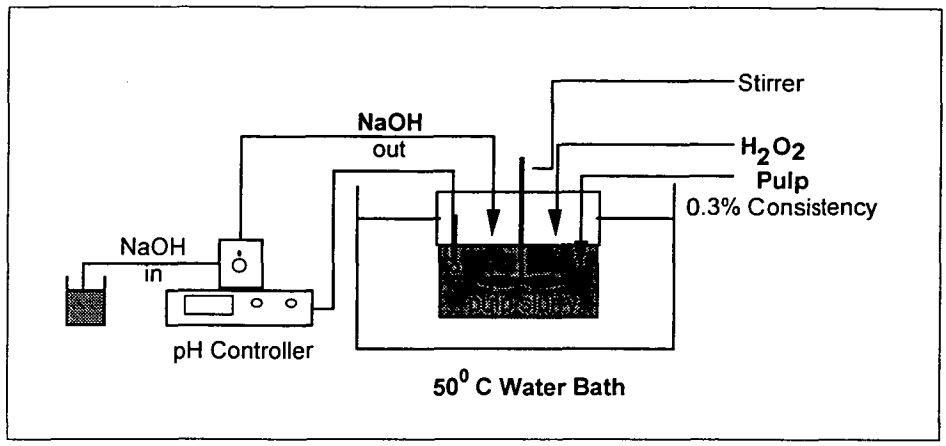

Figure 2.2 Experimental setup for the constant reagent concentrations bleaching experiments.

Bleaching was initiated by simultaneously adding enough alkali and hydrogen peroxide to reach the target conditions. Subsequently, constant pH was maintained by adding alkali from a pH controller supplied by Cole-Parmer. The concentration of peroxide was maintained at constant levels by occasional addition of the necessary amount of hydrogen peroxide calculated from iodometric titration[1] of the bleaching liquor.

After initiation of bleaching, aliquots of pulp slurry (600 mL) were removed at the desired times to make pulp handsheets. The bleaching reaction was quenched by acidifying the slurry to pH 3 with sulphuric acid (2.5 M)[7], followed by filtration to remove the bleaching liquor. Pulp handsheets of 60-80 gram per square meter (g.s.m.) conditioned basis weight were formed by filtering the required volume of re-dispersed pulp slurry onto a 70 μm[5] nylon mesh placed on top of Whatman No. 540 filter paper. Using this procedure, 3 handsheets were obtained from each aliquot. The sheets were fan dried for several hours

at room temperature and were then allowed to equilibrate at constant temperature (25°C) and humidity (50%) so that conditioned basis weights could be obtained.

These so called 'constant conditions' is a well established technique for investigating peroxide bleaching kinetics and has the following advantages[4, 6, 8]:

- The effects of each variable are easily isolated and mathematical treatment of data is straightforward.
- The reaction conditions resemble those used in the bleaching of model chromophore compounds, enabling simple comparison of the bleaching of pulp and model compounds.
- The influence of diffusion on kinetic behaviour is minimised since each fibre is effectively surrounded by bleaching solution under the low pulp consistencies employed.

2.7 Measurement of Brightness

Brightness sheet were formed by filtering a sample of the pulp suspension on a Whatman number 1 filter paper. The brightness (%ISO) of bleached pulp handsheets were measured on either a Zeiss Elrepho, using a 457 nm filter or a Datacolor Elrepho 2000.

2.8 Measurement of Light Absorption Coefficient

After drying, black-backed and self-backed reflectance measurements were made on each sheet, at a wavelength of 457 nm, using an Elrepho 2000 reflectance spectrometer. Individual opacity (W), scattering coefficient (S) and light absorption coefficient (K) properties were calculated from the Kubelka-Munk equation[9-11] using a computer spreadsheet program (Appendix A). These properties were reported as the average per group of 3 handsheets.

2.9 UV-Visible Difference Absorption Spectra

The ultraviolet and visible spectra of the bleached and unbleached sheets were measured on samples 15 mm x 15 mm in the diffuse reflectance mode by using a Varian DRA diffuse reflectance accessory with a Varian model DMS100 ultraviolet-visible spectrophotometer.

The difference spectra were collected in absorbance at a spectral bandwidth of 2nm and at a rate of 100 nm/min between 260 and 540 nm. Whatman 40 filter paper was used as a reference.

To accommodate for further data manipulation and plotting, a custom program was written in BASIC which enables data collected from DMS100 to be saved as text file. The program is included in Appendix B.

2.10 Computational Chemistry Method

Geometry optimisations of minima and transition structures at the semi-empirical level were carried out using MOPAC 93 using the MNDO[12] and PM3[13] hamiltonians. For each minima, an approximation to the desired geometry was used as input for the calculation. For each transition structure, the calculation was performed using the TS option of the Eigenvector Following routine. The input for a transition structure calculation is approximated from the two minima on its left and right hand side of the reaction coordinate (involving a slight modification of one or more of a combination of bond length, bond angle and dihedral angle of the optimised minima).

Based on the starting geometry of the input file as described above, MOPAC 93 calculates the forces acting on the system, changing the geometry so as to lower the total energy. Internally, the SCF iterations of MOPAC 93 are stopped when two tests are satisfied. These are[14]:

1. when the difference in electronic energy, in eV, between any two consecutive iterations drops below the adjustable parameter, SELCON, and
2. the difference in density matrix elements on two successive iterations falls below a preset limit, which is a multiple of SELCON.

SELCON is set initially to 0.0001kcal/mol. In this work, this value has been made 100 times smaller by the use of the keyword PRECISE.

Optimised geometries of minima and transition structures from the semi-empirical calculations were then used for the *ab initio* calculations. The

6-31G(d) basis set[15] and Baker's Eigenvector Following (EF) optimisation algorithm[16] were used in the calculations. The MP2 calculations were performed on RHF geometries. The TS, EF TS, and QST3 algorithms in Gaussian 94 have also been used in one case where the transition structure could not be located at the semi empirical level.

2.11 References

1. Vogel, A. I., In *Quantitative Inorganic Analysis*, Longmans, Green and Co., London, 1947.

2. Hobbs, G. C. and Abbot, J., *J. Wood Chem. Technol.* 11 (3) :329 (1991).

3. Lundqvist, M., *Svensk Papperstidning* 82 (1) :16 (1979).

4. Moldenius, S. and Sjögren, B., *J. Wood Chem. Technol.* 2 (4) :447 (1982).

5. Heitner, C. and Schmidt, J. A., *Int. Symp. Wood Pulp. Chem.*, 1 :131 (1991).

6. Sjögren, B. and Moldenius, S., *1st Int. Symp. Wood and Pulp. Chem.*, 2 :125 (1981).

7. Wright, P. J. and Abbot, J., *J. Wood Chem. Technol.* 11 (3) :349 (1991).

8. Axegård, P., Moldenius, S. and Olm, L., *Svensk Papperstidning* 82 (5) :131 (1979).

9. Robertson, G. J., In *Fundamentals of Paper Performance*, "Chapter 9: General and Theoretical Concepts of the Optical Properties of Paper.", APPITA Technical Association, 1985.

10. Kubelka, P., *J. Opt. Soc. Am.* 38 (5) :448 (1948).

11. Kubelka, P., *J. Opt. Soc. Am.* 38 (12) :1067 (1948).

12. Dewar, M. J. S. and Thiel, W., *J. Am. Chem. Soc.* 99 (15) :4899 (1977).

13. Stewart, J. J. P., *J. Comput. Chem.* 10 210 (1989).

14. Stewart, J. J. P., In *MOPAC 93 Manual*, Fujitsu Limited, Tokyo, Japan, 1993.

15. Hariharan, P. C. and Pople, J. A., *Chem. Phys. Lett.* 66 217 (1972).

16. Baker, J., *J. Comput. Chem.* 7 385 (1986).

CHAPTER 3

Modelling Methods

3.1 Kinetic Modelling[1]

In the kinetic modelling of a reaction such as the one studied in this project, the first task was to superimpose the response of a proposed model to the experimental data by finding the parameters contained in the model equation which give the best fit. This can sometimes be done manually, although it generally requires considerable amount of time and sometimes, when the model equation has more than one minima, this method can lead to inaccurate solutions. A computerised method which uses an established algorithm in finding these parameters is generally preferred since it can be justified mathematically and also it normally requires much less time and effort.

Another complexity involved in kinetic modelling arises as a result of using many mathematical equations in the form of sets of differential equations to describe the change in the concentration of species with time. For some kinetic systems where the reaction mechanism involves only a few species, the solutions are sometimes quite easy to solve. However, for a development of a kinetic model, the proposed reaction mechanism can grow into a very complex one, in which case, the solutions are too complex to be solved by hand. In these cases,

sometimes only the application of computer techniques are able to provide a solution.

3.1.1 Fitting a Mathematical Model to Experimental Data

Consider the equilibrium model (Figure 3.1) reaction mechanism proposed for the alkaline peroxide bleaching of *Pinus radiata* TMP[2].

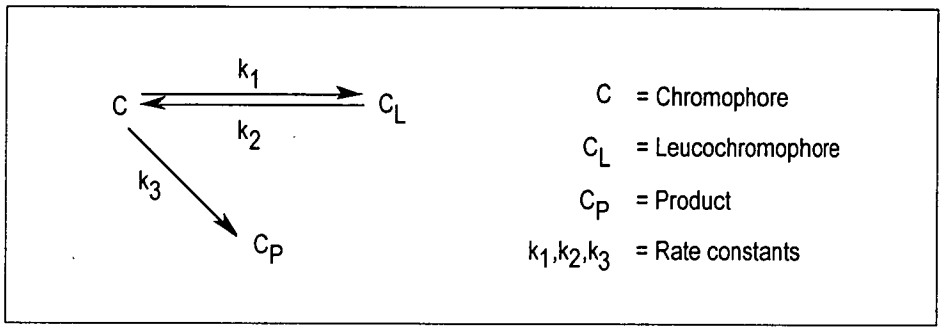

Figure 3.1 Equilibrium kinetic model for alkaline peroxide bleaching of *Pinus radiata* TMP.

The set of differential equations describing the change in the concentration of each of the species C, C_L, and C_P are :

$$-\frac{dC}{dt} = k_1C - k_2C_L + k_3C \quad (3.1)$$

$$-\frac{dC_L}{dt} = k_2C_L - k_1C \quad (3.2)$$

$$-\frac{dC_p}{dt} = -k_3C \quad (3.3)$$

Since only the changes in coloured species (C) can be observed, the analytical solution used in the fitting was the equation describing the

changes in the concentration of C with respect to time. Using Laplacian transformation methods (Appendix C) to solve Equations (3.1), (3.2), and (3.3), the variation of C with time is given by :

$$C = \frac{e^{bt}(bC_0+h) - e^{at}(aC_0+h)}{(b-a)} \tag{3.4}$$

where

$$b = -\frac{(k_1+k_2+k_3)+\sqrt{(k_1+k_2+k_3)^2-4\ k_2k_3}}{2}$$

$$a = -\frac{(k_1+k_2+k_3)-\sqrt{(k_1+k_2+k_3)^2-4\ k_2k_3}}{2}$$

$$h = (C_0+C_{L0})k_2$$

C_0 = initial concentration of C

C_{L0} = initial concentration of C_L

In the bleaching experiments, the chromophore concentration (C) was measured at different times (t) during bleaching reaction, in order to determine the value of constants k_1, k_2 and k_3. The constants k_1, k_2 and k_3 represent the first order rate constants for the reaction of

$$C \xrightarrow{k_1} C_L$$

$$C_L \xrightarrow{k_2} C$$

$$C \xrightarrow{k_3} C_P$$

respectively. The problem therefore lies in determining the values of k_1, k_2 and k_3 for a given set of t and C data such that the theoretical curve is the best fit to the experimental data.

In Equation (3.4) we have $C = \frac{e^{bt}(bC_0+h) - e^{at}(aC_0+h)}{(b-a)}$. In this equation, constants k_1, k_2 and k_3 do not vary within a set, whereas variables t and C do. During the bleaching experiment, we freely vary t, the independent variable. The dependent variable is C, which is dependent on t. The equilibrium equation as we have above when applied to an experiment forms a model with constants C_{L_0}, k_1, k_2 and k_3 as the model parameters. This equilibrium model has, therefore, one independent variable (t) and one dependent variable (C) which are described by an equation of four parameters (C_{L_0}, k_1, k_2 and k_3). To fit the curve we must estimate the best values for these parameters.

The equilibrium equation as shown here is not a linear equation and therefore a non-linear parametric fit is required. The methods used to handle this problem normally use recursive algorithms, that is, we must adjust the parameters in an iterative way, with no idea of how many repetitions we will need to achieve convergence or even, for that matter, if convergence can be reached. A non-linear parametric fit also requires initial estimates of the values sought.

3.1.2 Methods for Determining The Best Value for Model Parameters

Although the equilibrium model has a total of three dependent variables (C, C_L and C_P), the only measured species during the experiment is C. However, as shown in Equation (3.4), by assigning the initial value of C_L (denoted as C_{L_0}) and in the expectancy that C is also dependent on the value of t, we can use this equation as a model. The main thing we must do at this stage is to generalise the method in finding the best values for k_1, k_2 and k_3 for a set of t and C data.

First, we need a new representation of the data. In this new representation, if we choose arbitrary values for k_1, k_2 and k_3, we can determine the corresponding values of C for each experimental t from the model equation. Good values for k_1, k_2 and k_3 can adequately predict C values that are close to those experimentally observed.

To illustrate this, let us consider n data points obtained from an experiment. We can label each value of independent variables t as t_1, t_2, t_3, ..., t_n and each value of the dependent variable as C_1, C_2, C_3, ..., C_n. The predicted values of C generated using the equation using certain values of k_1, k_2 and k_3 can be labelled as C_1', C_2', C_3', ..., C_n'. With this, any pair of k_1, k_2 and k_3 values thus produces a set of C_i' values corresponding to the experimental t_i set.

The sum $(C_1 - C_1')^2 + (C_2 - C_2')^2 + ... + (C_n - C_n')^2$ is called the sum of the squares of the residuals (SS_R) and can be written $\Sigma_i (C_i - C_i')^2$. The lower

this sum is, the better the curve fits between model and experimental points. This is called the least-squares criterion. For random errors randomly distributed, which is a reasonable assumption in our case, this is the best criterion of all.

Thus the problem of finding the best values for a function's unknown parameters becomes the problem of finding the minimum of a new function, SS_R. In our problem, we can picture k_1, k_2 and k_3 as the independent variables and SS_R as the dependent one. Since we have three parameters to be optimised, our SS_R is a four dimensional surface. A bad set of k_1, k_2 and k_3 will give a high value of SS_R. As we move toward better values, the response surface dips toward a minimum. The best values of k_1, k_2 and k_3 lie at this minimum.

3.1.3 The Simplex Algorithm

The simplex method is relatively new. It was proposed by J. A. Nedler and R. Mead in 1965 to find mathematical function minima[3]. Since then, various applications of the algorithm to fitting problems have been developed.

Simplex itself refers to a geometric figure that has one more vertex than the space in which it is defined has dimensions. In our three parameters model the simplex is a tetrahedron. The basic idea in the simplex method is to build a simplex in (m+1)-dimensional space described by

the parameters we want to fit. In our problem, since we have three parameters, k_1, k_2 and k_3, we can consider them as the three planes formed by three axes on which we create a simplex (a tetrahedron). Each vertex is then characterised by four values: k_1, k_2, k_3, and the response SS_R.

To reach the lowest value of SS_R, the program moves the simplex 'downhill', accelerating and slowing down as needed. It follows the rule: find which vertex has the highest (worst) response and which has the lowest (best), then reject the highest and substitute another one for it. The program computes the new vertex according to one of the following mechanisms: reflection, expansion, contraction, and shrinkage.

The simplex strategy as applied in this work has the following advantages[1]:

1. Divergence is impossible.
2. We need to compute the response value only once or at most a few times for each iteration.
3. We do not need any knowledge of derivative or numerical differentiation. This avoids rounding-off errors and allows the handling of non-continuous functions.
4. No matrix operation is involved.

In terms of chemical kinetic modelling, the simplex algorithm can be programmed to implement contour conditions, that is the values of k_1, k_2 and k_3 must be positive. This can be carried out by assigning very high values to SS_R points corresponding to out-of-boundary parameter values to prevent the simplex from ever entering these regions.

3.1.4 Computer Fitting Program Description

SIMP (Appendix D) was written in the 'C' programming language and was designed to run under various computer platforms. The version which was used in this study was compiled using SunOS Unix 'C' Compiler to run under Sun 3 or Sun 4 computers[4].

To operate the program to suit our modelling environment, the function declaration and constants from the original program have been modified. In general use, the constants which need to be modified are:

m = the number of parameters to be fitted.
nvpp = the total number of variables per data point.

For the equilibrium model as an example, nvpp is 2 (1 independent variable, t, and 1 dependent one, C) and m is 3 (k_1, k_2, k_3).

The program input is a disk file with a specified format (Appendix D). Procedure *enter* reads the input file. SIMP directs *enter* to produce a screen output. Next, the program computes the starting simplex values, represented as a square matrix n x n, where n is the number of parameters we want to fit plus one. Each matrix row is a different vertex, for which the first n-1 columns are the individual parameter values, and the n^{th} column stores the response value to be minimised from the procedure *sum_residual.*

Procedure *sum_residual* receives a set of parameter values, and from these, combined with the experimental data, computes the response

surface value at the corresponding point. That is, it computes the sum of the squares of the differences between individual experimental dependent variable values and those calculated for the same independent variable values using the parameters being tested. In our calculation, the statistical weight of each of the data points are assumed to be equal.

Function *f* computes a single dependent variable value, C', from the parameters and a given independent variable value. The program spends most of its time in this function. A highly optimised code in function *f* will greatly save computation time required.

SIMP calls procedure *order* to identify the highest and lowest value of the parameters and the response surface from among all vertices. It uses this information to compute the errors and make decisions for the simplex's next movement.

The main program loop moves the simplex according to the rules previously given. Procedure *new_vertex* substitutes the rejected vertex with a new one. SIMP exits the loop when the error (the percent difference between the extreme values) for all parameters falls below the necessary limits or reaches the maximum number of iterations.

Once the program exits the main loop, procedure *report* directs the results to the screen which shows the fitted points and the computed residuals (the quantities C_i-C_i').

3.2 Computational Chemistry Methods[5]

Two broad areas in the calculations of molecules and their reactivity exist within computational chemistry. They are molecular mechanics and electronic structure theory. Both of them perform the same basic types of calculations[5] :

- Computing the energy of a particular molecular structure (physical arrangement of atoms or nuclei and electrons). Some methods allow for the prediction of properties related to the energy.
- Performing geometry optimisation, which locate the lowest energy molecular structure in close proximity to the specified starting structure. Geometry optimisations depend primarily on the gradient of the energy, the first derivative of the energy with respect to atomic positions.
- Computing the vibrational frequencies of molecules resulting from interatomic motion within the molecule. Frequencies depend on the second derivative of the energy with respect to atomic structure, and frequency calculations may also predict other properties which depend on second derivatives. Frequency calculations are not possible or practical for all computational chemistry methods.

3.2.1 Molecular Mechanics

Molecular mechanics calculations are based on a simple classical-mechanical model of molecular structure. It treats the molecule as an array of atoms governed by a set of classical-mechanical potential functions. There are many different molecular mechanics methods. Each one is characterised by its particular force field with the following components[5]:

- A set of equations defining how the potential energy of a molecule varies with the locations of its component atoms.
- A series of atom types, defining the characteristics of an element within a specific chemical context. Atom types prescribe different characteristics and behaviour for an element depending upon its environment. For example, a carbon atom in a carbonyl is treated differently than one bonded to three hydrogens. Atom type depends on hybridisation, charge and the types of the other atoms to which an atom is bonded.
- One or more parameter sets that fit the equations and atom types to experimental data. Parameter sets define force constants, which are values used in the equations to relate atomic characteristics to energy components, and structural data such as bond lengths and angles.

Molecular mechanics calculations don't explicitly treat the electrons in a molecular system. Instead, they perform computations based upon the interactions among the nuclei. Electronic effects are implicitly included in force fields via their parameterization.

The use of this approximation makes molecular mechanics computations quite inexpensive computationally which therefore allows them to be used for very large systems containing thousands of atoms. However, it also carries several limitations as well. Firstly, particular force fields achieve good results only for a limited class of molecules, related to those for which it was parameterized. No force field can be generally used for all molecular systems of interest. Secondly, neglect of electrons means that molecular mechanics methods cannot treat chemical problems where electronic effects predominate[5]. For example, it cannot describe bond formation or bond breaking or predict molecular properties which depend on molecular orbital interactions.

3.2.2 Electronic Structure Methods

Electronic structure methods use the laws of quantum mechanics rather than classical physics as the basis for their computations. Quantum mechanics states that the energy and other related properties of a molecule may be obtained by solving the Schrödinger equation:

$$H\Psi = E\Psi \tag{3.5}$$

Exact solutions for the Schrödinger equation are generally not practical except for the smallest and totally symmetric systems. Various mathematical approximations to the solution of the Schrödinger equation characterise the electronic structure methods. There are two major classes of electronic structure methods[5]:

- Semi-empirical methods which use parameters derived from experimental data to simplify the computation. They solve an approximate form of the Schrödinger equation that depends on having appropriate parameters available for the type of chemical system in question.
- *Ab initio* methods which unlike either molecular mechanics or semi-empirical methods, use no experimental parameters in their computations. Instead, their computations are based solely on the laws of quantum mechanics- the first principles referred to in the name *ab initio* and on the values of a small number of physical constants (the speed of light, the masses and charges of electrons and nuclei and Planck's constant).

Ab initio methods compute solutions to the Schrödinger equation using a series of rigorous mathematical approximations. Compared to the semi empirical methods, there is a trade-off between computational cost and accuracy of results. Semi-empirical calculations are relatively

inexpensive and provide reasonable qualitative descriptions of molecular systems where good parameter sets exists. In contrast, *ab initio* computations provide high quality quantitative predictions for a broad range of systems. They are not limited to any specific class of system. Although early *ab initio* programs were quite limited in the size of system they could handle, modern *ab initio* programs can generally compute the energies and related properties for systems containing a dozen heavy atoms in just a few minutes.

Prior to the availability of relatively cheap and powerful computers, the solution of quantum mechanical problems was considered to be impractical for any but the simplest molecules. In the past, researchers usually avoided the use of *ab initio* calculations because of the relatively expensive computing time required. During that period, several semi-empirical methods were normally employed for large molecules. The semi empirical methods judiciously use approximations and assumptions to give considerably accurate calculations with relatively small computing time for molecular orbital calculations on large molecules.

In this study, both the semi-empirical and *ab initio* calculations have been used. MOPAC[6] and Gaussian[7] were used for the semi-empirical and *ab initio* calculations respectively. The types of calculation which were performed during this study include single point energy calculation, geometry optimisation and frequency calculation.

3.2.3 Single Point Energy Calculations

The energy and related properties for a molecule with a specific geometric structure is predicted using a single point energy calculation. In this type of calculation, the calculation is performed at a single, fixed point on the potential energy surface for the molecule. It is usually performed with the purpose of obtaining basic information about a molecule, finding a molecular geometry to be used as the starting point for an optimisation, or computing very accurate values for the energy and other properties for an optimised geometry[5].

3.2.4 Geometry Optimisations

Structural changes within a molecule usually produce differences in the molecule energy and other properties. The way the energy of a molecular system varies with small changes in its structure is specified by its potential energy surface.

3.2.5 Potential Energy Surfaces

Potential energy surface is a mathematical relationship linking molecular structure and the resultant energy. A diatomic molecule will have a two-dimensional plot with the internuclear separation on the X-axis, and the energy at that bond distance on the Y-axis, producing a curve. For a molecule with N atoms, the surface has 3N - 6 dimensions, or as many as

the number of degrees of freedom within the molecule. Such a surface is conceptually unmanageable, and therefore potential energy diagrams are often reduced to graphs of one or two dimensions, such as shown in Figure 3.2a for the simple reaction profile and in Figure 3.2b for the potential surface.

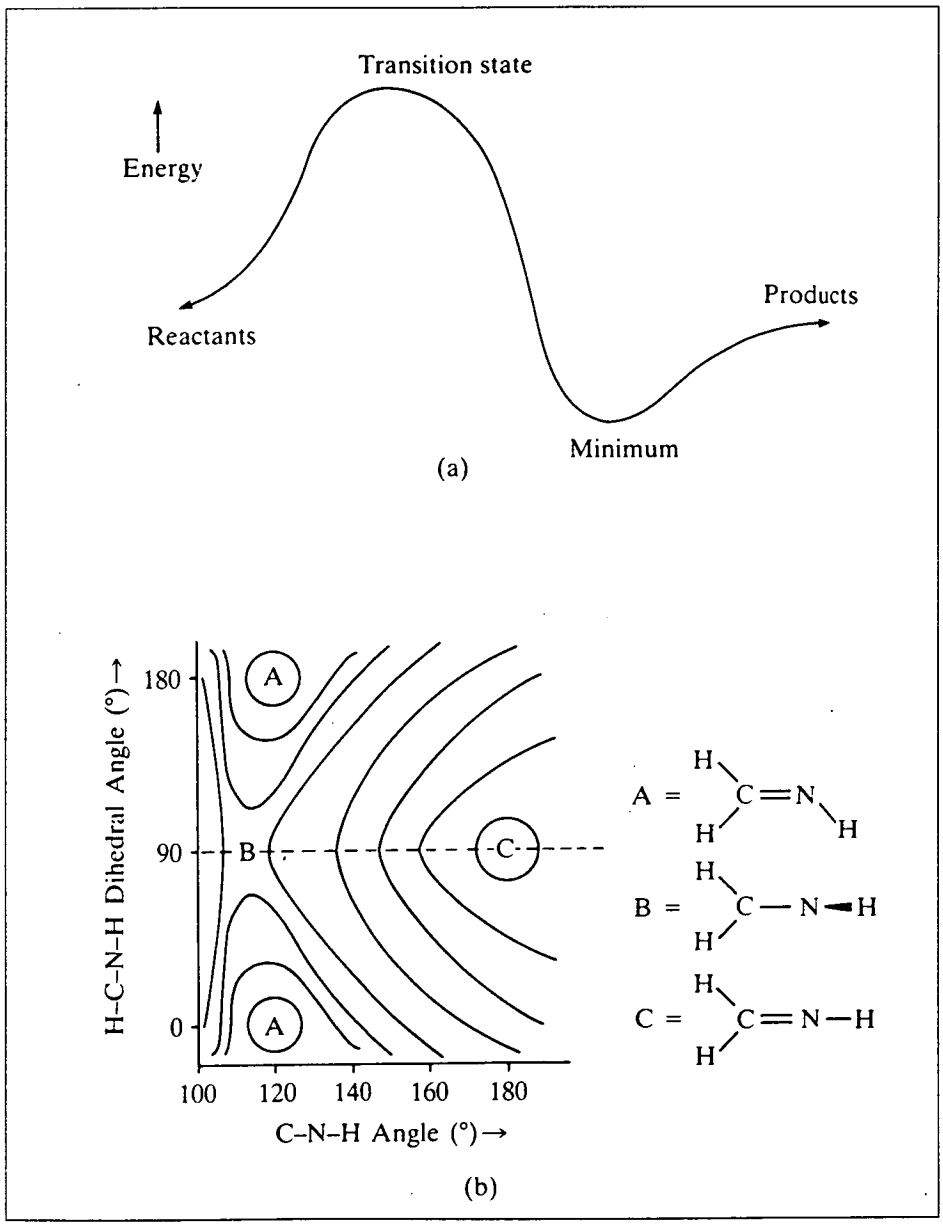

Figure 3.2 (a) Simple reaction profile and (b) Contour diagram of a potential surface.[8]

Potential energy surfaces (PES) are often represented by illustrations like the one shown in Figure 3.3. This drawing considers only two of the degrees of freedom within the molecule, and plots the energy above the plane defined by them, creating a literal surface. Each point corresponds to the specific values of the two structural variables, and thus represents a particular molecular structure, with the height of the surface at that point corresponding to the energy of that structure[5].

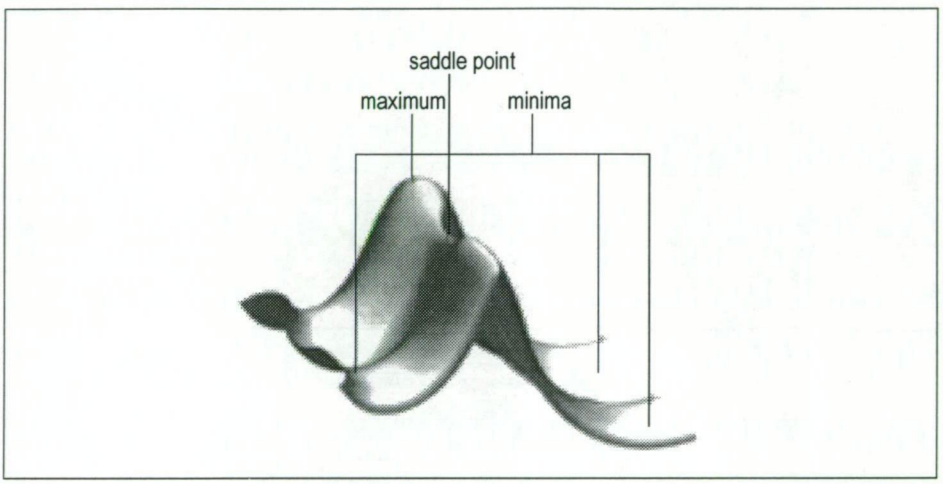

Figure 3.3 Representation of a potential energy surface.[5]

There are three minima on this potential surface. A minimum is the bottom of a valley on the potential surface. From such a point, a motion in any direction - a physical metaphor corresponding to changing the structure slightly - leads to a higher energy. A minimum can be a local minimum, meaning that it is the lowest point in some limited region of the potential surface, or it can be the global minimum, the lowest point anywhere on the potential surface. Minima occur at equilibrium structures for the system, with different minima corresponding to

different conformations or structural isomers in the case of single molecules, or reactant and product molecules in the case of multicomponent systems[5].

Peaks and ridges correspond to maxima on the potential energy surface. A peak is a maximum in all directions (i.e., both along and across the ridge). A low point along a ridge - a mountain pass in our topographical metaphor - is a local minimum in one direction (along the ridge), and a maximum in the other. A point which is a maximum in one direction and a minimum in the other (or in all others in the case of a larger dimensional potential surface) is called a saddle point. For example, the saddle point in Figure 3.3 is a minimum along its ridge and a maximum along the path connecting minima on either side of the ridge. A saddle point corresponds to a transition structure connecting the two equilibrium structures[5]. It should be noted however that the reduction of a n-dimensional PES to a reaction coordinate becomes less meaningful as the dimensions of the surface, or number of atoms in the molecule, increases.

3.2.6 Locating Minima

Geometry optimisation programs are usually designed to find minima. In some cases, they may also be used to locate transition structures. Optimisations to minima are also called minimisations[5].

At both minima and saddle points, the first derivative of the energy, known as the gradient, is zero. Since the gradient is the negative of the forces, the forces are also zero at such a point. This makes sense within the topographic metaphor: the derivative of the surface with respect to its coordinates is zero when the surface is flat. A point on the potential energy surface where the forces are zero is called a stationary point. All successful optimisations locate a stationary point, although not always the one that was intended[5].

A geometry optimisation begins at the molecular structure specified as its input, and steps along the potential energy surface. It computes the energy and the gradient at that point and then determines how far and in which direction to make the next step. The gradient indicates the direction along the surface in which the energy decreases most rapidly from the current point as well as the steepness of that slope[5].

Most optimisation algorithms also estimate or compute the value of the second derivative of the energy with respect to the molecular coordinates, updating the matrix of force constants known as the Hessian. These force constants specify the curvature of the surface at that point, which provides additional information useful for determining the next step[5].

3.2.7 Convergence Criteria

An optimisation is complete when it has converged: essentially, when the forces are zero, the next step is very small, below some preset value defined by the algorithm, and some other conditions are met. These are the convergence criteria used by Gaussian[5] (one of the popular *ab initio* program):

- The forces must be essentially 0. Specifically the maximum component of the force must be below a certain cutoff value (interpreted as 0).
- The root-mean-square of the forces must be 0 (within the defined tolerance).
- The calculated displacement for the next step must be smaller than the defined cutoff value.
- The root-mean-square of the displacement for the next step must be also below its cutoff value.

Note that the change in energy between the current and next points is not an explicit criterion for convergence. It is reflected in the tests of the size of the next step, since small steps near a minimum will usually result in small changes in energy[5].

The presence of four distinct convergence criteria prevents a premature identification of the minimum. For example, in a broad, nearly flat valley on the potential energy surface, the forces may be near zero (within the tolerance) while the computed steps remain quite large as the optimisation moves toward the very bottom of the valley. Or in extremely steep regions, the step size may become very small while the forces remain quite large. Checking the root-mean-squares of the items

of interest also guards against bad tolerance values for any of the criteria leading to an incorrect prediction of the minimum[5].

3.3 References

1. Caceci, M. S. and Cacheris, W. P., *Byte Mag.* (May) :340 (1984).

2. Abbot, J. and Ginting, Y. A., *J. Pulp Paper Sci.* 18 (3) :J85 (1992).

3. Nedler, J. A. and Mead, R., *Computer J.* 7 308 (1965).

4. Whitbeck, M., *REACT Chemical Analysis Software*, 1991.

5. Foresman, J. B. and Frisch, Æ., In *Exploring Chemistry with Electronic Structure Methods: A Guide to Using Gaussian*, Gaussian Inc., Pittsburgh, PA 15213, 1993.

6. Stewart, J. J. P., *MOPAC 93*, 1993.

7. Frisch, M. J., Trucks, G. W., Head-Gordon, M., Gill, P. M. W., Wong, M. W., Foresman, J. B., Johnson, B. G., Schlegel, H. B., Robb, M. A., Replogle, E. S., Gomperts, R., Andres, J. L., Raghavachari, K., Binkley, J. S., Gonzalez, C., Martin, R. L., Fox, D. J., Defrees, D. J., Baker, J., Stewart, J. J. P. and Pople, J. A., *GAUSSIAN 92*, 1992.

8. Clark, T., In *A Handbook of Computational Chemistry*, John Wiley and Sons, New York, 1985.

CHAPTER 4

Development of Kinetic Models

4.1 Literature Review

There are two different approaches when formulating kinetic models to describe bleaching and pulping. The first approach uses process variables such as temperature, stock concentration, initial or final reagent concentration and time to formulate the model in the form of mathematical expression. This type of approach, which produces empirical kinetic expressions, can be useful in predicting the response of pulp when changing one or more process variables under mill conditions and have been mostly employed in the development of many delignification processes such as those for kraft[1, 2] and alkaline pulping[3-6] as well as chlorine[7], chlorine dioxide[8] and oxygen bleaching[9]. The main criteria for the validity of models developed using this approach is that there is a reasonable degree of statistical significance in the correlation between experimental and predicted values. One example of an equation of this type is the kinetic model for alkaline pulping as shown in Equation (4.1).

$$dL / dt = k [L]^a [X]^b [Y]^c \quad (4.1)$$

where L = lignin concentration, usually measured as Kappa number
X, Y = concentrations of pulping or bleaching reagents
eg. X = AQ and Y = OH^- for soda-anthraquinone pulping
k = rate constant
a, b, c = orders of reaction

Since the main purpose of empirical kinetic expressions is to facilitate control and optimisation of industrial processes[1, 4, 5, 7-11], this approach suffers the drawback of providing little insight into basic chemical processes occurring during a reaction. In Equation (4.1) for example, the orders of reaction have no chemical significance and are considered only as variable parameters, the values of which are determined by fitting an empirical expression to experimental data.

The second approach formulates the model in a manner similar to the type found in classical chemical kinetics which is based on the relation between the changes in concentration of reacting species to their instantaneous concentrations. Initially, a model devised using this approach still needs to be treated as an empirical expression, however, with a suitable analysis of the kinetic relationship obtained from it, it is possible that the underlying process can be partially unravelled. This type of formulation is generally more difficult to perform, especially

when one remembers the inherent complexity of the chemical composition of wood or pulp.

4.1.1 Empirical Models

Most of the results of the applications of empirical equations to bleaching and pulping process were hard to interpret in a chemically meaningful way. The reaction orders found using this method are generally of a high value and non integral. Some of the reported values for the reaction orders for pulping and bleaching were in the range of 3-5[7, 8, 10-13].

In addition to this and despite several attempts to provide an explanation of chemical significance of such high orders of reaction, many authors rejected the application of empirical equations. This is due to the lack of molecular consideration of the structure of lignin[3-5, 14-16].

These authors further attempted to include the molecular factor of lignin by using Flory - Stockmayer theory. It was assumed that polymeric branching in lignin occurs in a tree-like fashion. Using this theory, delignification was then treated as the depolymerisation of extensive three dimensional networks. The branched polymer is characterised in terms of a statistical molecular weight distribution and equal reactivity is assumed among functional groups in the polymer. Despite its simplicity, the Flory - Stockmayer theory requires complex expressions to be used to describe the statistical distribution of molecular weights and reaction

rates in lignin depolymerisation. This necessitates the use of many assumptions and approximations before the theory can be used practically[17]. Using this theory, several kinetic models have been able to describe delignification in a chemically meaningful way[4, 5] such as the application to soda and kraft pulping which produced a 'two-gel' kinetic model which then suggested a first order delignification reaction with respect to lignin monomer[4]. This forward reaction was opposed by a reverse reaction which was found to be second order in lignin monomer. Kinetic evidence indicated that the opposing reaction could be associated with lignin recondensation while the forward reaction was associated with depolymerisation by pulping chemicals.

4.1.2 Application of Empirical Models to Alkaline Peroxide Bleaching

Although the application of hydrogen peroxide bleaching for high yield pulp has been on the increase, the development of the kinetic models have so far been minimal in comparison to those carried out for the delignification process. The earliest investigation on a kinetic model of peroxide bleaching on high yield pulps was carried by Martin[18] using Eastern spruce. During the investigation, the rate of total peroxide consumption was found to be a first order process at constant pH levels in the range of 10.5 - 12.0. The rates of peroxide decomposition and reaction with groundwood were also found to be first order processes over the same pH range. He then proposed the equation describing peroxide disappearance during the bleaching at a constant pH as:

$$- d[H_2O_2]_{total} / dt = (k_d + k_r)[H_2O_2]_{total} \quad (4.2)$$

where k_d , k_r = pseudo-first order rate constants for decomposition reaction with pulp respectively

$[H_2O_2]_{total}$ = the sum of both $[H_2O_2]$ and $[HO_2^-]$

Significant amounts of evolved oxygen were reported to be consumed at a rate independent of the peroxide concentration during bleaching. Martin suggested that this observation is due to alkaline oxidation reactions which produced appreciable quantities of carbon dioxide

A 'constant conditions' experiment for the study of the peroxide bleaching kinetics was reported by Lundqvist[12] in 1979. The experiments were carried out at constant temperature with reagent concentrations (alkali and peroxide) maintained at constant levels. A low consistency pulp of 0.3% was used to reduce the rate of alkali and peroxide consumption in order to enable easier replenishment of its amount as the reaction proceed. In this work, the elimination of chromophores in the spruce groundwood pulp during bleaching was studied as a function of time by measuring the light absorption coefficients (K) of bleached pulp handsheets. The results of these bleaching experiments were fitted to an empirical mathematical model of the form:

$$dC_K / dt = k [H_2O_2]^a [OH^-]^b C_K^n (3) \quad (4.3)$$

where C_K = the concentration of chromophores estimated by light absorption coefficient (K)
k = reaction rate constant
t = reaction time
a, b, n = orders of reaction.

The order of reaction with respect to peroxide concentration, a, was determined to be 1.0 in agreement with the earlier work of Martin[18]. The remaining orders of reaction, b and n, were found to have values of 0.3 and 5 respectively. From a mechanistic standpoint, Lundqvist recognised that a reaction order of 5 in chromophore concentration was highly improbable since, in strict kinetic terms, it would require the reaction of 5 chromophores with each other in a rate determining step. Instead it was proposed that a reaction involving three parallel first order reactions might imitate a single process of higher order.

The approach taken by Lundqvist was further extended by Moldenius and Sjögren[10, 11] who examined the peroxide bleaching kinetics of a number of softwood mechanical and thermomechanical pulps. Bleaching experiments were conducted under constant conditions and also under 'differential conditions' which closer resemble the declining concentrations of peroxide and alkali encountered in industrial peroxide bleaching. Experimental results obtained under constant conditions at 0.3% consistency were fitted to the empirical model in Equation (4.3) and resulted in reaction orders of a = 1.0, b = 0.45 and n = 4.8. Orders of

reaction for experiments carried out under differential conditions at 15% consistency were approximately half the values obtained in constant conditions experiments. It was proposed that physical factors such as diffusion might influence the rate determining step at higher consistencies leading to the observed difference in reaction orders under differential and constant reagent conditions. Moldenius and Sjögren also reported a maximum in the rate of bleaching at *p*H 11.5 in constant conditions experiments, even though Equation (4.3) predicted an indefinite increase in bleaching rate with alkali concentration. The maximum in bleaching rate was ascribed to a balance in the bleaching action of perhydroxyl anion (HO_2^-) and colour creation by alkali in condensation reactions.

In another report, Allison and Graham[13] used the empirical model (as in Equation (4.3)) for kinetics analysis of the bleaching of *Pinus radiata* TMP fractions. For a constant conditions experiments carried out at 60^0C with pulp consistency of 1%, they found that the reaction orders for the peroxide bleaching of whole TMP have the values of a = 1.2, b = 0.25 and n = 4.8. The bleaching of pulp fines gave similar results with a = 1.2, b = 0.21 and n = 5.0. From the similar kinetic response of fibre and fines, reflected in similar orders of reaction, it was concluded that fibre and fines lignin contain similar chromophoric structures.

In a recent study of alkaline peroxide bleaching of *Eucalyptus regnans* SGW under constant reagent conditions, Wright and Abbot[19] explained

the phenomenon of limiting brightness levels after extended bleaching in terms of a two chromophore consecutive reaction model. In this model it was assumed that there are at least two categories of chromophores which contribute to the pulp colour as measured by the light absorption coefficient at 457 nm as illustrated in Figure 4.1.

In the proposed model, they argued that two categories of chromophore may exist within the original pulp (C_1 and C_2). Chromophore C_1 can undergo rapid initial reaction to give colourless products C_p. Chromophore C_2 is eliminated much more slowly in the presence of alkaline peroxide. Furthermore, as this reaction progresses, in addition to the reaction pathway to produce C_p, C_1 can be converted to C_2 through a parallel reaction process. They also reported that the rate of removal of C_1 is strongly dependent on the concentration of peroxide present while the removal of C_2 is not strongly dependent on peroxide concentration.

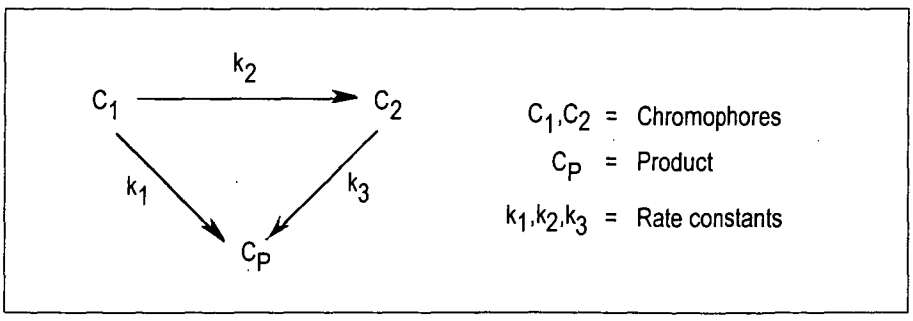

Figure 4.1 Two chromophore model.[19]

This formulation has been found to result in a better fitting of the experimental results compared with the previous empirical model and has an advantage that the overall bleaching response is defined in terms of first order processes. The model also predicts a maximum in the rate of bleaching at a pH in the range of 11-12 in agreement with experimental results. This result was a significant improvement on the previous empirical model which would predict a continuous increase in the bleaching rate without limit.

In a more recent work, a new kinetic model for the alkaline peroxide brightening of mechanical pulp which provides a good fit to data obtained from experiments was proposed on the basis of hydroxide and peroxide anion concentration in the fibre wall[20]. In this model, reactions are assumed to be controlled by a spectrum of activation energies and zero-order reaction kinetics with respect to the chromophore concentration. It was reported that the reaction order of the peroxide anion concentration within the fibre wall was found to be less than one which is attributed to hydrogen peroxide adsorption on the fibre pore surfaces.

4.2 Introduction

As mentioned above, the two chromophore model as proposed by Wright and Abbot[19] defines the bleaching response in terms of first order

processes. Although the model offers a significant improvement of the fitting of experimental data over the previously reported empirical kinetic models[10-13, 21], the validity of the model should be established by its ability to reflect chemical reaction processes taking place between pulp and bleaching reagents. That is to say that an apparent adequate fitting of data points should not be used as the sole criteria of the model without comparison to experimental behaviour.

In this chapter, bleaching of *Pinus radiata* TMP with alkaline hydrogen peroxide will be studied. In particular, a series of experiments using both the differential method and the constant conditions method were carried out to test the validity of the two chromophore model. The model has been considered and reviewed in terms of a limiting brightness increase which was observed during normal bleaching and the repeated bleaching experiments. These experiments will now be discussed.

4.3 Experimental

The chemicals and procedure for the differential and constant reagent concentrations bleaching experiments of *Pinus radiata* TMP were identical to those described in Chapter 2. The same range of hydrogen peroxide concentration as used by previous researchers[11, 12] on similar studies was used in order to maintain relatively constant concentration

and to ease the process of keeping the reagent concentration at a constant level by regularly measuring the remaining peroxide and adding more.

Light absorption coefficients at 457 nm were used as the measure of chromophore removals during constant reagent concentrations bleaching. The computer data sheets used for the calculation of the light absorption coefficient - time which was used for the kinetics study are detailed in Appendix A.

For the differential bleaching, the brightness measurement were carried out on a Zeiss Elrepho as described in section 2.7 in Chapter 2.

4.4 Results

4.4.1 Limits to Brightness Achieved

Experimental result using the differential method for *Pinus radiata* TMP using 18% hydrogen peroxide on oven dried pulp (o.d. pulp) and 2% NaOH on o.d. pulp at 4% consistency and 50^{0}C is shown in Figure 4.2. The progress of the colour removal in the pulp has been monitored by the increase in brightness value (%ISO) of handsheets made from pulp samples withdrawn from the reaction vessel at different intervals of time during bleaching.

The bleaching response as shown in Figure 4.2 resembles alkaline peroxide bleaching under mill conditions and is typical of many reported

results which exhibits an initial rapid increase in brightness, indicating a fast rate of chromophore removal, which then decreases as time progresses. Under differential bleaching conditions, the peroxide concentration (Figure 4.3) and pH (Figure 4.4) of the system are allowed to decline throughout the bleaching process.

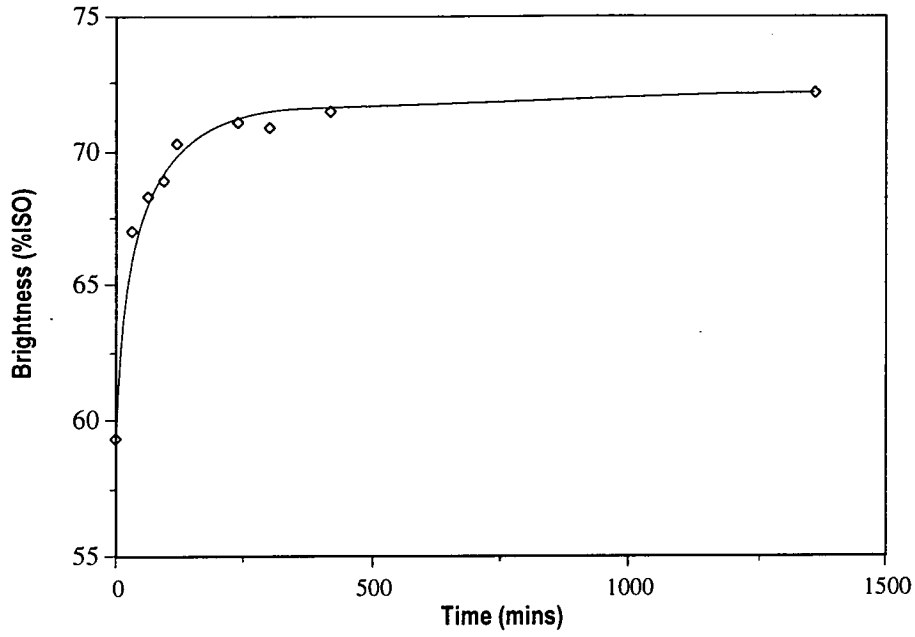

Figure 4.2 Increase in brightness with time of the differential bleaching experiment of *Pinus radiata* TMP at 50°C, 4% consistency.
Initial conditions : 18% hydrogen peroxide on o.d. pulp and 2% NaOH on o.d. pulp

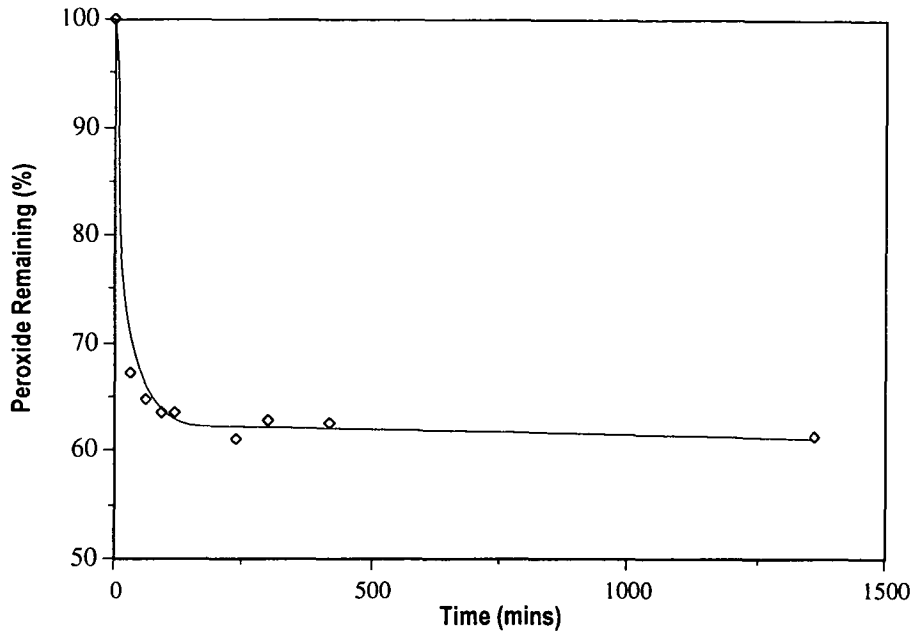

Figure 4.3 Decrease in peroxide charge with time of the differential bleaching experiment of *Pinus radiata* TMP at 50°C, 4% consistency.
Initial conditions: 18% hydrogen peroxide on o.d. pulp and 2% NaOH on o.d. pulp

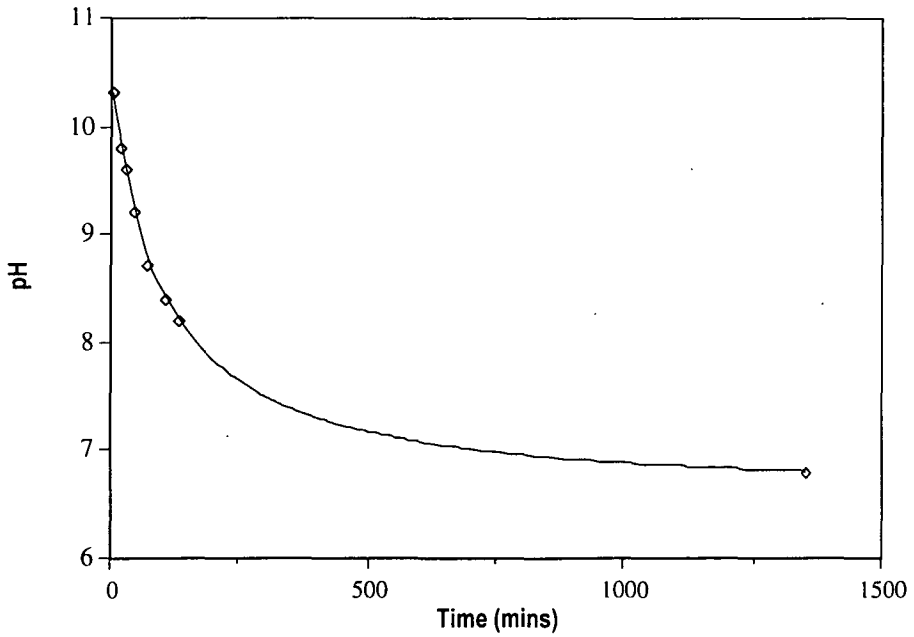

Figure 4.4 Decrease in pH with time of the differential bleaching experiment of *Pinus radiata* TMP at 50°C, 4% consistency.
Initial conditions: 18% hydrogen peroxide on o.d. pulp and 2% NaOH on o.d. pulp

In Figure 4.2 we can see that after the first 250 minutes of bleaching, the pulp can be considered to have attained a limiting brightness of 72% ISO. After the attainment of this limiting brightness, further increase in brightness is very minimal unless very long periods are considered. By referring to Figure 4.3 and Figure 4.4 where the concentration of active bleaching species decreases over time, we interpret the reduction in the rate of chromophore removal as resulting from a loss of the active bleaching species. That is, the apparent limiting brightness observed during bleaching was due to lack of reagents, and thus can be regarded as a 'reagent limited' reaction.

In order to further examine the concept of brightness limits under given bleaching conditions, a series of experiments were carried out using *Pinus radiata* TMP at 95°C and 4% consistency. The reason for conducting the experiments at 95°C becomes clear by inspection of Figure 4.5 which shows plots of brightness against time for various levels of initial peroxide addition at constant initial alkali addition. In each case, an almost constant level of brightness is attained within a few minutes of bleaching. This allows us to accurately define a limiting brightness level associated with each set of experimental conditions.

The results for pulps bleached using an initial peroxide charge of 18% on o.d. pulp as shown in Figure 4.5 indicated that the brightness limit occurs at 69.3% ISO. Higher brightness limits were attained at higher initial peroxide concentrations, and using very high initial levels of peroxide,

brightness levels of >80% ISO were found to be achievable. If the limit of 69.3% ISO was solely due to the availability of active bleaching species (reagent limited), in theory it should be possible to remove additional chromophores and increase brightness by isolating the pulp after reaction, and repeating the bleaching process, starting with the same initial reagent concentrations.

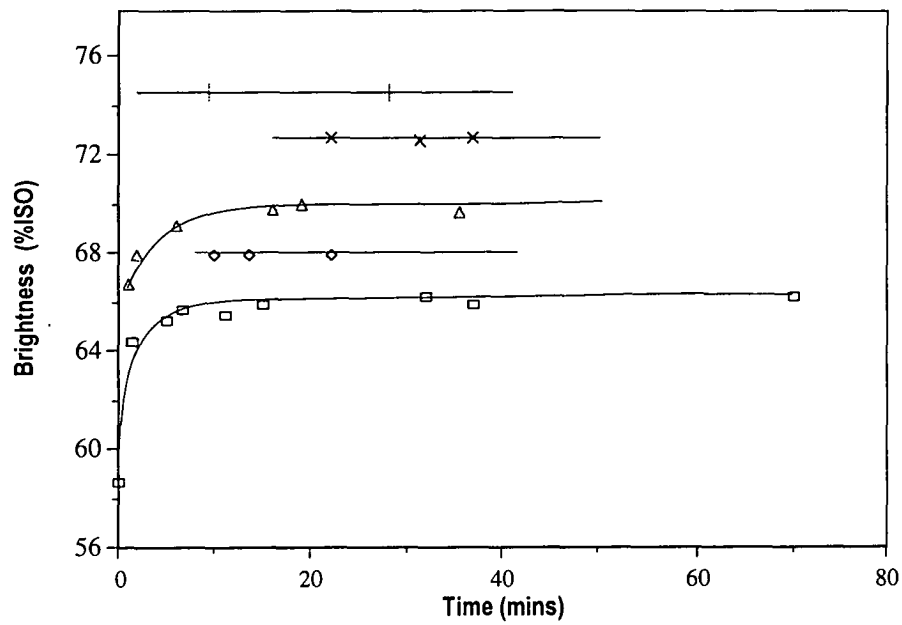

Figure 4.5 Differential bleaching of *Pinus radiata* TMP at 95°C, 4% consistency.
Bleaching conditions:

peroxide charge	:	□ = 6%, ◇ = 9%, △ = 18%, × = 36%, + = 72% (on o.d. pulp)
NaOH	:	2% on o.d. pulp

To investigate this theory, an experiment in which a pulp was repeatedly bleached using the same initial peroxide concentration after isolating the pulp by filtration prior to each bleaching cycle was carried out .

The effect of a series of such bleaching cycles is shown below in Table 4.1.

Table 4.1 Repeated differential bleaching of *Pinus radiata* TMP at 95°C and 4% consistency.

Cycle	Brightness (% ISO)
1	69.3
2	71.5
3	71.4
5	71.7

Bleaching conditions:

peroxide charge	=	18% on o.d. pulp
NaOH	=	2% on o.d. pulp
duration	=	10 min./cycle

It is apparent from Table 4.1 that a limit to brightness gain is achieved after the second bleaching experiment, with the pulp brightness settling at 71.5% ISO. This brightness level remains virtually unchanged after a further set of four cycles. These results show that, even though active bleaching species are constantly available for reaction with chromophores in the pulp, no further significant brightness gain is achieved, and we might conclude that some change has occurred to the chromophores in the original pulp so that they are no longer easily removed by alkaline peroxide under bleaching conditions. Therefore we can consider that the reaction has become a 'pulp limited' reaction. Such a limitation might arise if some of the chromophores initially present in

the pulp are transformed to a state in which their removal is very slow under alkaline peroxide conditions as previously suggested by Wright and Abbot[19]. Alternatively, all the bleachable chromophores originally present may have been removed, while new chromophores are simultaneously created so that the net effect results in the brightness limit observed.

These effects can also be illustrated by reference to Figure 4.6. With an initial peroxide charge of 6% on oven dried (o.d.) pulp, a limit to the brightness gain is observed at 66.0% ISO during the first cycle. Restoration of initial reagent conditions after 15 minutes does not increase the brightness limit for the pulp. Even repeatedly restoring the initial reagent concentrations over 5 cycles at 8 minute intervals does not yield a pulp of higher final brightness.

All the above experiments were undertaken under conditions where both pH and peroxide concentration decreased during the bleaching. However since the formation of active bleaching species, the perhydroxyl anions HO_2^-, is dependent on both hydrogen peroxide concentration and pH, investigations into the bleaching profile of the pulp when there is no reduction in both pH and hydrogen peroxide would be interesting (especially in order to deduce the validity of the 'reagent limited' concept).

A set of experiments using constant conditions of reagent were carried out, with the progress of the bleaching process being monitored using

both brightness and light absorption coefficient. Typical results using brightness measurement and light absorption coefficient for a constant conditions bleaching experiment can be seen in Figure 4.7 and Figure 4.8 respectively.

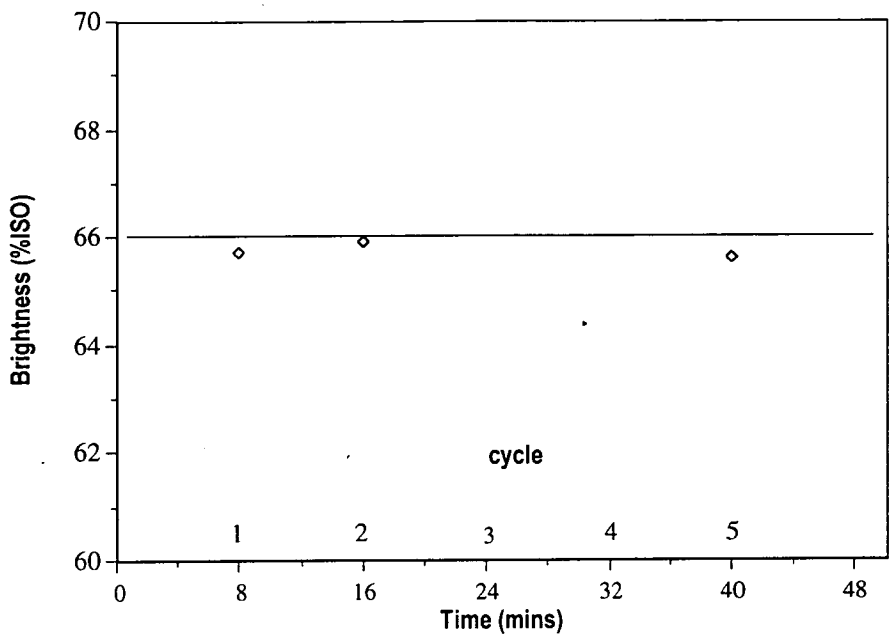

Figure 4.6 Effect of repeated differential bleaching of five cycles at 95°C, 4% consistency. Bleaching conditions:

peroxide charge	=	6% on o.d. pulp
NaOH	=	2% on o.d. pulp
duration	=	8 min./cycle

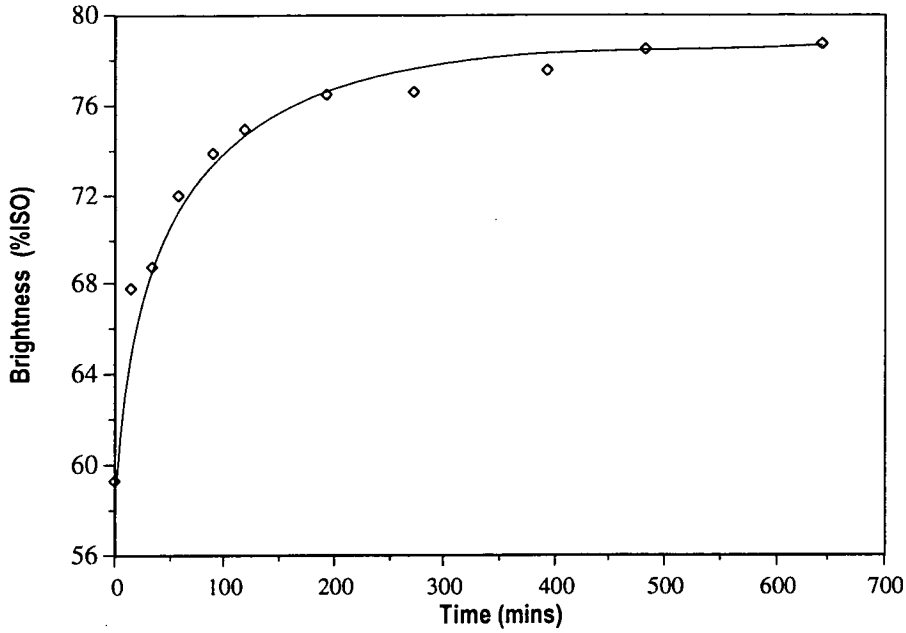

Figure 4.7 Brightness profile of the constant conditions bleaching of *Pinus radiata* TMP at 50°C and 0.3% consistency.
Bleaching conditions:

peroxide charge	=	4g/L
pH	=	11.0

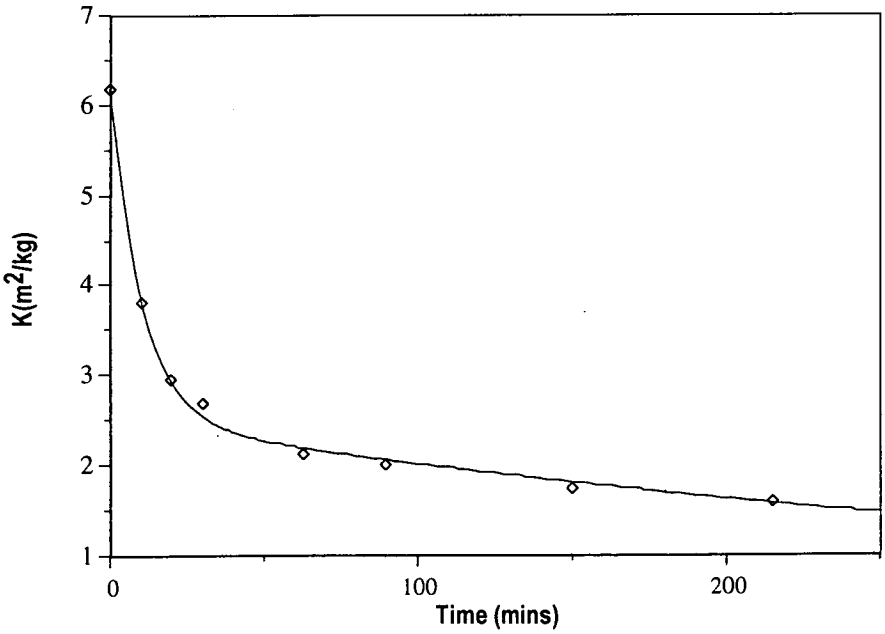

Figure 4.8 Light absorption coefficient (K) profile for the constant conditions bleaching of *Pinus radiata* TMP at 50°C and 0.3% consistency.
Bleaching conditions:

peroxide charge	=	4g/L
pH	=	11.0

Under these conditions, both pH and peroxide concentration are maintained at constant levels throughout the bleaching experiment. As we can see, even when there is no reduction in peroxide concentration or pH, the bleaching profile exhibits an apparent limit in the rate of the chromophore removal as was observed during the differential method.

Further experiments carried out using various constant concentrations of reagents showed that the light absorption coefficient at which the rate of chromophore elimination reaches a low, approximately constant level depends on both pH and peroxide concentration (Figure 4.9). This is in agreement with several studies reported earlier[11-13, 19]. In view of these results, the brightness limit of 78 % ISO illustrated in Figure 4.7 might be described as 'pulp limited'.

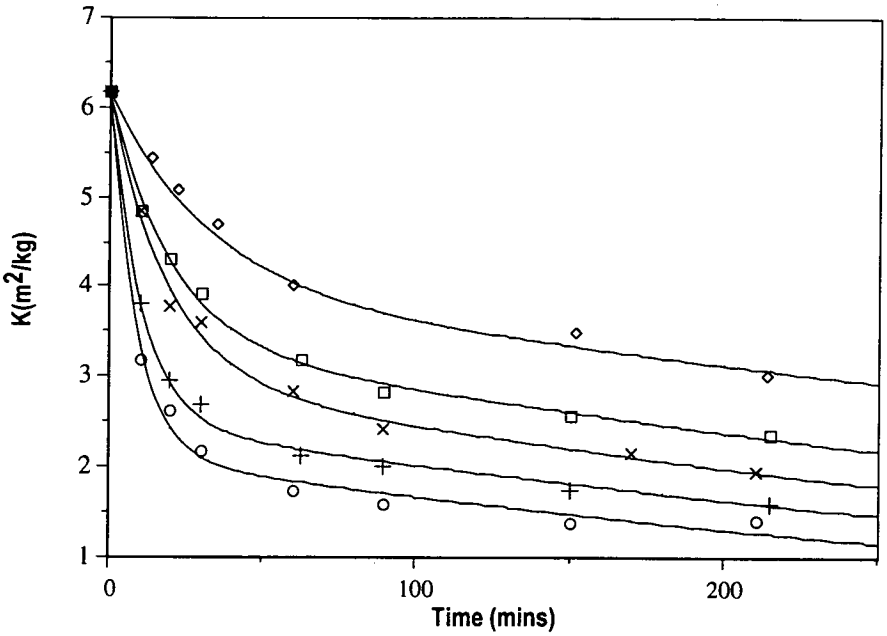

Figure 4.9 Constant conditions bleaching of *Pinus radiata* TMP at 50°C and 0.3% consistency.
Bleaching conditions:
peroxide charge = ◆ 0.5g/L, □ 1g/L, × 2g/L, + 4g/L, ○ 6g/L
pH = 11.0

Having completed the experiments under constant reagent conditions, it was thought that it would be interesting to examine the two kinetic models as mentioned earlier in section 4.1.1 and section 4.1.2. Investigation concerning the ability of the models to match experimental response curves was then carried out.

In section 4.1.2, a two chromophore kinetic model has been proposed to describe the kinetic behaviour of alkaline peroxide bleaching. Figure 4.10 shows a typical profile of chromophore elimination with time, generated by a computer simulation program using the two chromophore model.

Figure 4.10 shows that this model can simulate the general behaviour of chromophore elimination seen under constant conditions (Figure 4.8), with the rapid initial rate of chromophore elimination declining to an almost constant rate after longer bleaching times. Results for isothermal bleaching of *Eucalyptus* SGW under constant conditions of pH and peroxide concentration have been successfully fitted to this two chromophore consecutive reaction model[19]. Results for peroxide bleaching of softwood pulps including *Pinus radiata* TMP taken from the literature[11-13] have also been adequately fitted by this model[19].

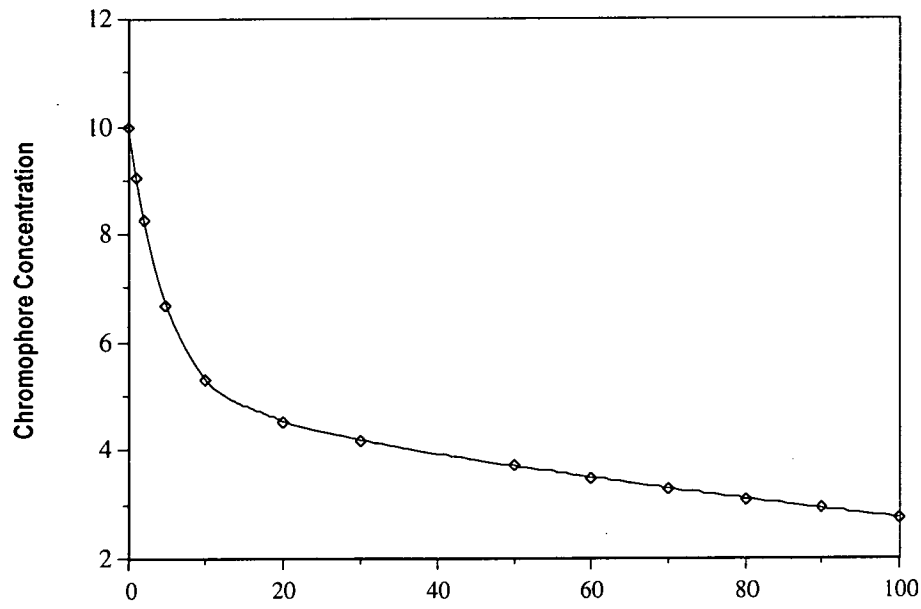

Figure 4.10 Typical chromophore elimination profile of the two chromophore model as generated by computer simulation program. The two chromophore model equation is given on page 15 on Appendix D.

At this stage it is useful to compare the two chromophore model with the empirical kinetic model as described in section 4.1.1. One of the previously reported kinetic models based on the empirical formulation[11-

[13] was found to have reaction orders corresponding to those shown in Equation (4.4).

$$-\frac{dC_k}{dt} = k\left[H_2O_2\right]_{total}\left[OH^-\right]^{0.3} C_k^5 \qquad (4.4)$$

High values in the reaction order with respect to chromophore concentration, C_k, are necessary to give an adequate correlation between the empirical formulation and experimental results. These apparent high orders of reaction have been interpreted in the literature[12] as representing a set of chromophore elimination processes as shown in Figure 4.11, where $k_1 > k_2 > k_3 ... > k_n$.

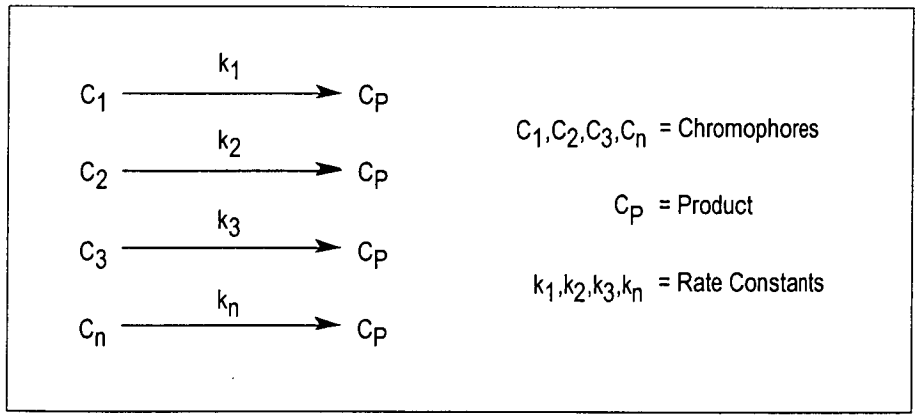

Figure 4.11 Parallel chromophore elimination model.
An explanation to the high value of reaction order with respect to chromophore concentration in empirical kinetic model as in Equation (4.4).

A computer simulation representing chromophore elimination as a function of time using Equation (4.4) is shown in Figure 4.12.

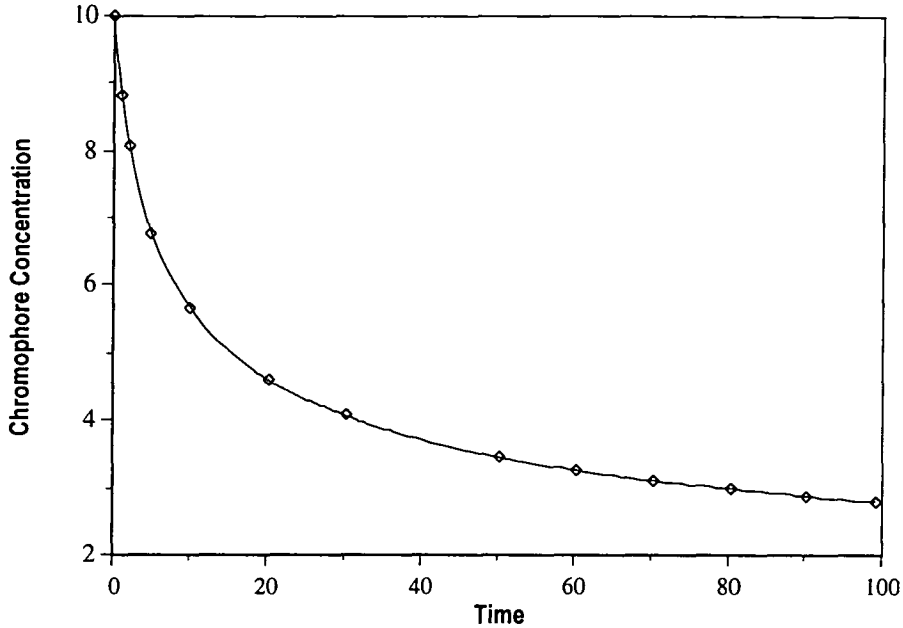

Figure 4.12 Typical chromophore elimination profile of the parallel chromophore elimination model (Equation 4.4) as generated by computer simulation program.

Although the output can provide a reasonable description of chromophore elimination under conditions of constant reagent concentrations[11-13] as mentioned in section 4.1.1, this model has been found to give an inferior fit compared to the two-chromophore model[19]. In addition to poor fitting, Equation (4.3) also does not provide a description for a chromophore creation or a transformation step which is required to account for a limit to brightness gain arising from "pulp limitation" (Figure 4.5 and Figure 4.6).

Another shortcoming of Equation (4.3) is that it would predict that, as the total peroxide charge and pH are increased, the rate of bleaching should increase indefinitely. In practice it is generally observed that as

the pH is increased, the rate of bleaching passes through a maximum value using both constant conditions of reagents[11] and normal mill bleaching conditions[22, 23].

With reference to the two chromophore model, an analysis of the behaviour of rate constant k_1 from this model[19] has shown that it probably represents a reaction process with consecutive steps involving intermediate species. The overall dependence of k_1 on peroxide and alkalinity has the form:

$$k_1 \approx \frac{\left[HO_2^-\right]^a}{\left[OH^-\right]^b} \qquad (4.5)$$

Using this expression, the observation of a maximum in the bleaching rate as pH is increased can therefore be described. In comparison to Equation (4.3), this expression is also preferable since it contains a concentration dependence on the active species HO_2^- rather than the sum of two species (H_2O_2 and HO_2^-) represented by $[H_2O_2]_{total}$.

4.4.2 Chromophore Creation by The Action of Alkali

The two-chromophore model appears to provide an adequate description of kinetic phenomena during alkaline peroxide bleaching by assuming

creation of a second chromophore type which leads to a 'pulp limited' rate of bleaching. Under the conditions used in this study it could be concluded that the rate of removal of C_2 is very low indeed, leading to an almost constant brightness level at 95°C. However, the reaction process leading to the formation of the second chromophore type has not yet been determined.

During industrial bleaching of mechanical pulps with alkaline hydrogen peroxide, the need to retain some level of peroxide concentration at the end of the bleaching process is well known. The presence of this residual peroxide prevents the process of "alkali darkening"[24, 25] which has been attributed to chromophore creation by the action of alkali. Figure 4.13 shows the effect of alkali on the pulp in the absence of peroxide at 95°C, with an initial pH level (11.0) equivalent to that for repeated bleaching with 6% peroxide on o.d. pulp (as in Figure 4.6).

The loss of brightness of the pulp attributable to alkali darkening is approximately 3 units after 15 minutes. This drop in brightness is much smaller than that necessary to account for a limiting brightness level of 66 %ISO (Figure 4.6) when one considers that it is possible to reach levels >80 %ISO at high peroxide concentrations. It should be noted however that peroxide degradation which produces radical species may contribute to the darkening during the bleaching reaction which potentially is not reversible.

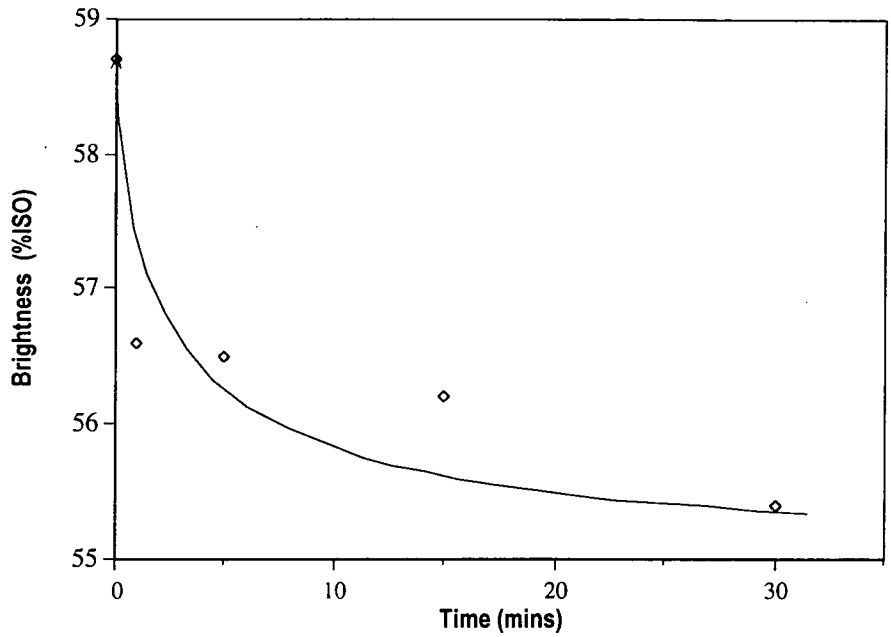

Figure 4.13 Alkali darkening of *Pinus radiata* TMP at 95°C, consistency 4%. Initial alkali charge = 2% on o.d. pulp

Experiments conducted on a two stage process in which bleaching is followed by an alkali darkening stage indicated that the brightness of the pulp falls to a level below that of the initial unbleached pulp (Figure 4.14). This investigation was carried out by bleaching the pulp using 6% peroxide on o.d pulp and 2% NaOH on o.d. pulp until the attainment of a limiting brightness level. The pulp was then isolated and washed and finally exposed to NaOH (2% on o.d. pulp) in the absence of peroxide.

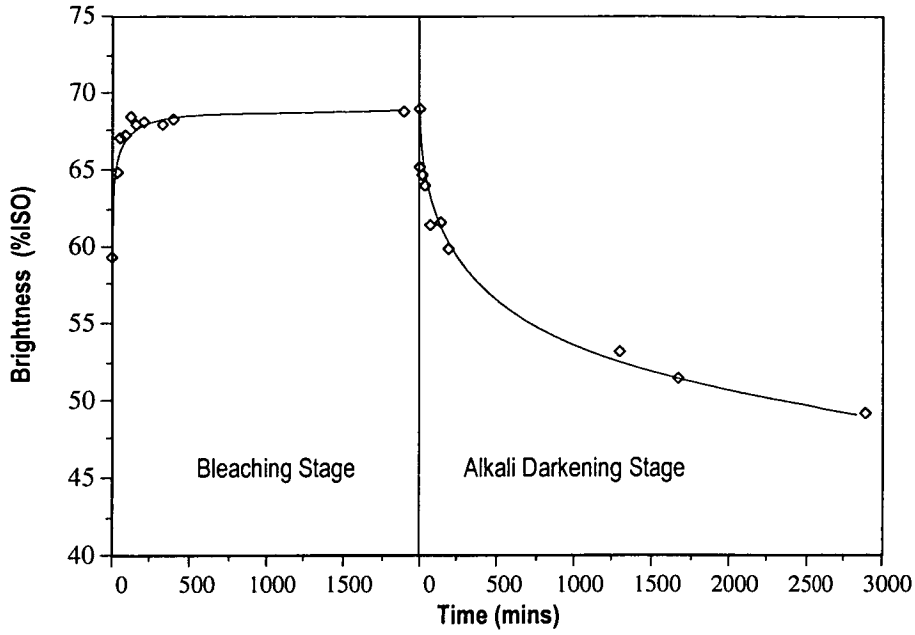

Figure 4.14 Alkali darkening of bleached *Pinus radiata* pulp, 4% consistency and 50°C
First stage (bleaching) initial conditions : 6% peroxide on o.d. pulp, 2% NaOH on o.d. pulp
Second stage (alkali darkening) initial condition : 2% NaOH on o.d. pulp

The bleaching and darkening processes were also found to be reversible. This is clear by inspection of Figure 4.15 which shows that a pulp which has been alkali darkened can be bleached with alkaline peroxide to the same limiting brightness level as the untreated pulp.

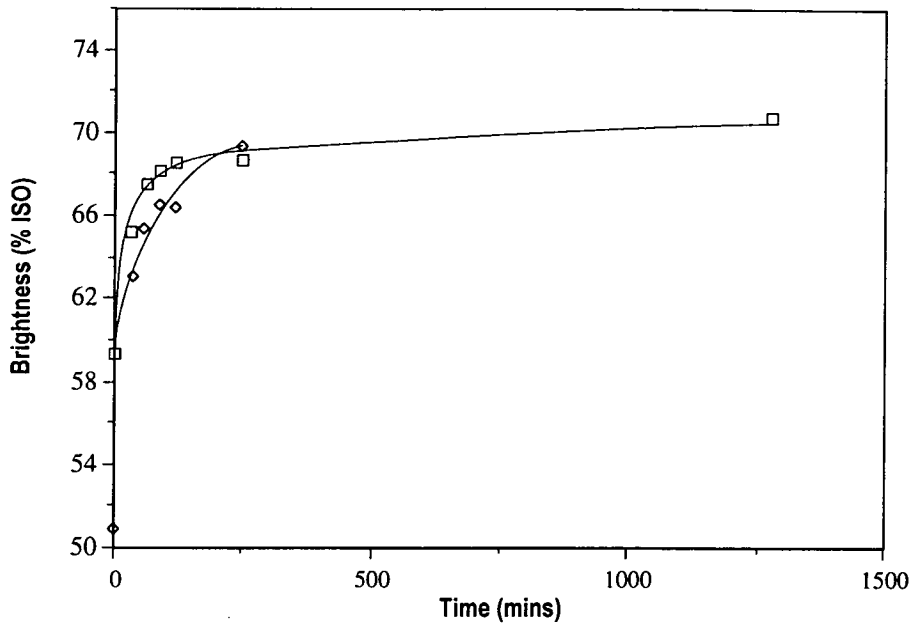

Figure 4.15 Alkaline peroxide bleaching of alkali darkened *Pinus radiata* pulp, 4% consistency and 50°C. ◇ = alkali darkened pulp, □ = normal pulp
Initial bleaching conditions:

peroxide	=	6% on o.d. pulp
NaOH	=	2% on o.d. pulp

4.4.3 Equilibrium Model

Figure 4.16 shows that a simulated kinetic curve generated using Equation (4.3) can be closely duplicated using suitable parameters in the two-chromophore kinetic model. However, as mentioned previously, the latter model is more satisfactory in its representation of chemical phenomena involved during peroxide bleaching, as it considers other criteria such as the need for a chromophore creation step, or prediction of a maximum in bleaching rate with pH. Figure 4.16 illustrates an important principle, showing that fitting a model to experimental results does not necessarily mean a particular model is valid. In light of this, the

two-chromophore model was subjected to further tests, based on predicted behaviour, to ascertain whether it was adequate.

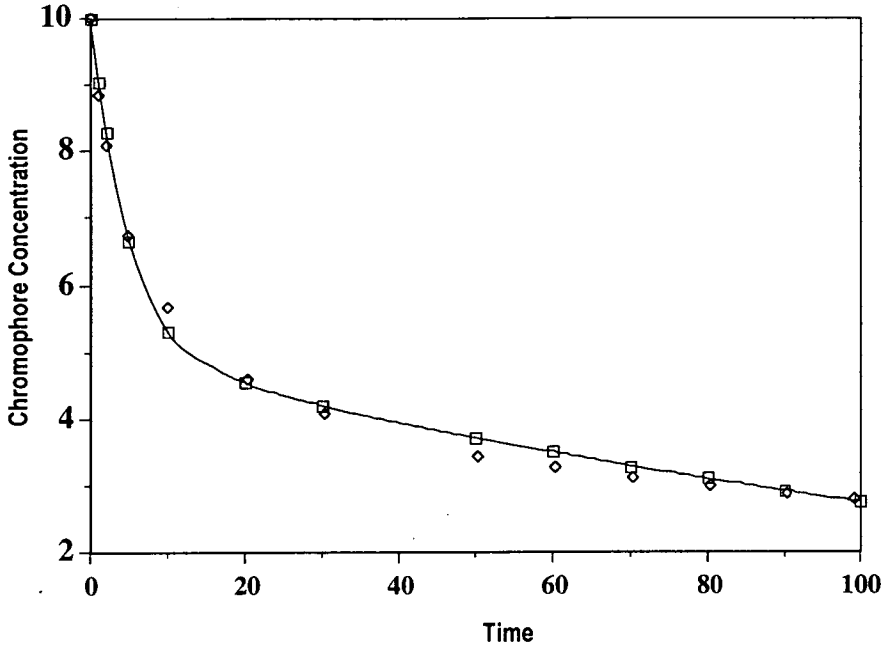

Figure 4.16 Computer simulations for chromophore elimination using parallel process and two chromophore models. □ = Parallel process model (Equation 4.4), ◇ = Two chromophore model (model equation is given on page 15 on Appendix D).

The experiments using repeated bleaching cycles (Table 4.1 and Figure 4.6) showed that a limiting brightness is reached when the pulp is repeatedly exposed to the same initial reagent conditions. In terms of the two chromophore consecutive model, all bleachable chromophores have been converted to C_2, which can only be eliminated very slowly. For example, with repeated cycles at 6% peroxide on o.d. pulp (4% consistency and 95^{0}C) the brightness is restricted to a limit of 66.0 %ISO. However, introduction of additional peroxide to bring the level to

18% on o.d. pulp after "limiting brightness" had been reached, very rapidly increased the brightness, to approach that corresponding to the level attained after initial bleaching with 18% peroxide on o.d. pulp (Figure 4.17).

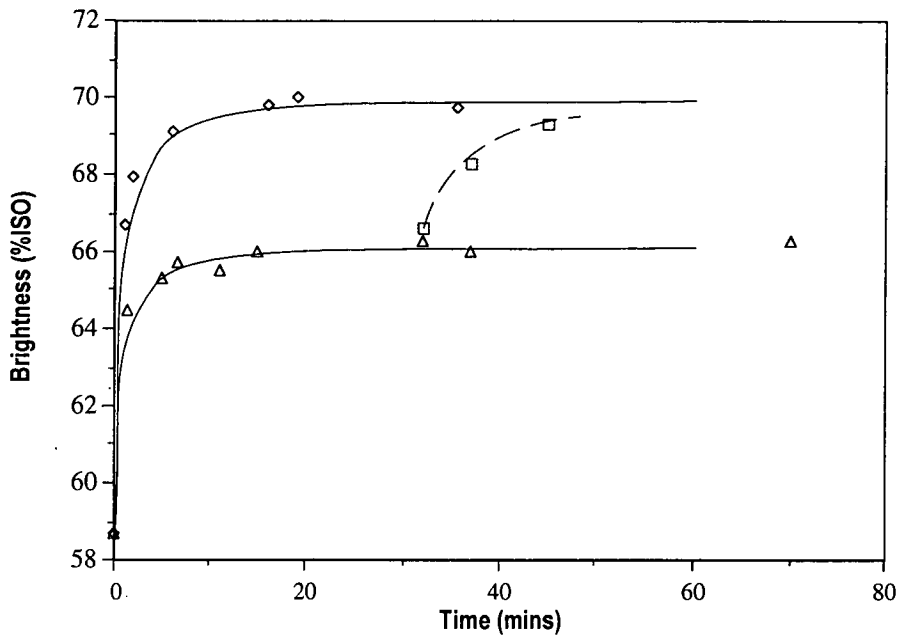

Figure 4.17 The effect of introducing additional peroxide after attainment of limiting brightness level at 95^{0}C and 4% consistency.
Bleaching conditions:

initial peroxide	=	△ 6% on o.d. pulp
		◇ 18% on o.d. pulp
		□ 6% then 18% on o.d. pulp
initial alkali	=	2% on o.d. pulp

If all chromophores were in the C_2 state, simply increasing the concentration of peroxide by a factor of three should not have produced this effect if the two chromophore model were correct. Similar observations were made under other conditions. For example, addition

of excess peroxide after repeated cycles at 18% on o.d. pulp (Table 4.1) rapidly increased the brightness level to >75 % ISO.

These observations suggested that it was necessary to modify the two-chromophore model in order to account for the observed chemical phenomena. The concept of two reacting species was retained, but now the chromophoric species (represented by C), are considered to be in equilibrium with colourless species (C_L). This enables the C_L species to be reversibly interconverted to coloured species C in the presence of alkaline peroxide (Figure 4.18).

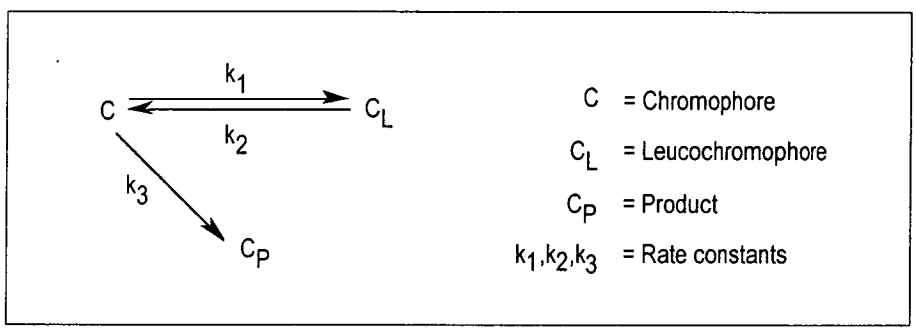

Figure 4.18 Equilibrium kinetic model for alkaline peroxide bleaching of *Pinus radiata* TMP.

The C_L species can be identified with the concept of leucochromophores, i.e. colourless functional groups which can be transformed into chromophores. In this formulation, the rate of conversion of C to C_L is determined primarily by the concentration of active species derived from peroxide (e.g. HO_2^- or possibly OH^-) whereas the reverse process is favoured by hydroxide ion. With constant concentrations of peroxide

and alkali, establishment of an equilibrium position can be associated with the brightness level at which the rates of forward and reverse reactions are balanced. The slow residual rate of chromophore elimination can be described by an irreversible process in which C is slowly converted to colourless products C_p (Figure 4.18). Under normal bleaching conditions, where both peroxide concentration and pH fall, an equilibrium position will be established which may vary from that corresponding to initial reagent conditions. This explains why some shift in limiting brightness may be observed after repeated bleaching cycles (Table 4.1). After attainment of an equilibrium position, with falling concentrations of both peroxide and hydroxide ion, the rates of both forward and reverse processes will decline very rapidly. Under these conditions a shift away from equilibrium due to prevailing reactant concentrations during the later stages of bleaching will be slow. An exception to this, however, may occur if all the peroxide is consumed and the pulp is left in a medium of high pH, when alkali darkening can occur[24, 25]. In our case, this effect is as shown previously in Figure 4.14.

The computer simulation shown in Figure 4.19 shows that with suitable parameters the equilibrium model shown in Figure 4.18 can simulate the type of behaviour found under bleaching conditions. Figure 4.20 shows a set of simulations for the three models discussed above.

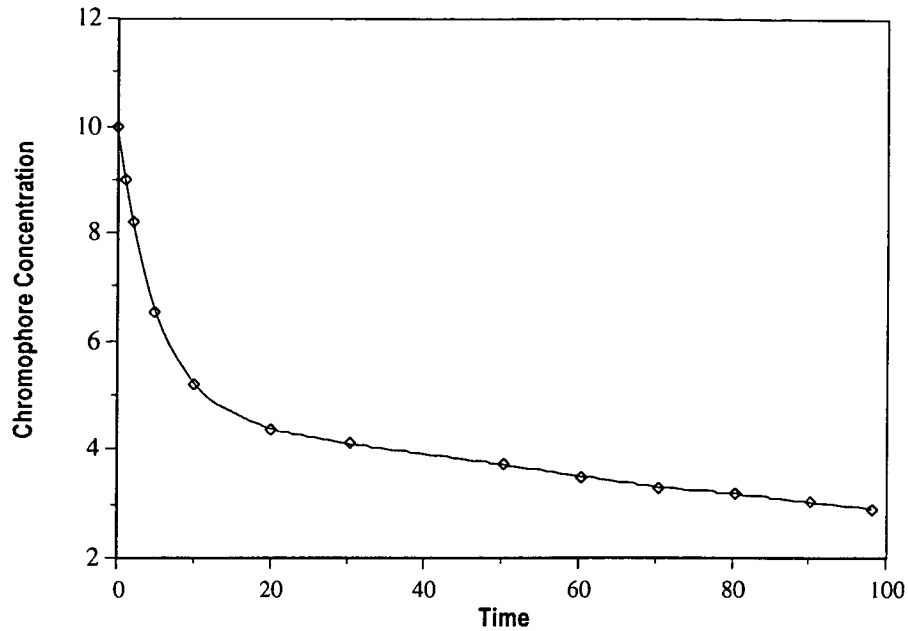

Figure 4.19 Typical chromophore elimination profile of the equilibrium model as generated by computer simulation program. The equilibrium model equation is given on page 14 on Appendix D.

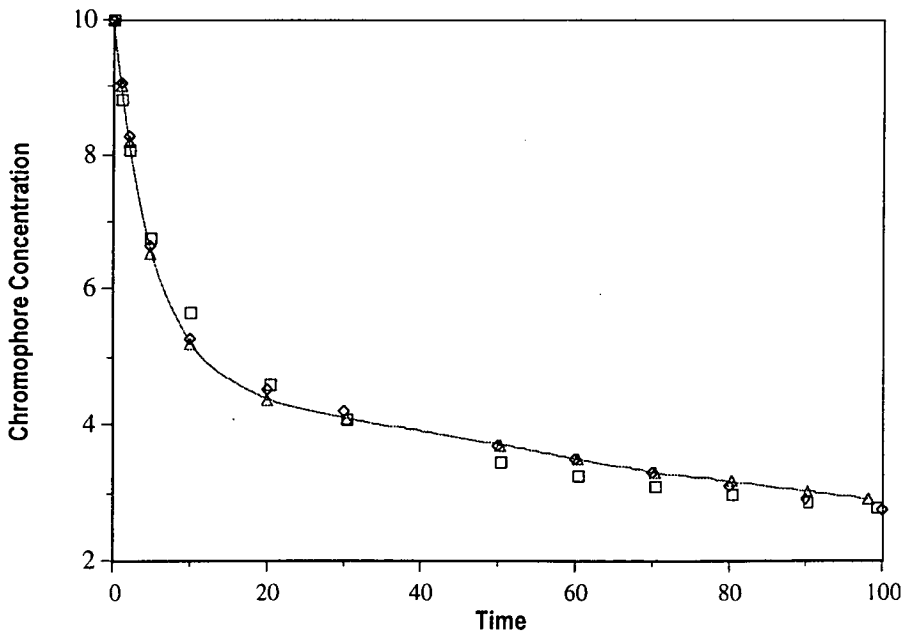

Figure 4.20 Computer simulations for kinetic models of alkaline peroxide bleaching. ◇ = Parallel process model (Equation 4.4), □ = Two chromophore model (model equation is given on page 15 on Appendix D), △ = Equilibrium model (model equation is given on page 14 on Appendix D).

Figure 4.20 illustrates the fact that, with suitable values for parameters, a given curve generated by one model can be closely approximated by the other models. This also suggests that a given set of experimental data can be simulated by more than one plausible model, and demonstrates the requirements to test the predicted chemical behaviour based on a particular model.

4.5 Conclusions

Bleaching of *Pinus radiata* TMP with alkaline hydrogen peroxide has been studied. Factors affecting maximum brightness attained have also been examined for various bleaching conditions. The concepts of limiting brightness due to either reagent concentrations or changes in the pulp itself have been considered, as well as observations based on the effects of repeated bleaching cycles.

Three different kinetic models for alkaline peroxide bleaching have been considered. The general characteristics of bleaching profiles with time can be simulated by all three models. Analysis of the results has shown that the two chromophore consecutive reaction kinetic model is unable to describe the behaviour of the bleaching when the peroxide level is suddenly increased during bleaching.

A model which is based on the concept of a rapid establishment of an equilibrium between chromophores and leucochromophores, coupled

with a slower irreversible elimination reaction, was found to be superior in that it can account for experimental observations.

Computer simulations show that very similar simulations for various kinetic models can be produced by appropriate adjustment of parameters. This suggests that it is difficult to differentiate between various models based only on the adequacy of fitting alone and therefore it is important to formulate tests to compare experimental behaviour with model predictions as a means to establishing model validity.

4.6 References

1. Olm, L. and Tistad, G., *Svensk Papperstidning* 82 (15) :458 (1979).

2. Obst, J. R., *Tappi J.* 68 (2) :100 (1985).

3. Yan, J. F., *Tappi* 63 (11) :154 (1980).

4. Yan, J. F. and Johnson, D. C., *J. Applied Polymer Sci.* 26 1623 (1981).

5. Yan, J. F., *Macromolecules* 14 1438 (1981).

6. Abbot, J., *J. Wood Chem. Technol.* 9 (4) :467 (1989).

7. Axegård, P., *Svensk Papperstidning* 82 (12) :361 (1979).

8. Germgård, U. and Teder, A., *Trans. Tech. Sect. CPPA* 6 (2) :TR31 (1980).

9. Olm, L. and Teder, A., *Tappi* 62 (12) :43 (1979).

10. Sjögren, B. and Moldenius, S., *1st Int. Symp. Wood and Pulp. Chem.*, 2 :125 (1981).

11. Moldenius, S. and Sjögren, B., *J. Wood Chem. Technol.* 2 (4) :447 (1982).

12. Lundqvist, M., *Svensk Papperstidning* 82 (1) :16 (1979).

13. Allison, R. W. and Graham, K. L., *J. Pulp Paper Sci.* 15 (4) :J145 (1989).

14. Szabo, A. and Goring, D. A. I., *Tappi* 51 (10) :440 (1968).

15. Bolker, H. I. and Brenner, H. S., *Science* 170 173 (1970).

16. Bolker, H. I., Rhodes, H. E. W. and Lee, K. S., *J. Agric. Food Chem.* 25 (4) :708 (1977).

17. Schöön, N. H., *Svensk Papperstidning* 85 (15) :R185 (1982).

18. Martin, D. M., *Tappi* 40 (2) :65 (1957).

19. Wright, P. J. and Abbot, J., *J. Wood Chem. Technol.* 11 (3) :349 (1991).

20. Been, J., *Tappi J.* 78 (8) :144 (1995).

21. Axegård, P., Moldenius, S. and Olm, L., *Svensk Papperstidning* 82 (5) :131 (1979).

22. Dence, C. W. and Omori, S., *Tappi J.* 71 (10) :120 (1986).

23. Moldenius, S., *Svensk Papperstidning* 85 (15) :R116 (1982).

24. Allison, R. W. and Graham, K. L., *J. Pulp Paper Sci.* 16 (1) :J28 (1990).

25. Kutney, G. W. and Evans, T. D., *Svensk Papperstidning* 88 (9) :R84 (1985).

CHAPTER 5

Testing of the Equilibrium Kinetic Model

5.1 Introduction

In the previous chapter, the kinetic behaviour associated with the bleaching of *Pinus radiata* thermomechanical pulp was examined under both differential and constant reagent conditions. The two chromophore consecutive reaction model was also found to be inadequate in explaining the experimental behaviour when reagent concentrations are changed during bleaching. If peroxide bleaching behaviour under mill conditions is to be described, a valid kinetic model must ultimately account for bleaching responses when reagent concentrations are not held at constant levels.

In this chapter, the validity of the equilibrium kinetic model in describing alkaline peroxide bleaching process was investigated using the constant conditions of reagents bleaching method. The concentration of chromophores (C) in the bleached pulp was followed by measuring the value of light absorption coefficient (K) of the pulp at intervals during the bleaching.

5.2 Peroxide Bleaching of *Pinus radiata* Under Constant Conditions

To assess the validity of the equilibrium model, two different tests were carried out. In the first test, the adequacy of the model in reproducing experimental bleaching curves was studied. The criteria used here to judge the goodness of fit was the sum of squares of the residuals of the model as shown in Equation (3.4) when fitted to the experimental data. The computer simulation program was used in the second test to investigate the correlation between predicted and experimental bleaching responses when the concentration of reagents were changed to new constant levels during bleaching. In this test, the effects of both increasing and decreasing reagent concentrations were considered.

5.2.1 Fitting of Experimental Data

Constant conditions bleaching of *Pinus radiata* TMP was studied at pH 11.0 and 50^{0}C using six different levels of peroxide concentration ranging from 0.5 - 6.0 g/Litre. Experimental measurements in the form of sets of light absorption coefficient and time data at each peroxide level were used to find the best values for the first order rate constants k_1, k_2 and k_3 in the equilibrium model as shown in Equation (3.4). The fitting method has been discussed previously in chapter 3.

During the fitting of equilibrium model equation into the experimental results, it was found that two extremes for the value of initial leucochromophore concentration (C_{L_0}) could be used. An initial leucochromophore concentration of zero ($C_{L_0} = 0$) was used to represent conditions where any leucochromophoric species are not considered to be present in the original unbleached pulp. In this case, the leucochromophores are formed as a result of the reaction between alkaline peroxide and chromophoric species C (Figure 4.18). Values of sum of squares of the residuals (SS_R) for the fittings when $C_{L_0} = 0$ are shown in Table 5.1.

Table 5.1 Fitting results for equilibrium kinetic model for $C_{L_0} = 0$

H_2O_2 (g/L)	HO_2^- (M)	k_1 (min^{-1})	k_2 (min^{-1})	k_3 (min^{-1})	Sum of Squares of Residual (SS_R)
0.5	1.30E-03	1.07E-02	1.11E-02	7.77E-09	5.86E-02
1.0	2.59E-03	2.07E-02	2.88E-02	3.15E-03	9.94E-02
2.0	5.19E-03	2.45E-02	2.71E-02	4.08E-03	1.15E-01
4.0	1.04E-02	5.22E-02	4.04E-02	5.42E-03	8.00E-02
5.0	1.30E-02	6.83E-02	4.19E-02	6.09E-03	5.85E-02
6.0	1.56E-02	6.94E-02	4.13E-02	6.83E-03	1.58E-01

Figure 5.1 shows the best fit curves generated using the parameters listed in Table 5.1.

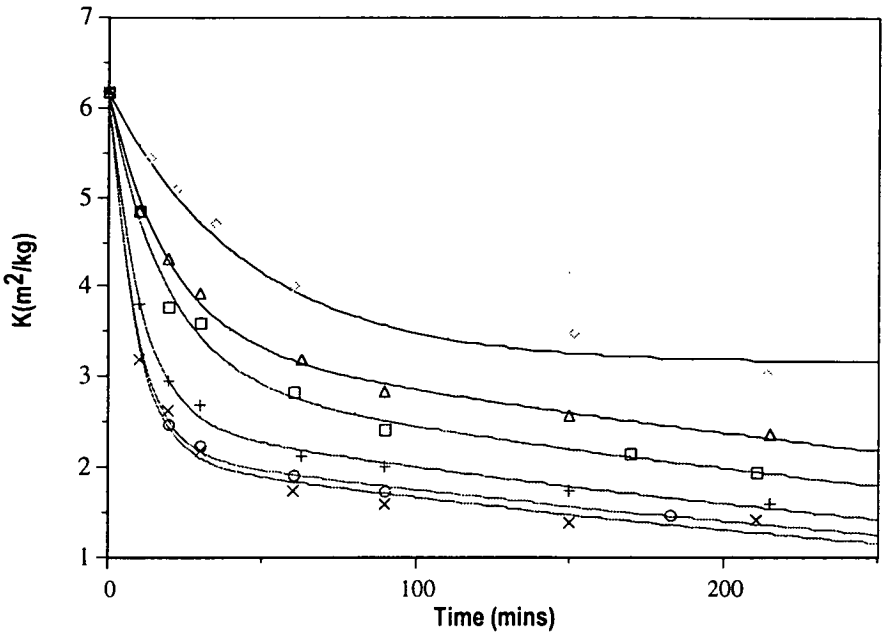

Figure 5.1 Equilibrium model best fit curves when C_{L_0} = 0 m²/kg for constant conditions bleaching of *Pinus radiata* TMP at 50°C, 0.3% consistency and pH 11.0.
Hydrogen peroxide charge:
◇ = 0.5 g/L, △ = 1 g/L, □ = 2 g/L, + = 4 g/L, ○ = 5 g/L, × = 6 g/L.
Lines are computer generated and points are experimentally obtained.

Very high initial leucochromophore values (e.g. C_{L_0} = 400 m²/kg) were also used based on the idea that the potential chromophores (leucochromophores) are part of the bulk lignin structure and hence exist in reasonably high concentrations. The value of 400 was selected arbitrarily to represent a much higher value compared to the initial chromophore C concentration as measured by the light absorption coefficient (C_0 ~ 6). The computer fitting results for the case where C_{L_0} = 400 m²/kg are listed in Table 5.2 and are plotted in Figure 5.2.

Table 5.2 Fitting results for equilibrium kinetic model for C_{L0} = 400 m²/kg

H_2O_2 (g/L)	HO_2^- (M)	k_1 (min^{-1})	k_2 (min^{-1})	k_3 (min^{-1})	Sum of Squares of Residual (SS_R)
0.5	1.30E-03	2.07E-10	1.84E-04	2.27E-02	5.86E-02
1.0	2.59E-03	4.96E-08	2.35E-04	3.58E-02	1.77E-01
2.0	5.19E-03	2.70E-07	2.18E-04	3.89E-02	1.96E-01
4.0	1.04E-02	1.23E-07	3.64E-04	7.35E-02	2.01E-01
5.0	1.30E-02	1.17E-06	3.89E-04	8.69E-02	1.68E-01
6.0	1.56E-02	3.60E-07	3.75E-04	9.00E-02	2.30E-01

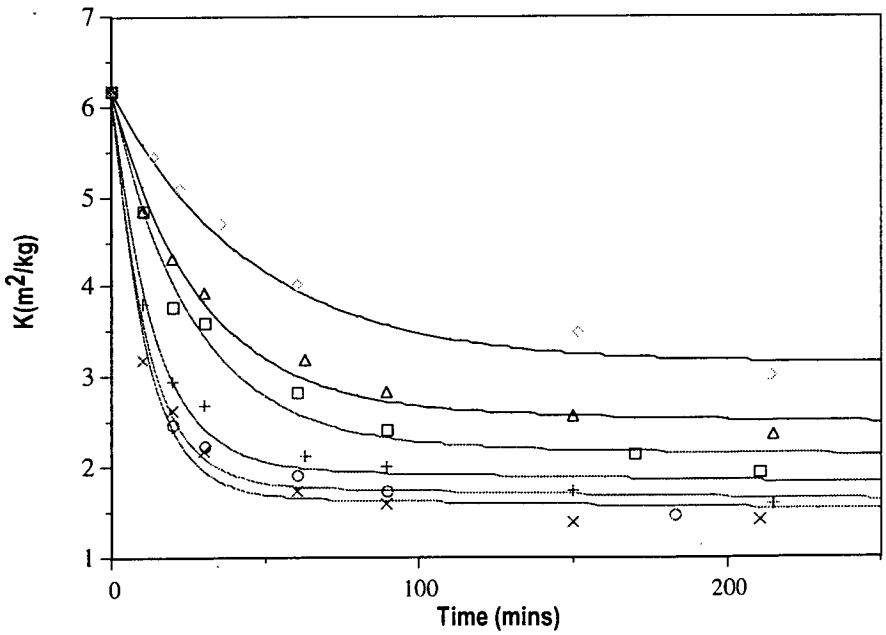

Figure 5.2 Equilibrium model best fit curves when C_{L0} = 400 m²/kg for constant conditions bleaching of *Pinus radiata* TMP at 50°C, 0.3% consistency and pH 11.0.
Hydrogen peroxide charge:
◇ = 0.5 g/L, △ = 1 g/L, □ = 2 g/L, + = 4 g/L, ○ = 5 g/L, × = 6 g/L.
Lines are computer generated and points are experimentally obtained.

Tables 5.1 and 5.2 show that the adequacy of fitting for the two cases are very similar as judged by the values of SS_R. This implies that, from a mathematical standpoint, we cannot easily distinguish between situations where the initial concentrations of structural units which can potentially be converted into chromophores are either zero or very high in comparison to the initial chromophore concentration (~6 in this case). However, further inspection of the magnitude of the SS_R in Table 5.1 and Table 5.2 shows that the fitting for the case when $C_{L_0} = 0$ is consistently better. Setting up the computer fitting program to allow the value of C_{L_0} to be varied revealed that a slightly better fitting was obtained when C_{L_0} approached zero.

5.2.2 Testing of Model Response

The validity of the proposed equilibrium model was also tested by conducting experiments in which the concentration of peroxide was changed from one level to another during the course of bleaching. Figure 5.3 shows the effect of changing the concentration of peroxide at pH 11.0 from 0.5g/L to 5g/L after 105 minutes bleaching, then maintaining the concentration at the higher level.

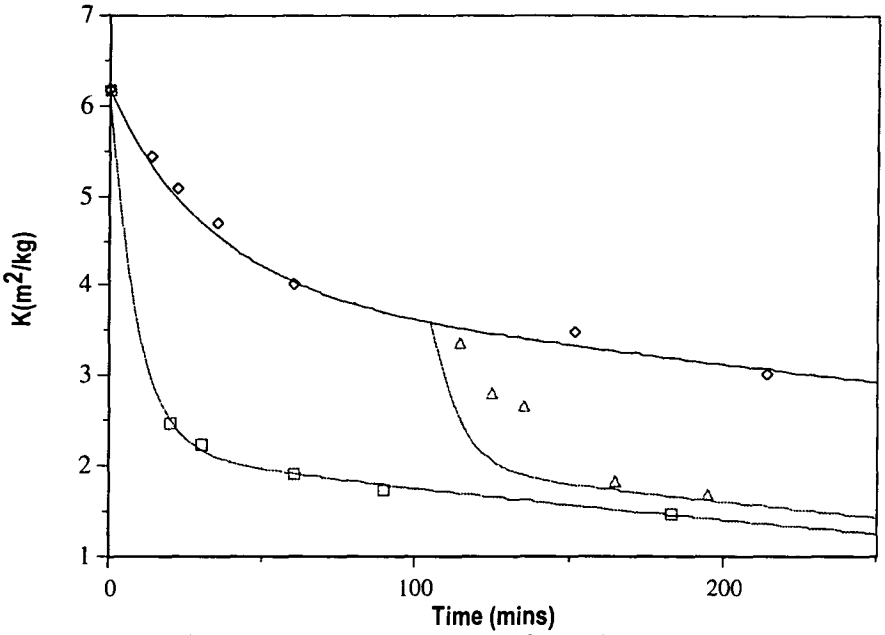

Figure 5.3 Effect of increasing the concentration of peroxide during constant condition bleaching of *Pinus radiata* TMP at 50°C, 0.3% consistency and pH 11.
Hydrogen peroxide charge:
◇ = 0.5 g/L, □ = 5 g/L, △ = 0.5 g/L for 105 minutes then 5 g/L
Solid lines are the computer predicted paths.

It is apparent that there is a transition in the course of the K-time relationship, moving from the 0.5g/L level towards the 5g/L level. The course of this transition was then compared with a calculated path which has been computed using the equilibrium model by changing the values of the rate constants to correspond to the 5g/L level after the appropriate time. It can be seen that there is a reasonable correspondence between the observed result and predicted course of the bleaching process.

Interestingly, computer simulation of the equilibrium model also predicts that darkening of the pulp should occur if the peroxide concentration is reduced at constant pH. This was more difficult to test experimentally as the peroxide concentration cannot be instantaneously reduced without

other concurrent changes in the system. An investigation in which peroxide levels were reduced was carried out by bleaching a pulp at a constant peroxide level of 5g/L and pH 11.0 for 90 minutes then isolating the pulp by filtration, followed by washing. Subsequently the pulp was introduced into a liquor at pH 11.0 at 0.5g/L peroxide. The result of this treatment is shown in Figure 5.4 together with the predicted response.

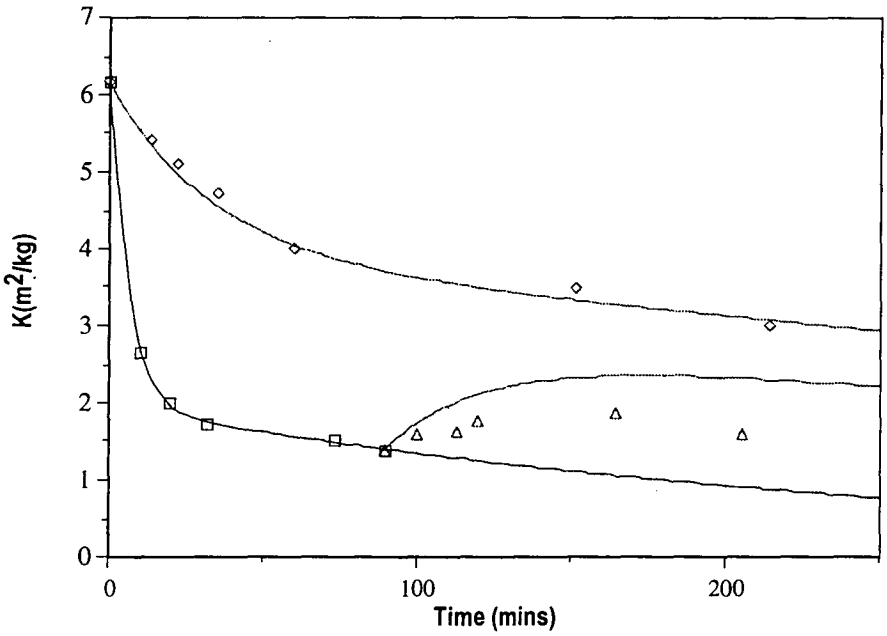

Figure 5.4 Effect of decreasing the concentration of peroxide during constant condition bleaching of *Pinus radiata* TMP at 50°C, 0.3% consistency and pH 11.
Hydrogen peroxide charge:
◇ = 0.5 g/L, □ = 5 g/L, △ = 5 g/L for 90 minutes then 0.5 g/L
Solid lines are the computer predicted paths.

It is clear from Figure 5.4 that the pulp did indeed undergo darkening and the absorption coefficient increased towards the level representing bleaching under constant conditions of 0.5g/L peroxide and pH 11.0, although it is somewhat lower than the predicted response. In the next

section, the possible chemical processes which may be responsible for brightening and darkening of pulps as described by the equilibrium model will be discussed.

5.3 Chemical Significance of The Equilibrium Model for Peroxide Bleaching

It is well known that peroxide-bleached mechanical pulp can undergo darkening in the presence of alkali[1]. The phenomenon of alkali darkening can occur during industrial bleaching if hydrogen peroxide decomposition is excessive, resulting in low levels of residual peroxide. However it has also been demonstrated that darkening of the pulp can occur when bleached pulps are introduced into liquors containing alkaline hydrogen peroxide[2], even using concentration levels comparable to conventional bleaching conditions. This has been observed particularly when peroxide decomposition is induced by addition of transition metal ions, such as manganese or copper. Kutney[2] has shown that significant reversion of a bleached groundwood pulp occurred during peroxide decomposition induced by manganese addition, even though most of the peroxide was still present. These experiments suggested that it may be products from the decomposition of hydrogen peroxide, particularly radical species such as the hydroxyl radical, $OH^{\cdot}$, which can give rise to chromophore formation during alkaline peroxide bleaching. Attention has recently been focused on the role of radical

species during peroxide bleaching processes[3-5], although it is not yet clear under what circumstances the net effect of radicals is either beneficial or detrimental to brightness development. Studies with model compounds have also shown that formation of a coloured species can be promoted by the presence of metal ions in alkaline peroxide systems [6].

The phenomenon of brightness reversion of bleached mechanical pulps when exposed to light is well known and has recently been reviewed by Heitner and Schmidt[7]. The participation of free radical species have also been implicated in these photochemical processes. Studies have shown that it is possible to reversibly darken and bleach mechanical pulp by application of radiation of specific wavelengths in the UV and visible region respectively[8]. Recent investigations with diffuse reflectance spectroscopy[9, 10] show that specific absorption bands removed by peroxide bleaching can be restored on exposure to light, which implies a reversibility of these chemical processes.

Such a reversibility of chemical processes whereby chromophores are converted to leucochromophores and vice versa can be described in the context of the proposed equilibrium model. As has already been shown, an adequate fitting can be obtained on the assumption that the initial concentration of leucochromophores in the pulp is either very small or very large in comparison with the concentration of chromophores. We can consider the implications of both situations in turn. It is known that there are several types of chemical structures which can be identified

with chromophores susceptible to removal with alkaline hydrogen peroxide. The two most common chromophore types are α,β-unsaturated carbonyls and *o*- or *p*- quinones[11, 12]. Components which form stilbenes, condensation products, and alpha-hydroxyl components which are oxidised to carbonyl structures have characteristics required to become leucochromophoric structure, nevertheless, there is only a limited number of literature references which provide descriptions of its nature.

5.4 Explanation of Reaction Mechanisms When $C_{L_0} = 0$

This model requires that the chromophoric species C reacts rapidly and reversibly to produce a structural unit C_L. The chemical structure of C_L must be closely related to that of C for this to occur. If the formation of C_L is accompanied by extensive fragmentation, particularly involving the C_9 lignin monomeric unit, it is difficult to see how C could readily be reformed. Model compound studies with both α,β–unsaturated carbonyl compounds and quinones have been reported. In both cases, the proposed mechanisms[13, 14] involve addition of oxygen to the conjugated carbonyl structure, to give an epoxide prior to further reaction involving fragmentation leading ultimately to carboxylic acids (Figure 5.5).

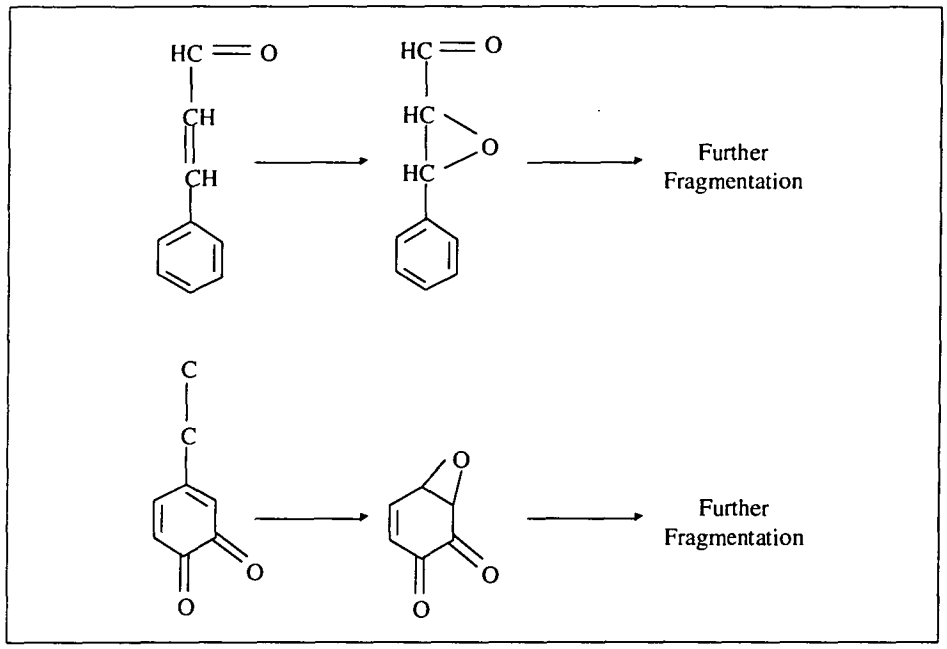

Figure 5.5 Reactions of chromophore in alkaline hydrogen peroxide leading to epoxide structures.[13, 14]

It is conceivable that the reaction process to produce the epoxide is reversible, as the structural integrity of the carbon skeleton is maintained. However, further reaction processes involve rupture of C-C bonds and cannot be conceived to be easily reversible. If epoxide structures were to be identified with C_L, it would be necessary for the epoxide to be a stable intermediate with subsequent reaction to oxidised fragments occurring much more slowly. Extensive studies of relative rates of formation of epoxides and further oxidation products have not been reported. However, it has been reported that the epoxide is relatively stable, and has been isolated in some cases[13].

Correlation of C_L with epoxide structures would also necessitate proposing a mechanism whereby the original chromophore can be easily regenerated to give C in the presence of alkaline peroxide. As already discussed, an involvement of free radical species might be postulated although no evidence in the literature for conversion of an epoxide to give conjugated carbonyl structures could be found.

Figure 5.6 shows the calculated concentration - time profiles for C, C_L and C_P corresponding to a constant peroxide concentration of 2.0 g/L. This shows the initial rapid conversion of chromophores (C) to leucochromophoric species C_L, with a slower conversion to the final product C_P. Figure 5.7 shows the dependence of the three rate constants k_1, k_2 and k_3 on the calculated concentrations of perhydroxyl anion HO_2^-. Rate constants k_1 and k_2 are an order of magnitude larger than k_3. For practical purposes the levelling off of the brightness (or for that matter, light absorption coefficient) is essentially controlled by the position of the equilibrium between C and C_L (i.e. the rate constants k_1 and k_2). None of the rate constants are directly proportional to the concentration of the active bleaching species (HO_2^-), and this indicates that the steps involved in the bleaching mechanism cannot be elementary reaction processes (i.e. they would involve more than one step).

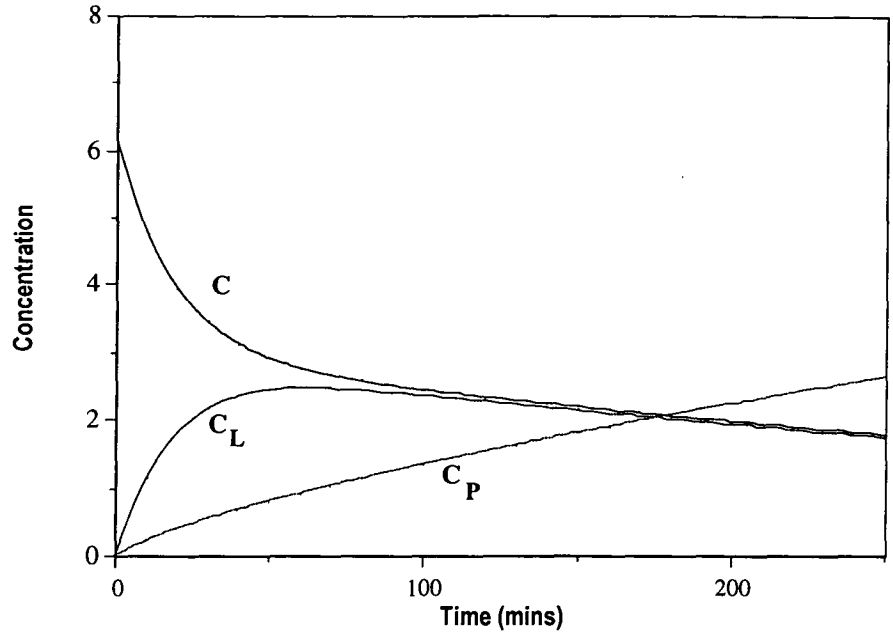

Figure 5.6 Calculated concentration profiles for C, C_L and C_P for the case when C_{L0} = 0 m²/kg.

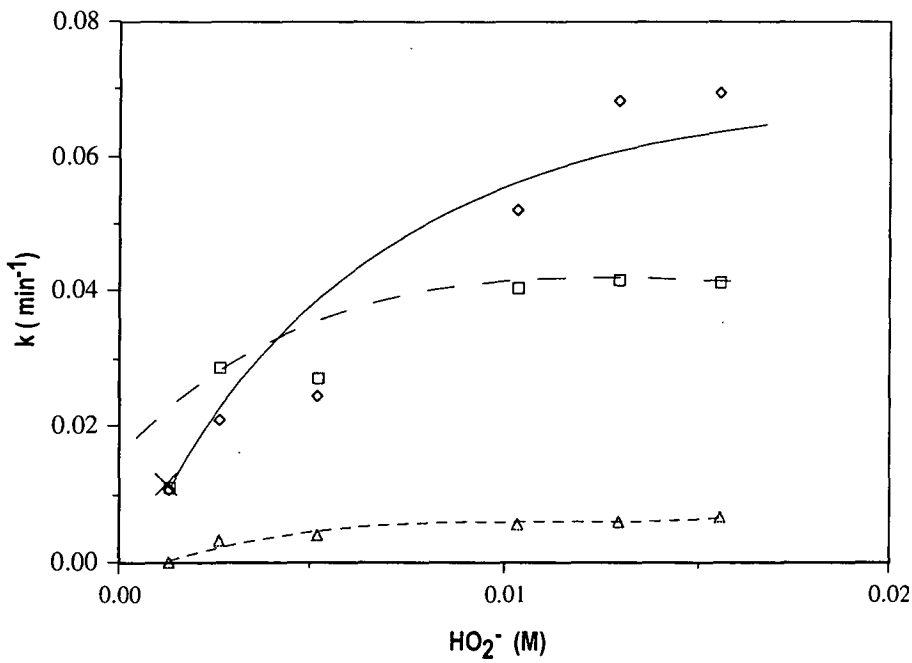

Figure 5.7 Dependence of rate constant k_1, k_2 and k_3 on the concentration of perhydroxyl anion (HO_2^-) for the case when C_{L0} = 0 m²/kg. ◇ = k_1 , □ = k_2 , △ = k_3

5.5 Explanation of Reaction Mechanisms When $C_{L_0} = 400$

This model assumes that the initial concentration of leucochromophoric species is very high compared to that of the chromophores present. The value of 400 used in this fitting procedure was selected arbitrarily, since it was shown that any value such that $C_{L_0} >> C_0$ will produce a satisfactory fitting. The main implication of this condition is that the concentration of leucochromophores (C_L) remains almost constant throughout the course of the bleaching process. In fact, the result is that the rate of chromophore creation can be regarded as almost constant such that Equation (3.1) and Equation (3.2) can be rewritten as

$$-\frac{dC}{dt} = k_1 C - k_2' + k_3 C \qquad (5.1)$$

$$-\frac{dC_L}{dt} = k_2' - k_1 C \qquad (5.2)$$

Under this condition k_2' represents a pseudo-zero order reaction. In chemical terms, this would suggest that chromophores can possibly be created at a constant rate from a large pool of potential sites (or leucochromophores) embedded in the lignin structure. The simplest explanation would be to suggest that, in fact the lignin structure itself is an almost infinite source of chromophores. In comparison, the total number of chromophoric structures (C), both conjugated carbonyl and

quinones, has been found to make up only about 6% of the total C_9 lignin units [12].

Interestingly, setting the value of C_L to a high initial value resulted in two possible mathematical solutions, which had similar adequacy of fitting as judged by the sum of squares of residuals. The behaviour of the system corresponding to concentration of C, C_L and C_P with time for both condition is shown in Figure 5.8. In both situations, the lignin structure (or leucochromophores) is the major source of material eventually converted to the final product C_P, rather than the chromophores C initially present in the pulp. However the two solutions differ in the relative magnitude of rate constants. For the first solution the $k_1 << k_2 < k_3$. This showed that the equilibrium step could be replaced by an irreversible step, resulting in the mechanism

$$C_L \xrightarrow{k_2} C \xrightarrow{k_3} C_P$$

representing the overall process. For the second solution, the equilibrium process dominated the overall behaviour, with a slower irreversible step controlled by the rate constant k_3.

It is also interesting to note that, with appropriate parameters, a three component consecutive model such as shown in the previous paragraph will also fit the observed experimental data. Assuming that $k_2 = k'[HO^-] + k''[HOO^-]$ and given that this equation would have a negative effect on brightness at high pH and competing reactions in peroxide anion

concentration, it may address the balance between bleaching and yellowing reactions and the problems with the two chromophore model. For $C > C_L$ this would produce the desired change in the brightness. The conversion of leucochromophore to chromophores would lead to the observed high order in chromophores as described in Equation (4.4). Also such a model would predict results shown in Figure 5.4 when peroxide is added after most of the initial concentration of chromophores has been depleted. The weakness of this model is of course the complete conversion of both C_L and C into C_P at a very long bleaching time which disagrees with the observation of the existence of various levels of brightness at which the bleaching seems to have been completed depending on the peroxide concentration.

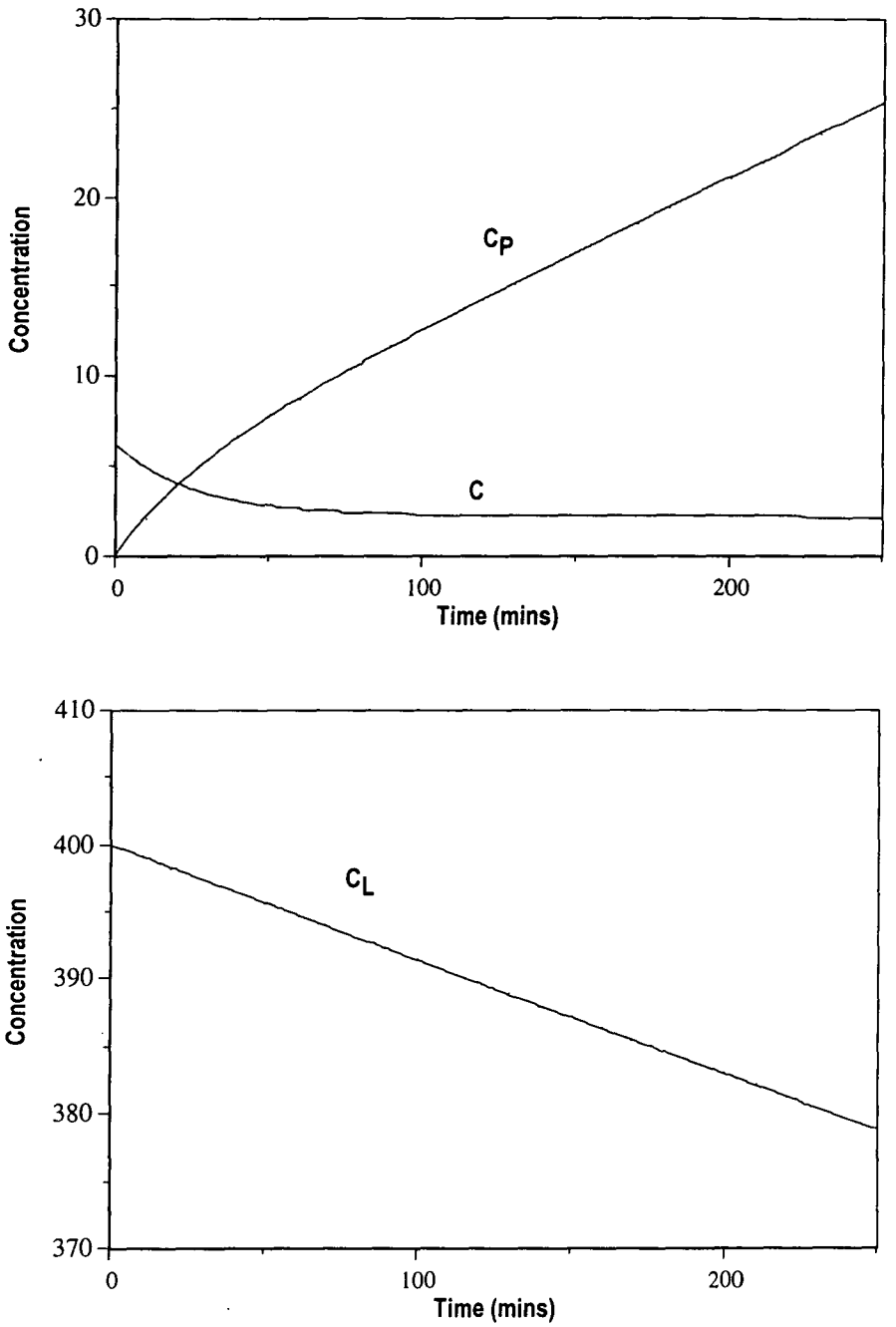

Figure 5.8 Calculated concentration profiles for C, C_L and C_P for the case when C_{L_0} = 400 m²/kg.

5.6 Conclusions

Two equilibrium kinetic models for alkaline peroxide bleaching of *Pinus radiata* thermomechanical pulp were investigated and were found to adequately duplicate experimental observations. The models can also account for observed changes in chromophore content when the peroxide concentration is changed to either higher or lower constant levels.

The models allow for the concurrent formation and removal of chromophores in the presence of alkaline peroxide and can account for darkening reactions which are observed when the peroxide concentration is reduced.

Consideration of the available chemical evidence suggests that the leucochromophores can be considered as specific chemical structures which can be reversibly interconverted between chromophores and leucochromophores.

5.7 References

1. Kutney, G. W. and Evans, T. D., *Svensk Papperstidning* 88 (6) :R78 (1985).

2. Kutney, G. W. and Evans, T. D., *Svensk Papperstidning* 88 (9) :R84 (1985).

3. Reitberger, T., Gierer, J., Jansbo, K., Yang, E. and Yoon, B. H., *6th Int. Symp. Wood and Pulp. Chem.*, 1 :93 (1991).

4. Sjögren, B., Reitberger, T. and Zachrison, H., *5th Int. Symp. Wood and Pulp. Chem.*, 161 (1989).

5. Reitberger, T., *Holzforschung* 42 (6) :351 (1988).

6. Pero, R. W. and Dence, C. W., *J. Pulp Paper Sci.* 12 (6) :J192 (1986).

7. Heitner, C. and Schmidt, J. A., *Int. Symp. Wood Pulp. Chem.*, 1 :131 (1991).

8. Forsskahl, I. and Janson, J., *Int. Symp. Wood Pulp. Chem.*, 255 (1991).

9. Michell, A. J., Chin, C. W. J. and Nelson, P. J., *Appita* 44 (5) :333 (1991).

10. Michell, A. J., Nelson, P. J. and Chin, C. W. J., *Appita* 42 (6) :443 (1989).

11. Holah, D. G. and Heitner, C., *Tappi Int. Mech. Pulp. Conf. Proceedings* 177 (1992).

12. Lebo, S., Lonsky, W., McDonough, T., Medvecz, P. and Dimmel, D., *J. Pulp Paper Sci.* 16 (5) :J139 (1990).

13. Gellerstedt, G. and Agnemo, R., *Acta Chem. Scand.* B34 (4) :275 (1980).

14. Gellerstedt, G., Hardell, H. L. and Lindfors, E. L., *Acta Chem. Scand.* B34 (9) :669 (1980).

CHAPTER 6

Molecular Orbital Calculations

Improvements in kinetic models for alkaline peroxide bleaching of *Pinus radiata* TMP have been investigated in the preceding chapters. To further refine the understanding of the reaction of chromophoric groups in lignin, a theoretical study has been undertaken.

There are three main chromophoric groups in the lignin polymer (with the most commonly used model chromophores as shown in Figure 6.1) which account for the value of light absorption coefficient at 457 nm.

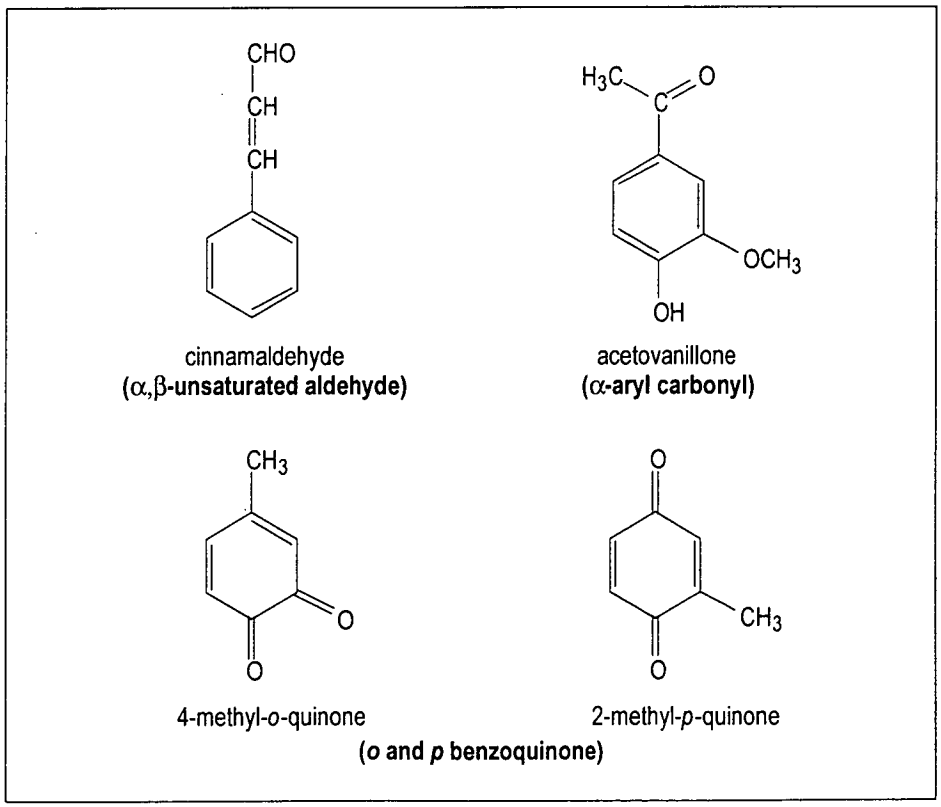

Figure 6.1 Examples of chromophoric structures thought to be present in lignin.

The α,β-unsaturated aldehydes are thought to account for a significant proportion of the colour of lignin[1]. Many studies have been carried out on the reaction mechanisms between this chromophoric group and alkaline peroxide resulting in several descriptions on the mechanism of the reactions. One of the proposed mechanisms involves the formation of an epoxide intermediate[2]. The formation of this epoxide intermediate has been confirmed experimentally[3].

With the ready availability of computational methods in the investigation of reaction mechanism, it is of great interest to perform a comparison between the suggested mechanisms for the reaction between alkaline peroxide and α,β-unsaturated aldehydes to those obtained computationally.

In this chapter, evidence of the existence of α,β-unsaturated aldehydes and their importance in relation to the colour of pulp will be discussed. The study of possible reaction pathways of the epoxidation of cinnamaldehyde with alkaline peroxide by means of *ab initio* and semi-empirical molecular orbital theory will then be reported.

6.1 Literature Review

Studies on the topic of α,β-unsaturated aldehydes and the reaction mechanism during alkaline peroxide bleaching that have been carried out in the past have been primarily undertaken either *in situ* or by means of model lignin chromophores. Numerous reviews exist discussing the relationship amongst α,β-unsaturated aldehydes, lignins and mechanical pulps. Studies such as the assessment of the numbers and types of α,β-unsaturated aldehydes, their formation in lignin and their reactions with various pulping as well as spectroscopic properties have been well reviewed in the past[4-7] and no attempt has been made here to provide an exhaustive review of the available literature. Rather, the current review is confined to relatively recent studies in which the roles of α,β-unsaturated aldehydes during peroxide bleaching are examined. Several studies on the applications of computational methods in the study of wood chemistry will also be discussed.

6.1.1 Existence of α,β-Unsaturated Aldehydes in Lignin

It is generally believed that α,β-unsaturated carbonyls are present naturally in native lignin. A study of the constituents of softwood lignin by means of hydrolysis[8], acidolysis[9], acetolysis[10] and solvolysis[11] found that lignins contain α,β-unsaturated aldehydes such as coniferaldehyde (3-hydroxy-4-methoxy-cinnamaldehyde) and coniferaldehyde methyl ether (3,4-dimethoxy-cinnamaldehyde) as shown

in Figure 6.2. The existence of these structures have also been confirmed with a more direct approach using spectroscopic methods (UV-visible, infra-red and ^{13}C-nmr).

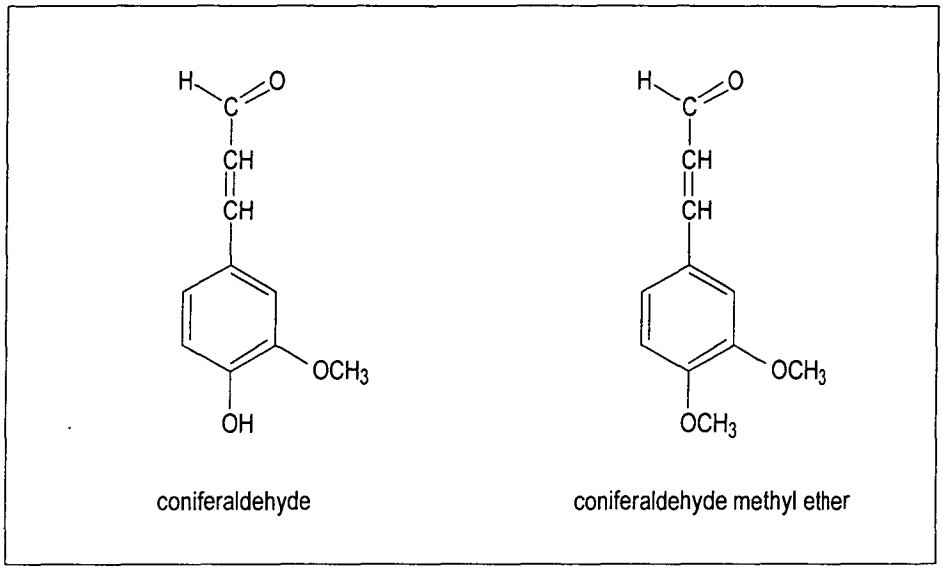

Figure 6.2 α,β-Unsaturated aldehyde structures in softwood lignins.

Under a UV-visible spectrometer, mechanical pulps display a peak at about 300 nm with a pronounced shoulder occurring around 400 nm[12-14] which is consistent with the feature of the presence of α,β-unsaturated aldehydes.

In 1961, in a study based on the behaviour of model lignin compounds, Marton[15] proposed that α,β-unsaturated aldehydes were partly responsible for the absorption of light by spruce lignin in the region above 300 nm. This work was later extended by Pew and Connors to

include an investigation on the effects of aromatic substituents on light absorption characteristics[16]. From this study, they found that α,β-unsaturated aldehydes in hardwoods absorbed more visible light than in softwoods and their removal from mechanical pulp resulted in a net reduction in absorption at around 350 nm.

Observations under infra-red spectroscopy by Polcin and Rapson[12] have shown that α,β-unsaturated aldehydes are partly responsible for the signal at 1670 cm^{-1}, which is in the area of characteristic bands in the region of 1650-1670 cm^{-1} attributed to carbonyl stretch[12-14, 17, 18]. Infra-red studies employing second derivative spectra have also indicated the presence of α,β-unsaturated aldehyde groups in *Eucalyptus regnans* cold soda pulps[14]. A recent application of pyrolysis-gas chromatography-photo ionisation-mass spectroscopy (Py-GC-MS) on beech milled wood lignin showed the presence of small but significant amounts of guaiacyl and syringyl α,β-unsaturated aldehydes in lignin[19].

Although evidence of the presence of α,β-unsaturated aldehydes in native lignin is widespread, the origin of these structures is still not well understood. Several processes are generally believed to cause their formation. For example enzymatic reduction of hydroxycinnamic acid produced during lignification has been shown to produce the corresponding α,β-unsaturated aldehydes and alcohols[20]. It has also been reported that enzymatic dehydrogenation of coniferyl alcohol structures in lignin produces coniferaldehyde structures[21].

6.1.2 Amount of α,β-Unsaturated Aldehydes in Lignin

The most common techniques for measuring the amount of α,β-unsaturated aldehydes in lignin are by means of chemical derivatisation and/or application of colouring agents followed by spectrophotometric measurement. Only a short summary of these techniques will be presented here.

Adler and Ellmer[8], using a *p*-aminobenzoic acid (phloroglucinol) colour test estimated the content of coniferaldehyde structures in spruce wood lignin to be about 2 to 2.5 for every 100 phenylpropane units. Later, catalytic hydrogenation was employed to rapidly and selectively reduce ethylenic and carbonyl functionalities, including coniferaldehyde structures in spruce milled wood lignin[15]. UV-visible difference spectra was then carried out which showed a decrease in the absorbance above 300 nm. From this investigation, it was estimated that the spruce milled wood lignin contains approximately 3 etherified coniferaldehyde structures and less than 1 phenolic coniferaldehyde unit per 100 phenylpropane units.

A direct method for the measurement of the content of α,β-unsaturated aldehydes was developed for Japanese red pine milled groundwood by Hirashima and Sumimoto[22] in 1987. In this method, the absorbance of the groundwood sheets was measured after application of the phloroglucinol - HCl colour reagent developed earlier by Adler.

Calibration curves prepared by impregnation of lignin free sheets with coniferaldehyde and coniferaldehyde methyl ether were used to calculate the content of α,β-unsaturated aldehydes obtained from the absorbance of the coloured sheets. From this study, they reported approximately 1.1 to 1.5 coniferaldehyde units and 1.4 to 3.0 coniferaldehyde methyl ether units for every 100 phenylpropane units.

6.1.3 Effects of Alkaline Peroxide on α,β-Unsaturated Aldehydes

Most of the studies on the topic of the effect of alkaline peroxide on α,β-unsaturated aldehydes indicated their ready destruction. In a series of studies carried out on black spruce and balsam fir using a colour test employing phloroglucinol and resorcinol, it was found that α,β-unsaturated carbonyls are responsible for a large part of the absorption of visible light[23]. Application of alkaline peroxide to the pulp showed the absence of colour in the phloroglucinol and resorcinol test, indicating that peroxide bleaching completely removed α,β-unsaturated aldehydes from black spruce and balsam fir lignins.

Holmbolm and co-workers[24] employed ^{13}C-nmr techniques and also observed the removal of α,β-unsaturated aldehyde groups from mechanical pulp lignins during alkaline peroxide bleaching. Based on their experiments on spruce milled wood lignin, alkaline peroxide bleaching was reported to have completely removed a small signal at 196 ppm corresponding to the aldehyde carbon in α,β-unsaturated carbonyls.

The application of photoacoustic Fourier transform infra-red spectroscopy (FTIR-PAS) on the study of the alkaline peroxide bleaching of black spruce showed the loss in peak intensity at 1650 cm^{-1} attributed to the removal of conjugated carbonyl structures including α,β-unsaturated aldehydes[18]. Further observations on the removal of α,β-unsaturated aldehydes were reported from studies on oxidative-reductive processes of softwood mechanical pulps using UV-visible and infra-red[13], and bleaching of stone groundwood, TMP and CTMP employing ISO brightness and tristimulus L*, a* and b* measurements[25].

6.1.4 Reaction Mechanisms of α,β-Unsaturated Aldehydes with Alkaline Peroxide

Despite the numerous studies dealing with the reaction of α,β-unsaturated aldehydes and alkaline peroxide, there are contradictions concerning the mechanism. This is not surprising considering the complexity of lignin and the relatively minor occurrence of chromophores within it. Nevertheless, removal of α,β-unsaturated aldehydes from lignin in mechanical pulps has been confirmed from both pulp/milled wood lignin and model lignin chromophore studies. Most of the information regarding reaction mechanisms was obtained from studies of model lignin chromophores, and only some of them will be described here.

The first study on this topic was carried out by Payne[26] who reported to have isolated epoxides of unsaturated aldehydes upon application of hydrogen peroxide under mild alkali conditions to α,β-unsaturated aldehydes. Payne suggested that the ethylene bond of α,β-unsaturated aldehydes underwent nucleophilic attack by perhydroxyl anion (HO_2^-) at the β-carbon in a Michael addition similar to that reported for other α,β-unsaturated systems. In 1965, Reeves[27] carried out a study of the reactions of lignin-related model compounds with alkaline peroxide and reported rapid conversion of cinnamaldehyde (an α,β-unsaturated aldehyde) to benzaldehyde. Cleavage of the side chain to form benzaldehyde was proposed to occur by two possible mechanisms involving either epoxide intermediates or direct loss of the side chain.

Another study on the reaction of α,β-unsaturated aldehydes, which was thought to involve nucleophilic attack of perhydroxy anions on the β-carbon of the ethylene bond, was reported by Gellerstedt and Agnemo[28]. In a later study of the epoxidation kinetics of α,β-unsaturated aldehydes and esters by Rao[29], cinnamaldehyde in methanol solution was observed to undergo a mechanism similar to those observed in previous studies[26,28] involving nucleophilic attack of perhydroxyl anion at the β-carbon, followed by ring closure and elimination of hydroxide ion. Under the reaction conditions employed (pH 12, 30^0C), the epoxide ring was observed to undergo further cleavage to yield benzaldehyde.

6.2 Introduction

Although it is generally accepted that cinnamaldehydes react readily with alkaline peroxide, information regarding the mechanisms which are currently available have been almost exclusively obtained experimentally. With the availability of theoretical tools and with the assumption that the macroscopic properties are ultimately governed by molecular structure, it is of considerable interest to examine the results using theoretical methods in order to enrich the current information.

As described above, it is generally believed that cinnamaldehyde (an α,β-unsaturated aldehyde) reacts with hydrogen peroxide via nucleophilic attack by the perhydroxy anion at the β-position[3, 26, 28, 29] and formation of epoxide intermediates[3, 27, 29-31] as shown in Figure 6.3. In this chapter, this reaction mechanism of the epoxidation of cinnamaldehyde has been further studied using semi-empirical and *ab initio* molecular orbital theory.

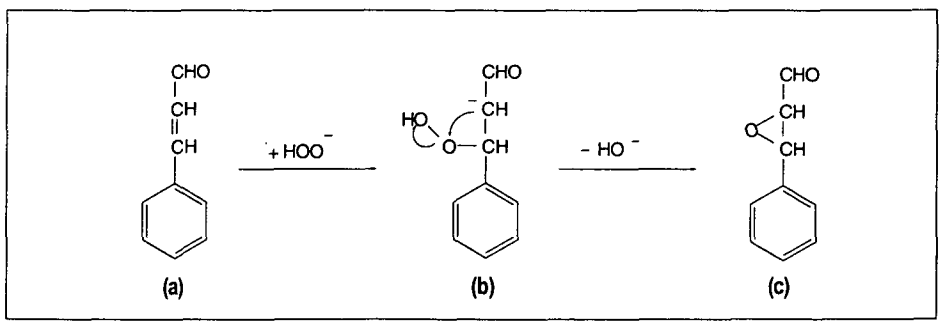

Figure 6.3 Mechanism for the formation of the epoxide of cinnamaldehyde[3].

6.3 Methods

Standard semi-empirical and *ab initio* molecular orbital calculations on the mechanism of epoxidation have been carried out with the MOPAC 93[32] and Gaussian 92[33] programs. The MNDO (modified neglect of diatomic overlap)[34] and PM3[35] hamiltonians have been used in the semi-empirical calculations. The *ab initio* calculations were carried out with the 6-31G(d) basis set[36] at the RHF and MP2 levels of theory. The core 1s electrons were frozen in the MP2 calculations.

Complete geometry optimisations of minima and transition structures were carried out at all levels of theory except MP2/6-31G(d) with the use of Baker's eigenvector following (EF) optimisation algorithm[37]. The MP2 calculations were performed on RHF geometries. The character of each stationary point has been determined by calculating vibrational frequencies at the appropriate level. The transition structures were 'followed downhill' to confirm that they connected with the appropriate minima.

In all calculations, the MNDO method which is the least sophisticated and the least in computation time was always performed first. The optimised structure obtained from the MNDO method was then used as a starting point for the PM3 method which in turn provided a starting point for the RHF calculation.

Wherever geometry of a structure is given, bond lengths are reported in angstroms. Both angles and dihedral angles are reported in degrees. This can be clearly described with a reference of Figure 6.4. The bond lengths and bond angles represent the interatomic separation between atoms I and J and angle between atoms IJK respectively. The dihedral angle is the angle between vectors IJ and KL, a positive value indicate that it is measured clockwise from I to L.

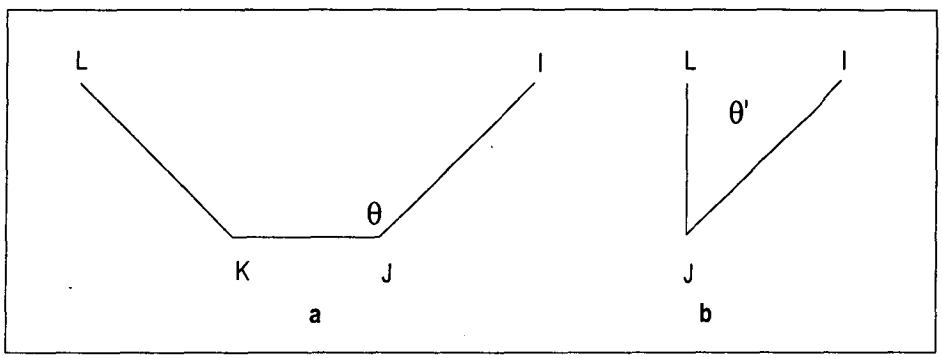

Figure 6.4 Illustration of geometric dimensions[38].
a) I-J is bond length, and θ represents the bond angle IJK.
b) View along the JK axis showing that the dihedral angle (θ') is the angle between vectors IJ and KL.

6.4 Results

The reaction of the formation of cinnamaldehyde epoxide that has been examined involves cinnamaldehyde (Figure 6.3 a) and its intermediate (Figure 6.3 b). Examination of possible reaction pathways was carried out by assessing the properties of both the ground state and the anionic intermediate of the cinnamaldehyde.

6.4.1 Cinnamaldehyde Ground State

Although the experimental study on the reactions taking place when cinnamaldehyde is oxidised by alkaline peroxide as reported by Wright and Abbot[3] was carried out on cinnamaldehyde with more than 99.5% abundance of the *trans* isomer, in this study the energy calculations have also, whenever relevant, been carried out for both the *trans* and *cis* isomers.

The atom numbering for the *trans* cinnamaldehyde structure which was used in the calculation is as shown in Figure 6.5. The geometries of the optimised *trans* cinnamaldehyde at PM3 level of theory are listed in Table 6.1 and shown in Figure 6.6. For the *cis* cinnamaldehyde, the atom numbering, the geometries and visual representation are given in Figure 6.7, Table 6.2 and Figure 6.8 respectively.

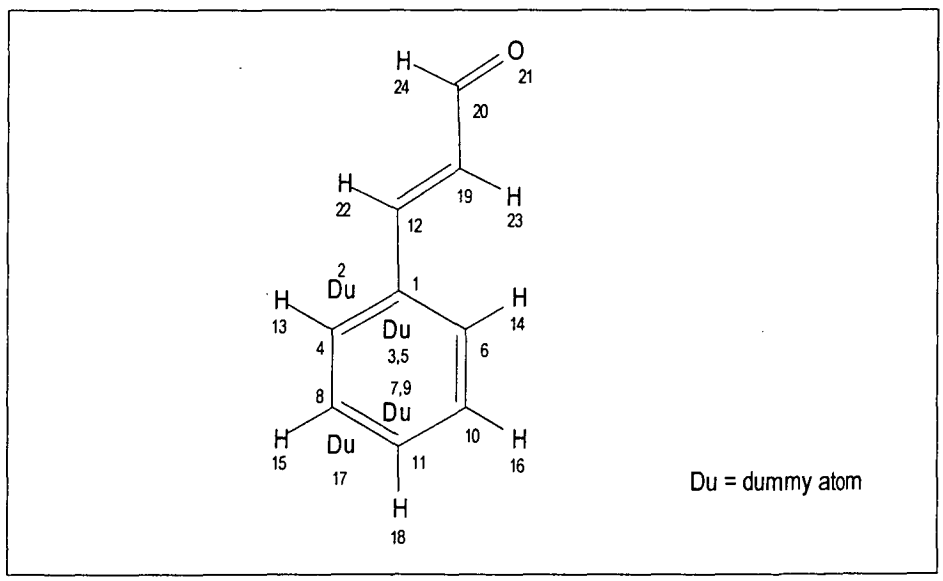

Figure 6.5 Atom numbering for *trans* cinnamaldehyde geometry in Table 6.1.

Table 6.1 Optimised geometry for *trans* cinnamaldehyde (at PM3).

Atom number I	Bond length (angstrom) IJ	Bond angle (degree) IJK	Dihedral angle (degree) IJKL	J	K	L
1	0.000	0.0	0.0	0	0	0
2 (Du)	1.000	0.0	0.0	1	0	0
3 (Du)	0.705	90.0	0.0	1	2	0
4	1.209	90.0	0.0	3	1	2
5 (Du)	0.707	90.0	0.0	1	2	4
6	1.207	90.0	180.0	5	1	2
7 (Du)	2.094	90.0	0.0	1	2	4
8	1.205	90.0	0.0	7	1	2
9 (Du)	2.096	90.0	0.0	1	2	4
10	1.205	90.0	-180.0	9	1	2
11	2.791	90.0	0.0	1	2	4
12	1.459	89.4	180.0	1	2	3
13	1.096	150.2	0.0	4	3	1
14	1.102	149.0	0.0	6	5	1
15	1.095	150.0	180.0	8	7	1
16	1.095	150.0	-180.0	10	9	1
17 (Du)	1.000	90.0	0.0	11	1	2
18	1.095	89.9	180.0	11	17	1
19	1.339	122.8	-179.9	12	1	4
20	1.477	121.5	180.0	19	12	1
21	1.211	122.4	-179.9	20	19	12
22	1.100	120.9	0.0	12	19	20
23	1.103	120.1	0.0	19	12	1
24	1.103	120.2	-180.0	20	21	19

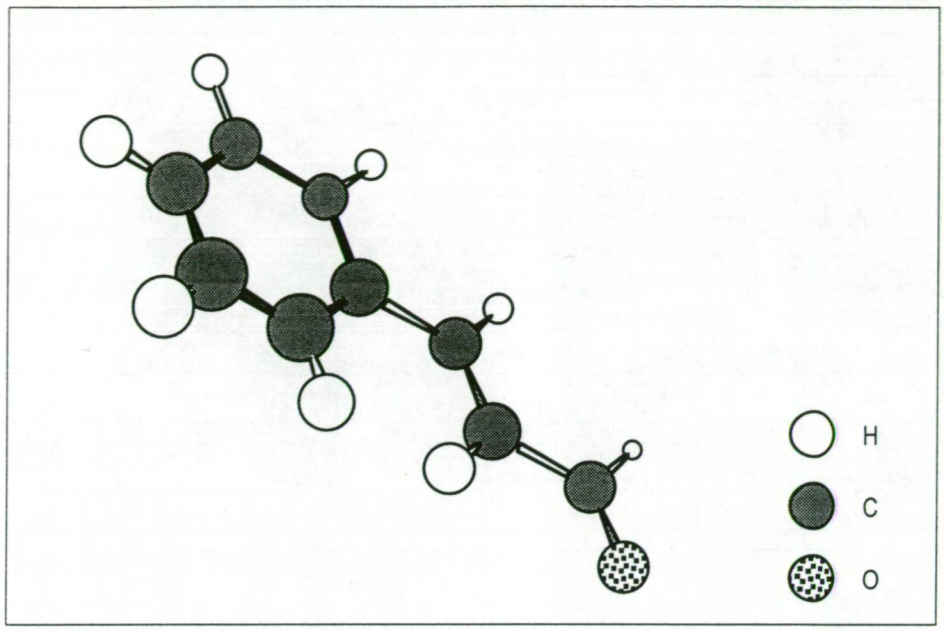

Figure 6.6 Optimised *trans* cinnamaldehyde (at PM3).

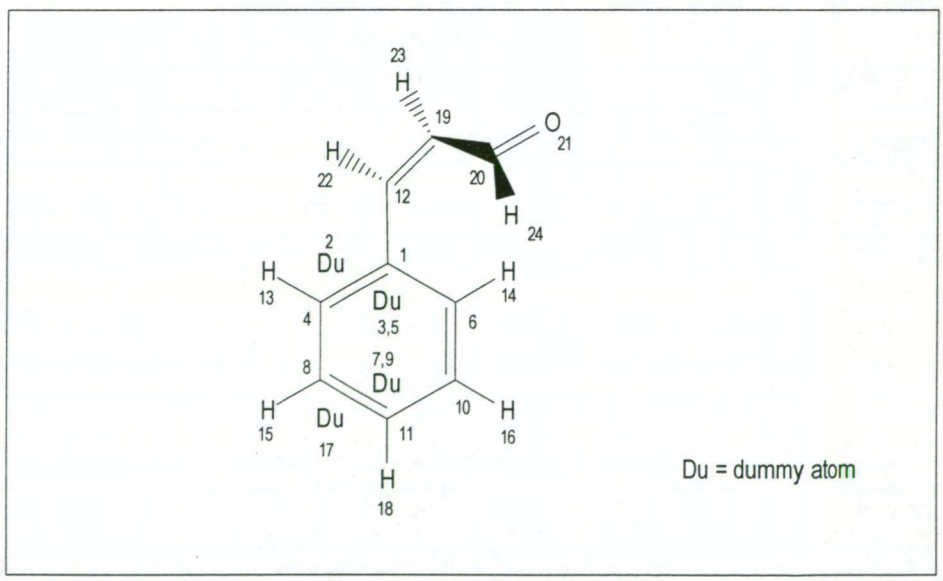

Figure 6.7 Atom numbering for *cis* cinnamaldehyde geometry in Table 6.2.

Table 6.2 Optimised geometry for *cis* cinnamaldehyde (at PM3).

Atom number I	Bond length (angstrom) IJ	Bond angle (degree) IJK	Dihedral angle (degree) IJKL	J	K	L
1	0.000	0.0	0.0	0	0	0
2 (Du)	1.000	0.0	0.0	1	0	0
3 (Du)	0.701	90.0	0.0	1	2	0
4	1.209	90.0	0.0	3	1	2
5 (Du)	0.700	90.0	0.0	1	2	4
6	1.208	90.0	180.0	5	1	2
7 (Du)	2.091	90.0	0.0	1	2	4
8	1.205	90.0	-0.6	7	1	2
9 (Du)	2.091	90.0	0.0	1	2	4
10	1.204	90.0	-179.8	9	1	2
11	2.787	90.0	-0.3	1	2	4
12	1.464	88.9	178.4	1	2	3
13	1.096	150.0	0.9	4	3	1
14	1.096	150.0	-1.1	6	5	1
15	1.095	150.0	179.6	8	7	1
16	1.095	150.0	-179.2	10	9	1
17 (Du)	1.000	90.0	0.0	11	1	2
18	1.095	90.0	179.9	11	17	1
19	1.336	125.6	121.2	12	1	4
20	1.480	123.8	-0.8	19	12	1
21	1.211	122.1	178.4	20	19	12
22	1.099	119.9	178.3	12	19	20
23	1.098	119.7	-180.0	19	12	1
24	1.103	120.4	180.0	20	21	19

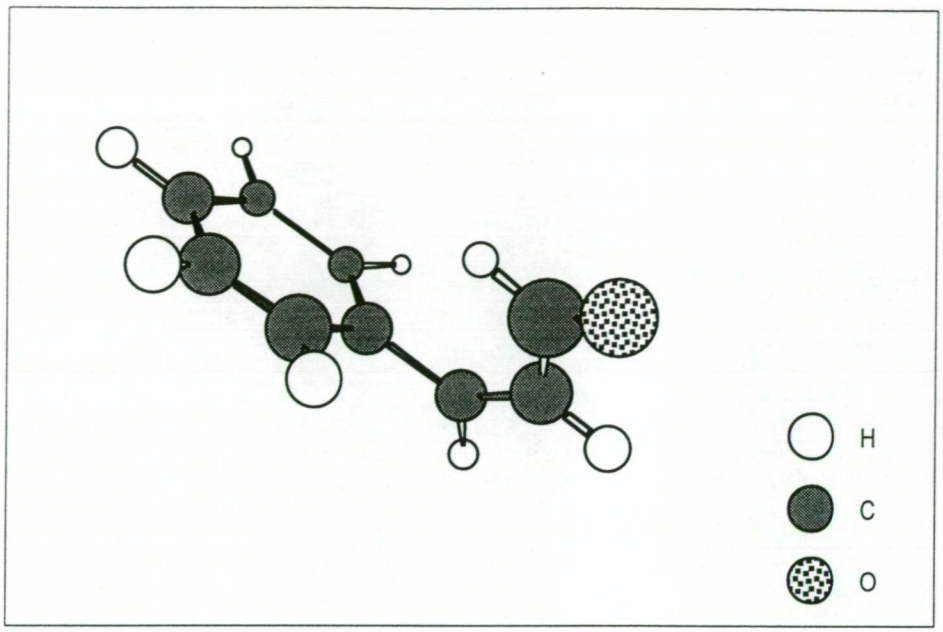

Figure 6.8 Optimised *cis* cinnamaldehyde (at PM3).

The absolute energies of the optimised *trans* and *cis* cinnamaldehyde at all levels of theory are given in Table 6.3.

Table 6.3 Optimised absolute energies of cinnamaldehyde

Methods	Units	*trans* cinnamaldehyde	*cis* cinnamaldehyde
MNDO	ev	-1584.7943	-1584.7647
PM3	ev	-1482.1884	-1482.0783
RHF/6-31G(d)	a.u.	-420.318233	-420.311654
MP2/6-31G(d)[a]	a.u.	-421.618579	-421.618166

[a] Single-point calculation on RHF/6-31G(d) optimised geometry

From Table 6.3, it can be concluded that computationally, the *trans* isomer is lower in energy and thus a more stable form of

cinnamaldehyde than the *cis* isomer. For this reason, the *trans* isomer was the focus in the rest of the calculations.

The optimised absolute energies of the perhydroxy anion (HOO^-), which is also part of the starting molecules in the reaction, are given in Table 6.4.

Table 6.4 Optimised absolute energies of perhydroxy anion (HOO^-)

Methods	Energies
MNDO	-655.8383 ev
PM3	-600.2245 ev
RHF/6-31G(d)	-150.125561 a.u.
MP2/6-31G(d)[a]	-150.486667 a.u.

[a] Single-point calculation on RHF/6-31G(d) optimised geometry

6.4.2 Positions of the Nucleophilic Attack

To predict the positions in cinnamaldehyde which are susceptible to the attack of the perhydroxy anion (HOO^-), a knowledge of charges at different carbon positions is required. To simplify the discussion, the atoms numbering has been modified to include only the atoms of interest (Figure 6.9). The selected atom charges calculated for the *trans* cinnamaldehyde at PM3 are shown in Table 6.5.

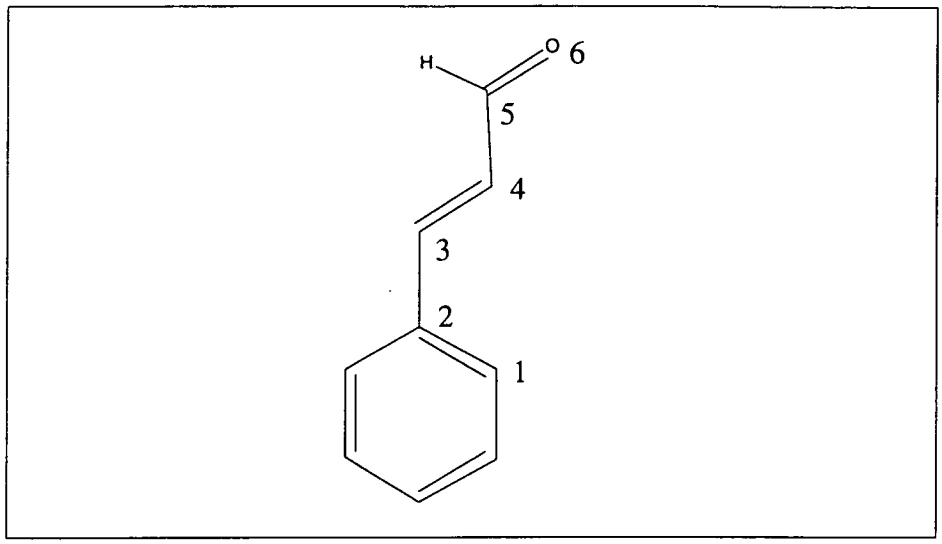

Figure 6.9 Numbering scheme for selected atomic charges data in Table 6.5.

Table 6.5 Charge for selected atoms in the optimised *trans* cinnamaldehyde (at PM3).

Atom Numbers	Charges
1	0.03
2	-0.08
3	0.09
4	-0.13
5	0.35
6	-0.31

The electronic theory of chemical reactivity states that nucleophiles (such as the perhydroxy anion) will attack positions that are deficient in electron density (net positive charge). Interestingly, from the data shown in Table 6.5, this would mean that on the basis of the value of the

positive charges alone, the attack of the perhydroxy anion would preferentially occur at the carbonyl carbon (C_5) instead of at the β-carbon (C_3).

Energy calculations performed on intermediate structures arising from both positions of attack, however, indicated that an attack at the C_5 position was found to be consistently higher in energy across all levels of theory than that at C_3 (the β-carbon). The results of the calculations are compared in Table 6.6.

Table 6.6 Energy differences (ΔE kJ mol^{-1}) between the *trans* cinnamaldehyde ground state and the intermediates.

Methods	HOO^- at C_5 position	HOO^- at C_3 position (Figure 6.3 b)
MNDO	-111.83	-152.19
PM3	-147.87	-169.55
RHF/6-31G(d)	-156.18	-167.23
MP2/6-31G(d)[a]	-220.76	-238.20

[a] Single-point calculation on RHF/6-31G(d) optimised geometry

6.4.3 The Intermediate Structure

The calculations on the intermediate structure (Figure 6.3 b) were performed on the *trans* structure. The atom numbering, the visual representation and the geometries for the *trans* structure where the perhydroxy anion attacks at the β-carbon are given in Figure 6.10, Figure 6.11 and Table 6.7 respectively.

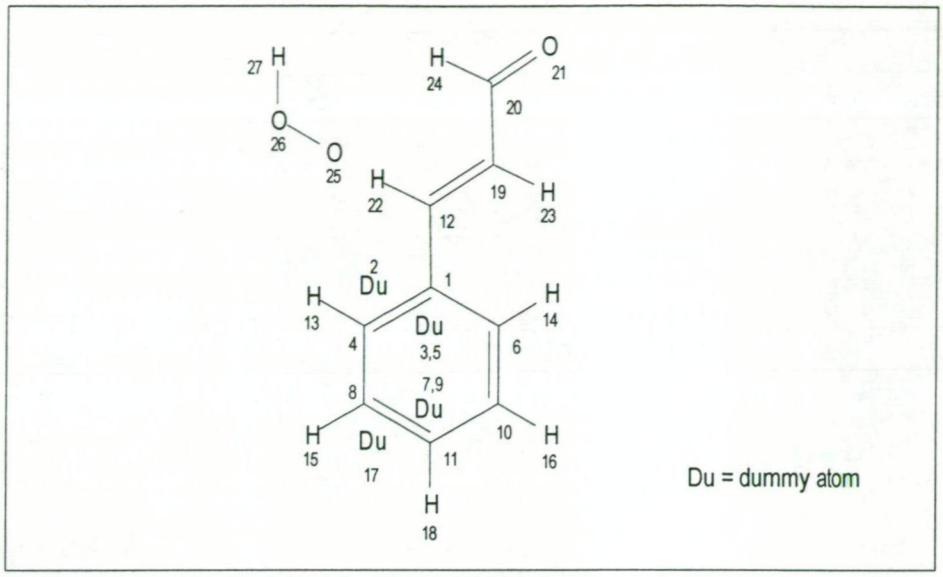

Figure 6.10 Atom numbering for data in Table 6.7.

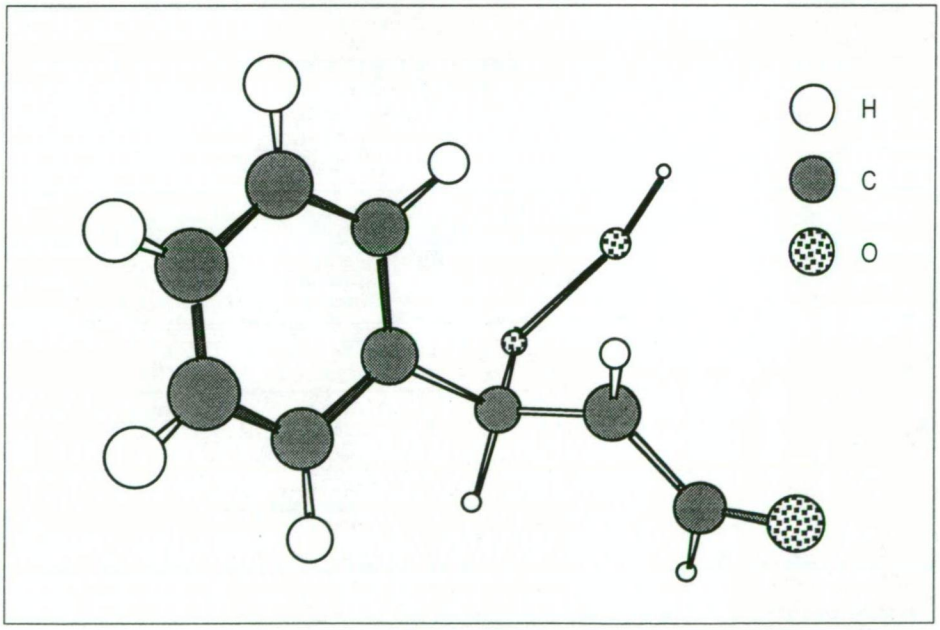

Figure 6.11 Optimised *trans* structure intermediate (at PM3).

Table 6.7 Optimised geometry for *trans* structure intermediate (at PM3).

Atom number I	Bond length (angstrom) IJ	Bond angle (degree) IJK	Dihedral angle (degree) IJKL	J	K	L
1	0.000	0.0	0.0	0	0	0
2 (Du)	1.000	0.0	0.0	1	0	0
3 (Du)	0.707	90.0	0.0	1	2	0
4	1.204	90.0	0.0	3	1	2
5 (Du)	0.708	90.0	0.0	1	2	4
6	1.203	90.0	180.0	5	1	2
7 (Du)	2.097	90.0	0.0	1	2	4
8	1.202	90.0	0.5	7	1	2
9 (Du)	2.099	90.0	0.0	1	2	4
10	1.202	90.0	179.8	9	1	2
11	2.796	90.0	0.3	1	2	4
12	1.517	91.1	-178.6	1	2	3
13	1.097	149.5	-0.9	4	3	1
14	1.096	150.1	1.5	6	5	1
15	1.094	150.1	-179.4	8	7	1
16	1.094	150.0	179.1	10	9	1
17 (Du)	1.000	90.0	0.0	11	1	2
18	1.094	90.0	-180.0	11	17	1
19	1.477	110.6	77.0	12	1	4
20	1.399	120.9	146.9	19	12	1
21	1.245	126.1	-175.5	20	19	12
22	1.119	113.5	23.2	12	19	20
23	1.092	118.0	-19.9	19	12	1
24	1.109	116.7	178.9	20	21	19
25	1.432	98.2	119.9	12	22	19
26	1.509	111.4	-146.6	25	12	22
27	0.964	96.3	26.2	26	25	12

6.4.4 Overall Mechanism

Figure 6.12 shows all intermediates and transition structures which form the overall mechanism of the epoxidation reaction of cinnamaldehyde with alkaline peroxide obtained from this study.

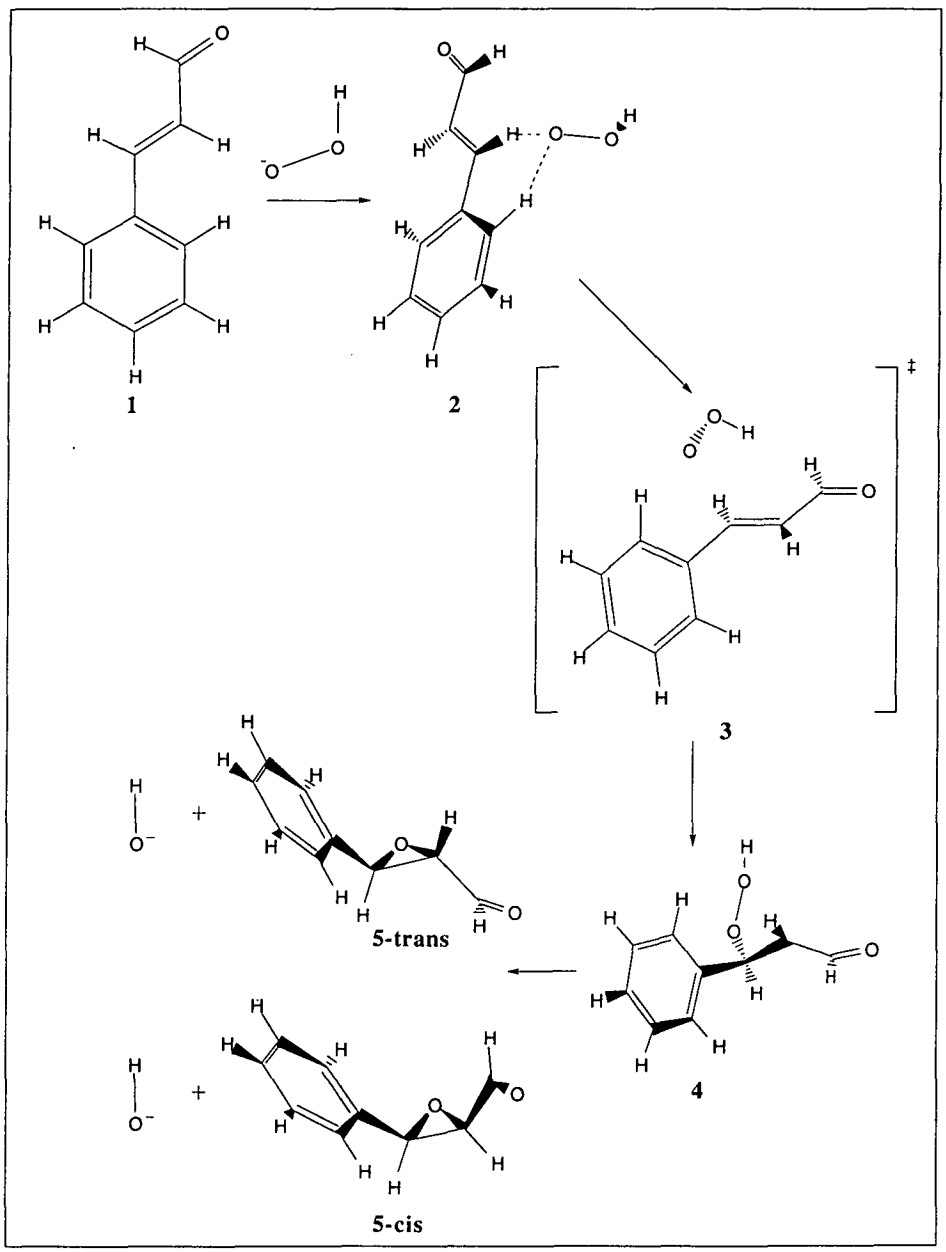

Figure 6.12 Computed structures for the epoxidation of cinnamaldehyde (based on atomic coordinates optimised at PM3).

From the calculations, it was found that cinnamaldehyde (structure 1 in Figure 6.12) reacts with perhydroxy anion ($^{-}$OOH) to form a weakly bound complex (structure 2). This is then followed by the attachment of the perhydroxy anion to the β-carbon via a transition structure 3 to form structure 4. From this point, the epoxide (structure 5) was formed via a transition structure which could not be well located at this stage.

Selected parameters for the optimised geometry at all levels of theory used in the study of each structure are shown in Table 6.8. The numbering scheme (Figure 6.13) has been simplified by showing only atoms of interest.

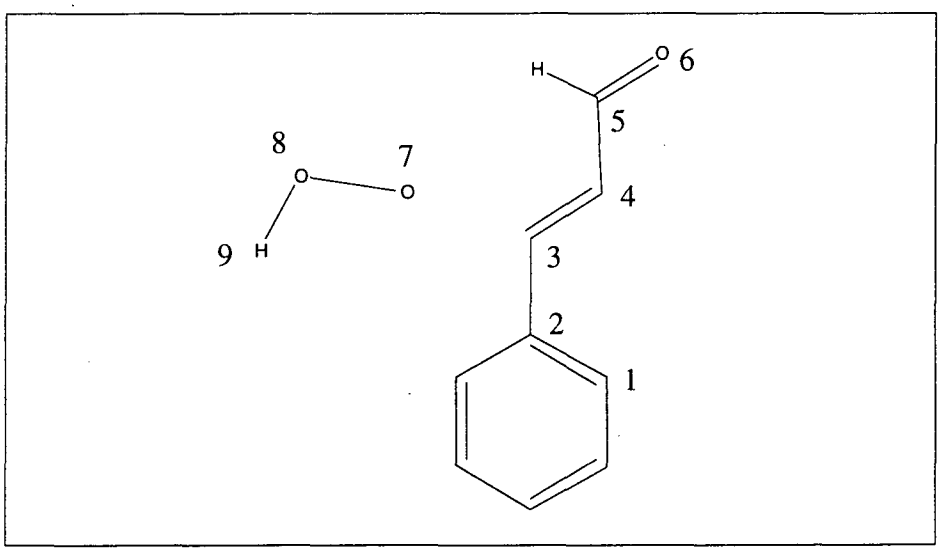

Figure 6.13 Numbering scheme for selected parameters in the optimised geometries.

Table 6.8 Selected parameters in the optimised geometries.

		1-cis	1-trans	2	3	4	5-cis	5-trans
	MNDO	∞	∞	3.479	2.291	1.455	1.418	1.420
C3-O7	PM3	∞	∞	2.809	2.131	1.432	1.433	1.434
	RHF/6-31G(d)	∞	∞	2.978	2.200	1.4482	1.394	1.395
	MNDO	-	-	111.0	95.2	104.9	120.3	119.9
C2-C3-O7	PM3	-	-	95.4	100.3	111.0	118.9	118.9
	RHF/6-31G(d)	-	-	99.7	98.9	109.2	118.0	118.1
	MNDO	-86.6	-91.0	62.5	-137.1	69.2	-77.8	-71.4
C1-C2-C3-C4	PM3	-60.6	0.1	0.0	-57.0	-101.4	-90.5	-94.1
	RHF/6-31G(d)	-46.3	0.1	-0.6	-45.2	-48.7	-98.5	-118.9

Complete values of absolute energies of the structures are shown in Table 6.9. Energies of all structures involved in the mechanism relative to the energies of the starting molecules (cinnamaldehyde and perhydroxy anion) are listed in Table 6.10. The reaction coordinate is shown in Figure 6.14.

Table 6.9 Optimised absolute energies.

	MNDO (ev)	PM3 (ev)	RHF/6-31G(d) (a.u.)	MP2/6-31G(d)[a] (a.u.)
1-trans	-1584.7943	-1482.1884	-420.31823	-421.61858
1-cis	-1584.7647	-1482.0783	-420.31165	-421.61817
2	-2240.9606	-2083.6556	-570.49056	-572.16297
3	-2240.6781	-2082.9631	-570.47138	-572.15948
4	-2242.2099	-2084.1702	-570.50749	-572.19597
5-trans	-1906.2796	-1774.9015	-495.14824	-496.63153
5-cis	-1906.2614	-1774.8721	-495.14639	-496.62996
·OOH	-655.8383	-600.2245	-150.12556	-150.48667
·OH	-334.8671	-308.0164	-75.326599	-75.512859

[a] Single-point calculation on RHF/6-31G(d) optimised geometry.

Table 6.10 Optimised relative energies (kJ mol^{-1} with respect to structure 1-*trans* + HOO·).

	MNDO	PM3	RHF/6-31G(d)	MP2/6-31G(d)[a]
1-*trans* + ·OOH	0.00	0.00	0.00	0.00
1-*cis* + ·OOH	2.85	10.62	17.27	1.08
2	-32.15	-119.8	-122.78	-151.56
3	-4.90	-53.71	-72.42	-142.38
4-*trans*	-152.70	-170.18	-167.23	-238.30
4-*cis*	-142.01	-163.09	-157.37	-230.85
5-*trans* + ·OH	-49.53	-48.65	-81.51	-102.78
5-*cis* + ·OH	-47.84	-45.89	-76.66	-98.65

[a] Single-point calculation on RHF/6-31G(d) optimised geometry.

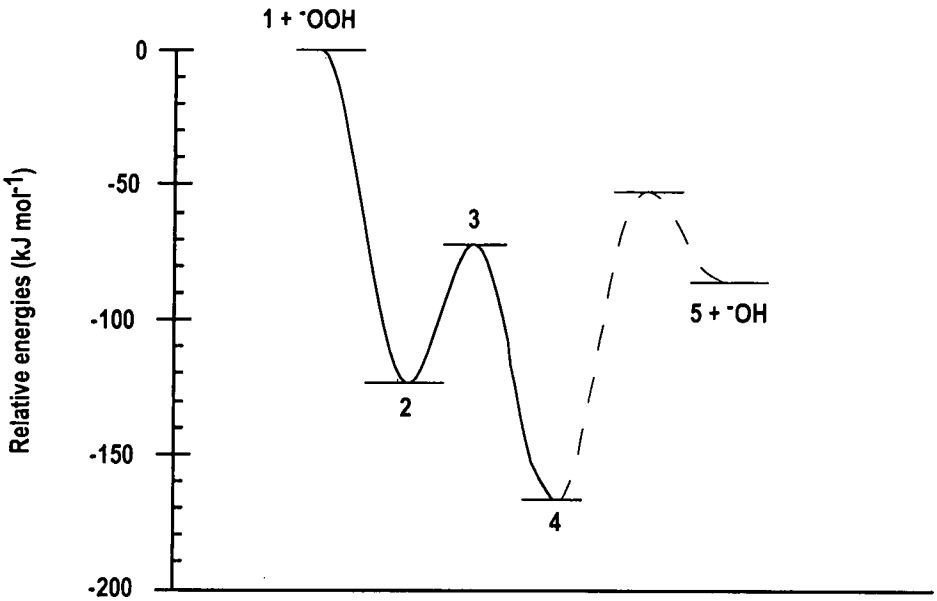

Figure 6.14 Reaction coordinate for the epoxidation of cinnamaldehyde (at PM3).

6.5 Discussion

In the mechanism of the epoxidation of cinnamaldehyde described in the previous section, the loosely bound complex structure 2 can be described as a structure where the perhydroxy anion is moving closer towards the cinnamaldehyde structure as shown in Figure 6.15.

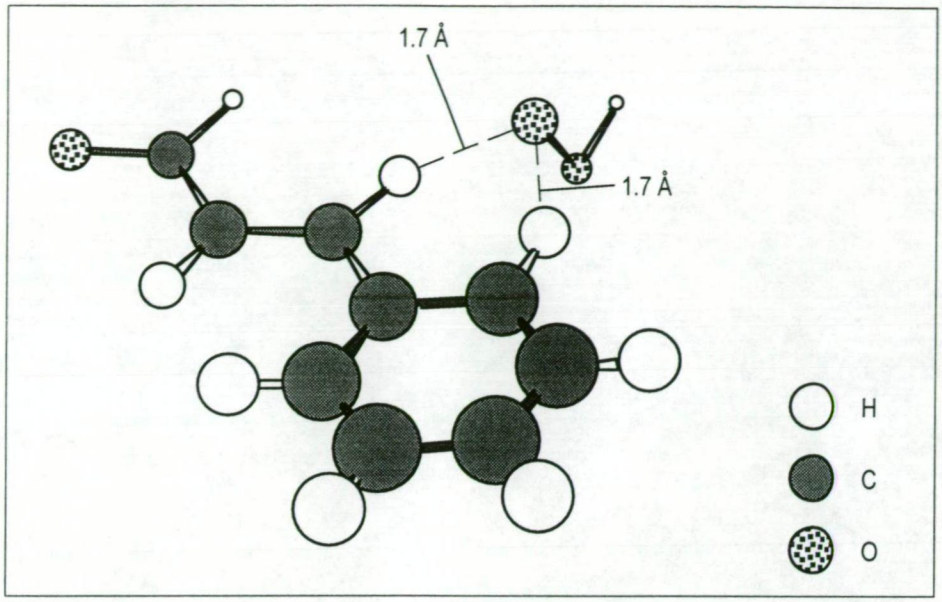

Figure 6.15 Structure 2. Perhydroxy anion is moving closer to the cinnamaldehyde (at PM3).

Transition structure 3 (Figure 6.16) shows the perhydroxy anion starting to form a bond to the β-carbon of the cinnamaldehyde.

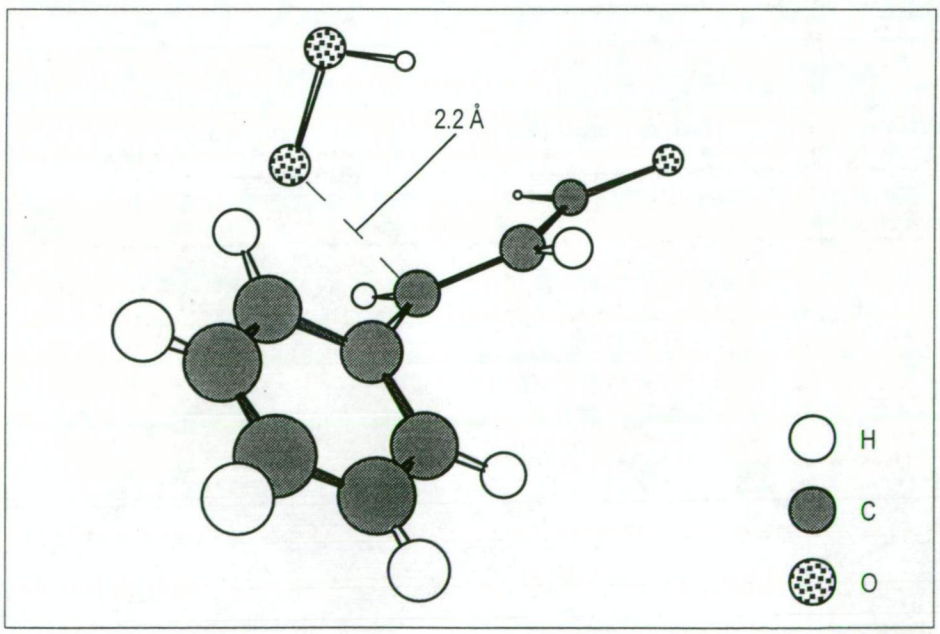

Figure 6.16 Structure 3. Perhydroxy anion is staring to form a bond to the β-carbon of the cinnamaldehyde (at PM3).

This structure leads to structure 4, which is calculated to be the most stable structure on the reaction coordinate at all levels of theory. The stability of this structure provides the driving force for the initial attack at the β-carbon of cinnamaldehyde. As expected, the C_4-C_5 bond is fairly short (1.389Å at RHF/6-31G(d)) and the C_5-O_6 bond is longer than a normal carbonyl bond (1.232Å in structure 4 versus 1.191Å in structure 1 at RHF/6-31G(d)) corresponding to the classical picture of the resonance structure for this intermediate (Figure 6.17). The delocalisation of the negative charge is also borne out by the Mulliken population analysis and is presumably the main factor leading to the stability of structure 4.

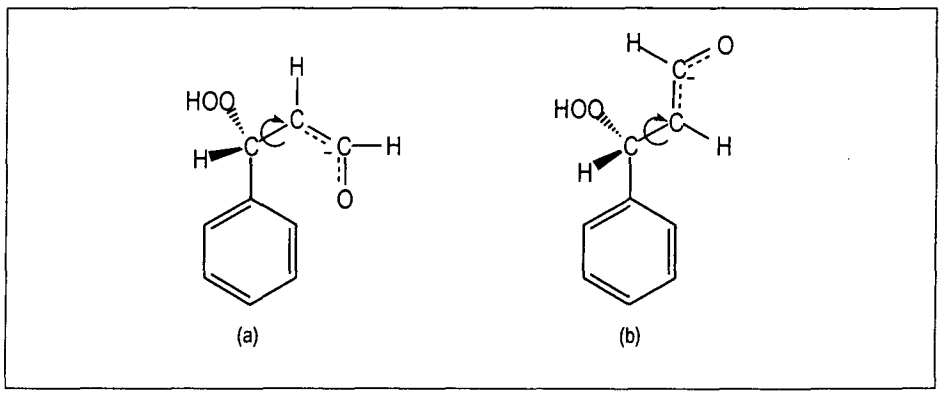

Figure 6.17 Resonance structure for structure 4.

Structure 4 then leads to the formation of the epoxide 5. Extensive searching of the potential surface was carried out using both the TS and SADDLE algorithms in MOPAC, and the TS, EF TS, and QST3 algorithms in Gaussian 94 to search for transition structures. About 25 different starting points were used in an attempt to find the right "guess"

of the transition structure. Approximate hessians and analytical hessians as starting points were used as well as various update schemes, and even full analytical hessians at every geometry with some levels of theory. A transition structure for the rearrangement of 4 to 5 was not located, even though a number of starting points from both "sides" of the barrier appeared promising. They inevitably ended up with rotational transition structures for isomerisation of different conformers. A weak complex between 5 and $^{-}$OH may exist, but in such structures the $^{-}$OH was found to be a considerable distance from the epoxide and this weak interaction may well disappear at higher levels of theory.

The epoxidation of cinnamaldehyde as studied here shows the possibility of the existence for both the *cis* and *trans* isomers. Unlike the epoxidation of several unsaturated ketones which has been observed to be a highly stereo-selective process[39], that of cinnamaldehyde is somewhat less stereo-selective. It was proposed that for unsaturated ketones, maximum overlap of electronic orbitals in the transition structure molecule by co-planar alignment is important in accounting for its stereo-selectivity. For α,β-unsaturated ketones, the ketone analogue of cinnamaldehyde, however, the maximum orbital overlap in the *cis* transition structure is seriously compromised by repulsion involving the acetyl group. For this reason, the epoxidation of the ketone analogue of cinnamaldehyde, benzalacetone, has been shown to yield the corresponding *trans* epoxide isomer exclusively[40].

The decrease in stereo-selectivity of cinnamaldehyde epoxidation can be explained by the fact that the acyl substituent has been replaced by a smaller hydrogen atom which reduces the repulsion which would otherwise diminish orbital overlap in the transition structure anion for the *cis* process.

From the calculations, it was found that there were two isomers (*cis* and *trans*) of the epoxide (structure 5), with the *trans* structure being the more stable one. The two isomers of the epoxide are shown in Figures 6.18 and 6.19 respectively.

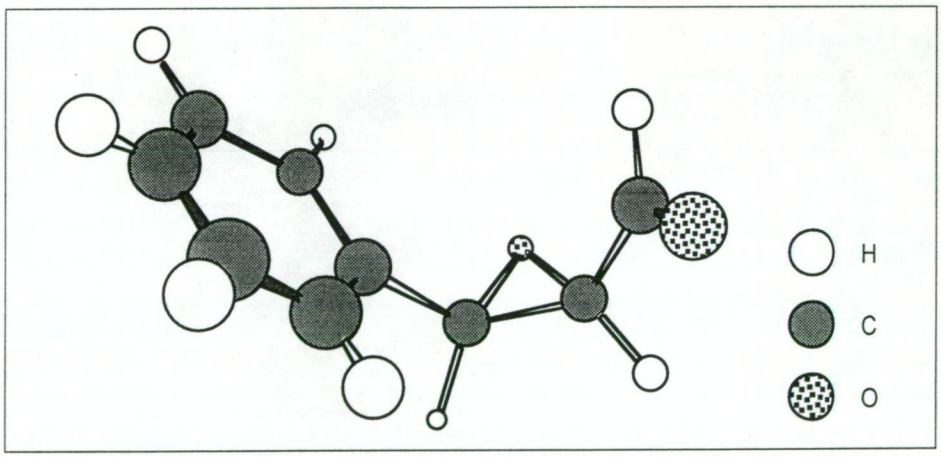

Figure 6.18 *Cis* isomer of the epoxide (structure 5).

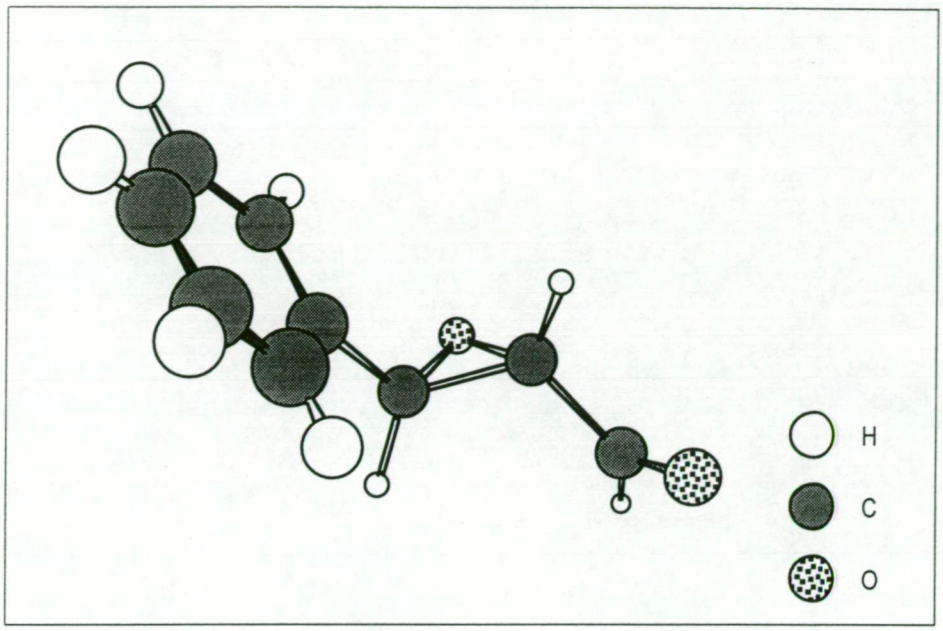

Figure 6.19 *Trans* isomer of the epoxide (structure 5).

The relative energies obtained for structure 4, the intermediates prior to the formation of the *cis* and *trans* epoxides, were -163.09 and -170.18 kJ mol^{-1} at PM3 for the *cis* and *trans* structures respectively. Theoretically, using the Boltzman distribution formula as shown in Equation (6.1), this would give a mole ratio of 1:17 (at T = 298) between the *cis* and the *trans* isomers. This is more than twice the experimental value of 1:8 reported from a previous study by Wright and Abbot[3]. The variation might suggest that the difference in relative energies is overestimated by the present calculations or that other factors are involved in the experimental situation.

$$\frac{n_b}{n_a} = e^{-\frac{\Delta H_f b - \Delta H_f a}{RT}} \qquad (6.1)$$

From the investigation of all the structures in this study, it appears that the mechanism for the alkaline peroxide attack on α,β-unsaturated ketones is as follows : first an initial loose complex (2) forms between the peroxy anion and the substrate; the oxygen of the peroxide bridges two protons, one on the β-carbon and the other on the neighbouring aromatic ring. Next, the peroxy anion moves perpendicular to the plane of the conjugated system and binds to the β-carbon to form a very stable intermediate (4). Then loss of $^{-}$OH occurs (probably concomitant) with formation of the epoxide. A loose complex of the epoxide and the $^{-}$OH anion initially forms (although this is not nearly as stable as structure 2), which then dissociates to the final species.

Atomic charges calculated for structure 1 at all levels of theory (Table 6.11) show that carbonyl carbon is consistently more positive than Cβ. However, energetically it was found that the Cβ is still the preferred site for an attack by the negatively charged perhydroxy anion.

Table 6.11 Selected atom charges for structure 1 at all levels of theory.

	C_3		C_4		C_5	
	cis	trans	cis	trans	cis	trans
MNDO	+ 0.06	+ 0.12	- 0.09	- 0.11	+ 0.31	+ 0.31
PM3	- 0.08	- 0.09	- 0.12	- 0.13	+ 0.36	+ 0.35
RHF/6-31G(d)	- 0.06	- 0.05	-0.06	- 0.07	+ 0.47	+0.47

Analysis of further nucleophilic attack to the epoxide (structure 5) indicates that based on the carbon atom charges, Cβ is also more likely to be the site of attack. Charges for selected carbon atoms of structure 5 are tabulated in Table 6.12.

Table 6.12 Selected atom charges for structure 5 at all levels of theory.

	C_3		C_4		C_5	
	cis	trans	cis	trans	cis	trans
MNDO	+ 0.12	+ 0.12	- 0.03	- 0.03	+ 0.28	+ 0.27
PM3	+ 0.09	+0.09	- 0.09	- 0.09	+ 0.29	+ 0.28
RHF/6-31G(d)	+ 0.09	+0.29	- 0.02	+ 0.21	+ 0.32	+ 0.49

6.6 Conclusions

The epoxidation of cinnamaldehyde was found to be exothermic with an overall activation energy close to zero. This would suggest that the formation of the epoxide during the reaction of cinnamaldehyde with alkaline peroxide is theoretically feasible. The experimental presence of

two epoxide isomers with the *trans* isomer as the preferred product agrees with the results of our calculations.

Good agreement between the results of the less sophisticated PM3 calculations and the more sophisticated *ab initio* calculations at RHF/6-31G(d) suggest that PM3 can be used for further studies without sacrificing significant accuracy of the results. PM3 is also computationally preferred since it generally requires less computation time to perform.

6.7 References

1. Wright, P. J., *PhD Thesis*, Department of Chemistry, University of Tasmania (1993).

2. Gellerstedt, G., Petterson, I. and Sundin, S., *1st Int. Symp. Wood and Pulp. Chem.*, II :120 (1981).

3. Wright, P. and Abbot, J., *Int. J. Chem. Kin.* 25 901 (1993).

4. Sarkanen, K. V., In *Lignins - Occurrence, Formation, Structure and Reactions.*, "Chapter 4: Precursors and Their Polymerization", Sarkanen, K. V. and Ludwig, C. H. (Eds.), Wiley-Interscience, New York, 1971.

5. Fengel, D. and Wegener, G., In *Wood: Chemistry, Ultrastructure, Reactions*, De Gruyter, Berlin, 1984.

6. Casey, J. P., In *Chemistry and Chemical Technology, Volume 1: Pulp and Paper*, Wiley-Interscience, New York, 1980.

7. Sjöstrom, E., In *Wood Chemistry*, Academic Press, New York, 1984.

8. Adler, E. and Ellmer, L., *Acta Chem. Scand.* 2 839 (1948).

9. Lundqvist, K., *Acta Chem. Scand.* 18 (5) :1316 (1964).

10. Fukuzumi, T. and Terasawa, M., *Mokuzai Gakkaishi* 8 77 (1962).

11. Wallis, A. F. A., In *Lignins - Occurrence, Formation, Structure and Reactions*, "Chapter 9: Solvolysis by Acids and Bases", Sarkanen, K. V. and Ludwig, C. H. (Eds.), Wiley-Interscience, New York, 1971.

12. Polcin, J. and Rapson, W. H., *Pulp and Paper Mag. Can.* 72 (3) :69 (1971).

13. Polcin, J. and Rapson, W. H., *Pulp and Paper Mag. Can.* 72 (3) :80 (1971).

14. Michell, A. J., Nelson, P. J. and Chin, C. W. J., *Appita* 42 (6) :443 (1989).

15. Marton, J. and Adler, E., *Acta Chem. Scand.* 15 (2) :370 (1961).

16. Pew, J. C. and Connors, W. J., *Tappi* 54 (2) :245 (1971).

17. Hergert, H. L., In *Lignins - Occurrence, Formation, Structure and Reactions*, "Chapter 7: Infra-red Spectra", Sarkanen, K. V. and Ludwig, C. H. (Eds.), Wiley-Interscience, New York, 1971.

18. St. Germain, F. and Gray, D., *J. Wood Chem. Technol.* 7 (1) :33 (1987).

19. Genuit, W. and Boon, J., *Anal. Chem.* 59 508 (1987).

20. Higuchi, T. and Brown, S. A., *Can. J. Biochem. and Physiol.* 41 613 (1963).

21. Freudenberg, K. and Schluter, H., *Chem. Ber.* 88 617 (1955).

22. Hirashima, H. and Sumimoto, M., *Mokuzai Gakkaishi* 33 (1) :31 (1987).

23. Gupta, V. N., *Pulp and Paper Mag. Can.* 73 (6) :57 (1972).

24. Holmbolm, B., Ekman, R., Sjoholm, R. and Thornton, J., *Das Papier* 45 (10A) :16 (1992).

25. Holah, D. G., Heitner, C. and therein, r. c., *J. Pulp Paper Sci.* 18 (5) :J161 (1992).

26. Payne, G. B., *J. Am. Chem. Soc* 26 250 (1961).

27. Reeves, R. H. and Pearl, I. A., *Tappi* 48 (2) :121 (1965).

28. Gellerstedt, G. and Agnemo, R., *Acta Chem. Scand.* B34 (4) :275 (1980).

29. Sri Rama Rao, D., *J. Indian Chem. Soc.* 60 300 (1983).

30. Tishchenko, I. G., Burd, V. N. and Revinskii, I. F., *Zh. Org. Khim.* 22 (3) :669 (1986).

31. Sugiyama, S., Kubo, S. and Hayashi, H., *Chem. Express* 4 (7) :433 (1989).

32. Stewart, J. J. P., *MOPAC 93*, 1993.

33. Frisch, M. J., Trucks, G. W., Head-Gordon, M., Gill, P. M. W., Wong, M. W., Foresman, J. B., Johnson, B. G., Schlegel, H. B., Robb, M. A., Replogle, E. S., Gomperts, R., Andres, J. L., Raghavachari, K., Binkley, J. S., Gonzalez, C., Martin, R. L., Fox, D. J., Defrees, D. J., Baker, J., Stewart, J. J. P. and Pople, J. A., *GAUSSIAN 92*, 1992.

34. Dewar, M. J. S. and Thiel, W., *J. Am. Chem. Soc.* 99 (15) :4899 (1977).

35. Stewart, J. J. P., *J. Comput. Chem.* 10 210 (1989).

36. Hariharan, P. C. and Pople, J. A., *Chem. Phys. Lett.* 66 217 (1972).

37. Baker, J., *J. Comput. Chem.* 7 385 (1986).

38. Elder, T. J. and Worley, S. D., *Holzforschung* 39 (3) :173 (1985).

39. Zimmerman, H. E., Singer, L. and Thyagarajan, B. S., *J. Am. Chem. Soc.* 81 108 (1959).

40. Kwart, H. and Kirk, L. G., *J. Org. Chem.* 22 (1) :116 (1957).

CHAPTER 7

Conclusions and Discussion

The equilibrium models have been shown to be able to describe the kinetic bleaching response of *Pinus radiata* TMP under constant reagent conditions. Ability to describe experimental kinetic behaviour, including bleaching responses when bleached pulp is exposed to a new set of constant reagent conditions, form the main advantages of the equilibrium models which are not possessed by previously reported kinetic models. This success is attributed to the inclusion of a chromophore creation step in the reaction scheme. Perhydroxyl anions are found to be responsible for the main bleaching reactions while alkali produces an inhibiting effect. Limited observation shows that the pseudo-first order rate constants exhibit non-linear dependence on reagent concentration and indicates that more complex reactions take place than are assumed in the kinetic model schemes.

Computational studies of the previously reported mechanism for the reaction of cinnamaldehyde with alkaline peroxide which involves the formation of an epoxide intermediate, has shown that it is theoretically feasible. The Calculation results which show the *trans* isomer of the epoxide as the preferred isomer also agree with experimental observation.

It was found that the computationally less expensive PM3 calculations are in good agreement with the more expensive *ab initio* calculations at RHF/6-31G(d). This suggests that PM3 can be used for further study without sacrificing the accuracy of the results.

7.1 Directions for Future Work

There are many questions which remain unanswered regarding the kinetics of reactions under alkaline peroxide bleaching reactions. There are numerous factors which have not been fully taken into account in this study. Future development of a good model for peroxide bleaching requires the following independent events which have been experimentally shown to occur during alkaline peroxide brightening to be taken into account:

- Reaction of hydrogen peroxide and the hydrogen peroxide anion with colour producing chromophores such as coniferaldehyde, α-carbonyl structure and ortho and para quinones. These reactions lead to brightening. Model compound results indicate that these reactions are normally first order in peroxide and chromophore concentration. Among the significant differences between model compound results and results from pulp is the non-linearity of the ln(brightness) graph compared to the first order situation for model compounds.
- The reaction of hydroxyl anions with lignin to generate coloured components. Among those which are probably produced, stilbenes and condensation products will not be formed in an equilibrium. The generation of α-carbonyl structures may be a reversible reaction and certainly leads to a component which may then be attacked by alkaline peroxide.
- The formation of chromophores by radical processes. The decomposition of hydrogen peroxide to hydroxyl radicals and superoxide is dependent on the

base concentration and is second order in peroxide concentration. Also this degradation may be catalysed by certain metals. The radical degradation products generated from peroxide will lead to greater amounts of conjugated structures and colour producing chromophores.

- The heterophase nature of the brightening reaction as this undoubtedly leads to the significant difference between model compound work and the work with real pulp.
- The pKa of the hydrogen peroxide and the lignin components.
- Dependency of the hydrogen peroxide brightening of wood on removal of lignin components as shown by the following equation:

$$\frac{dC}{dT} = -\sum_{m} k_m \left[\sum_{i} k_i [C][HOO^-] + \sum_{j} k_j [C][HOOH] \right] + \sum_{k} k_j [C_{L1}][HO^-] + \sum_{l} k_k [C_{L2}][R]$$

R	Radical components, presumably at a steady stage depending on metals, pH, peroxide, lignin concentrations.
C_{L1}	Leucochromophores which are reactive to base
C_{L2}	Leucochromophores which are reactive to radical species
C_i	Different chromophoric components
k_m	Mass transfer or diffusion rate of product removal.

- Conditions where the hydrogen peroxide and alkali are kept constant during the reaction will eliminate reactions such as the degradation of carbohydrate structures which have little effect on the pulp brightness but consume reagents.
- Strategy for measuring C_L and K_3 using very extreme or very mild conditions for further study of the equilibrium models.

The colour producing reactions, as previously discussed, need to be investigated further which creates considerable scope for future work related to the characterisation of darkening reactions during peroxide bleaching. To start with, model compound studies focussing on the reactions of the main non-chromophoric units in lignin with alkaline peroxide and radical species generated by peroxide decomposition are required in order to identify the likely reaction mechanism responsible for chromophore formation during peroxide bleaching. Structural units which are easily oxidised to quinones such as phenolic compounds[1-3]

and structures such as phenylcoumarans and 1,2-diarylpropane-1,3-diols which may give rise to α,β-unsaturated structures such as stilbenes upon oxidation[4, 5] are worthy of further study. Once the principal darkening routes have been identified and taking advantage of the fact that both quinones and stilbenes exhibit characteristic signals in ^{13}C-nmr[4], verification of the occurrence of the same darkening reactions in pulp or in lignin preparations such as milled wood lignin can then be carried out.

Several techniques are available for studying the elimination of α,β-unsaturated aldehydes from pulp or milled wood lignin under conventional peroxide bleaching conditions which can be useful in further study. The techniques include the use of specific colour reagents, such as the phloroglucinol-HCl reagent[6-8] and derivatisation by thioacidolysis followed by Raney nickel desulfuration[9].

7.2 References

1. Kempf, A. W. and Dence, C. W., *Tappi* 58 (6) :104 (1975).

2. Bailey, C. W. and Dence, C. W., *Tappi* 52 (3) :491 (1969).

3. Stone, T. J. and Waters, W. A., *J. Chem. Soc.* 1488 (1965).

4. Sjöholm, R., Holmbolm, B. and Åkerback, N., *J. Wood Chem. Technol.* 12 (1) :35 (1992).

5. Gellerstedt, G. and Agnemo, R., *Acta Chem. Scand.* B34 (6) :461 (1980).

6. Adler, E. and Ellmer, L., *Acta Chem. Scand.* 2 839 (1948).

7. Gupta, V. N., *Pulp and Paper Mag. Can.* 73 (6) :57 (1972).

8. Hirashima, H. and Sumimoto, M., *Mokuzai Gakkaishi* 33 (1) :31 (1987).

9. Pan, X. and Lachenal, D., *J. Wood Chem. Technol.* 12 (2) :135 (1992).

Appendix A

Computer Spreadsheet Program For Calculations Of Physical Properties Of Paper

	A	B	C	D	E	F	G	H	I
1	SHEET								
2		1			2			3	
3	R Infinity	R Zero	Mass	R Infinity	R Zero	Mass	R Infinity	R Zero	Mass
4	60.66	60.16	0.5382	60.07	59.97	0.5394	60.47	59.96	0.4971
5	67.09	66.01	0.5205	66.31	65.63	0.5261	66.42	65.72	0.5427
6	68.98	67.58	0.5436	68.98	67.37	0.5152	68.93	67.50	0.5000
7	70.16	68.68	0.5206	70.36	68.73	0.5195	70.54	69.23	0.5078
8	72.59	70.26	0.5241	72.50	70.72	0.5274	72.66	70.16	0.5159
9	74.05	70.91	0.5420	73.85	70.76	0.5238	73.75	71.43	0.5000
10	75.15	72.16	0.5315	75.47	72.33	0.5413	75.42	73.15	0.5693
11	76.15	73.11	0.5684	76.41	73.13	0.5400	76.75	73.71	0.5254
12									
13	Basis-Weight_1	s_1	k_1	Basis-Weight_2	s_2	k_2	Basis-Weight_3	s_3	k_3
14	0.081	51.501	6.570	0.081	68.933	9.148	0.075	55.137	7.124
15	0.078	55.225	4.458	0.079	59.947	5.130	0.082	57.929	4.917
16	0.082	52.618	3.670	0.078	53.192	3.710	0.075	56.736	3.973
17	0.078	56.482	3.584	0.078	55.349	3.455	0.076	60.949	3.749
18	0.079	53.047	2.745	0.079	57.561	3.002	0.078	52.690	2.710
19	0.082	48.580	2.209	0.079	50.191	2.324	0.075	58.279	2.723
20	0.080	52.751	2.167	0.081	51.466	2.052	0.086	55.167	2.210
21	0.086	51.031	1.906	0.081	52.667	1.918	0.079	56.586	1.993
22									

	K	Devn.	Std.Dev
23			
24	7.614	1.023	0.960
25	4.835	0.252	0.243
26	3.784	0.126	0.116
27	3.596	0.102	0.104
28	2.819	0.122	0.113
29	2.418	0.203	0.191
30	2.143	0.061	0.058
31	1.939	0.036	0.033

Date	=
pH	=
Peroxide	=

NOTE

Microsoft Excel Formula Sheet

	A	B	C
1		R Infinity	60.66
2	Sheet 1	R Zero	60.16
3		Mass	0.5382
4		R Infinity	60.07
5	Sheet 2	R Zero	59.97
6		Mass	0.5394
7		R Infinity	60.47
8	Sheet 3	R Zero	59.96
9		Mass	0.4971
10			
11		Basis-Weight_1	=(C3*0.001)/(PI()*(0.5*0.092)^2)
12		s_1	=(((C1*0.01)/(1-((C1*0.01))^2))*LN((1-(((C2*0.01)/(C1*0.01))*((C1*0.01))^2))/(1-((C2*0.01)/(C1*0.01))))))/C11
13		k_1	=((0.5*((1/(C1*0.01))+(C1*0.01)))-1)*C12
14			
15		Basis-Weight_2	=(C6*0.001)/(PI()*(0.5*0.092)^2)
16		s_2	=(((C4*0.01)/(1-((C4*0.01))^2))*LN((1-(((C5*0.01)/(C4*0.01))*((C4*0.01))^2))/(1-((C5*0.01)/(C4*0.01))))))/C15
17		k_2	=((0.5*((1/(C4*0.01))+(C4*0.01)))-1)*C16
18			
19		Basis-Weight_3	=(C9*0.001)/(PI()*(0.5*0.092)^2)
20		s_3	=(((C7*0.01)/(1-((C7*0.01))^2))*LN((1-(((C8*0.01)/(C7*0.01))*((C7*0.01))^2))/(1-((C8*0.01)/(C7*0.01))))))/C19
21		k_3	=((0.5*((1/(C7*0.01))+(C7*0.01)))-1)*C20
22			
23		K	=(C13+C17+C21)/3
24			
25		Devn.	=(ABS(C23-C13)+ABS(C23-C17)+ABS(C23-C21))/3
26			
27		Std.Dev	=SQRT(((C23-C13)^2+(C23-C17)^2+(C23-C21)^2))/2

Appendix B

Computer Program For Controlling Varian DMS100 UV-Vis Spectrometer

```
REM ================================================================================
REM =                              REM Program DMSC                                  =
REM ================================================================================
REM =   This program is to be used to externally Control DMS100 UV-VIS             =
REM =                                Spectrometer                                    =
REM ================================================================================
REM =                           Created 17 November 1992                             =
REM =                                 Yos Ginting                                    =
REM =                         Chemistry Dept. Uni of Tasmania                        =
REM ================================================================================


'                                  ===== CONSTANTS =====
STX$ = CHR$(&H2)             ' start transmission character
ETX$ = CHR$(&H3)             ' end transmission character
ACK$ = CHR$(&H6)             ' msg acknowledged character
NAK$ = CHR$(&H15)            ' msg not acknowledged character
DIM SPECTRAVAL(12000)        ' array to store DMS data
$COM1 4096                   ' set 4 kb buffer for COM1
TAKE% =  5                   ' Take data for every 5 nm, change it to suit your need

'                               ===== MAIN PROGRAM LOOP ======
REM It starts with an introduction and followed with a menu
REM It keeps running until user select to Quit


GOSUB OpenDMS                                   ' opens line between COM1 and DMS
GOSUB Introduction                              ' Introduce user about program
CALL DisplayMenu(USERCHOICE$,CONTINUE$)         ' Display menu to user
WHILE CONTINUE$="YES"                           ' As long as user want to continue
                                                ' Check what user want
  IF USERCHOICE$ = "1" THEN                     ' User want to set some parameters
    GOSUB SetDMSPar
    WHILE U$ <>"7"
      GOSUB SetDMSPar
    WEND
  ELSEIF USERCHOICE$ = "2" THEN                 ' User want to do Baseline program
    GOSUB BaseLineProg
  ELSEIF USERCHOICE$ = "3" THEN                 ' User want to start scanning
    GOSUB PrepareScanning
    GOSUB LockDMS
    GOSUB StartScan
    GOSUB UnlockDMS
  ELSEIF USERCHOICE$ = "4" THEN                 ' User want to download data
    GOSUB LockDMS
    GOSUB Download
    GOSUB UnlockDMS
    CHOICE$=""
    GOSUB WhichOutput
  ELSEIF USERCHOICE$ = "5" THEN                 ' User want to scan and download
    GOSUB LockDMS
    GOSUB StartScan
    GOSUB Download
    GOSUB UnlockDMS
    CHOICE$=""
    GOSUB WhichOutput
  ELSEIF USERCHOICE$ = "6" THEN                 ' User needs help
```

```
    GOSUB MainHelp
    END IF
  CALL DisplayMenu(USERCHOICE$,CONTINUE$)
' Re display menu
WEND
GOSUB CloseDMS                                  ' close connection
END


'             ===== BELOW ARE ALL SOUBROUTINES USED ====


'            ==== SUBROUTINE TO OPEN CONNECTION TO DMS100 ====

REM opening connection via RS232 TO DMS100
REM DMS is in COM1, 2400 BAUD, Even parity, 8 data bits,1 stop bit
REM options available but not used are used are :
REM                    RS (Supress the RTS Line)
REM                    CS (Control CTS) ,Default 1000 msec
REM                    DS (Control DSR) ,Default 1000 msec
REM                    PE (Turn on parity checking)
REM Do not use LF options to DMS !!!!!!

OpenDMS :
  CLS
   OPEN "COM1: 2400, E, 8, 1 " AS #1
   'PRINT "COM LINE OPENED SUCCESFULLY"
  RETURN


'            ==== SUBROUTINE TO INTRODUCE DMSC PROGRAM ====

REM subroutine introduction
REM Tell user about what the program does
Introduction :
  CLS
  CALL DrawLine("=")
  PRINT
  CALL CenterMSG("VARIAN DMS 100 PROGRAM CONTROLLER")
  CALL CenterMSG("1st Version, Nov 1992")
  CALL CenterMSG("=======")
  PRINT "               BEFORE GOING FURTHER, PLEASE CHECK AND DO THE FOLLOWING"
  PRINT "                   * DMS MODE is in Scan Mode"
  PRINT "                   * Set slit width  (e.g =2)"
  PRINT "                   * Set Change source (e.g 300)"
  PRINT "                   * Set Max and Min Wavelength (e.g 200 -700)"
  PRINT "                   * Finally, check the connection"
  PRINT "                     - Computer connection is via COM1"
  PRINT "                     - DMS connection is via RS232 on its back panel"
  PRINT "                     - DMS RS232 Setting should be 01011100"
  PRINT
  CALL DrawLine("=")
  CALL WaitKey("PRESS ANY KEY TO GO TO MAIN MENU")
  RETURN
```

```
'            ==== SUBROUTINE TO DISPLAY AVAILABLE FUNCTIONS ====

SUB DisplayMenu(UC$,CONTINUE$)
  CLS
  CALL DrawLine("=")
  PRINT
  PRINT " SELECT OPERATION :"
  PRINT "   1. SET DMS PARAMETERS AND ACCESS OTHER KEYBOARD FUNCTIONS"
  PRINT "   2. BASELINE PROGRAM"
  PRINT "   3. START SCAN"
  PRINT "   4. DOWNLOAD LAST SPECTRA (VALUE IS % T)"
  PRINT "   5. SCAN AND DOWNLOAD AT ONCE"
  PRINT "   6. HELP"
  PRINT "   7. EXIT DMS CONTROLLER PROGRAM"
  PRINT
  CALL DrawLine("=")
  INPUT "SELECT AN OPERATION = ",UC$
  WHILE (UC$ <>"1") AND (UC$ <>"2") AND (UC$ <>"3") AND (UC$ <>"4") AND (UC$ <>"5")
AND (UC$ <>"6") AND (UC$ <>"7")
    BEEP 1
    COLX% = POS(0)
    ROWY% = CSRLIN
    LOCATE (ROWY%-1),1
    INPUT "SELECT AN OPERATION = ",UC$
    LOCATE ROWY%,COLX%
  WEND
  IF (UC$ = "7") THEN
    CONTINUE$="NO"
  ELSE
    CONTINUE$="YES"
  END IF
END SUB

'            ==== SUBROUTINE TO PERFORM SOME DMS KEYBOARD FUNCTIONS====

SetDMSPar :
  CLS
  CALL DrawLine("=")
  PRINT
  PRINT " SELECT OPERATION :"
  PRINT "   1. CLEAR SCREEN"
  PRINT "   2. LOCK KEYBOARD"
  PRINT "   3. UNLOCK KEYBOARD"
  PRINT "   4. PLOT SCAN"
  PRINT "   5. CLEAR SCREEN AND SHOW LAST SCAN"
  PRINT "   6. HELP"
  PRINT "   7. GO BACK TO MAIN MENU"
  PRINT
  CALL DrawLine("=")
  INPUT "SELECT AN OPERATION = ",U$
  WHILE (U$ <>"1") AND (U$ <>"2") AND (U$ <>"3") AND (U$ <>"4") AND (U$ <>"5") AND
(U$ <>"6") AND (U$ <>"7")
    BEEP 1
    COLX% = POS(0)
    ROWY% = CSRLIN
    LOCATE (ROWY%-1),1
    INPUT "SELECT AN OPERATION = ",U$
    LOCATE ROWY%,COLX%
```

```
  WEND
  IF U$ = "1" THEN
    GOSUB ClearScreen
  ELSEIF U$ = "2" THEN
    GOSUB LockDMS
  ELSEIF U$ = "3" THEN
    GOSUB UnlockDMS
  ELSEIF U$ = "4" THEN
    GOSUB UnlockDMS
    GOSUB PlotToPrinter
  ELSEIF U$ = "5" THEN
    GOSUB LockDMS
    GOSUB ShowLastPlot
    GOSUB UnlockDMS
  ELSEIF U$ = "6" THEN
    GOSUB HelpFunctionKey
  END IF
RETURN


'               ==== SUBROUTINE TO CLEAR SCREEN ====

ClearScreen:
  CLS
  LDI$="E"                    ' E is external computer address, that's us
  MI$ ="C"                    ' Follows are C(ommand)
  MD$ ="F"                    ' KeyCode
  MQ$ =CHR$(&H34)             ' Clear SCreen Key
  GOSUB SendMessage           ' send it to DMS
  ANS$ = INPUT$(1, #1)        ' Does DMS ACKnowledge our message
  WHILE ANS$ <> ACK$          ' while not ACKnowledge our message
    GOSUB SendMessage         ' keep sending and trying
    ANS$ = INPUT$(1, #1)        ' Does DMS ACKnowledge our message
  WEND
  RETURN

'            ==== SUBROUTINE TO LOCK DMS KEYBOARD ====

REM the format used is :
REM         Send STX Character                (02 Hex)
REM         Send byte count of message        (a single binary byte)
REM         Send all bytes in the message     (several bytes)
REM         Send checksum                     (a single binary byte)
REM         Send ETX Character                (03 Hex)
REM And for locking, we send STX -Count - ECA - CheckSum -ETX
REM Refers to section 9.1 and 92 pp 47-49 of DMS100 Manual

LockDMS:
  CLS
  LDI$="E"                    ' E is external computer address, that's us
  MI$ ="C"                    ' Follows are C(ommand)
  MD$ ="A"                    ' Lock Keyboard message
  MQ$ =""                     ' No Message Qualifier
  GOSUB SendMessage           ' send it to DMS
  ANS$ = INPUT$(1, #1)        ' Does DMS ACKnowledge our message
  WHILE ANS$ <> ACK$          ' while not ACKnowledge our message
    'PRINT "DMS IS HAVING PROBLEM LOCKING ITS KEYBOARD, STILL TRYING = "
    'PRINT 'ITS CURRENT MESSAGE IS = ", ANS$
```

```
    GOSUB SendMessage          ' keep sending and trying
    ANS$ = INPUT$(1, #1)         ' Does DMS ACKnowledge our message
  WEND
  'PRINT "DMS KEYBOARD IS SUCCESFULY LOCKED"
  RETURN


'             ==== SUBROUTINE TO UNLOCK DMS KEYBOARD ====

REM unlocking DMS keyboard
REM the format used is the same as in LockDMS
UnlockDMS:
  CLS
  LDI$="E"                    ' E is external computer address, that's us
  MI$ ="C"                    ' Follows are C(ommand)
  MD$ ="B"                    ' Unlock Keyboard message
  MQ$ =""                     ' No Message Qualifier
  GOSUB SendMessage           ' send it to DMS
  ANS$ = INPUT$(1, #1)        ' Does DMS ACKnowledge our message
  WHILE ANS$ <> ACK$          ' while not ACKnowledge our message
   ' PRINT "DMS IS HAVING PROBLEM UNLOCKING ITS KEYBOARD, STIL TRYING .."
   ' PRINT "ITS CURRENT MESSAGE IS = ", ANS$
    GOSUB SendMessage         ' keep sending and trying
    ANS$ = INPUT$(1, #1)        ' Does DMS ACKnowledge our message
  WEND
 ' PRINT "DMS KEYBOARD IS SUCCESFULY UNLOCKED"
  RETURN

'             ==== SUBROUTINE TO PLOT SCREEN TO PRINTER ====

PlotToPrinter:
  CLS
  CALL Highlight("SENDING PLOT TO PRINTER MESSAGE")
  LDI$="E"                    ' E is external computer address, that's us
  MI$ ="C"                    ' Follows are C(ommand)
  MD$ ="F"                    ' Lock Keyboard message
  MQ$ =CHR$(&H35)             ' Command contains no data, so leave out
  GOSUB SendMessage           ' send it to DMS
  ANS$ = INPUT$(1, #1)        ' Does DMS ACKnowledge our message
  WHILE ANS$ <> ACK$          ' while not ACKnowledge our message
    'PRINT "DMS IS HAVING PROBLEM SENDING PLOT SCAN MSG, STILL TRYING = "
    'PRINT 'ITS CURRENT MESSAGE IS = ", ANS$
    GOSUB SendMessage         ' keep sending and trying
    ANS$ = INPUT$(1, #1)        ' Does DMS ACKnowledge our message
  WEND
  ' PRINT "SENDING PLOT SCAN MSG IS SENT SUCCESFULY"
  '  ANS$ = INPUT$(1, #1)                                    ' get ANS$
  '  WHILE ANS$ <> STX$                      ' While it is not the start of data
  '    PRINT "STILL WAITING FOR -START TRANSMISSION- CHARACTER FOR PLOT SCAN .."
  '    ANS$ = INPUT$(1, #1)                                  ' keep asking for it
  '    PRINT "ITS CURRENT MESSAGE IS = ", ANS$
  '  WEND
  'ANS$ = INPUT$(1, #1)       ' get ANS$
  'WHILE ANS$ <> ETX$         ' While it is not the start of data
  '  PRINT "STILL WAITING FOR -END TRANSMISSION- CHARACTER FOR PLOT SCAN.."
  '  ANS$ = INPUT$(1, #1)     ' keep asking for it
  '  PRINT "ITS CURRENT MESSAGE IS = ", ANS$
  'WEND
```

```
  GOSUB WaitDMSMessage
  WHILE (DMSMSG$<>"ICI") AND (DMSMSG$<>"MCI") AND (DMSMSG$ <> "INA") AND (DMSMSG$ <>
"MNA") AND (DMSMSG$ <> "ICC") AND (DMSMSG$ <> "MCC")
    GOSUB WaitDMSMessage
  WEND
  RETURN


'          ==== SUBROUTINE TO CLEAR SCREEN AND COMPUTE LAST SCAN ====

ShowLastPlot:
  CLS
  CALL Highlight("SENDING CLEAR AND COMPUTE MESSAGE")
  LDI$="E"                    ' E is external computer address, that's us
  MI$ ="C"                    ' Follows are C(ommand)
  MD$ ="F"                    ' Key Code
  MQ$ =CHR$(&H34)             ' Clear Screen key
  GOSUB SendMessage           ' send it to DMS
  ANS$ = INPUT$(1, #1)        ' Does DMS ACKnowledge our message
  WHILE ANS$ <> ACK$          ' while not ACKnowledge our message
    GOSUB SendMessage         ' keep sending and trying
    ANS$ = INPUT$(1, #1)        ' Does DMS ACKnowledge our message
  WEND

  LDI$="E"                    ' E is external computer address, that's us
  MI$ ="C"                    ' Follows are C(ommand)
  MD$ ="F"                    ' Key Code
  MQ$ =CHR$(&H23)             ' Compute key
  GOSUB SendMessage           ' send it to DMS
  ANS$ = INPUT$(1, #1)        ' Does DMS ACKnowledge our message
  WHILE ANS$ <> ACK$          ' while not ACKnowledge our message
    GOSUB SendMessage         ' keep sending and trying
    ANS$ = INPUT$(1, #1)      ' Does DMS ACKnowledge our message
  WEND

  GOSUB WaitDMSMessage
  WHILE (DMSMSG$ <> "INA") AND (DMSMSG$ <> "MNA") AND (DMSMSG$ <> "ICC") AND (DMSMSG$
<> "MCC")
    GOSUB WaitDMSMessage
  WEND
  RETURN

'       ==== SUBROUTINE TO DISPLAY HELP ON DMS KEYBOARD FUNCTION  MENU ====

HelpFunctionKey  :
  CLS
  PRINT
  PRINT
  PRINT
  CALL DrawLine("=")
  PRINT
  CALL CenterMSG(" THIS PROGRAM IS ORIGINALLY DESIGNED TO DOWNLOAD DATA OBTAINED")
  CALL CenterMSG(" DURING DIFFUSE REFLECTANCE MEASUREMENT OF PAPER.")
  CALL CenterMSG(" HOWEVER, IT ALSO PROVIDES CONTROLS TO DO OTHER FUNCTION
AVAILABLE")
  CALL CenterMSG(" IN THE VARIAN DMS 100 SPECTROMETER")
```

```
  CALL DrawLine("=")
  PRINT "1. ENSURE THAT THE CONNECTOR ON BOTH DMS100 AND THIS COMPUTER ARE"
  PRINT "   PROPERLY INSTALLED"
  PRINT "2. SWITCH ON DMS 100 AND ALLOW FOR SELF CALIBRATION TO FINISH"
  PRINT "3. SET ALL VARIABLES SUCH AS SCAN SPEED, SLIT WIDTH, MIN AND"
  PRINT "   MAX WAVELENGTH TO SUIT YOUR PARTICULAR REQUIREMENTS"
  PRINT "4. FOR DIFFUSE REFLECTANCE MEASUREMENT, TYPICALLY :"
  PRINT "              * SLIT WIDTH     = 2"
  PRINT "              * WAVELENGTH     = 200 - 700 nm"
  PRINT "              * SOURCE CHANGE = 300 nm"
  PRINT "              * MODE IS SCAN MODE"
  PRINT
  CALL DrawLine("=")
  CALL WaitKey("PRESS ANY KEY TO GO BACK TO MENU")
  RETURN


'            ==== SUBROUTINE TO DISPLAY HELP ON MAIN MENU ====

REM HELP
MainHelp  :
  CLS
  PRINT
  PRINT
  PRINT
  PRINT
  PRINT
  CALL DrawLine("=")
  CALL CenterMSG("SELECTING ANY OF THE DISPLAYED FUNCTION WILL HAVE THE")
  CALL CenterMSG("SAME EFFECT AS IF YOU DO IT DIRECTLY VIA DMS KEYBOARD")
  CALL DrawLine("=")
  PRINT "1. CLEAR SCREEN WILL CLEAR ANY PLOT PREVIOUSLY DRAWN"
  PRINT "2. LOCK KEYBOARD WILL PREVENT ANY ACCESS TO DMS KEYBOARD"
  PRINT "   VERY HANDY IF YOU ARE GOING TO LEAVE THE UNIT FOR SOMETIME"
  PRINT "3. UNLOCK KEYBOARD WILL ALLOW KEYBOARD ACCESS BACK"
  PRINT "4. PLOT TO PRINTER WILL PLOT THE CURRENT SCREEN DISPLAY TO PRINTER"
  PRINT "5. SHOW LAST PLOT WILL CLEAR THE SCREEN AND REDRAW ONLY THE LAST SCAN"
  PRINT
  CALL DrawLine("=")
  CALL WaitKey("PRESS ANY KEY TO GO BACK TO MAIN MENU")
  RETURN

'            ==== SUBROUTINE TO SEND MESSAGE TO DMS ====

REM calculate ByteCount, Checksum and then send it
REM NOTE.., DON'T FORGET TO PUT ";" ON PRINT STATEMENTS DIRECTED TO DMS
REM Otherwise it will send CR/LF to DMS and crash it immediately

SendMessage :
  MESSAGE$ = LDI$ + MI$ + MD$ + MQ$    ' Refers to section 9.2 for message format
  IF MQ$ = "" THEN                     ' If nothing in Message Qualifier's filed
    SUM = (1 +LEN(MESSAGE$) + ASC(LDI$) + ASC(MI$) + ASC(MD$)) MOD 256
  ELSE
    SUM = (1+LEN(MESSAGE$) + ASC(LDI$) + ASC(MI$) + ASC(MQ$) + ASC(MD$)) MOD 256
  END IF
  CSM$ = CHR$(256 - SUM)                                              ' checksum
  REM again.., don't forget ";" in the end of message directed to DMS
  PRINT #1,STX$ + CHR$(1+LEN(MESSAGE$)) + MESSAGE$ + CSM$ + ETX$;
```

```
  'PRINT "MESSAGE SENT"
  RETURN


'            ==== SUBROUTINE TO WAIT DMS INTERMEDIATE MESSAGE ====

REM Waits for DMS message.
REM Use it when you request DMS for functions which when in normal
REM operations (from DMS console), it wil lock its keyboard
REM For example, Scanning, Plotting, BaselineProgram etc
REM No need to be used in :
REM        Locking/unlocking keyboard
REM        Changing ScanMode/MultiMode
REM        Changing Min - Max Value
REM        and any other keys not normally locking DMS keyboard when operated


WaitDMSMessage:
  ANS$ = INPUT$(1, #1)                                              ' get ANS$
  ' PRINT "ITS CURRENT MESSAGE IS = ", ANS$
  WHILE ANS$ <> STX$                          ' While it is not the start of data
    'PRINT "STILL WAITING FOR -START TRANSMISSION- CHARACTER .."
    ANS$ = INPUT$(1, #1)     ' keep asking for it
    'PRINT "ITS CURRENT MESSAGE IS = ", ANS$
  WEND

  DATACOUNT% = ASC(INPUT$(1, #1)) - 4      ' read the byte count, exclude 4 bytes
                                             ' for 3 bytes in 3 fields plus CSM
  DMSMSG$ = INPUT$(3, #1)                         ' read 3 bytes for LDI,LI, MD
  'PRINT " NEXT BYTE COUNT IS = ", DATACOUNT%
  'PRINT "NEXT DMS MESSAGE IS = ", DMSMSG$

  REM getting End of Transmission message
  ANS$ = INPUT$(1, #1)                                              ' get ANS$
  WHILE ANS$ <> ETX$               ' While it is not End of Transmission message
    ANS$ = INPUT$(1, #1)                                        ' keep asking for it
  WEND
  PRINT #1, ACK$;                ' yes, we acknowledged your End of Transmission
  RETURN

'            ==== SUBROUTINE TO DRAW A LINE ACROSS THE SCREEN ====

REM subroutine to draw a line consisting of 80 BORDER$ chars
SUB DrawLine(BORDER$)
  FOR N% =1 TO 80
    PRINT BORDER$;
  NEXT N%
END SUB

'            ==== SUBROUTINE TO NOTIFY USER BEFOE SCANNING ====

REM subroutine attention before scan is performed
PrepareScanning :
  CLS
  CALL DrawLine("=")
  PRINT
  CALL CenterMSG("MAKE SURE YOU HAVE PLACED YOUR SAMPLE")
  PRINT
```

```
  CALL DrawLine("=")
  CALL WaitKey("PRESS ANY KEY TO BEGIN SCAN")
  RETURN

'            ==== SUBROUTINE TO CENTER A MESSAGE STRING ====
SUB CenterMSG(MESSG$)
  SPACE% = INT((80 - LEN(MESSG$))/2)     ' calculate space for centering message
  FOR SPACECOUNT% =1 TO SPACE%
    PRINT " ";
  NEXT SPACECOUNT%
  PRINT MESSG$                             ' print message
END SUB

'            ==== SUBROUTINE TO HIGHLIGHT MESSAGE ====

REM subroutine highlight
SUB Highlight(MESG$)
  COLX% = POS(0)                          ' Get cursor position (column)
  ROWY% = CSRLIN                          ' Get cursor position (row)
  LOCATE 2,3                              ' locate cursor to row 2, column 3
  COLOR 31,0                              ' change color
  CALL CenterMSG(MESG$)                   ' print message to be highlighted
  COLOR 7,0                               ' change color again
  LOCATE ROWY%,COLX%                      ' recover cursor postion
END SUB

'            ==== SUBROUTINE TO ASK USER TO PRESS ANY KEY ====

REM display message and wait for any key to be pressed
SUB WaitKey(MSG$)
  COLX% = POS(0)                          ' Get cursor position (column)
  ROWY% = CSRLIN                          ' Get cursor position (row)
  LOCATE 2,1                              ' locate cursor to row 2, column 3
  COLOR 31,0                                ' change color
  CALL CenterMSG(MSG$)                    ' print message
  COLOR 7,0                               ' change color again
  LOCATE ROWY%,COLX%                      ' recover cursor postion
  WHILE NOT INSTAT
   ' DO NOTHING
  WEND
  PRINT INKEY$
END SUB


'            ==== SUBROUTINE TO DOWNLOAD TRACE BUFFER ====

REM downloading trace buffer

Download:
  CLS
  CALL Highlight("DOWNLOADING  TRACE BUFFER....WAIT")
  LDI$ = "E"                          ' E is external computer address, that's us
  MI$  = "C"                                          ' Follows are C(ommand)
  MD$  = "H"                                       ' Send Trace Buffer Command
  MQ$  = ""                                            ' No Message Qualifier
  GOSUB SendMessage                                          ' send it to DMS
  ANS$ = INPUT$(1, #1)                        ' Does DMS ACKnowledge our message
  WHILE ANS$ <> ACK$                         ' while not ACKnowledge our message
```

```
  ' PRINT "STILL TRYING SENDING -SEND TRACE BUFFER- COMMAND..."
  ' PRINT "ITS CURRENT MESSAGE IS = ", ANS$
  GOSUB SendMessage                                    ' keep sending and trying
  ANS$ = INPUT$(1, #1)                          ' Does DMS ACKnowledge our message
WEND

'PRINT "WAITING FOR -START TRANSMISSION- CHARACTER "
ANS$ = INPUT$(1, #1)                                                  ' get STX$
' PRINT "ITS CURRENT MESSAGE IS = ", ANS$
WHILE ANS$ <> STX$                             ' While it is not the start of data
  'PRINT "STILL WAITING FOR -START TRANSMISSION- CHARACTER .."
  ANS$ = INPUT$(1, #1)                                    ' keep asking for it
  'PRINT "ITS CURRENT MESSAGE IS = ", ANS$
WEND
'PRINT "DMS IS READY TO TRANSMIT DATA"

COUNTER%     = 0                                        'initialise Data counter
DMSMSG$      = ""                                ' initialising DMS message status
K%           = 0                                ' initialising trace buffer counter
J%           = 0                               ' initialising data received counter
TRASH$       =""

'PRINT "READING BYTE COUNT OF THE DATA"
DATACOUNT% = ASC(INPUT$(1, #1)) - 4      ' read the byte count, exclude 4 bytes
                                         ' (INH or IPH plus ETX$
'PRINT "BYTE COUNT VALUE IS = ",DATACOUNT%
'PRINT "READING POSITIVE TRACE BUFFER TRANSFER FROM DMS -IPH- .."
DMSMSG$ = INPUT$(3, #1)                                ' is it INH or IPH we have
'PRINT "ITS CURRENT MESSAGE IS = ", DMSMSG$

WHILE DMSMSG$ = "IPH"                                  ' DMS giving Positve reply
  REM now getting the trace buffer
  FOR N% = 1 TO (DATACOUNT%/4)                ' we are reading it in 4 bytes/loop
    J% =J% + 1
    IF (J% MOD (5 * TAKE%) ) = 1 THEN               ' note dms reads every 0.2 nm
      REM DMS trace buffer is values for every 0.2 nm
      REM so, change the J% MOD 25 line above to suit your need
      REM If you want to read every 1 nm, then change line into
      REM IF (J% MOD 5) = 1 THEN
      REM Note that LOW and HIGH are of type LONG integer

      LOW&  = ASC(INPUT$(1, #1))                   ' read the low mantissa value
      'PRINT "LOW VALUE IS = " ,LOW&
      HIGH& = ASC(INPUT$(1, #1))                  ' read the high mantissa value
      'PRINT "HIGH = ", HIGH&
      THESIGN& = ASC(INPUT$(1, #1))          ' read the sign value . 0 = positive
                                                             ' 80H = negative
      IF THESIGN& = &H80 THEN
        SIGN& = -1
      ELSE
        SIGN& = +1
      END IF

      'PRINT "SIGN = ", SIGN&
      EXPON& = ASC(INPUT$(1, #1))                    ' read the exponent value

      IF EXPON& > 127 THEN
        EXPON& = EXPON& - 256
```

```
    END IF
    'PRINT "EXPON = ", EXPON&

    REM The above values are 2 , 16 unsigned bits
    REM We have added absolute value below for safety
    REM infact, it will give wrong value in Turbo Basic
    REM if you do not take the absolute value

    MANTISSA = (LOW& + (256 * HIGH&))/65536

    REM the way spectra value is calculated is explained in page 50
    REM basically it is performed as folows:
    REM 1. Convert all reading (low, high etc) into ASCII value
    REM    note that value without letter H is already in decimal value of ASCII
    REM    see ASCII table value if you want to convert from Hexadecimal to
    REM    decimal value.
    REM 2. Mantissa = (Low + 256 * High )/65536
    REM 3. Actual value is = Mantissa * 2^ Exponent

    REM we multiply with 100 for easier reading, since actual data ranging only
    REM from 0.5 (80000H) to 0.999(FFFFH). See page 50

    K% = K% + 1
    'PRINT "K VALUE IS = ", K%
    SPECTRAVAL(K%) = 100! * SIGN& * MANTISSA * (2^ EXPON&)
    'PRINT "SPECTRA VALUE IS = ",SPECTRAVAL(K%)
    'PRINT USING "###.##" ; SPECTRAVAL(K%)
  ELSE
    'PRINT "TRASHING UNUSED VALUE ..."
    TRASH$ = INPUT$(4, #1)                          ' we throw away this data
  END IF
NEXT N%

REM receive checksum. it is not checked for this version
REM But probably ned to be added in future version

CSM% = ASC(INPUT$(1, #1))                           ' receive checksum value
'PRINT "CHECKSUM RECEIVED OF VALUE =" ,CSM%

REM receive End of transmission Char (ETX$).
REM it is not checked for this version , we trust DMS ...
REM By the way.., the checking code is included for you
REM SInce this version works okay.., we do not use it

ANS$ = INPUT$(1, #1)                                          ' receive ETX$
' PRINT "ITS CURRENT MESSAGE IS = ", ANS$
' WHILE ANS$ <> ETX$                          ' While it is not the end of data
  ' PRINT "STILL WAITING FOR -END TRANSMISSION- CHARACTER .."
  ' ANS$ = INPUT$(1, #1)                                  ' keep asking for it
  ' PRINT "ITS CURRENT MESSAGE IS = ", ANS$
' WEND
' PRINT "END OF TRANSMISSION CHAR = ", ANS$

REM tell DMS that we acknowledged its message
REM Not to forget the semi colon !!
PRINT #1, ACK$;

REM at this point, DMS should be ready for further data (if any)
```

```
    REM so ask it the Start Transmission sign (STX$)

    ANS$ = INPUT$(1, #1)                                              ' get ANS$
    'PRINT "ITS CURRENT MESSAGE IS = ", ANS$
    WHILE ANS$ <> STX$                        ' While it is not the start of data
      'PRINT "STILL WAITING FOR -START TRANSMISSION- CHARACTER .."
      ANS$ = INPUT$(1, #1)                                  ' keep asking for it
      'PRINT "ITS CURRENT MESSAGE IS = ", ANS$
    WEND


    DATACOUNT% = ASC(INPUT$(1, #1)) - 4   ' read the byte count, exclude 4 bytes
                                          ' (I,N,H or I,P,H plus ETX$
    DMSMSG$ = INPUT$(3, #1)               ' is it INH or IPH we have
    ' PRINT " NEXT BYTE COUNT IS = ", DATACOUNT%
    ' PRINT "NEXT DMS MESSAGE IS = ", DMSMSG$
  WEND

  'PRINT "MESSAGE IS NO LONGER IPH, IT IS = ", DMSMSG$
  REM getting End of Transmission message
  ANS$ = INPUT$(1, #1)       ' get ANS$
  WHILE ANS$ <> ETX$         ' While it is not End of Transmission message
    ANS$ = INPUT$(1, #1)     ' keep asking for it
  WEND
  PRINT #1, ACK$;             ' yes, we acknowledged your End of Transmission

  TOTALDATA% =K%
  'PRINT "TOTAL NUMBER OF DATA IS = " , TOTALDATA%
  'PRINT "                                TRANSFER DATA COMPLETED"
  BEEP 2
  RETURN


'          ==== SUBROUTINE TO MAKE INPUT LETTER UPPERCASE ====

SUB UpperCase(LETTER$)
  IF (ASC(LETTER$) >96) AND (ASC(LETTER$) <123) THEN ' lower case
    LETTER$ = CHR$(ASC(LETTER$) - 32)     ' Make letter upperCase
  END IF
END SUB

'     ==== SUBROUTINE TO ASK FILE NAME OUTPUT FOR TRACE BUFFER DATA ====

WhichOutput:

  DO UNTIL (CHOICE$ ="E")
  CLS
  INPUT "SELECT OUTPUT ,S(creen) , D(isk) or E(xit) = ", CHOICE$
  CALL UpperCase(CHOICE$)                                  ' make input Uppercase
  WHILE (CHOICE$ <> "S") AND (CHOICE$ <> "D") AND (CHOICE$ <> "E")
    BEEP 1
    COLX% = POS(0)
    ROWY% = CSRLIN
    LOCATE (ROWY%-1),1
    INPUT "SELECT OUTPUT ,S(creen) , D(isk) or E(xit) = ", CHOICE$
    CALL UpperCase(CHOICE$)
    LOCATE ROWY%,COLX%
  WEND
```

```
  IF (CHOICE$ = "S") THEN
      GOSUB DisplayToScreen
  ELSEIF (CHOICE$ = "D") THEN
      GOSUB SaveToDisk
  ELSE
      'DO NOTHING
  END IF
  LOOP
RETURN
'               ==== SUBROUTINE TO SAVE DATA TO DISK ====

SaveToDisk :
  CLS
  CALL DrawLine("*")
  PRINT
  CALL CenterMSG(" ENTER THE NAME OF THE FILE FOR THIS DATA")
  CALL CenterMSG(" IF THE FILE NAME SPECIFIED IS NOT PRESENT, IT WILL BE CREATED.")
  CALL CenterMSG(" IF THERE IS FILE WITH THE SAME NAME, IT WILL BE APPENDED.")
  PRINT
  CALL DrawLine("*")
  INPUT "ENTER NAME FOR THIS DATA = ", OutName$
  WHILE OutName$ =""
    BEEP 1
    INPUT "INVALID NAME, RE-ENTER NAME FOR THIS DATA = ", OutName$
  WEND
  OPEN OutName$ FOR APPEND AS #2

  PRINT #2, "THIS FILE WAS CREATED ON "; DATE$;
  PRINT #2, "  AT "; TIME$
  PRINT #2,
  FOR K% =1 TO TOTALDATA%
    PRINT #2, USING "+###.###"; SPECTRAVAL(K%)
  NEXT K%
  CLOSE #2
RETURN
'               ==== SUBROUTINE TO DISPLAY DATA TO SCREEN ====

DisplayToScreen:
  CLS
  SCRN%=INT(TOTALDATA%/19)
  COUNTER%=0
  FOR L% =1 TO SCRN%
    CALL Drawline("=")
    PRINT "DATA INDEX","% TRANSMITTANCE"
    CALL Drawline("=")
    FOR M% =1 TO 19
      COUNTER%= COUNTER% +1
      PRINT COUNTER%,
      PRINT USING "+###.###"; SPECTRAVAL(COUNTER%)
    NEXT M%
    PRINT "Strike any key when ready ...."
    WHILE NOT INSTAT
      ' do nothing
    WEND
    JUNKKEY$= INKEY$
    CLS
  NEXT L%
```

```
  CALL Drawline("=")
  PRINT "DATA INDEX","% TRANSMITTANCE"
  CALL Drawline("=")
  REMAIN% = TOTALDATA% - COUNTER%
  FOR Z% =1 TO REMAIN%
    COUNTER%=COUNTER%+1
    PRINT COUNTER%,
    PRINT USING "+###.###"; SPECTRAVAL(COUNTER%)
  NEXT Z%
  CALL DrawLine("=")
  PRINT "Strike any key to return to output options ...."
  WHILE NOT INSTAT
    ' do nothing
  WEND
  JUNKKEY$= INKEY$
  RETURN

'            ==== SUBROUTINE TO AUTODOWNLOAD TRACE BUFFER ====
REM Scan and automatically receive trace buffer
AutoDownload :
  CLS
  GOSUB LockDMS
  GOSUB StartScan
  GOSUB Download
  GOSUB UnlockDMS
  CHOICE$=""
  GOSUB WhichOutput
  RETURN


'              ==== SUBROUTINE TO SEND START SCAN ====
REM Start scan is an example of process which DMS locks its keyboard when
REM it is being performed.
REM During the process, DMS sends various messages which we must take care of.
REM Since the Message format is known (always STX-ByteCount-3 bytes status -
REM CSM -ETX, we have employed the WaitDMSMEssage to take care of any messages sent
REM during process.
REM Without this.., it will just crash DMS

StartScan:
  CLS
  CALL Highlight("SENDING START SCAN MESSAGE")
  LDI$="E"                    ' E is external computer address, that's us
  MI$ ="C"                    ' Follows are C(ommand)
  MD$ ="F"                    ' Lock Keyboard message
  MQ$ =CHR$(&H2E)             ' Command contains no data, so leave out
  GOSUB SendMessage           ' send it to DMS
  ANS$ = INPUT$(1, #1)        ' Does DMS ACKnowledge our message
  WHILE ANS$ <> ACK$          ' while not ACKnowledge our message
    'PRINT "DMS IS HAVING PROBLEM LOCKING ITS KEYBOARD, STILL TRYING = "
    'PRINT 'ITS CURRENT MESSAGE IS = ", ANS$
    GOSUB SendMessage         ' keep sending and trying
    ANS$ = INPUT$(1, #1)        ' Does DMS ACKnowledge our message
  WEND
  CLS
  CALL Highlight("NOW SCANNING .... WAIT")
  'PRINT "DMS KEYBOARD IS SUCCESFULY LOCKED"
  GOSUB WaitDMSMessage
```

```
  WHILE (DMSMSG$ <> "ICC") AND (DMSMSG$ <> "MCC")     ' DMS identity can be either
                                                      ' I or M, see manual
    GOSUB WaitDMSMessage
  WEND
  BEEP 2
  RETURN


'              ==== SUBROUTINE TO SET DMS SCAN MODE ====

REM Set Scan Mode is an example of process which DMS does not lock its keyboard
REM when it is being performed.
REM Similar to what we have in Locking and Unlocking DMS keyboard, no need to
REM employ WaitDMSMessage in here

SetScanMode:
  CLS
  CALL Highlight("SENDING SET SCAN MODE MESSAGE")
  LDI$="E"                    ' E is external computer address, that's us
  MI$ ="C"                    ' Follows are C(ommand)
  MD$ ="F"                    ' Key Code
  MQ$ =CHR$(&H26)             ' HEX 26 is Scan Mode key, see p 49 DMS manual
  GOSUB SendMessage           ' send it to DMS
  ANS$ = INPUT$(1, #1)        ' Does DMS ACKnowledge our message
  WHILE ANS$ <> ACK$          ' while not ACKnowledge our message
    'PRINT "DMS IS HAVING PROBLEM SETTING ITS KEY, STILL TRYING = "
    'PRINT 'ITS CURRENT MESSAGE IS = ", ANS$
    GOSUB SendMessage         ' keep sending and trying
    ANS$ = INPUT$(1, #1)        ' Does DMS ACKnowledge our message
  WEND
  'PRINT "DMS KEY IS SUCCESFULY SET"
  RETURN


'            ==== SUBROUTINE TO DO BASELINE PROGRAMMING ====

BaseLineProg:
  CLS
  CALL Highlight("RUNNING BASELINE PROGRAM, PLEASE WAIT .....")
  LDI$="E"                    ' E is external computer address, that's us
  MI$ ="C"                    ' Follows are C(ommand)
  MD$ ="F"                    ' Key Code
  MQ$ =CHR$(&H0F)             ' HEX OF is Scan Mode key, see p 49 DMS manual
  GOSUB SendMessage           ' send it to DMS
  ANS$ = INPUT$(1, #1)        ' Does DMS ACKnowledge our message
  WHILE ANS$ <> ACK$          ' while not ACKnowledge our message
    'PRINT "DMS IS HAVING PROBLEM SENDING BASELINE PROG MSG , STILL TRYING = "
    'PRINT 'ITS CURRENT MESSAGE IS = ", ANS$
    GOSUB SendMessage         ' keep sending and trying
    ANS$ = INPUT$(1, #1)        ' Does DMS ACKnowledge our message
  WEND
  'PRINT "BASELINE PROG MSG IS SENT SUCCESFULY"
  GOSUB WaitDMSMessage
  WHILE (DMSMSG$ <> "ICC") AND (DMSMSG$ <> "MCC")
    GOSUB WaitDMSMessage
  WEND
  RETURN
```

```
'              ==== SUBROUTINE TO READ WHATEVER DMS SENDS VI RS232 ====
REM use this routine to analyse DMS behaviour when its key is pressed
REM or when a task is being carried.
REM The easiest way is to open COM1 and go to this routine.
REM Then perform normal task via DMS Keyboard and observe its output.
ReadJunk:
  JUNK$ = INPUT$(1, #1)       ' get ANS$
  WHILE NOT INSTAT          ' While key is not pressed
    PRINT "JUNK = ", JUNK$
    JUNK$ = INPUT$(1, #1)     ' keep reading COM1 line
  WEND
  RETURN


'            ==== SUBROUTINE TO CLOSE CONNECTION TO DMS100 ====

REM closing connection
CloseDMS :
  CLS
  CLOSE #1
  RETURN
```

Appendix C

Analytical Solution For The Differential Equations Of Equilibrium Kinetic Models

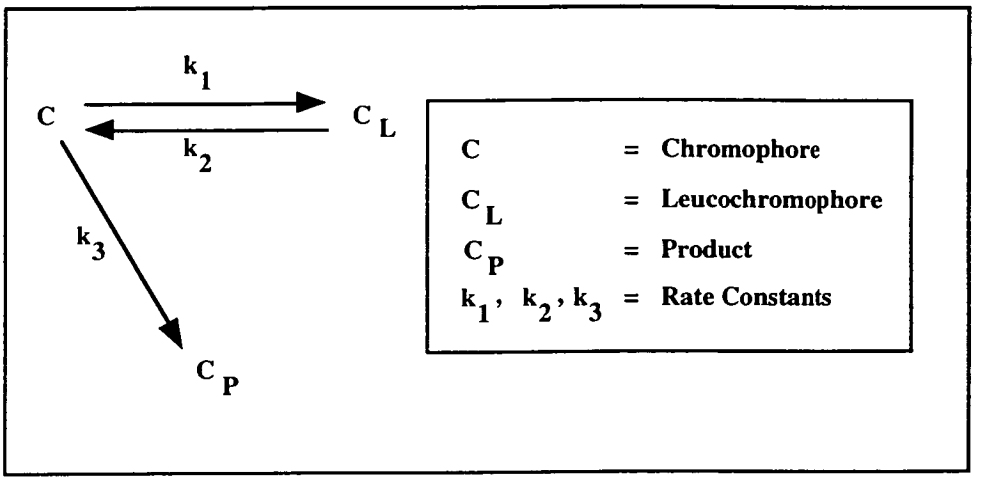

The concentration of each species with respect to time are given in the following set of differential equations.

Rate of the disappearance of chromophore C :

$$-\frac{dC}{dt} = k_1C - k_2C_L + k_3C \qquad \text{(i)}$$

Rate of the disappearance of leucochromophore C_L :

$$-\frac{dC_L}{dt} = k_2C_L - k_1C \qquad \text{(ii)}$$

Rate of the formation of product C_P :

$$\frac{dC_P}{dt} = k_3C \qquad \text{(iii)}$$

To solve the above set of differential equations, Laplace transform will be used. The use of Laplace transform will simplify the process, since the transformed equations can be manipulated using simple algebra rules.

The Laplace transform of (i) :

$$-(sC - C_0) = k_1C - k_2C_L + k_3C \qquad \text{(iv)}$$

The Laplace transform of (ii) :

$$-(sC_L - C_{L_0}) = k_2C_L - k_1C \qquad \text{(v)}$$

The Laplace transform of (iii) :

$$(sC_P - C_{P_0}) = k_3 C \qquad \text{(vi)}$$

Let us consider equation (v) where

$$- (sC_L - C_{L_0}) = k_2 C_L - k_1 C$$

that is

$$- sC_L + C_{L_0} = k_2 C_L - k_1 C$$

on rearranging, we have

$$sC_L + k_2 C_L = k_1 C + C_{L_0}$$

and therefore

$$C_L = \frac{k_1 C + C_{L_0}}{s + k_2} \qquad \text{(vii)}$$

Now, consider equation (iv), where we have

$$- (sC - C_0) = k_1 C - k_2 C_L + k_3 C$$

$$= (k_1 + k_3) C - k_2 C_L$$

Substituting the value of C_L obtained from (vii) to this equation we have

$$- s C + C_0 = (k_1 + k_3) C - k_2 \frac{k_1 C + C_{L_0}}{s + k_2}$$

rearranging to give

$$C_0 = (s + k_1 + k_3) C - \frac{k_1 k_2}{s + k_2} C - \frac{k_2 C_{L_0}}{s + k_2}$$

$$= \frac{[(s + k_1 + k_3) (s + k_2) - k_1 k_2]}{s + k_2} C - \frac{k_2 C_{L_0}}{s + k_2} \qquad \text{(viii)}$$

on bringing the $- \frac{k_2 C_{L_0}}{s + k_2}$ term to the left hand side, we have

$$C_0 + \frac{k_2 C_{L_0}}{s + k_2} = \frac{[(s + k_1 + k_3) (s + k_2) - k_1 k_2]}{s + k_2} C$$

that is

$$\frac{C_0 (s + k_2) + k_2 C_{L_0}}{s + k_2} = \frac{[(s + k_1 + k_3) (s + k_2) - k_1 k_2]}{s + k_2} C$$

and hence

$$C_0 (s + k_2) + k_2 C_{L_0} = [(s + k_1 + k_3) (s + k_2) - k_1 k_2] C \quad \text{(ix)}$$

Solving for C in equation (ix) we have

$$C = \frac{C_0 (s + k_2) + k_2 C_{L_0}}{(s + k_1 + k_3) (s + k_2) - k_1 k_2}$$

$$= \frac{C_0 s + C_0 k_2 + k_2 C_{L_0}}{(s + k_1 + k_3) (s + k_2) - k_1 k_2}$$

$$= \frac{C_0 s + k_2 (C_0 + C_{L_0})}{(s + k_1 + k_3) (s + k_2) - k_1 k_2}$$

$$C = \frac{C_0 s + H}{(s + k_1 + k_3) (s + k_2) - k_1 k_2} \quad \text{(x)}$$

where

$$H = k_2 (C_0 + C_{L_0})$$

Now, let us consider the denominator in (x)

$$(s + k_1 + k_3)(s + k_2) - k_1 k_2 = s^2 + s k_2 + k_1 s + k_1 k_2 + k_3 s + k_3 k_2 - k_1 k_2$$

$$= s^2 + (k_1 + k_2 + k_3) s + k_2 k_3$$

$$= s^2 + \mu s + \gamma \qquad \text{(xi)}$$

where

$\mu = (k_1 + k_2 + k_3)$ and $\gamma = k_2 k_3$

For the inverse Laplace transform, the denominator is required in the for

$$(s - a)(s - b)$$

i.e.

$$s^2 - (a + b) s + ab \qquad \text{(xii)}$$

by referring equation (xii), we have in equation (xi)

$$\mu = -(a + b) \qquad \text{(xiii)}$$

and

$$\gamma = ab \quad \text{or} \quad b = \frac{\gamma}{a} \qquad \text{(xiv)}$$

now, we have equation (xiii) as

$$a + b + \mu = 0$$

since $b = \frac{\gamma}{a}$, therefore

$$a + \frac{\gamma}{a} + \mu = 0$$

and on multiplying by a, we have

$$a^2 + \mu a + \gamma = 0$$

The value of a, can then be calculated as follows

$$a = \frac{-\mu \pm \sqrt{\mu^2 - 4\gamma}}{2}$$

taking only the positive root, we have

$$a = \frac{-\mu + \sqrt{\mu^2 - 4\gamma}}{2}$$

$$= \frac{-p + q}{2}$$

where

$p = \mu$ and $q = \sqrt{\mu^2 - 4\gamma}$

but from (xiii)

$$b = -\mu - a$$

$$= -\mu - \frac{(-p + q)}{2}$$

$$= -p + \frac{p}{2} - \frac{q}{2}$$

$$= -\frac{p}{2} - \frac{q}{2}$$

$$= -\frac{(p + q)}{2}$$

thus

$$a = -\frac{(p - q)}{2} \text{ and } \quad b = -\frac{(p + q)}{2}$$

now (x) can be written as

$$C = \frac{C_0 s}{(s-a)(s-b)} + \frac{H}{(s-a)(s-b)}$$

Using the inverse Laplace transform, we have

$$C = C_0 \left[\frac{b e^{bt} - a e^{at}}{b-a} \right] + \frac{H}{b-a} \left(e^{bt} - e^{at} \right)$$

$$= C_0 \frac{b e^{bt}}{b-a} - C_0 \frac{a e^{at}}{b-a} + \frac{H e^{bt}}{b-a} - \frac{H e^{at}}{b-a}$$

And finally this gives us the relation of the value of C at any given time as

$$C = \frac{e^{bt} (b C_0 + H) - e^{at} (a C_0 + H)}{(b-a)}$$

where

$$a = -\frac{(p-q)}{2}$$

$$b = -\frac{(p+q)}{2}$$

$$p = k_1 + k_2 + k_3$$

$$q = \sqrt{p^2 - 4 (k_2 k_3)}$$

and

$$H = k_2 (C_0 + C_{L_0})$$

Appendix D

Listing Of Simplex Curve Fitting Program

```
/*
This program was written by Dr. Michael Whitbeck of the Desert
Research Institute at Reno, Nevada USA. It is a C port of the
original version written in Pascal by Cacheci and Cacheris (Byte
Magazine, May Edition 1984, page 340).

The description of the Simplex algorithm is given on the following
paper:
      Nedler, J. A and Mead, R., Computer Journal 7:308 (1965).

*/
```

File 'Simplex.h'

```
#include <math.h>
#include <stdio.h>


#define MNP    200
#define ALPHA  1.0
#define BETA   0.5
#define GAMMA  2.0
#define LW     5
#define ROOT2  1.414214


extern int M,NVPP,N;
extern int       *h, *l;
extern int       np, maxiter, niter;
extern double    *next, *mean, *error, *maxerr, *step, **simp;
extern double    **data;
extern double     C0, CL0;
extern FILE      *fpdata;


extern double    f();
```

'Main .C' (the main simplex routine)

```
#include <stdio.h>
#include "simplex.h"

double **matrix(nr,nc)
{
int i;
double **m;
m = (double **) malloc((unsigned) (nr+1)*sizeof(double *));
for(i = 0; i <= nr; i++){
  m[i] = (double *)malloc((unsigned)(nc+1)*sizeof(double));
  if (!m[i]){
    printf("out of memory\n"); exit(0);
  }
}
return m;
}

int M, NVPP, N, *h, *l;
double *next, *mean, *error, *maxerr, *step, **data, **simp;
double CL0, C0;

main(argc,argv)
int argc; char *argv[];
{
extern int sfit();

M = 3; NVPP = 2; N = M+1;
h = (int *) malloc(N*sizeof(int));
l = (int *) malloc(N*sizeof(int));
next = (double *)malloc(N*sizeof(double));
mean  = (double *)malloc(N*sizeof(double));
error = (double *)malloc(N*sizeof(double));
maxerr = (double *)malloc(N*sizeof(double));
step = (double *)malloc(N*sizeof(double));
simp = matrix(N,N);
data = matrix(200,NVPP);

sfit(argv[1]);

free(h); free(l); free(next); free(mean);
free(error); free(maxerr); free(step);


}
```

File 'Enter.c'

```
#include "simplex.h"

enter(fname)
char *fname;
{
     register int   i, j;

     printf("EQUILIBRIUM MODEL 1 C=CL ; CL -> CP\n");
     printf("SIMPLEX Optimization for \"\%s\"\n",fname);
     fscanf(fpdata,"%F %F", &C0, &CL0);
     printf("starting values: %10.4f %10.4f\n", C0,CL0);
     fscanf(fpdata, "%d", &maxiter);
     for (i=0 ; i<M ; i++)  fscanf(fpdata, "%F", &simp[0][i]);


     for (i=0 ; i<M ; i++)  fscanf(fpdata, "%F", &step[i]);

     printf("\n\n");

     for (i=0 ; i<N ; i++)  fscanf(fpdata, "%F", &maxerr[i]);

     np = 0;
     while (!feof(fpdata)) {
          for (j=0 ; j<NVPP ; j++) {
               if (fscanf(fpdata, "%F", &data[np][j]) == EOF)
                    break;
          }
          np++;
     }
     np--;

}
```

File 'First.c'

```
#include "simplex.h"

first()
{
     register int   i, j;

     printf("Starting Simplex\n");
     for (j=0 ; j<N ; j++) {
          printf(" simp[%d]", j+1);
          for (i=0 ; i<N ; i++) {
               if ((i+1) % LW == 0)
                    printf("\n");
               printf("  %e", simp[j][i]);
          }
          printf("\n");
     }
     printf("\n");
}
```

File 'MakeFile'

```
CFLAGS= -g
SRC= sfit.c enter.c    new_vert.c report.c f.c  main.c \
      order.c  sum_resi.c

FILES= sfit.o enter.o    new_vert.o report.o f.o  main.o \
      order.o  sum_resi.o

simplex: $(FILES)
      cc -o simplex $(FILES) -lm

hc: $(SRC)
      vgrind -lc -Plw268 $(SRC)
```

File 'Order.c'

```
#include "simplex.h"

order()
{
     register int   i, j;

     for (j=0 ; j<N ; j++)
          for (i=0 ; i<N ; i++) {
               if (simp[i][j] < simp[l[j]][j])
                    l[j] = i;
               if (simp[i][j] > simp[h[j]][j])
                    h[j] = i;
          }
}
```

File 'New_Vert.c'

```
#include "simplex.h"

new_vertex()
{
     register int   i;

     for (i=0 ; i<N ; i++) {
          simp[h[N-1]][i] = next[i];
     }
}
```

File 'Report.c' (executes output report)

```
#include "simplex.h"

report()
{
     register int   i, j;
     double         y, dy, sigma;

     printf("\nProgram exited after %d iterations.\n\n", niter);

     printf("The mean is:");
     for (i=0 ; i<N ; i++) {
          if ((i+1) % LW == 0)
               printf("\n");
          printf("  %e", mean[i]);
     }
     printf("\n\n");

     printf("The estimated fractional error is:");
     for (i=0 ; i<N ; i++) {
          if ((i+1) % LW == 0)
               printf("\n");
          printf("  %e", error[i]);
     }
     printf("\n\n");

     printf("\n\n");

     printf("   #          X              Y              Y''
DY\n");
     sigma = 0.0;
     for (i=0 ; i<np ; i++) {
          y = f(mean, data[i][0]);
          dy = data[i][1] - y;
          sigma += (dy*dy);
          printf("%4d  ", i);
          printf("%13e  %13e  ", data[i][0], data[i][1]);
          printf("%13e  %13e\n", y, dy);
     }
     printf("\n");
     sigma = sqrt(sigma);
     printf("The standard deviation is %e\n\n", sigma);
     sigma /= sqrt((double) (np-M));
     printf("The estimated error of the function is %e\n\n",
sigma);
}
```

File 'Sfit.c'

```
#include "simplex.h"

#define until(x) while (!(x))

int       np, maxiter, niter;

FILE      *fpdata;

sfit(name)
char  *name[];
{
   register int   i, j, done;
   double *center, *p, *q;

   center = (double *)malloc((unsigned)N*sizeof(double));
   p = (double *)malloc((unsigned)N*sizeof(double));
   q = (double *)malloc((unsigned)N*sizeof(double));

   if ((fpdata = fopen(name, "r")) == NULL) {
      fprintf(stderr, "simplex: can't open %s\n", name);
      exit(1);
   }

   enter(name);

   /* First Vertex */
   sum_residual(simp[0]);

   /* Compute offset of Vertices */
   for (i=0 ; i<M ; i++) {
      p[i] = step[i] * (sqrt((double) N) + M - 1) / (M * ROOT2);
      q[i] = step[i] * (sqrt((double) N) - 1) / (M * ROOT2);
   }

   /* All Vertices of the Starting Simplex */
   for (i=1 ; i<N ; i++) {
      for (j=0 ; j<M ; j++)
         simp[i][j] = simp[0][j] + q[j];
      simp[i][i-1] = simp[0][i-1] + p[i-1];
      sum_residual(simp[i]);
   }

   /* Preset */
   for (i=0 ; i<N ; i++) {
      l[i] = 1;
      h[i] = 1;
   }
   order();

   niter = 0;
```

```
    /* Iterate */
    do {
       /* Wish it were True */
       done = 1;
       niter++;

       /* Compute Centroid...Excluding the Worst */
       for (i=0 ; i<N ; i++)
          center[i] = 0.0;
       for (i=0 ; i<N ; i++)
          if (i != h[N-1])
             for (j=0 ; j<M ; j++)
                center[j] += simp[i][j];

       /* First Attempt to Reflect */
       for (i=0 ; i<N ; i++) {
          center[i] /= M;
          next[i] = (1.0+ALPHA) * center[i] - ALPHA * simp[h[N-
1]][i];
       }
       /* changed from plural to singular 9-28-89
       sum_residuals(next);
       */
       sum_residual(next);

       if (next[N-1] <= simp[l[N-1]][N-1]) {
          new_vertex();
          for (i=0 ; i<M ; i++)
             next[i] = GAMMA * simp[h[N-1]][i] + (1.0-GAMMA) *
center[i];
          sum_residual(next);
          if (next[N-1] <= simp[l[N-1]][N-1])
             new_vertex();
       }
       else {
          if (next[N-1] <= simp[h[N-1]][N-1])
             new_vertex();
          else {
             for (i=0 ; i<M ; i++)
                next[i] = BETA * simp[h[N-1]][i] + (1.0-BETA) *
center[i];
             sum_residual(next);
             if (next[N-1] <= simp[h[N-1]][N-1])
                new_vertex();
             else {
                for (i=0 ; i<N ; i++) {
                   for (j=0 ; j<M ; j++)
                      simp[i][j] = BETA * (simp[i][j] + simp[l[N-
1]][j]);
                   sum_residual(simp[i]);
                }
             }
```

```
            }
         }

         order();

         /* Check For Convergence */
         for (j=0 ; j<N ; j++) {
            error[j] = (simp[h[j]][j] - simp[l[j]][j]) /
simp[h[j]][j];
            if (done)
               if (error[j] > maxerr[j])
                  done = 0;
         }

   } until(done || (niter == maxiter));

   /* Average Each Parameter */
   for (i=0 ; i<N ; i++) {
      mean[i] = 0.0;
      for (j=0 ; j<N ; j++)
         mean[i] += simp[j][i];
      mean[i] /= N;
   }

   report();
free(center);free(p);free(q);
}
```

File 'Sum_Resid.c'

```
#include "simplex.h"

#define sqr(x) ((x) * (x))

sum_residual(x)
double    *x;
{
     register int   i;

     x[N-1] = 0.0;

     for (i=0 ; i<np ; i++)
          x[N-1] += sqr(f(x, data[i][0]) - data[i][1]);
/* mod to force all params to be > 0 */
     for (i=0 ; i< M ; i++)
      {
      if (x[i] < 0.0) x[N-1]= 9.999e99;
      }
}
```

File 'M1f.c'
(contains the explicit equations for equilibrium model #1 to be solved by the simplex algorithm).

```
#include "simplex.h"

double f(x, d)
double    *x;
double   d;
{

/* C = CL; CL -> CP  model */

float p,prod,h,q,a,b,result;
float k1,k2,k3,t;

t =  d;
k1 = x[0];
k2 = x[1];
k3 = x[2];

p    = k1+k2+k3;
prod = k1*k3;
h    = (k2+k3) + (k2 *CL0/C0);
q    = sqrt(p*p-4.0*prod);
a    = -(p-q)/2.0;
b    = -(p+q)/2.0;

result= C0/(b-a) *  (exp(b*t)*(b+h)-exp(a*t)*(a+h));

return (result);
}
```

Program 'M2f.c'
(contains the explicit equations for equilibrium model #2 to be solved by the simplex algorithm).

```
#include "simplex.h"

double f(x, d)
double    *x;
double   d;
{

/* C = CL; C -> CP  model */

float p,prod,h,q,a,b,result;
float k1,k2,k3,t;

t =  d;
k1 = x[0];
k2 = x[1];
k3 = x[2];

p    = k1+k2+k3;
prod = k2*k3;
h    = (C0+CL0)*k2;
q    = sqrt(p*p-4.0*prod);
a    = -(p-q)/2.0;
b    = -(p+q)/2.0;

result= (exp(b*t)*(C0*b+h)-exp(a*t)*(C0*a+h))/(b-a);

return (result);
}
```

Program 'M3f.c'
(contains the explicit equations for the two chromophore consecutive reaction model to be solved by the simplex algorithm).

```
#include "simplex.h"

double f(x, d)
double    *x;
double   d;
{

/* C1 -> C2;  C2 -> CP;  C1 -> CP  model */

float a, b,h,result;
float k1,k2,k3,t;

t =  d;
k1 = x[0];
k2 = x[1];
k3 = x[2];

a = -(k1 + k2);
b = - k3;
h = (C20 * -a) + (C10 * k2);

result=( C10 * exp(a*t) ) + (exp(b*t)/(b-a))*(C20*b+h)-
(exp(a*t)/(b-a))*(C20*a+h);

return (result);
}
```

Sample Input File

```
10.63    0         0
1000
0.01     0.01      0.001
0.001    0.001     0.0005
1e-05    1e-05     1e-06     1e-04
0      10.63
5      9.51
10     8.73
15     8.64
20     8.10
30     7.80
60     6.48
120    4.71
240    3.44
420    2.97
```

Explanation of Input File

Line 1

```
  10.63  =  initial value for chromophoric group C
      0  =  initial value for leuco-chromophoric group CL
      0  =  initial value for chromophoric products CP
```

Line 2

```
   1000  =  maximum number of iterations allowed
```

Line 3

```
   0.01  =  initial guess for k1
   0.01  =  initial guess for k2
  0.001  =  initial guess for k3
```

Line 4

```
  0.001  =  step increment for k1
  0.001  =  step increment for k2
 0.0005  =  step increment for k3
```

Line 5

```
  1e-05  =  maximum error allowed in k1
  1e-05  =  maximum error allowed in k2
  1e-06  =  maximum error allowed in k3
  1e-04  =  maximum total error allowed
```

Lines 6-15

contains the raw data (time in minutes, light absorption coefficient) to be fitted.

```
0      10.63
5      9.51
```

10	8.73
15	8.64
20	8.10
30	7.80
60	6.48
120	4.71
240	3.44
420	2.97

Sample Output File "2gLpH10.opt"

```
EQUILIBRIUM MODEL 2  C <-> CL;   C -> CP
SIMPLEX Optimisation for "2gLpH10"
Starting values:10.63   0.0000      0.0000


Program exited after 122 iterations.

The mean is: 1.187054e-02      1.963894e-02      3.261121e-03

The estimated fractional error is: 4.468377e-07   4.504017e-07
                                   6.331946e-07   1.052956e-05
```

#	X	Y	Y''	DY
0	0.000000e+00	1.063000e+01	1.063000e+01	-1.144409e-07
1	5.000000e+00	9.510000e+00	9.888348e+00	-3.783476e-01
2	1.000000e+01	8.730000e+00	9.249465e+00	-5.194650e-01
3	1.500000e+01	8.640000e+00	8.698060e+00	-5.806004e-02
4	2.000000e+01	8.100000e+00	8.221127e+00	-1.211266e-01
5	3.000000e+01	7.800000e+00	7.448082e+00	+3.519176e-01
6	6.000000e+01	6.480000e+00	6.051359e+00	+4.286413e-01
7	1.200000e+02	4.710000e+00	4.900240e+00	-1.902404e-01
8	2.400000e+02	3.440000e+00	3.813954e+00	-3.739539e-01
9	4.200000e+02	2.970000e+00	2.692344e+00	+2.776556e-01

```
The standard deviation is 9.997949e-01

The estimated error of the function is 3.778870e-01
```

Explanation of Output

Line 1

Model Scheme = C <-> CL; C -> CP

Line 2

"2gLpH10" = input file

Line 3

10.63 = initial Value of C
0.0000 = initial Value of CL
0.0000 = initial Value of CP

Line 4

122 = no. of iterations required for optimisation of fit

Line 5

1.187054e-02 = fitted value of k_1
1.963894e-02 = fitted value of k_2
3.261121e-03 = fitted value of k_3

Line 6

4.468377e-07 = fractional error in k_1
4.504017e-07 = fractional error in k_2
6.331946e-07 = fractional error in k_3
1.052956e-05 = fractional error in the function

Lines 7 - 17

contains the raw data and fitted data points

# = data set number
X = x - co-ordinate (time in minutes)
Y = y - co-ordinate (light absorption coefficient)
Y'' = model values of Y calculated using k_1, k_2, k_3
DY = delta y (Y-Y'')

Line 18

9.997949e-01 = standard deviation in the fit

Line 19

3.778870e-01 = standard error in the function

Appendix E

Supplementary Table for The Molecular Orbital Calculations

Supplementary Table. Selected parameters in the optimised geometries (Figure 6.13).

		1-cis	1-trans	2	3	4	5-cis	5-trans
	MNDO	1.479	1.481	1.480	1.483	1.540	1.500	1.500
C2-C3	PM3	1.464	1.459	1.461	1.474	1.517	1.485	1.484
	RHF/6-31G(d)	1.483	1.473	1.476	1.495	1.528	1.498	1.494
	MNDO	1.345	1.349	1.351	1.377	1.486	1.531	1.529
C3-C4	PM3	1.336	1.340	1.343	1.360	1.477	1.498	1.497
	RHF/6-31G(d)	1.329	1.329	1.336	1.356	1.487	1.469	1.468
	MNDO	1.491	1.486	1.487	1.458	1.404	1.518	1.519
C4-C5	PM3	1.480	1.477	1.464	1.450	1.399	1.508	1.507
	RHF/6-31G(d)	1.478	1.472	1.460	1.440	1.388	1.495	1.493
	MNDO	1.221	1.224	1.229	1.235	1.251	1.220	1.220
C5-O6	PM3	1.211	1.211	1.220	1.224	1.245	1.208	1.208
	RHF/6-31G(d)	1.193	1.191	1.202	1.207	1.232	1.187	1.187
	MNDO	infinity	infinity	3.479	2.291	1.455	1.418	1.420
C3-O7	PM3	infinity	infinity	2.809	2.131	1.432	1.433	1.434
	RHF/6-31G(d)	infinity	infinity	2.978	2.200	1.448	1.394	1.395
	MNDO	1.265	1.265	1.265	1.259	1.283	infinity	infinity
O7-O8	PM3	1.491	1.491	1.471	1.453	1.509	infinity	infinity
	RHF/6-31G(d)	1.479	1.479	1.458	1.429	1.394	infinity	infinity
	MNDO	127.6	124.9	125.1	124.3	112.7	125.5	123.9
C2-C3-C4	PM3	125.6	122.8	122.3	120.3	110.6	122.4	120.6
	RHF/6-31G(d)	128.3	128.1	126.8	121.6	114.3	124.2	121.8
	MNDO	127.0	126.8	123.8	124.1	124.7	125.2	124.0
C3-C4-C5	PM3	123.8	121.5	120.2	120.9	120.9	120.8	119.3
	RHF/6-31G(d)	126.0	120.5	119.3	120.5	121.6	121.3	119.6
	MNDO	124.2	125.7	123.0	125.3	124.7	122.2	122.4
C4-C5-O6	PM3	122.0	122.4	123.1	123.9	120.9	121.2	121.4
	RHF/6-31G(d)	122.4	124.1	125.0	126.6	129.7	121.8	123.0

Supplementary Table. (cont.)

		1-cis	1-trans	2	3	4	5-cis	5-trans
C2-C3-O7	MNDO	-	-	111.0	95.2	104.9	120.3	119.9
	PM3	-	-	95.4	100.3	111.0	118.9	118.9
	RHF/6-31G(d)	-	-	99.7	98.9	109.2	118.0	118.1
C3-O7-O8	MNDO	-	-	119.6	120.1	116.4	-	-
	PM3	-	-	109.6	116.1	111.4	-	-
	RHF/6-31G(d)	-	-	88.5	106.9	109.6	-	-
O7-O8-H9	MNDO	109.5	109.5	109.4	109.7	110.3	-	-
	PM3	95.3	95.3	96.2	97.0	96.3	-	-
	RHF/6-31G(d)	100.7	100.7	101.4	102.0	100.5	-	-
C1-C2-C3-C4	MNDO	-86.6	-91.0	62.5	-137.1	69.2	-77.8	-71.4
	PM3	-60.6	0.1	0.0	-57.0	-101.4	-90.5	-94.1
	RHF/6-31G(d)	-46.3	0.1	-0.6	-45.2	-48.7	-98.5	-118.9
C2-C3-C4-C5	MNDO	-1.3	180.0	177.7	172.2	122.5	-2.9	149.9
	PM3	-0.8	180.0	180.1	175.6	146.9	-3.0	148.8
	RHF/6-31G(d)	-5.4	180.0	179.9	168.1	141.4	-1.7	151.9
C3-C4-C5-O6	MNDO	104.9	1.1	158.7	-176.3	180.5	96.0	-80.3
	PM3	178.5	180.1	180.6	-176.9	-175.5	123.3	-117.3
	RHF/6-31G(d)	174.0	180.0	180.3	180.7	-177.8	134.8	-135.8
C2-C3-O7-O8	MNDO	-	-	80.7	90.4	-176.5	-	-
	PM3	-	-	102.7	108.4	98.7	-	-
	RHF/6-31G(d)	-	-	88.2	79.2	84.9	-	-
C2-C3-C4-O7	MNDO	-	-	-106.4	-110.4	-119.5	-106.0	-106.4
	PM3	-	-	-107.3	-117.2	-125.4	-106.4	-107.3
	RHF/6-31G(d)	-	-	-105.8	-116.5	-127.2	-104.6	-105.8

Appendix F

Publications

JOURNAL OF WOOD CHEMISTRY AND TECHNOLOGY, 12(1), 111-134 (1992)

KINETIC MODELS FOR PEROXIDE BLEACHING UNDER ALKALINE CONDITIONS, PART 2. EQUILIBRIUM MODELS.

P. J. Wright, Y. A. Ginting and J. Abbot
Department of Chemistry
University of Tasmania
Hobart, Tasmania, Australia

ABSTRACT

The validity of a previously proposed kinetic model for alkaline peroxide bleaching has been tested by changing reagent concentrations during bleaching. The model has been revised to account for experimental observations and now includes a reversible reaction between chromophoric and leucochromophoric groups. Analysis of model first order rate constants indicates that ionic and radical species may both play an important role in alkaline peroxide bleaching.

INTRODUCTION

There is currently widespread interest in the expansion of markets for mechanical and chemi-mechanical pulps bleached with hydrogen peroxide. In addition, there is also a growing potential for substitution of high brightness mechanical pulps into products traditionally manufactured from bleached chemical pulps. However, problems arising from reversion processes, for example after exposure to light, may limit the extent of replacement. It is now generally believed that radical induced processes participate in reversion reactions induced by both heat and light[1-6]. Reactions involving radical species have also been the subject of

recent debate during the alkaline bleaching process itself. It is now thought that radicals, in particular the hydroxyl radical ($OH^{\cdot}$), may play an important role in bleaching[7-10] in addition to the perhydroxyl anion (HO_2^-) which has long been considered to be the active reagent[11]. However, there is conflicting evidence as to whether the involvement of radicals leads to brightening or darkening processes.

In part 1 of this study[12] we undertook an examination of the kinetics of alkaline peroxide bleaching processes under conditions of constant reagent concentrations at low consistency. Several plausible kinetic schemes were examined in detail, including a two chromophore consecutive reaction model. In the present paper we have extended our study to include a model which allows for a reversible reaction in which chromophores are created as well as removed. The analysis of peroxide bleaching kinetics in terms of a reversible reaction has also been considered in the context of identifying the possible contributions of radical induced processes in the overall reaction scheme.

RESULTS AND DISCUSSION

THE TWO CHROMOPHORE CONSECUTIVE REACTION MODEL

In the previous paper[12], the kinetic behaviour associated with the bleaching of *E. regnans* mechanical pulp was examined under constant reagent conditions by following the change in light absorption coefficient (K) with time. The light absorption coefficient has been found to be the the most suitable variable to monitor since it is known to relate proportionally to the chromophore concentration[13-16]. Analysis of bleaching behaviour led to the formulation of a peroxide bleaching model based on two distinct chromophore types (C_1 and C_2). Both chromophores were considered to be initially present in the pulp and, under bleaching conditions, were assumed to react via first order processes to yield colourless products (C_p) via the mechanism presented in Figure 1(a) (the other mechanisms outlined in Figure 1 will be discussed later).

Chromophore type C_1 was assumed to react rapidly via two routes, with rate constants k_1 and k_2, to form C_p and C_2 respectively. Hence the disappearance of C_1 was correlated with the rapid initial decrease in light absorption coefficient

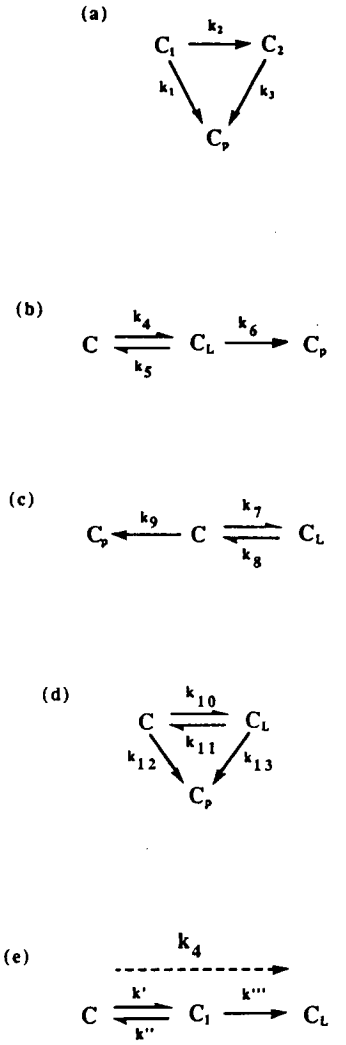

FIGURE 1 : Kinetic model reaction schemes. (a) The two chromophore consecutive reaction model, (b) & (c) 3 parameter equilibrium models, (d) 4 parameter equilibrium model (e) Postulated mechanism for C to C_L conversion.

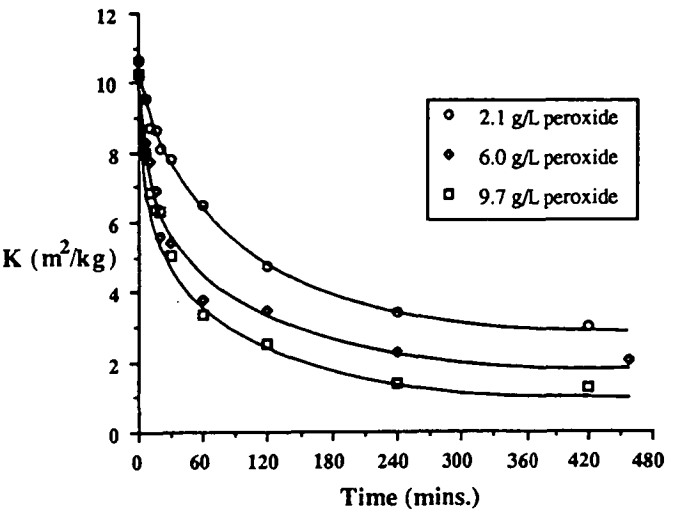

FIGURE 2 : Typical variation in light absorption coefficient (K) with time for an *E. regnans* pulp bleached under constant conditions (pH 10, 50°C, 0.3% pulp consistency).

which is evident during the first 30 minutes of bleaching (Figure 2). The chromophoric group C_2 was assumed to be more resistant to bleaching and was identified as being responsible for the much slower final bleaching phase. The rate constant associated with the conversion of C_2 to C_p (k_3) was found to be small and independent of reagent concentration and coincided with the levelling off in the rate of bleaching at longer times.

Computer evaluation of the rate constants (k_1, k_2 and k_3) allowed the features of the two chromophore consecutive reaction model to be examined in more detail. The model was initially favoured for several reasons. Firstly, a good fitting between experimental and theoretical data was obtained and secondly, the reaction steps could be defined in terms of chemically meaningful first order processes. Finally, a maximum bleaching rate in the pH range 11-12 was predicted which is in agreement with experimental observations[11,17,18], whereas previously published empirical models[15,17,18] predict a continuous increase in bleaching rate with pH.

Two Chromophore Consecutive Reaction Model Tests

Although the fitting obtained between experimental data and theoretical behaviour predicted by the consecutive reaction model was a significant improvement on previously proposed kinetic models, this is not sufficient to establish the validity of the proposed scheme[15]. As is the case with any complex multi-parameter kinetic model, an apparent adequate fitting of data points should not be used as the sole criterion of model validity. It is important to attempt to formulate tests to compare experimental behaviour with model predictions.

The experiments undertaken here to test the consecutive reaction model were essentially consecutive two stage bleaching sequences carried out under constant conditions at 50°C and 0.3% consistency. The aim of these experiments was to check the ability of the present model to predict the effects of sudden changes in reagent conditions.

(i) Increase in Peroxide Concentration at Constant pH

An *E. regnans* pulp was bleached under constant conditions (4 g/L peroxide, pH 11) for 3 hours at 50°C. Bleaching progress was monitored by following the decrease in the light absorption coefficient (K) with time. After 3 hours bleaching, enough hydrogen peroxide was added to raise the peroxide concentration to 6 g/L while maintaining the pH at 11. Light absorption coefficients were followed for a further 1 hour. The results of this bleaching procedure, shown in Figure 3(a), indicate that when the total peroxide concentration is increased at constant pH, the absorption coefficients slowly shift from the 4 g/L bleaching profile to the 6 g/L profile. In other words, increasing the peroxide concentration increases the rate of bleaching.

In terms of the two chromophore consecutive reaction model, this effect is unexpected. At the stage of bleaching when the peroxide concentration was increased (after 3 hours) the consecutive reaction model predicts chromophores would exist exclusively in the difficult to remove C_2 state (Figure 4). Therefore the decrease in absorption coefficient after 3 hours is a result of C_2 being converted to the colourless C_p type, the rate constant being represented by k_3. This rate constant had previously been shown[12] to be small and independent of alkali and peroxide concentration which is clearly in conflict with experimental observations.

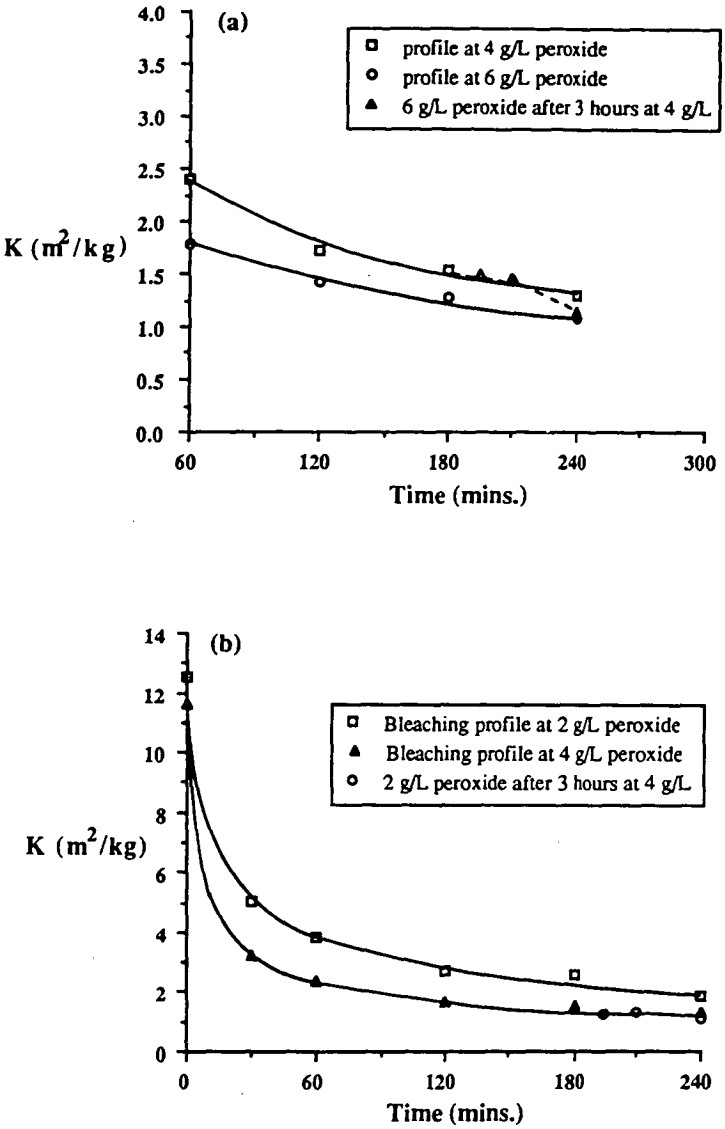

FIGURE 3 : Effect on light absorption coefficient (K) when reagent conditions are changed during bleaching. (a) Peroxide levels increased at constant pH, (b) Peroxide levels decreased at constant pH, (c) pH increased at constant peroxide concentration.

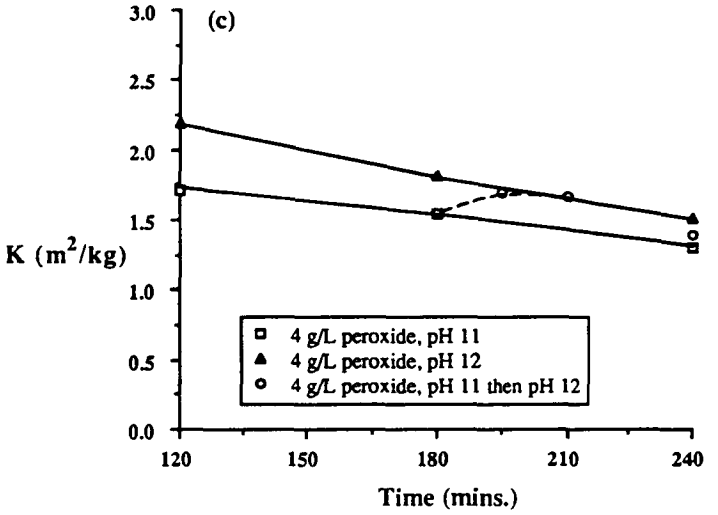

Fig. 3 (continued)

(ii) Decrease in Peroxide Concentration at Constant pH

An *E. regnans* pulp was bleached for 3 hours using an identical procedure to that in (i). After 3 hours the reaction was quenched by cooling and acidifying the slurry to pH 3, followed by filtration of the pulp. The pulp was then bleached at pH 11 and 2 g/L peroxide for a further hour and light absorption coefficients were followed.

Figure 3(b) shows that when peroxide levels are decreased at constant pH, light absorption coefficients tend to remain constant rather than shifting towards a bleaching profile corresponding to a lower amount of peroxide. This implies that reducing the amount of peroxide by half does not significantly impede bleaching rate. This observation has been noted before in the context of industrial peroxide bleaching[19]; as long as there is some residual peroxide present at the end of a bleaching stage the pulp will not darken. Figure 3(b) is also consistent with the predictions of the two chromophore consecutive reaction model since the rate constant which controls the removal of chromophore C_2 (k_3) has been shown to not be greatly influenced by a decrease in peroxide concentration.

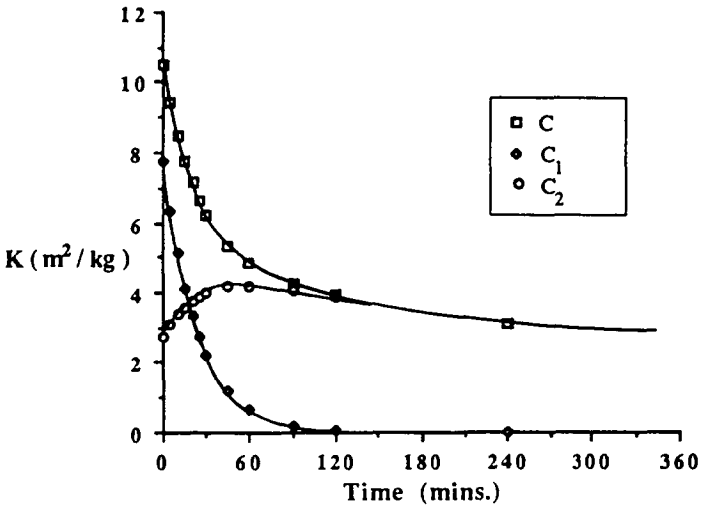

FIGURE 4 : Example of variation of two chromophore consecutive reaction model species C_1, C_2 and C_p with time. Points calculated from rate constants at pH 10, 4 g/L peroxide.

(iii) Increase in pH at Constant Peroxide Concentration

An *E. regnans* pulp was bleached for 3 hours under identical conditions to those in (i). After 3 hours the alkalinity was increased from pH 11 to pH 12 by addition of sodium hydroxide (2 M) and the reaction was allowed to proceed for a further hour. The change in light absorption coefficient with time is shown in Figure 3(c). From this figure it can be observed that when pH is increased from 11 to 12, absorption coefficients increase and move from the pH 11 bleaching profile to that at pH 12. This behaviour causes the pulp to darken. Such a darkening is somewhat surprising considering that formation of the active bleaching species[11], the perhydroxyl anion HO_2^-, is favoured by increasing pH (Table 1). This information implies that the action of (HO_2^-) is substantially impeded at high pH in agreement with studies, including this work, which show a maximum bleaching rate in the pH 11-12 range (Figure 5).

The darkening observed in Figure 3(c) is also indicative of a reversible reaction which cannot be explained in terms of the consecutive reaction model. The

TABLE 1

Effects of Increasing pH on the Formation of Perhydroxyl Ions at 50°C (Calculated from the Equation of Teder & Tormund[20]).

Concentration H_2O_2 (g/L)	pH	Concentration HO_2^- (M)
2.0	9	5.7 e-05
4.0	9	1.1 e-04
6.0	9	1.7 e-04
2.0	10	5.7 e-04
4.0	10	1.1 e-03
6.0	10	1.7 e-03
2.0	11	5.2 e-03
4.0	11	1.0 e-02
6.0	11	1.6 e-02
2.0	12	2.9 e-02
4.0	12	5.8 e-02
6.0	12	8.7 e-02

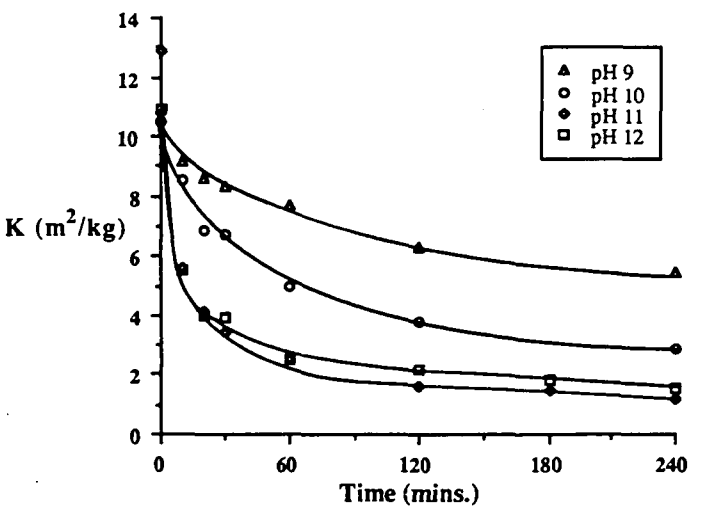

FIGURE 5 : Evidence for maximum bleaching rate in the pH range 11-12. *E. regnans* pulp bleached under constant conditions (4 g/L peroxide, 50°C, 0.3% pulp consistency).

model predicts that, after 3 hours, chromophore type C_1 will have been fully converted to C_2 and C_p. The darkening which occurs on increasing the pH suggests that C_1 is being somehow reformed from C_2 and C_p, a possibility which is not taken into account by the current model.

EQUILIBRIUM MODELS

The model tests mentioned above clearly illustrate some of the deficiencies in the two chromophore consecutive reaction model. Although this model appears to adequately describe the kinetics of chromophore removal under conditions of constant peroxide concentration and pH, it does not account for the observed effects which occur during changes in reagent concentration. Ultimately, if we wish to be able to describe peroxide bleaching behaviour under mill conditions, a valid kinetic model must account for behaviour under conditions where reagent concentrations are not maintained at constant levels.

In particular, the consecutive reaction model is unable to describe the darkening which occurs when pH is increased from 11 to 12 at constant peroxide levels. This observation suggests that a reversible step should be incorporated in the model. Several plausible models containing a reversible step are presented in Figures 1(b), 1(c) and 1(d). Light absorption coefficients also appear to reach approximately limiting values after long bleaching times, and these values are dependent on the amount of peroxide present (Figure 2). This type of behaviour can be explained by the concept of attainment of an equilibrium. Indeed, inconsistencies in the consecutive reaction model were recently noted in its application to the peroxide bleaching of *P. radiata* TMP at high temperatures[21], particularly with regard to explaining the effect of repeated bleaching cycles. As a result, a model involving an equilibrium between a chromophoric group (C) and a colourless leucochromophoric group (C_L) followed by an irreversible conversion to a colourless product (C_p) was postulated as a better description of experimental data (Figure 1(b)).

The equilibrium model outlined in Figure 1(b) was fitted to existing kinetic data[12] from the bleaching of *E. regnans* pulps under constant conditions at 50°C. The concentration of chromophores (C) present before bleaching was considered to correspond to the light absorption coefficient of unbleached handsheets while the

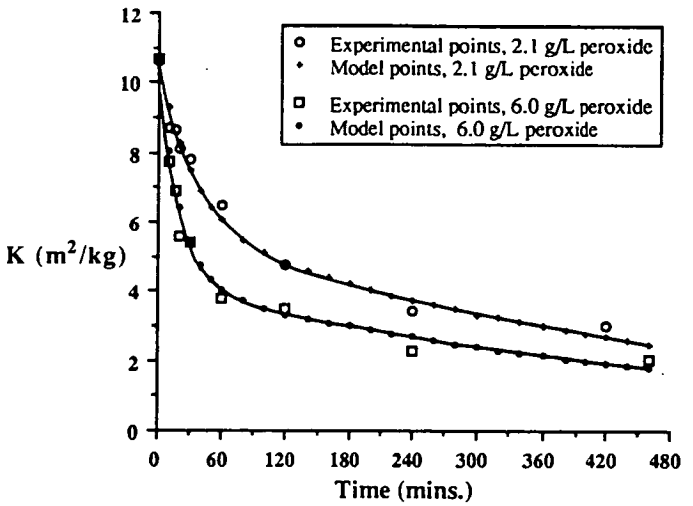

FIGURE 6 : Examples of equilibrium model fits of experimental bleaching curves. *E. regnans* pulp bleached under constant conditions (pH 10, 50°C, 0.3% pulp consistency).

initial concentrations of leucochromophores (C_L) and colourless products (C_p) were set to zero.

Differential equations describing the changes in C, C_L and C_p with time were solved by Laplace transformation to yield explicit equations for the variation in each of the chromophore types with time. The rate constants were computed using an iterative procedure whereby different combinations of k_4, k_5 and k_6 were substituted into the explicit equations to generate theoretical bleaching curves. Standard deviations between theoretical and experimental points were calculated and iterations were ceased once minimisation of standard deviations had occurred. The rate constants corresponding to the minimum standard deviation were regarded as the optimum solutions. Figure 6 illustrates some model fits of experimental data and from Table 2 it is evident that these fits are generally very good.

Features of the Equilibrium Model

A typical plot of the variation in equilibrium model species C, C_L and C_p with time is shown in Figure 7. An advantage of the equilibrium model over the

TABLE 2

Standard Deviations in the Fitting of the Equilibrium Model to Experimental Data from the Bleaching of *E. regnans* at 50°C.

	Standard Deviation in K (m^2 / kg)			
Peroxide dose (g/L)	pH 9	pH 10	pH 11	pH 12
2	0.207	0.323	0.354	0.186
4	0.294	0.337	0.389	0.308
6	0.307	0.374	0.391	0.167

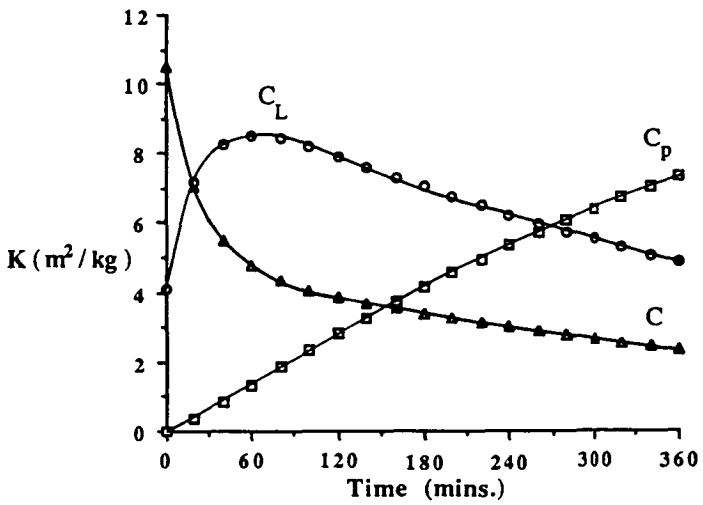

FIGURE 7 : Example of variation of equilibrium model species C, C_L and C_p with time. Points calculated from rate constants at pH 10, 4 g/L peroxide.

two chromophore consecutive reaction model is that the behaviour observed in Figures 3(a) and 3(c) when reagent conditions were changed part way through a bleach can now be described in terms of a model (Figures 8(a) and 8(c)). These figures show the predicted behaviour when either the peroxide concentration is increased at constant pH, or pH is increased at constant peroxide concentration. Theoretical lines have been generated corresponding to behaviour under constant conditions using values of the rate constants previously obtained by computer optimisation. The third line in each graph shows the predicted behaviour obtained by a sudden change in reagent concentration (ie. changing values of the rate constants) after 180 minutes. By comparison with Figure 3 it can be seen that the predicted response in terms of change in chromophore concentration is close to that observed experimentally.

Interestingly, the model also predicts that darkening should occur when peroxide levels are reduced at constant pH (Figure 8(b)), although this effect was not observed in the current work (Figure 3(b)). Further testing at lower peroxide concentrations than studied here may be required to investigate whether darkening can occur when peroxide levels are reduced at constant pH, as the model would predict.

(i) Behaviour of Rate Constant, k_4

Figure 9(a) shows the dependence of k_4, the dominant rate constant responsible for removal of colour, with the concentration of perhydroxyl ion (HO_2^-) which may be considered to be the primary active bleaching species.

It is apparent that the magnitude of k_4 increases with the concentration of HO_2^- at a given pH, but the relationship is non-linear and falls off at higher concentrations of the anion. At very high concentrations of HO_2^-, the rate constant appears to reach a limiting value (as shown here for pH 12). This behaviour suggests that the process described by the conversion of C to C_L does not take place in either a single step (ie. an elementary process in which HO_2^- reacts with C) or through a sequential mechanism in which only C and HO_2^- participate in a rate determining step.

It is also clear that the results at different pH levels in Figure 9(a) do not fall on a common curve. This shows that the dominant process for chromophore removal is strongly influenced by the hydroxide ion (OH^-) as well as the

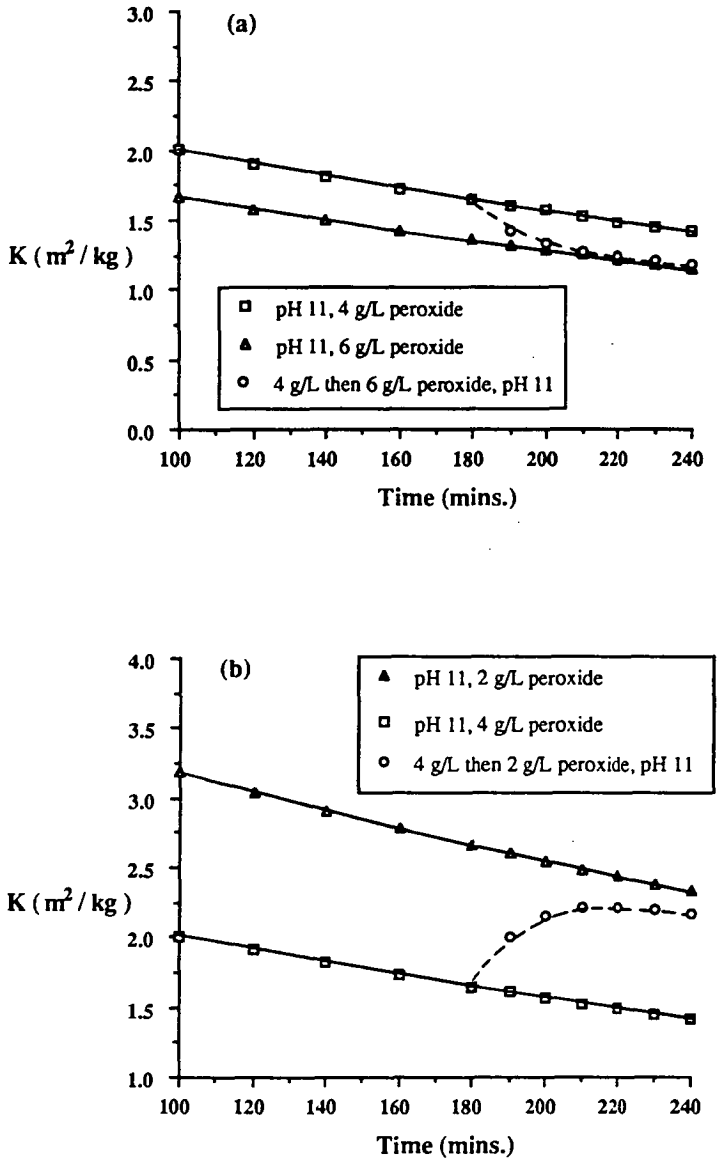

FIGURE 8 : Equilibrium model predictions of the change in light absorption coefficients when reagent concentrations are changed during bleaching. (a) Peroxide levels increased at constant pH, (b) Peroxide levels decreased at constant pH, (c) pH increased at constant peroxide concentration.

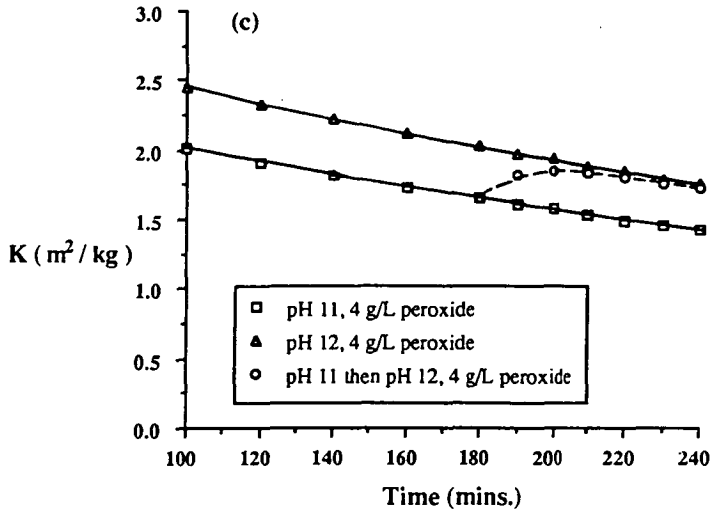

Fig. 8 (continued)

perhydroxyl anion (HO_2^-). The trend shown in Figure 9(a) implies that the forward reaction of C to C_L is promoted by the presence of HO_2^- and inhibited by the presence of OH^-.

A plausible mechanism to account for the kinetic behaviour of k_4 is shown in Figure 1(e). In this mechanism we postulate the formation of an intermediate species (C_I). The rate of formation of C_I is directly proportional to the concentration of HO_2^- (rate constant k') while the reverse process is proportional to the concentration of OH^- (rate constant k''). Formation of the leucochromophoric product (C_L) takes place in a single irreversible step (rate constant k''') which is assumed to be independent of HO_2^- and OH^-. Assuming this type of mechanism it is possible to generate a family of curves, as in Figure 9(b), which resemble the experimental curves in Figure 9(a). The postulated mechanism would explain the non-linear dependence of k_4 on HO_2^-, the limiting value of k_4 at very high HO_2^- concentrations and the inhibiting influence of the hydroxide ion.

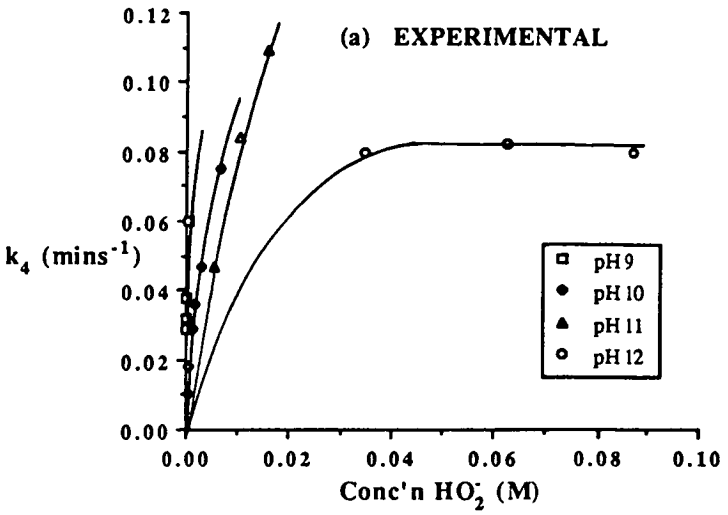

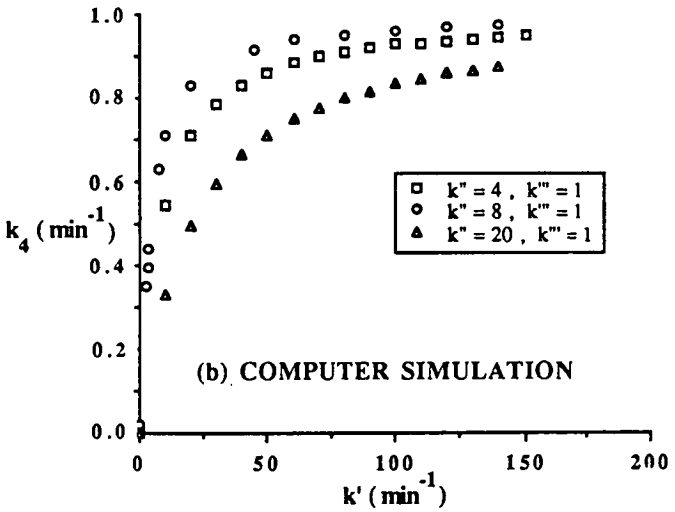

FIGURE 9 : Variation in equilibrium model rate constants with perhydroxyl ion concentration. (a) Rate constant k_4, (b) Simulation of behaviour of k_4, (c) Rate constant k_5, (d) Limiting rate constant k_6.

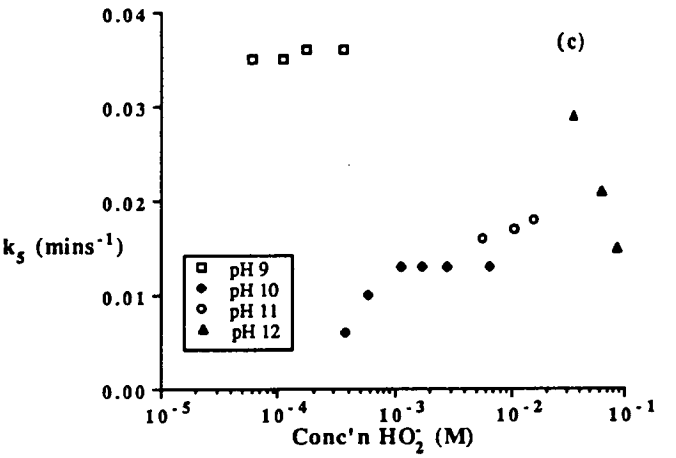

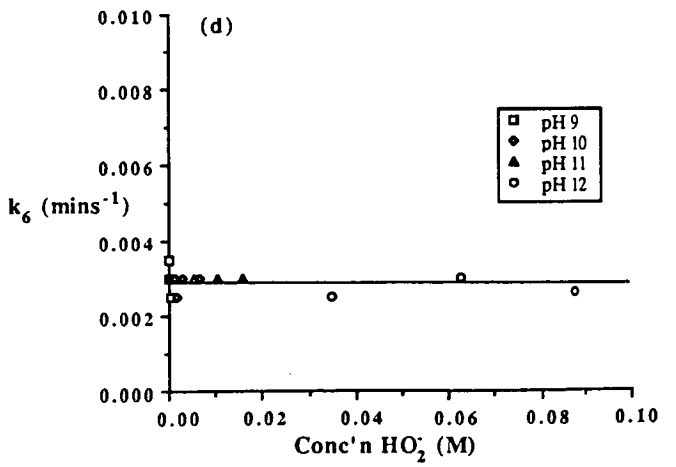

Fig. 9 (continued)

TABLE 3
Rate Constants and Standard Deviations for the Fitting of 4 Different Models to a Single Peroxide Bleaching Curve (pH 10, 3.9 g/L Peroxide).

Model Type	Figure 1(a)	Figure 1(b)	Figure 1(c)	Figure 1(d)
Rate Constants (min^{-1})	$k_1 = 0.025$ $k_2 = 0.021$ $k_3 = 0.002$	$k_4 = 0.030$ $k_5 = 0.014$ $k_6 = 0.003$	$k_7 = 0.025$ $k_8 = 0.016$ $k_9 = 0.006$	$k_{10} = 0.027$ $k_{11} = 0.014$ $k_{12} = 0.003$ $k_{13} = 0.002$
Std. Deviation (m^2/kg)	0.337	0.337	0.338	0.338

(ii) Behaviour of Rate Constants k_5 and k_6

The dependence of rate constant k_5 on perhydroxyl ion concentration is depicted in Figure 9(c) over the pH range 9-12. At constant pH, k_5 appears to be almost independent of perhydroxyl ion concentration. Despite the perhydroxyl ion and alkali concentrations varying by a factor of approximately 1000, Figure 9(c) shows that k_5 changes by a factor of about 3 in the pH range 10-12. From this observation it can be concluded that k_5 is much less sensitive to alkali and peroxide concentrations than k_4.

The rate at which the model leucochromophoric group (C_L) is irreversibly converted to a colourless product (C_p) is described by the rate constant k_6. This rate constant is reflected in the residual rate of reaction after equilibrium has been achieved. As was the case for the two chromophore consecutive reaction model, k_6 has been found to be considerably smaller than both k_4 and k_5 indicating that the conversion of C_L to C_p is the slowest step of all. The rate constant also appears to be insensitive to both alkali and peroxide levels (Figure 9(d)) suggesting that little can be done to accelerate this reaction step by way of changing reagent concentrations. Over the entire range of conditions examined, k_6 was invariably found to have a value between 0.0025-0.0030 min^{-1}.

PEROXIDE BLEACHING MECHANISMS

Table 3 shows that the adequacy of fitting obtained for the consecutive reaction model (Figure 1(a)), two 3 parameter equilibrium models (Figures 1(b) and

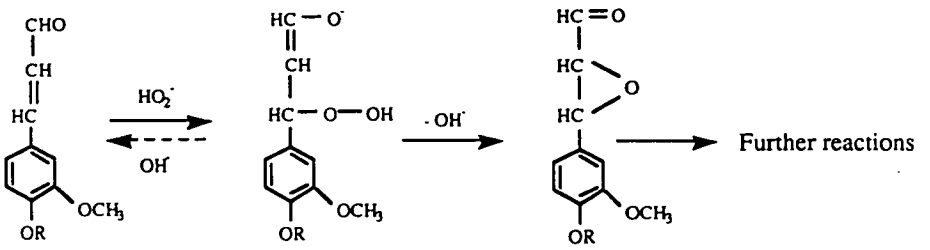

FIGURE 10 : Proposed mechanism for peroxide bleaching of lignin model compound, coniferaldehyde[23].

1(c)) and a 4 parameter equilibrium model (Figure 1(d)) are very similar. It is therefore impossible to distinguish between these models solely on the basis of fitting between experimental and theoretical points. However, as already demonstrated, the favoured equilibrium model (Figure 1(b)) can predict the response of a pulp under constant reagent conditions when the concentrations of either peroxide or hydroxide are increased. This model can apparently also explain behaviour when a pulp is repeatedly bleached in a series of consecutive stages with the same initial conditions[21].

Application of the equilibrium model under constant reagent conditions leads to the conclusion that the principle reaction leading to elimination of chromophores is controlled by ionic species as demonstrated by the behaviour of k_4. This reaction proceeds through an intermediate species the formation of which depends directly on the perhydroxyl anion and is retarded by the hydroxide ion. The existence of such an intermediate has recently been discussed in the context of two stage acid/alkaline peroxide bleaching[22]. A possible example of this type of reaction process might be envisaged for conjugated carbonyl groups[23] (Figure 10). This type of chromophore is believed to contribute a significant proportion of the colour in mechanical pulps, and is reactive towards alkaline peroxide. The mechanism shown illustrates how an intermediate species may be involved in the overall mechanism of chromophore removal. It is conceivable that the postulated intermediate would undergo elimination of hydroxide ion to produce the epoxide at a rate which is strongly dependent on the ionic species OH^- and HO_2^-. Detailed examination of the kinetic behaviour of selected model compounds in the presence

of alkaline peroxide should be valuable in interpretation of the observed kinetic phenomena for mechanical pulps.

Our analysis also shows that the values of rate constants k_5 and k_6 in the equilibrium model are more or less insensitive to the concentrations of the OH^- and HO_2^- ions. A plausible explanation for this phenomena might be to assign these reactions to radical dependent processes. There has been considerable interest in the possible participation of radical species in peroxide bleaching reactions over the past decade[7-10]. Although it appears that the hydroxyl radical ($OH^{\cdot}$) may play a significant role, there is evidence that radical species may participate in both chromophore elimination and chromophore creation processes[9,10,24]. This is an interesting observation in view of our equilibrium model which may imply the participation of radical induced reactions in both brightening processes (k_6) and darkening processes (k_5).

Although the equilibrium model can apparently explain the behaviour of pulps under constant reagent conditions and when the concentrations of ionic reagents (HO_2^- and OH^-) are increased, the response to decreasing concentrations of these species is not predicted (Figure 8(b)). For example, a strict application of the model would predict that washing the pulp with water after prolonged bleaching should result in darkening ($k_4 \rightarrow 0$, k_5 independent of ion concentrations). This is not observed in practice but can possibly be rationalized in terms of a rapid quenching of radical processes associated with the conversion of C_L to C. Further studies will be required to provide supporting evidence for participation of ionic species and radicals as suggested by the present kinetic analysis.

CONCLUSION

The two chromophore consecutive reaction model for peroxide bleaching has been tested by carrying out a series of two stage bleaching experiments under constant reagent conditions. When peroxide levels or pH are suddenly increased during bleaching, the consecutive reaction model is unable to describe the resulting experimental behaviour. An equilibrium model was investigated and found to be capable of duplicating experimental observations while retaining the benefits of the consecutive reaction model in terms of adequacy of fitting between theoretical and experimental results.

The behaviour of the model rate constants indicate that initial chromophoric species, C, are converted to stable leucochromophores, C_L, through a series of steps which are dependent on ionic species. Furthermore, these leucochromophores can be eliminated to form colourless products (Cp) or they may be reconverted to coloured species (C). These processes can possibly be assigned to reactions involving radicals, in particular the hydroxyl radical ($OH^{\cdot}$).

The present model based on an equilibrium concept can adequately describe the kinetic behaviour of the chromophores in alkaline hydrogen peroxide under constant reagent conditions. It can also describe transient and final behaviour when increasing reagent concentrations to a new set of constant reagent conditions.

EXPERIMENTAL

Chemicals

Hydrogen peroxide (30%) and sulphuric acid (98%) were supplied by Ajax Chemicals. Semi-conductor grade sodium hydroxide (99.99%) obtained from Aldrich Chemicals was used as the alkali source to minimise the introduction of transition metal impurities.

Procedure

Alkaline groundwood pulp was prepared from approximately 150 year old *E. regnans* blocks which were soaked in Milli-Q water for three days prior to grinding. The wood was ground in a dilute solution of sodium hydroxide (~0.02 M) using a laboratory scale grindstone at Australian Newsprint Mills, Boyer. The resulting pulp was concentrated from 1.5% to 20% consistency by filtration and stored at 4°C until use.

Bleaching experiments were performed by adding sufficient *E. regnans* pulp to 6 L of Milli-Q water such that a pulp slurry of 0.3% consistency was achieved. The slurry was vigorously stirred in a polyethylene bucket immersed in a water bath such that a constant temperature of 50°C was maintained. Before each bleaching

run, an aliquot of pulp was removed to make blank handsheets so that changes in pulp, due to storage, could be monitored.

Bleaching was initiated by simultaneously adding enough alkali (2 M NaOH) and hydrogen peroxide to reach the target conditions. Subsequently, constant pH was maintained by adding alkali from a pH controller supplied by Cole-Parmer. The concentration of peroxide was maintained at constant levels by occasional addition of the necessary amount of hydrogen peroxide calculated from iodometric titration[25] of the bleaching liquor.

After initiation of bleaching, aliquots of pulp slurry (400 mL) were removed at the desired times to make pulp handsheets. The bleaching reaction was quenched by acidifying the slurry to pH 3 with sulphuric acid (2.5 M), followed by filtration to remove the bleaching liquor. Pulp handsheets of 40-45 g.s.m conditioned basis weight were formed by filtering the required volume of re-dispersed pulp slurry onto Whatman No. 540 filter paper[26]. Using this procedure, 3 handsheets were obtained from each aliquot. The sheets were fan dried for several hours at room temperature and were then allowed to equilibrate at constant temperature (25°C) and humidity (50%) so that conditioned basis weights could be obtained.

After drying, black-backed and self-backed reflectance measurements were made on each sheet, at a wavelength of 457 nm, using an Elrepho 2000 reflectance spectrometer. Individual opacity (W), scattering coefficient (S) and light absorption coefficient (K) properties were calculated from the Kubelka-Munk equation[13,27]. These properties were reported as the average per group of 3 handsheets.

ACKNOWLEDGEMENTS

Financial support for this work was provided by Australian Newsprint Mills Pty. Ltd., Interox Chemicals Pty. Ltd. and the Australian Research Council.

REFERENCES

1. J.A. Schmidt and C. Heitner, *6th Int. Symp. Wood and Pulp. Chem.*, Vol. 1, p. 263, (1991).

2. H. Tylli, I. Forsskåhl, C. Olkkonen, *5th Int. Symp. Wood and Pulp. Chem.*, Vol. 2, p. 361, (1989).

3. A. Castellan, N. Colombo, P. Fornier de Violet, A. Nourmamode and H. Bouas-Laurent, *5th Int. Symp. Wood and Pulp. Chem.*, Vol. 1, p. 421, (1989).

4. R. Agnemo, R.C. Francis, T.C. Alexander and C.W. Dence, *6th Int. Symp. Wood and Pulp. Chem.*, Vol. 1, p. 631, (1991).

5. J.A. Schmidt, C. Heitner, G.P. Kelly and F. Wilkinson, *5th Int. Symp. Wood and Pulp. Chem.*, Vol. 1, p. 607, (1989).

6. K. Fischer, I. Schmidt and H. Koch, *6th Int. Symp. Wood and Pulp. Chem.*, Vol. 1, p. 431, (1991).

7. R. Agnemo and G. Gellerstedt, *Acta Chem. Scand.*, B33, 337, (1979).

8. G. Gellerstedt, I. Pettersson and S. Sundin, *1st Int. Symp. Wood and Pulp. Chem.*, Vol. 2, p. 120, (1981).

9. B. Sjogren, J. Danielsson, P. Engstrand, G. Gellerstedt, T. Reitberger and H. Zachrison, *5th Int. Symp. Wood and Pulp. Chem.*, p. 161, (1989).

10. T. Reitberger, J. Gierer, K. Jansbo, E. Yang and B-H. Yoon, *6th Int. Symp. Wood and Pulp. Chem.*, Vol.1, p. 93, (1991).

11. D.H. Andrews and R.P. Singh, In The Bleaching of Pulp, Chapter 8, R.P. Singh (Ed.), Tappi Press, 1979.

12. P.J. Wright and J. Abbot, Submitted to *J. Wood Chem. Technol.*, 1990.

13. G.J. Robertson, In Fundamentals of Paper Performance, Chapter 9, Tech. Assoc. of Aust. and N.Z. Pulp and Paper Ind.

14. M. Lundqvist, *Sven. Papperstid.*, 82(1), 16, (1979).

15. P. Axegård, S. Moldenius and L. Olm, *Sven. Papperstid.*, 82(5), 131, (1979).

16. A. Teder and D. Tormund, Trans. Tech. Sect. CPPA, 3(2), TR41, (1977).

17. B. Sjogren and S. Moldenius, *1st Int. Symp. Wood and Pulp. Chem.*, Vol. 2, p. 125, (1981).

18. S. Moldenius and B. Sjogren, *J. Wood Chem. Technol.*, 2(4), 447, (1982).

19. V. Lorås, In Pulp and Paper - Chemistry and Chemical Technology, Chapter 5, J.P. Casey (Ed.), Wiley-Interscience, 1980.

20. A. Teder and D. Tormund, *Sven. Papperstid.*, 83(4), 106, (1980).

21. J. Abbot and Y.A. Ginting, Submitted to *J. Pulp Paper Sci.*, 1990.

22. G.C Hobbs and J. Abbot, *J. Wood Chem. Technol.*, 11(2), (1991).

23. G. Gellerstedt and R. Agnemo, *Acta Chem. Scand.*, B34(4), 275, (1980).

24. J. Gierer, E. Yang and T. Reitberger, *6th Int. Symp. Wood and Pulp. Chem.*, Vol. 2, p. 197, (1991).

25. A.I. Vogel, Quantitative Inorganic Analysis, p. 425, Longmans, Green and Co., London, 1947.

26. Appita Standard, P446s-82.

27. P. Kubelka, *J. Opt. Soc. Am.*, 38, 448, (1948).

10. BRYANT, C.W. and BARKLEY, W.A., Comparison of BOD, TSS and AOX Removals From Kraft Wastewaters in Activated Sludge Systems Versus Aerated Stabilization Basins, 1989 Western Branch CPPA Fall Conf. (Oct. 31-Nov. 2, 1989).
11. HYNNINEN, P. and PRYKE, D., Process Design Considerations in Finnish Pulp and Paper Mill Biological Purification Plants, Technical Section, CPPA Pacific Coast-Western Branches Conf. (May 17-19, 1989).
12. A Comparison of Air and Oxygen Activated Sludge Process Performance in the Pulp and Paper Industry, NCASI Tech. Bull. 359 (1989).
13. Standard Methods for the Examination of Water and Wastewater, Am. Public Health Assoc., Am. Water works Assoc. and Water Pollut. Control Fed., Washington, D.C., 16th Ed. (1985).
14. B.C. Provincial Guidelines and Laboratory Procedures for Measuring Lethal Toxicity of Liquid Effluents to Fish (1982).
15. Resin Acids Analysis — Methylated G.C., Environmental Protection Service (1983).
16. Experience with the Analysis of Pulp Mill Effluents for Chlorinated Phenols Using an Acetic Anhydride Derivatization Technique, NCASI Stream Improvement Bull. 347 (1981).
17. LEACH, J.M., MUELLER, J.C. and WALDEN, C.C., Biodegradeability of Toxic Compounds in Pulp Mill Effluents, *Trans. Tech. Sect. CPPA* 3(4): TR126-TR130 (1977).

Development of Kinetic Models for Alkaline Peroxide Bleaching

J. ABBOT and Y.A. GINTING

Bleaching of Pinus radiata TMP with alkaline hydrogen peroxide has been studied. In particular, factors affecting maximum brightness attained have been examined for various bleaching conditions. Results have been considered in the context of a previously proposed kinetic model based on the assumption of two chromophore types. The concepts of limiting brightness due to either reagent concentrations or changes in the pulp itself have been considered, as well as observations based on the effects of repeated bleaching cycles. The evidence suggests that a kinetic model based on an equilibrium between chromophores and leucochromophores provides a more satisfactory description of peroxide bleaching than previously proposed models which do not take simultaneous removal and formation of chromophores into account. The equilibrium concept has been applied to interpret the effects of temperature and the addition of magnesium ions during alkaline peroxide bleaching.

J. Abbot and Y.A. Ginting
University of Tasmania
GPO Box 252C
Hobart Tasmania 7001
Australia

INTRODUCTION

There have been numerous studies on bleaching of mechanical pulps with alkaline hydrogen peroxide in which the resulting brightness of pulps is reported as a function of time and reagent concentrations [1-5]. Most investigations have been carried out under conditions where the concentrations of hydrogen peroxide and hydroxide ion fall significantly through the course of the bleaching process. Although such conditions simulate industrial practice, the results are difficult to interpret in terms of kinetic phenomena associated with individual reaction processes. Over the past decade there have been some kinetic investigations reported [6-9] under conditions where the total peroxide concentration and pH have been maintained at constant levels, to facilitate interpretation of rate processes. These studies have usually been carried out at relatively low pulp consistencies, so that the rate of consumption of reagents is reduced to low levels, allowing monitoring and continuous readjustment to initial concentration values, as the bleaching process continues under isothermal conditions.

Recently we have proposed a kinetic model based on an examination of the bleaching of a *Eucalyptus* SGW [9] using on the assumption of two distinct chromophore types. In that study we have examined changes in the absorption coefficient (k) under constant conditions of pH and peroxide concentration, as k is found to show a better correlation with chromophore concentration than measurement of brightness [7]. The objective of these studies is to construct a kinetic formulation which relates to concentrations of reacting species (both chromophores and reagents), rather than formulate models which are limited to empirical formulation [10,11]. In the present study we have examined alkaline peroxide bleaching of *Pinus radiata* TMP [8,10,11] in the context of various kinetic models. Here we have used brightness as an indicator of chromophore content as we are concerned with trends which reflect the validity of proposed kinetic models, rather than accurate determination of exact kinetic parameters. It has been shown, however, that the general behaviour of brightness gain with time closely parallels changes in k for peroxide bleaching of *Pinus radiata* TMP [12]. Our objective in the present study is to attempt to differentiate between various possible models using a more qualitative

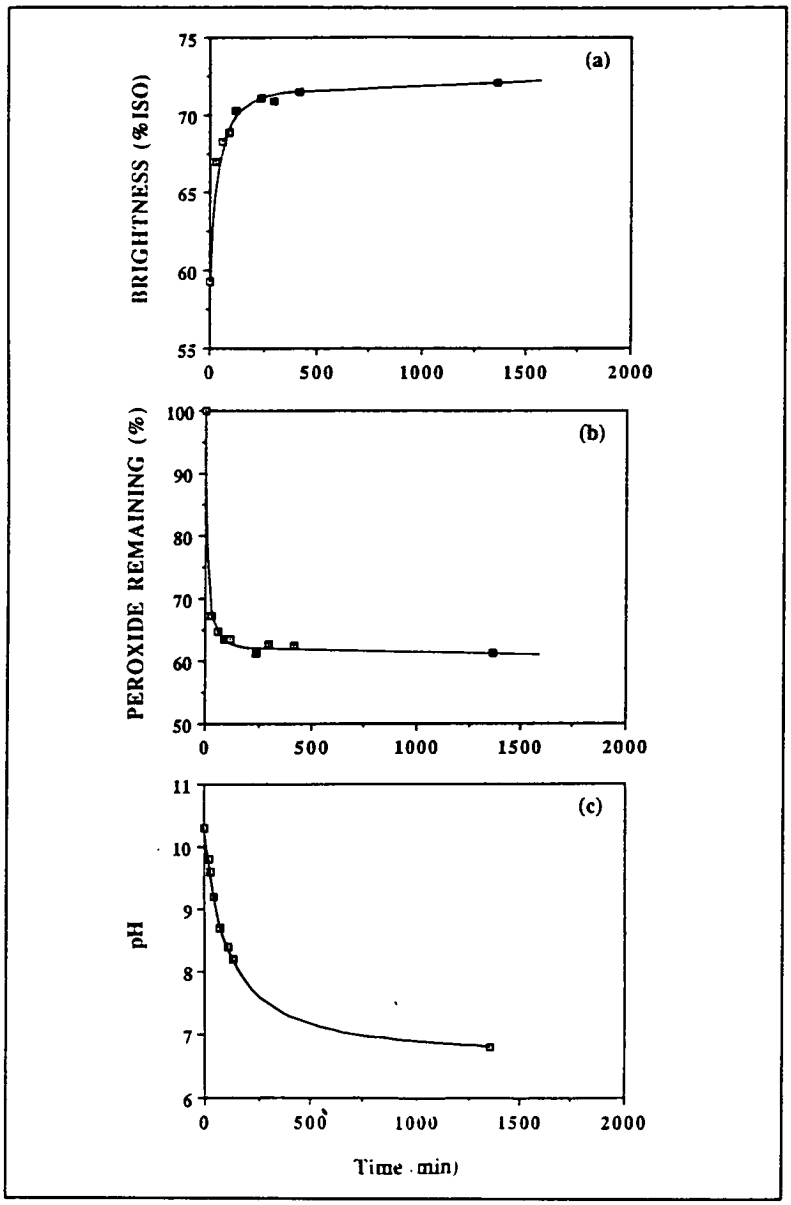

Fig. 1. Bleaching of *Pinus radiata* TMP at 50°C, 4% consistency. Initial conditions pH 11.0, 18% hydrogen peroxide 2% NaOH on o.d. pulp. (a) Increase in brightness with time; (b) Decrease in peroxide charge with time; (c) Decrease in pH with time.

approach, which can be applied in a rigorous manner once the most suitable model has been found.

EXPERIMENTAL

Hydrogen peroxide (30%) was obtained from Ajax Chemicals. Sodium hydroxide of semiconductor purity (99.99%) was supplied by Aldrich Chemicals. The *Pinus radiata* thermomechanical pulp was provided by Australian Newsprint Mills from TMP unit 2 at their Boyer mill in Tasmania. The pulp was stored at 8% consistency at 4°C until used. Analysis of transition metal ions present is given in Table I, as determined by atomic absorption after complete digestion of the pulp.

Bleaching studies were carried out in polyethylene or Teflon vessels maintained at either 50°C or 95°C in a constant temperature water bath. The pulp suspensions were rapidly stirred during the course of the bleaching reactions. The bleaching experiments were performed by mixing the required amounts of pulp, hydrogen peroxide and sodium hydroxide with the required volume of Milli-Q water to give a consistency of 4%. Sodium silicate was not introduced in the bleaching experiments, and the pulp was not pretreated by chelation. The pulp and dilution water were heated to reaction temperature before addition of reagents. Pulp samples were withdrawn at intervals to determine the brightness of the pulp and consumption of hydrogen peroxide. Residual peroxide concentrations were determined on filtrates by iodometric titration with standard sodium thiosulphate, after acidification and addition of potassium iodide and a few drops of saturated ammonium molybdate solution [13].

All pulp samples were thoroughly washed with deionized water. The brightness (% ISO) of bleached pulp handsheets was measured with a Zeiss Elrepho using a 457 nm filter. The measured brightness of the unbleached pulp was 59.3 ISO, and this was not found to vary over a 20-day period during storage.

Repeated Cycle Bleaching Experiments

For the repeated cycle experiments, the pulp suspensions and residual liquor were rapidly cooled to room temperature by addition to cold water at the end of each cycle. The pulp was then filtered and washed with Milli-Q water, before addition of fresh hydrogen peroxide and sodium hydroxide (at the required reaction temperature) to begin the next cycle.

RESULTS AND DISCUSSION

Figure 1a shows the increase in brightness with time for alkaline peroxide bleaching of *Pinus radiata* TMP at 50°C at 4% consistency. Under the conditions used, the peroxide concentration and pH decreased through the course of the bleaching reaction as shown in Figs. 1b and 1c, respectively. The bleaching profile shown in Fig. 1a is typical of many reported results where there is an initial rapid increase in brightness, with the rate of chromophore elimination eventually falling to a low value as time progresses [1-5]. In fact, unless very long time periods are considered, we can consider a limiting brightness to have been attained corresponding to a given set of experimental conditions. For the case illustrated in Fig. 1a this would correspond to a brightness of 72% ISO. This phenomenon can be interpreted on the basis of the reduction in the rate of chromophore elimination as the concentration of available active bleaching species is reduced. In this situation, an apparent limit to the increase in observed brightness of a pulp might be described as "reagent limited".

TABLE I
ANALYSIS OF TRANSITION METAL IONS OF *Pinus radiata* TMP

Metal Ion	Content (ppm)*
Iron	5.99
Manganese	32.05
Copper	4.2

* Determinated by atomic absorption after digestion of pulp.

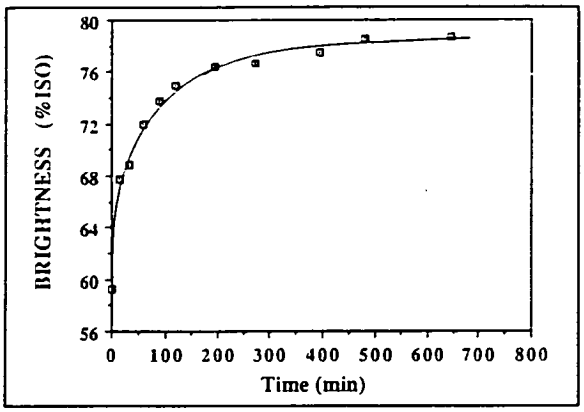

Fig. 2. Bleaching of *Pinus radiata* TMP at 50°C, 0.3% consistency under constant conditions of reagent concentration: pH 10.00, peroxide concentration 4 g/L.

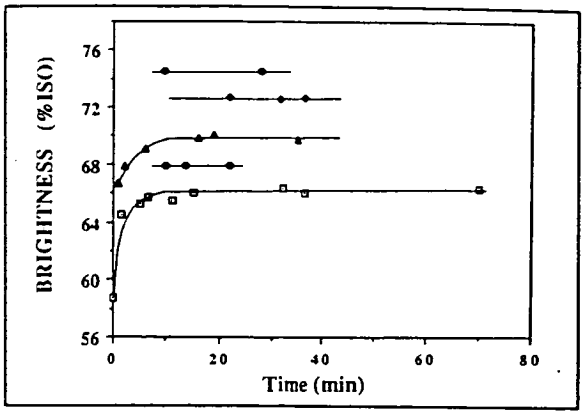

Fig. 3. Bleaching of *Pinus radiata* TMP at 95°C, 4% consistency. Initial conditions: NaOH, 2.0% on o.d. pulp. Hydrogen peroxide charge on o.d. pulp (initial pH levels in parentheses): □, 6% (10.6); ○, 9% (10.3); △, 18% (9.9); ◊, 36% (9.5); ●, 72% (9.2).

It is also possible to suggest that this apparent limit to brightness gain may be associated with properties of the pulp itself. This becomes evident by examination of Fig. 2, which shows results for peroxide bleaching of the TMP at 50°C under conditions of constant reagent concentrations [8]. Even when there is no reduction in peroxide concentration or pH during the course of the bleaching experiment, an apparent limit is reached where the rate of chromophore removal reaches a low, approximately constant level. Studies using various constant concentrations of reagents [6-9] have shown that the pulp brightness (or absorption coefficient) at which the rate of chromophore elimination reaches a low, approximately constant level depends on both pH and peroxide concentration. In this case the brightness limit illustrated in Fig. 2 at a brightness level of 78% ISO might be described as "pulp limited".

Bleaching at High Temperature

In order to examine the concept of limits to brightness increase observed under given bleaching conditions, a series of experiments was carried out with *Pinus radiata* TMP at 95°C and 4% consistency. The reason for conducting the experiments at high temperature becomes clear by inspection of Fig. 3, which shows plots of brightness against time for various levels of initial peroxide addition at constant initial alkali addition. In each case, an almost constant level of brightness is attained within a few minutes of bleaching. This allows us to accurately define a limiting brightness level associated with each set of experimental conditions.

Focusing on the results for pulps bleached using an initial peroxide charge of 18% on o.d. pulp, the brightness limit occurs at 69.3% ISO. Higher brightness limits were attained at higher initial peroxide concentrations, and using very high initial levels of peroxide, brightness levels of >80% ISO were found to be achievable for this pulp. If the limit of 69.3% ISO was due solely to availability of active bleaching species (reagent limited), in theory it should be possible to remove additional chromophores and increase brightness by isolating the pulp after reaction, and repeating the bleaching process, starting with the same initial reagent concentrations. The effect of a series of such bleaching cycles is shown in Table II. An apparent limit to brightness gain is achieved after the second bleaching experiment, with the pulp brightness at 71.5% ISO, which remains virtually unchanged after a further set of 4 cycles. This shows that, even though active bleaching species are available for reaction with chromophores in the pulp, no further significant brightness gain is achieved, and we might conclude that some change has occurred to the chromophores in the original pulp so that they are no longer susceptible to rapid removal by alkaline peroxide bleaching conditions ("pulp limited"). Such a limitation might arise if some of the chromophores initially present in the pulp are transformed to a state in which their removal is very slow under alkaline peroxide conditions, as we have previously suggested [9]. Alternatively, all the bleachable chromophores originally present could have been removed, but new chromophores are simultaneously created so that the net effect results in the brightness limit observed.

These effects can also be illustrated by reference to Fig. 4. With an initial peroxide charge of 6% on o.d. pulp, a limit to brightness gain is attained at 66.0% ISO during the 1st cycle (Fig. 4a). Restoration of initial reagent conditions after 15 min does not increase the brightness limit for the pulp (Fig. 4b). Even repeatedly restoring the initial reagent concentrations over 5 cycles at 8 min intervals does not yield a pulp of higher final brightness (Fig. 4c).

TABLE II
REPEATED BLEACHING OF *Pinus radiata* TMP AT 95°C WITH ALKALINE HYDROGEN PEROXIDE

Cycle	Brightness (% ISO)
1	69.3
2	71.5
3	71.4
5	71.7

Bleaching conditions: 4% consistency, 10 min/bleaching cycle.
Initial peroxide charge: Cycles 1-5, 18%; on o.d. pulp.
Initial alkali charge in each cycle 2.0% on o.d. pulp.

Kinetic Bleaching Models

We have previously proposed a kinetic model [9] to describe the kinetics of peroxide bleaching, as shown in Fig. 5a(i). This model was based on results from studies of alkaline peroxide bleaching of *Eucalyptus regnans* with constant reagent conditions. In the proposed model, we argued that two types of chromophore existed within the original pulp (C_1 and C_2). Chromophore C_1 can undergo rapid initial reaction to give colourless products C_p. Chromophore C_2 is eliminated much more slowly in the presence of alkaline peroxide. Furthermore, as this reaction progresses, in addition to the reaction pathway to produce C_p, C_1 can be converted into C_2 through a parallel reaction process. This type of kinetic model can be simulated by computer methods, by setting up differential equations to describe the model, and assigning values of the rate constants through a suitable fitting procedure. Figure 5a(ii) shows a typical profile of chromophore elimination with time, generated by computer simulation using this model. This shows that this model can simulate the general behaviour of brightness gain seen under

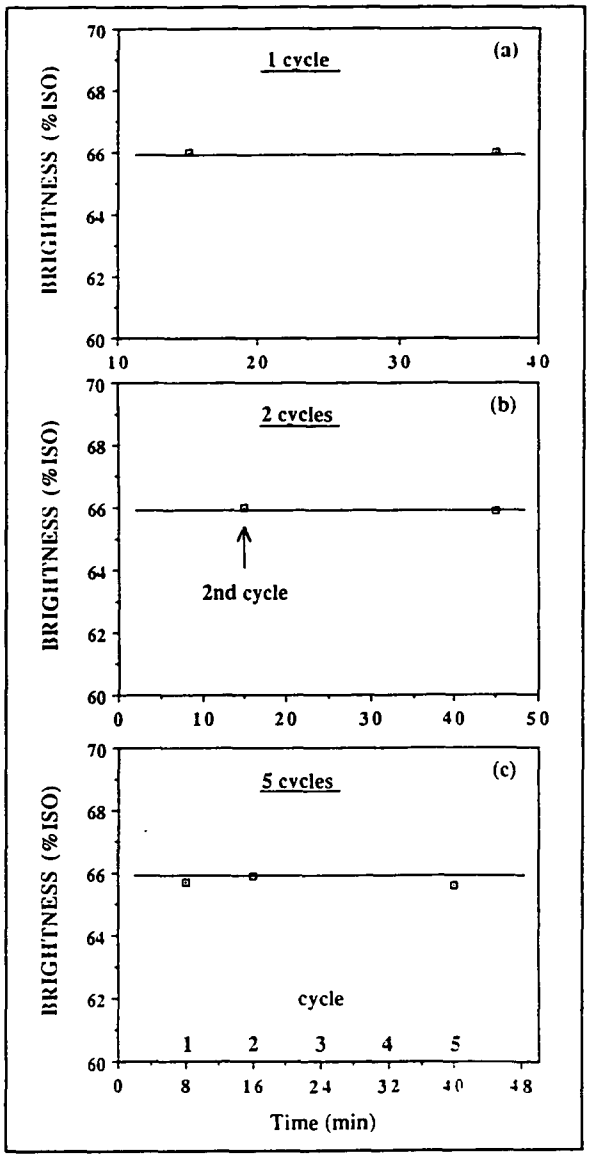

Fig. 4. Effect of repeated bleaching cycles at 95°C, 4% consistency. Initial conditions 2.0% NaOH, 6% peroxide on o.d. pulp. Initial reagent conditions restored at the start of each cycle. Initial pH in parentheses: (a) 1 cycle (10.6); (b) 2 cycles (10.9); (c) 5 cycles (10.9).

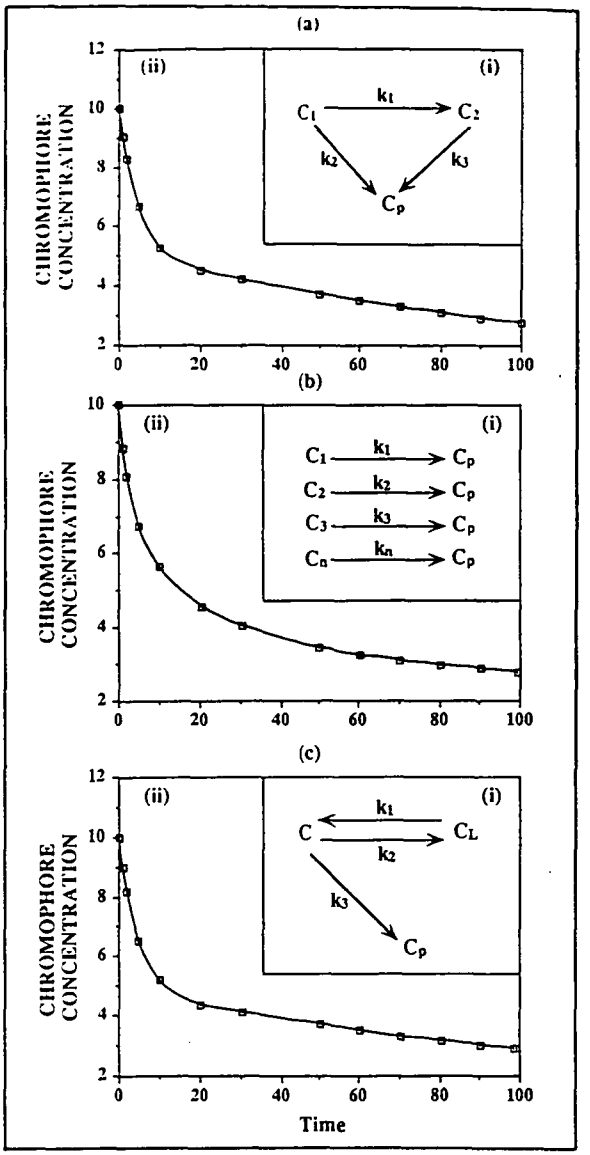

Fig. 5a(i). Two-chromophore consecutive reaction model for peroxide bleaching.
(ii). Computer simulation of chromophore elimination with time for the two-chromophore consecutive reaction model (k_1 = 0.1, k_2 = 0.1, k_3 = 0.006).

Fig. 5b(i). Kinetic model based on parallel processes.
(ii). Simulation of parallel process model using Eq. (1) for n = 4.0, k = 1.5×10^4.

Fig. 5c(i). The equilibrium model for peroxide bleaching.
(ii). Simulation of the equilibrium model k_1 = 0.1, k_2 = 0.1, k_3 = 0.01.

constant conditions (Fig. 2), with rapid initial rate of chromophore elimination declining to an almost constant rate after longer bleaching times [6-8]. Results for isothermal bleaching of *Eucalyptus* SGW under constant conditions of pH and peroxide concentration have been successfully fitted to this two-chromophore consecutive reaction model [9]. Results for peroxide bleaching of softwood pulps, including *Pinus radiata* TMP, taken from the literature [6-9] have also been adequately fitted by this model [9] .

At this stage it is useful to compare the two-chromophore model with previous interpretations of kinetic phenomena associated with peroxide bleaching. Equations of the type

$$-\frac{dC_k}{dt} = k[H_2O_2]_{total}\,[OH^-]^{0.3}\,C_k^n \qquad (1)$$

have been formulated to describe the rate of chromophore elimination during alkaline peroxide bleaching [6-8, 14-15]. High values in the reaction order with respect to chromophore concentration C_k are necessary to give an adequate correlation between Eq. (1) and experimental results, with values of n in the range 4-5 reported [6-8]. These apparent high orders of reaction have been interpreted in the literature [6] as representing a set of chromophore elimination processes as shown in Fig. 5b(i), where $k_1 > k_2 > k_3 \ldots > k_n$.

A computer simulation representing chromophore elimination as a function of time using Eq. (1) is shown in Fig.

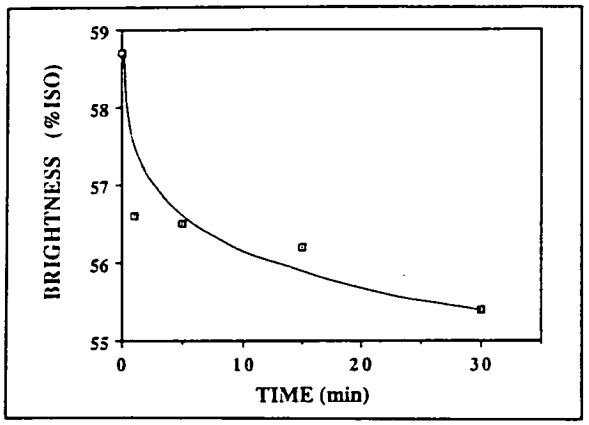

Fig. 6. Alkali darkening of TMP at 95°C. Initial pH 11.0, consistency 4%.

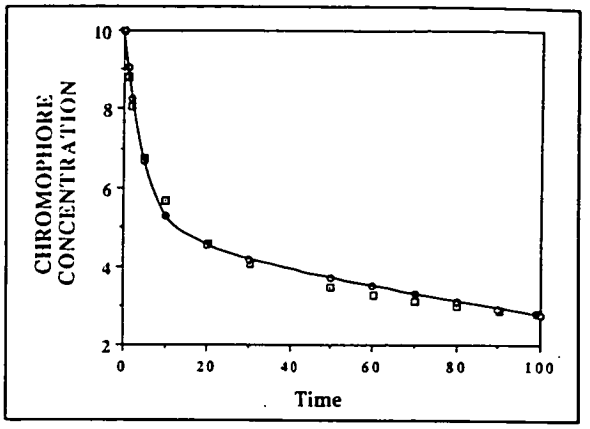

Fig. 7. Kinetic simulations for chromophore elimination by models for peroxide bleaching. Parallel process model, □; Consecutive two-chromophore model, ○.

5b(ii). Although the output can provide a reasonable description of chromophore elimination under conditions of constant reactant concentrations [6-8], it has been found to give an inferior fit compared to the two-chromophore model [9]. Equation (1) also does not provide for a chromophore creation or transformation step which could account for a limit to brightness gain arising from "pulp limitation" corresponding to different levels of reagent.

Another shortcoming of Eq. (1) is that it would predict that, as the total peroxide charge and pH are increased, the rate of bleaching should increase indefinitely. In practice it is generally observed that, as the pH is increased, the rate of bleaching passes through a maximum value using both constant conditions of reagents [7] and under normal bleaching conditions [3,4]. Analysis of the behaviour of rate constant k_1 from the consecutive reaction model [9] has shown that it probably represents a reaction process with consecutive steps involving intermediate species. The overall dependence of k_1 on peroxide and alkalinity has the form:

$$k_1 \approx \frac{[HO_2^-]^a}{[OH^-]^b} \qquad (2)$$

This expression allows for the observation of a maximum in the bleaching rate as pH is increased. It is also preferable to Eq. (1) in that it contains a concentration dependence on the active species HO_2^- rather than the sum of two species (H_2O_2 and HO_2^-) represented by $[H_2O_2]_{total}$ as in Eq. (1).

Chromophore Creation by the Action of Alkali

The two-chromophore model appears to provide an adequate description of kinetic phenomena during alkaline peroxide bleaching by assuming that creation of a second chromophore type leads to a "pulp-limited" rate of bleaching. Under the conditions used in this study it could be concluded that the rate of removal of C_2 is very low indeed, at 95°C leading to an almost constant brightness level. However, it still remains to identify the reaction process leading to the formation of the second chromophore type. During industrial bleaching of mechanical pulps with alkaline hydrogen peroxide, the need to retain some level of peroxide concentration at the end of the bleaching process is well known. The presence of this residual peroxide prevents the process of "alkali darkening" [16-17] which has been attributed to chromophore creation by the action of alkali. Figure 6 shows the effect of alkali on the pulp in the absence of peroxide at 95°C, with an initial pH level (11.0) equivalent to that for bleaching with 6% peroxide (as in Fig. 3). The reduction of brightness of the pulp after 15 min, attributable to alkali darkening, is approximately 3 units. This drop in brightness is much smaller than that necessary to account for a limiting brightness level of 66 (Fig. 4) when one considers that it is possible to reach levels >80 at high peroxide concentrations.

Equilibrium Models

Figure 7 shows that a simulated kinetic curve generated by using Eq. (1) can be closely duplicated by using suitable parameters in the two-chromophore kinetic model. We have shown that consideration of other criteria, such as the need for a chromophore creation step, or prediction of a maximum in bleaching rate with pH, implies that the two-chromophore model is more satisfactory than other proposed models in its representation of chemical phenomena observed during peroxide bleaching. This illustrates an important principle, showing that fitting a model to experimental results does not necessarily mean a particular model is valid. In light of this, the two-chromophore model was subjected to further tests, based on predicted behaviour, to ascertain whether it was adequate.

The experiments using repeated bleaching cycles (Table II and Fig. 4) showed that a limiting brightness is reached when the pulp is repeatedly exposed to the same initial reagent conditions. In terms of the consecutive model, all bleachable chromophores have been converted into C_2, which can only be eliminated very slowly. For example, with repeated cycles at 6% peroxide on o.d. pulp (4% consistency and 95°C) the brightness is restricted to a limit of 66.0% ISO. However, introduction of additional peroxide, to bring the level to 18% on o.d. pulp after "limiting brightness" had been reached, very rapidly increased the brightness, to approach that corresponding to the level attained after initial bleaching with 18% peroxide on o.d. pulp (Fig. 8). If all chromophores were in the C_2 state, simply increasing the concentration of peroxide by a factor of three should not have produced this effect if our two-chromophore model were correct. Similar observations were made under other conditions. For example, addition of an excess of peroxide after repeated cycles at 18% on o.d. pulp (Table II) rapidly increased the brightness level to >75% ISO.

These observations suggest that it is necessary to modify the two-chromophore model in order to account for observed chemical phenomena. The concept of two reacting species is retained, but now we propose an equilibrium between the chromophores present (C) and colourless species C_L which can be reversibly interconverted with C in the presence of alkaline peroxide [Fig. 5c(i)]. Species C_L can be identified with the concept of a leucochromophore. We propose that the rate of conversion of C into C_L is determined primarily by the concentration of active species derived from peroxide (e.g. HO_2^-, $OH^\bullet$) whereas the reverse process is favoured by hydroxide ion.

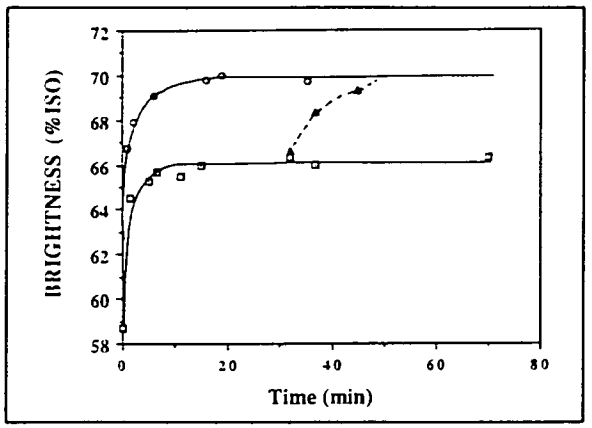

Fig. 8. The effect of introducing additional peroxide after attainment of limiting brightness level at 95°C and 4% consistency. Initial pH 10.6 (6% H_2O_2) and 9.9 (18% H_2O_2 on pulp). Bleaching conditions: initial alkali charge 2% NaOH on o.d. pulp; initial hydrogen peroxide charge on o.d. pulp: △ 6%; ○ 18%; □ 6%, than 18%.

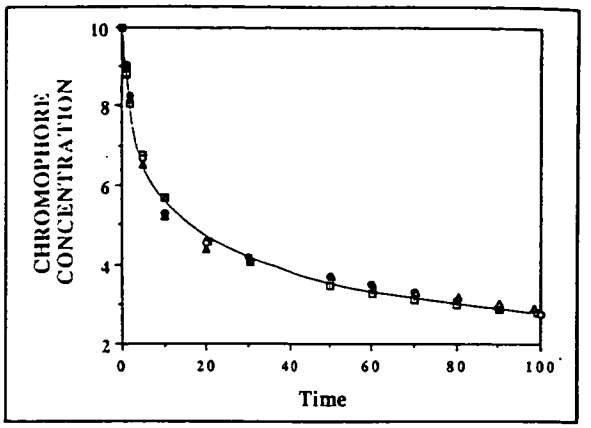

Fig. 9. Simulations for three models for peroxide bleaching. Parallel process models, □; Two-chromophore model, ○; Equilibrium model, △.

With constant concentrations of peroxide and alkali, establishment of an equilibrium position can be associated with the brightness level (ratio of C/C_L) at which the rates of forward and reverse reactions are balanced. The slow residual rate of chromophore elimination can be described by an irreversible process in which C is converted into colourless products C_p [Fig. 5c(i)]. Under normal bleaching conditions, where both peroxide concentration and pH fall, an equilibrium position will be established which may vary from that corresponding to initial reagent conditions. This explains why some shift in limiting brightness may be observed after repeated bleaching cycles (Table II). After attainment of an equilibrium position, with falling concentrations of both peroxide and hydroxide ion, the rates of both forward and reverse processes will decline very rapidly. Under these conditions, a shift away from equilibrium due to prevailing reactant concentrations during the later stages of bleaching will be slow. An exception to this, however, may occur if all the peroxide is consumed and the pulp is left in a medium of high pH, when alkali darkening can occur [16-17]. The computer simulation shown in Fig. 5c(ii) shows that with suitable parameters the equilibrium model shown in Fig. 5c(i) can simulate the type of behaviour found under bleaching conditions. Figure 9 shows a set of simulations for the three models discussed in this paper. This illustrates the fact that, with suitable values for parameters, a given curve generated for one model can be closely approximated by the other models. This also suggests that a given set of experimental data can be simulated by more than one plausible model, and demonstrates the requirements to test the predicted chemical behaviour based on a particular model, as we have illustrated in this study. The results presented here suggest that data available for peroxide bleaching under constant reagent conditions [6-9], using absorption coefficients as an accurate measure of chromophore content, should be reassessed by fitting to the equilibrium model. We are currently using computer methodology to try to fit it to our data for peroxide bleaching of *Eucalyptus regnans*. There are also implications of the proposed kinetic model in terms of multi-stage bleaching sequences [18,19]. For example, it would appear that attempts to achieve significant brightness gain by repeatedly subjecting pulp to the same initial conditions of pH and peroxide concentrations would prove an inefficient practice.

Equilibrium and the Effect of Temperature

There has been recent interest in the development of refiner bleaching using hydrogen peroxide [21,22]. This process has the advantage of reducing capital costs, as a separate bleaching facility is not required. Bleaching reactions may take place at significantly higher temperatures within a refiner than those normally encountered in conventional tower bleaching. Increasing the temperature of bleaching increases the rate of brightness gain, but there is also a concurrent increase in the rate of catalytic decomposition of peroxide due to transition metal ions [23-27]. This effect can lead to lower final brightness gain for a given initial peroxide charge or require a higher initial peroxide concentration to achieve a given brightness level. For example, it has been reported [28] that for peroxide bleaching of spruce TMP there is about 10% higher consumption of peroxide at 80°C compared to 65°C to produce an equivalent brightness gain.

Figure 10 shows a comparison for bleaching the TMP at 50°C and 95°C using the same initial conditions. It is clear that a higher brightness limit is achieved at the lower temperature, and that the residual level of peroxide concentration is higher at 50°C compared to 95°C. A higher limiting brightness was also observed at 50°C (Fig. 11) compared to 95°C after repeated bleaching cycles using the same initial reagent concentrations (75.0% ISO at 50°C compared to 71.5% ISO at 95°C).

Figure 12a shows limiting brightness levels for single-stage bleaching at 50° and 95°C process plotted as a function of the average peroxide concentration present. The average peroxide concentration was calculated as the arithmetic mean of initial and final concentrations of long reaction time (Fig. 1b). Although this parameter does not take into account the pH/peroxide profile in moving from initial to final conditions, this has been used here until a more sophisticated approach is developed. It is clear that the curve representing the results at 50°C lies above that for 95°C. In general there is a displacement of 1-2 units of brightness at the lower bleaching temperature. From this plot, it can also be deduced that this displacement is not due solely to additional peroxide consumption at 95°C, which is reflected by a lower average peroxide concentration during the bleaching reaction. For example, we can consider results corresponding to an initial peroxide charge of 18% on o.d. pulp shown as X and Y in Fig. 12a. A brightness level of 70.2 % ISO was achieved at 95°C (point Y). In order to reach a brightness level of 71.6% ISO corresponding to the brightness limit at 50°C, the average peroxide concentration would need to be in excess of the initial charge introduced (point Z). Clearly the brightness limit attained at 50°C (point X) cannot be reached even if there is complete peroxide stabilization at the higher

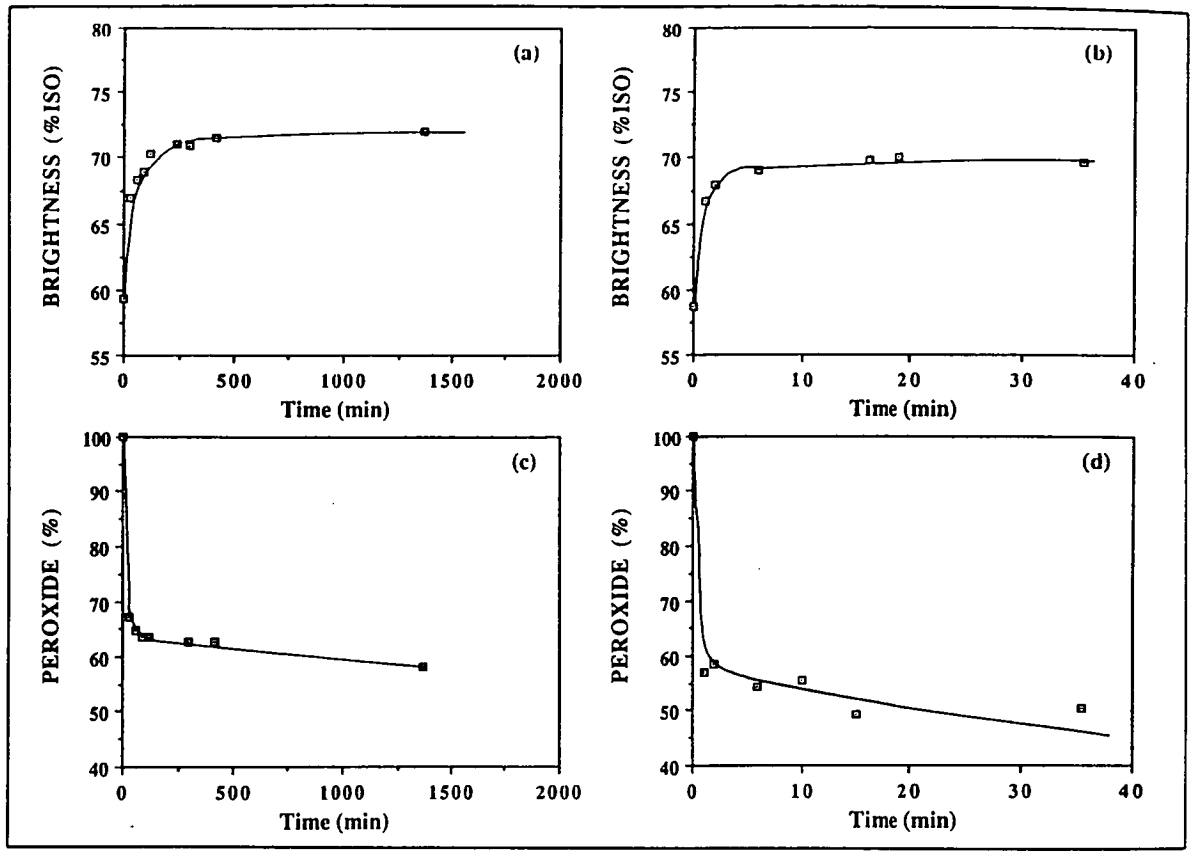

Fig. 10. Brightness gain and peroxide residuals for alkaline peroxide bleaching of *Pinus radiata* TMP at 50°C ('a' and 'b') and 95°C ('b' and 'd'). Initial alkali charge 2.0% NaOH on o.d. pulp; initial peroxide charge 18% on o.d. pulp.

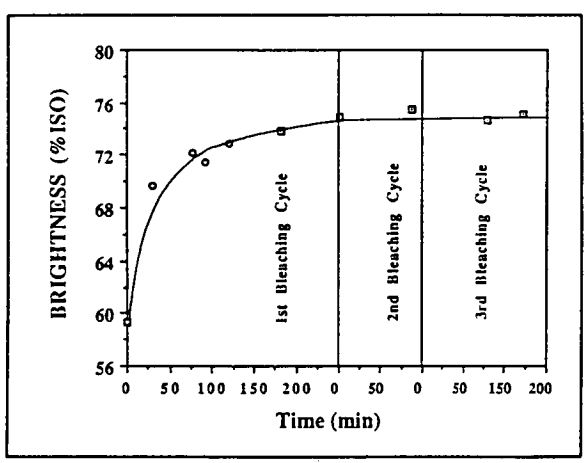

Fig. 11. Effect of repeated cycles for alkaline peroxide bleaching of *Pinus radiata* TMP at 50°C, 4% consistency. Initial alkali charge 2.0% NaOH on o.d. pulp. Initial peroxide charge 6% on o.d. pulp. Initial reagent conditions restored at the start of each stage.

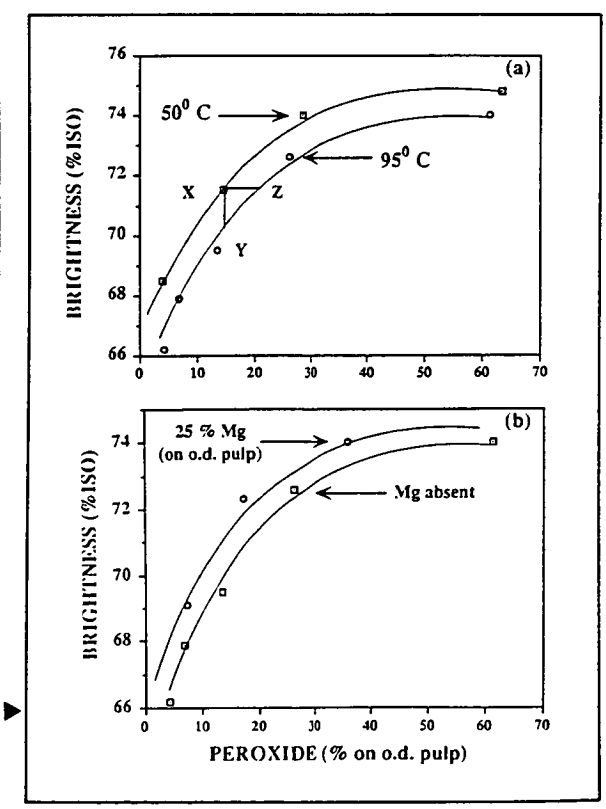

Fig. 12. Plots of limiting brigthness gain against average peroxide concentration. (a) Effect of temperature; (b) Effect of addition of magnesium nitrate (2.5% on o.d. pulp). Pulp consistency 4%. Initial alkali charge 2.0% NaOH on o.d. pulp. Bleaching temperature 95°C.

Testing of Equilibrium Kinetics Models for Peroxide Bleaching of *Pinus radiata* TMP

Y.A. GINTING and J. ABBOT

One of our proposed kinetic models for alkaline peroxide bleaching is based on the assumption that an equilibrium is established when the rate of chromophore removal is balanced by the rate of chromophore formation. We have tested this concept by comparing computer simulations with experimental results for the bleaching of Pinus radiata *thermomechanical pulp (TMP) at pH 11 with peroxide concentrations held constant at levels ranging from 0.5 to 6.0 g/L. The equilibrium model accounts for the observed relationships between absorption coefficient and time under constant conditions, and also explains the response of the pulp when the peroxide concentration is changed. Consideration of the available chemical evidence suggests that the chromophores and leucochromophores can be considered as specific chemical structures which can be reversibly interconverted. Sites on the lignin form a large pool of potential sources for formation of these structures.*

INTRODUCTION

There has been recent interest in kinetic phenomena during alkaline peroxide bleaching of mechanical and chemimechanical pulps [1-10]. Kinetic expressions have been formulated to describe brightness gain under normal process conditions, where the concentration of peroxide and pH fall continuously [1-4]. Experiments at low consistency with constant concentrations of peroxide and alkali also have been undertaken, and these studies can lead to kinetic formulations which can help to elucidate the mechanisms of the chemical processes involved [5-10]. There have also been attempts to relate the two approaches [1,6]. Our recent studies have suggested that peroxide bleaching should be regarded as a reversible process, in which chromophore formation as well as chromophore elimination should be considered simultaneously [10]. Photochemical reversibility of brightness gain is a well-known phenomenon when bleached pulps are exposed to light, particularly at wavelengths in the ultraviolet [11]. It is also known that bleached mechanical pulps and model compounds can undergo darkening processes when exposed to alkaline hydrogen peroxide under certain conditions [12-14]. In the present study, we have undertaken further testing of proposed kinetic models for alkaline peroxide bleaching for *Pinus radiata* thermomechanical pulp (TMP) [10], and have discussed possible chemical mechanisms which relate to the proposed kinetics.

Y.A. Ginting and J. Abbot
University of Tasmania
GPO Box 252C
Hobart, Tasmania 7001
Australia

EXPERIMENTAL

Hydrogen peroxide (30%) and sulphuric acid (98%) were obtained from Ajax Chemicals. Sodium hydroxide of semiconductor purity (99.99%) was supplied by Aldrich Chemicals. The *Pinus radiata* thermomechanical pulp was provided by Australian Newsprint Mills from TMP unit 2 at their Boyer mill in Tasmania. The pulp was stored at 8% consistency at 4°C until used. It contained Mn: 32.1 ppm, Cu: 4.20 ppm and Fe: 5.99 ppm, as determined by atomic absorption after complete acid digestion of the pulp.

For each bleaching run, sufficient pulp was added to 8 L of Milli-Q water to produce a pulp slurry of 0.3% consistency. The slurry was vigorously stirred in a polyethylene reaction vessel maintained at 50°C in a constant-temperature water bath. Before each run, an aliquot of the slurry was removed to make handsheets so that any changes caused by storage of pulp could be monitored.

Bleaching was initiated by simultaneously adding enough alkali and hydrogen peroxide to reach the target conditions. Subsequently, constant pH was maintained by adding alkali from a pH controller supplied by Cole Parmer*. The concentration of peroxide was maintained at constant levels by occasional addition of the necessary amount of hydrogen peroxide calculated from iodometric titration [15] of the bleaching liquor.

After initiation of bleaching, aliquots of the pulp slurry (600 mL) were removed at the desired times to make pulp handsheets. The bleaching reaction was quenched by acidifying the slurry to pH 3 with sulphuric acid (2.5 M), followed by filtration and washing. Pulp handsheets of 60-80 g/m^2 conditioned basis weight were formed by filtering 200 mL of the pulp slurry re-dispersed in 1 L deionized water onto a 70 μm [16] nylon mesh placed on top of Whatman No. 540 filter paper. Using this procedure, 3 handsheets were obtained from each aliquot. The sheets were fan-dried for several hours at room temperature and were then allowed to equilibrate at constant temperature (25°C) and humidity (50%) so that conditioned basis weights could be obtained.

After drying, black-backed and self-

* Cole Parmer Instrument Co.
7425 North Oak Park Avenue
Chicago, IL 60648-3884

backed reflectance measurements were made on each sheet, at a wavelength of 457 nm, using an Elrepho 2000 reflectance spectrometer. Individual opacity (W), scattering coefficient (S) and light absorption coefficient (K) properties were calculated from the Kubelka-Munk equation [17,18]. These properties were reported as the average per group of 3 handsheets.

KINETIC MODELS FOR PEROXIDE BLEACHING

There has been recent interest in developing kinetic models to describe the response of mechanical pulps to alkaline peroxide under mill conditions [1-4]. Various complex polynomial expressions have been tested in attempts to represent relationships between the brightness of a pulp and process variables including the consistency of the pulp and applied dosages of peroxide and alkali. For example, a 5-parameter model has been suggested [2] to represent conventional one-stage alkaline peroxide bleaching:

$$\begin{aligned} Brightness = \; & A_0 + A_1[H_2O_2] + A_2[H_2O_2]^2 \\ & + A_3{*}(consistency) + A_4{*}(consistency)^2 \\ & + A^5{*}(consistency){*}[H_2O_2] \end{aligned} \quad (1)$$

Even more complex expressions, with up to 12 parameters, have been reported to describe a two-stage peroxide bleaching sequence [3]. These types of relationships relate pulp brightness to a chosen set of controllable process variables such as initial pulp consistency and reagent concentration. The values of the parameters are varied to provide an adequate fitting between experimental and calculated brightnesses. The adequacy of the fitting can be improved by indroducing additional terms in the expression, each with its associated parameter. This type of expression results in a series of arbitrary terms in which there may be no specific meaning in any particular combination of variables. For example, there may be no fundamental significance to a term dependent on the square of consistency in the above expression. The term is included with its associated parameter, A_4, because the resulting calculated brightness is closer to the experimental value. Because these types of expression are not based on a series of terms which have individual significance, they cannot be expected to yield fundamental information concerning processes which occur during bleaching processes.

Another approach to describing kinetic phenomena during peroxide bleaching is based on the assumption that even complex phenomena can be described and understood by using the same approach as that applied to simpler chemical processes. This approach assumes that the rate of loss or formation of a particular chemical species depends on its concentration in the system, as well as on the concentration of other species with which it reacts. Analysis of kinetic phenomena is simplified by reducing the number of variables in a particular experiment. For alkaline peroxide bleaching this can be achieved by maintaining the pH and peroxide concentration at constant levels [5-9].

In the development of kinetic models for peroxide bleaching with constant reagent concentrations, the absorption coefficient (K) has been used as a measure of changes in the pulp. The absorption coefficient provides a better measure of chromophore concentration in the pulp than brightness, which also depends on light-scattering. Results relating changes in absorption coefficient with time under constant conditions have been reported for spruce stone groundwood (SGW) pulp [6], *Pinus radiata* thermomechanical pulp (TMP) [7] and *Eucalyptus regnans* SGW [8,9]. The general form of these K-time relationships under constant reagent conditions is the same in all cases, with an initial rapid decline in K, followed by a much slower rate of chromophore reduction at long bleaching times.

There have been various attempts to formulate expressions relating chromophore concentration and time in terms of conventional chemical kinetics. Lundqvist [5], and also Moldenius and Sjögren [6] have used expressions of the form:

$$-\frac{dC_k}{dt} = k\,[H_2O_2]^a\,[OH^-]^b\,C_k^c \quad (2)$$

where C_k is the chromophore concentration and the exponents a, b, and c can take non-integer values which must be determined experimentally. Values of c between 4 and 5 have been reported; thus, as pointed out by Lundqvist [5], this model may be rather improbable from a mechanistic standpoint because it implies that four or five chromophore species react with each other. The significance of the expression has been explained in terms of the net result of several parallel first-order processes with respect to C_k, each with its own first-order rate constant.

An alternative kinetic formulation has been advanced by Wright and Abbot [8], which assumes the mechanism shown in Fig. 1. This mechanism can provide a more adequate fitting of experimental data and is based on the assumption of a set of simple first-order processes. More recently, an alternative kinetic model has been proposed [9,10], in which chromophores (C) and leucochromophores (C_L) can be reversibly interconverted as shown in Fig. 2. This is coupled with a slower irreversible reaction in which chromophores are removed to give colourless products C_P. We proposed this equilibrium kinetic model on the basis of observations of changes in brightness of *Pinus radiata* TMP during multi-stage bleaching processes [10].

COMPUTER FITTING METHODS

For the equilibrium kinetic models shown in Fig. 2, the differential equations describing the changes in C, C_L and C_P with time are:

Model I:

$$-\frac{dC}{dt} = k_1C - k_2C_L \quad (3)$$

$$-\frac{dC_L}{dt} = -k_1C + k_2C_L + k_3C_L \quad (4)$$

$$\frac{dC_P}{dt} = k_3C_L \quad (5)$$

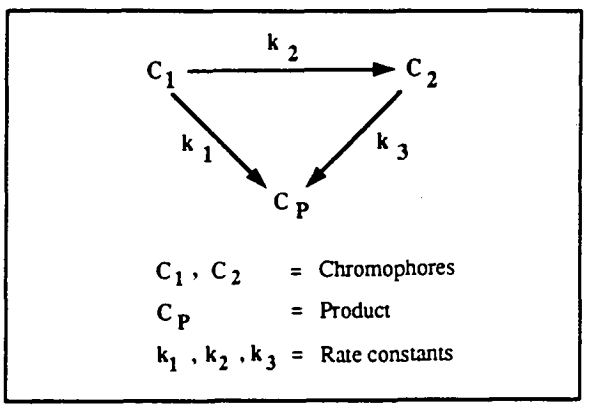

Fig. 1. The two-chromophore model for alkaline peroxide bleaching.

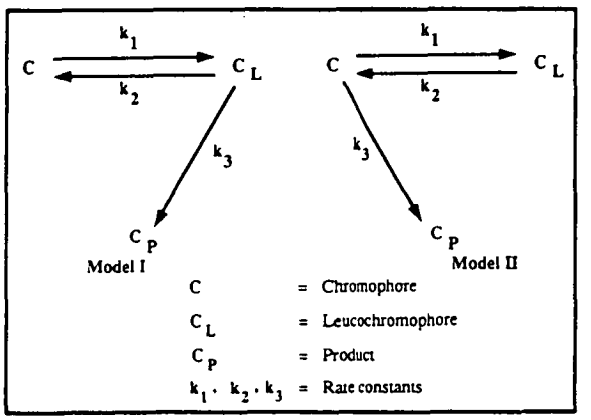

Fig. 2. The equilibrium models for alkaline peroxide bleaching.

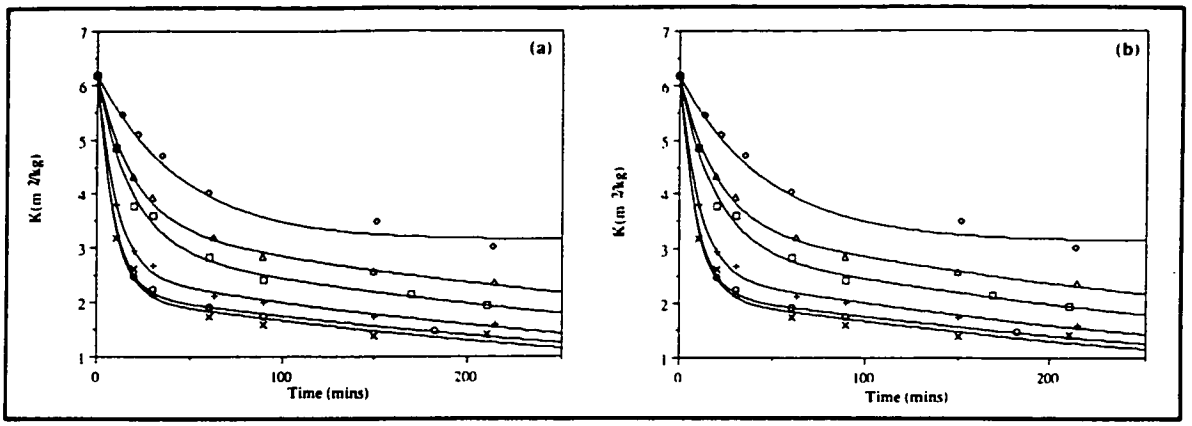

Fig. 3. Variation in absorption coefficient with time for alkaline peroxide bleaching of *Pinus radiata* TMP, fitted to equilibrium model I. Conditions: pH = 11.0; temperature = 50°C; consistency = 0.3%. Hydrogen peroxide charge: ◊ = 0.5 g/L, Δ = 1 g/L, □ = 2 g/L, + = 4 g/L, O = 5 g/L, x = 6 g/L. Solid lines are computer-generated and points are experimentally obtained. Fitting for: (a) $C_{L_0} = 0$, $C_{L_0} = 400$.

Model II:

$$-\frac{dC}{dt} = k_1C - k_2C_L + k_3C \quad (6)$$

$$-\frac{dC_L}{dt} = -k_1C + k_2C_L \quad (7)$$

$$\frac{dC_P}{dt} = k_3C \quad (8)$$

The equations can be solved to yield the analytical solutions for the variation in concentration of each of the chromophore types with time. Since only species C can be observed experimentally, the analytical solutions used in the fittings were the equations describing the changes in the concentration of C with respect to time. The variations of C with time are given by:

Model I:

$$C = \frac{C_0}{(b-a)}\left(e^{bt}(b+h) - e^{at}(a+h)\right) \quad (9)$$

where

$$a = -\frac{1}{2}\left((k_1+k_2+k_3) - \sqrt{(k_1+k_2+k_3)^2 - 4(k_1k_3)}\right)$$

$$b = -\frac{1}{2}\left((k_1+k_2+k_3) + \sqrt{(k_1+k_2+k_3)^2 - 4(k_1k_3)}\right)$$

$$h = (k_2+k_3) + \left(k_2\frac{C_{L_0}}{C_0}\right)$$

C_0 = initial concentration of C

C_{L_0} = initial concentration of C_L

Model II:

$$C = \frac{e^{bt}(bC_0+h) - e^{at}(aC_0+h)}{(b-a)} \quad (10)$$

where

$$a = -\frac{1}{2}\left((k_1+k_2+k_3) - \sqrt{(k_1+k_2+k_3)^2 - 4(k_2k_3)}\right)$$

$$b = -\frac{1}{2}\left((k_1+k_2+k_3) + \sqrt{(k_1+k_2+k_3)^2 - 4(k_2k_3)}\right)$$

$$h = (C_0 + C_{L_0})k_2$$

C_0 = initial concentration of C

C_{L_0} = initial concentration of C_L

Curves were fitted to the data by means of a program which uses a simplex algorithm [19] for the optimization. The program, which was run on a Sun SparcStation computer, was constrained to give only positive values of rate constants.

PEROXIDE BLEACHING OF *Pinus radiata* UNDER CONSTANT CONDITIONS

Figures 3 and 4 show experimental results for changes in absorption coefficient (K) with time under conditions of constant pH and peroxide concentration. Six levels of peroxide concentration from 0.5-6.0 g/L were studied at pH 11.0 and 50°C. The experimental data for bleaching at each peroxide level were fitted for equilibrium kinetic models by the computer techniques described above. For both equilibrium models represented in Fig. 2, fitting was carried out by trying two initial values of C_L. Figures 3a and 4a show experimental points and generated curves for $C_{L_0} = 0$, while Figs. 3b, 4b and 4c show experimental data and curves for $C_{L_0} = 400$. Figures 3 and 4 refer to models I and II, respectively. Two distinct solutions (Figs. 4b and c) were found for model II, corresponding to $C_{L_0} = 400$. The values of the residuals about the curves (Tables I-V) show that the adequacy of fitting for each case is similar. This implies that, from a mathematical standpoint, we cannot easily distinguish between situations where the initial concentrations of structural units which can potentially be converted into chromophores are either zero or very high in comparison to the initial chromophore concentration (~6 in this case). Inspection of the magnitude of the standard deviations in Tables I to V shows that the fitting is almost identical in the case where $C_{L_0} = 0$. Allowing C_{L_0} to be determined by the program as an additional variable was also undertaken. The best fitting was obtained when C_{L_0} approached zero.

The validity of the proposed equilibrium concept can be tested by experiments in which the concentration of peroxide is changed from one level to another during the course of bleaching. Figures 5a and 6a show the effect of changing the concentration of peroxide from

TABLE I
FITTING RESULTS FOR EQUILIBRIUM KINETIC MODEL I FOR $C_{L_0} = 0$
BLEACHING CONDITIONS: 0.3% CONSISTENCY, 50°C AND pH 11.0

H_2O_2 (g/L)	HO_2^- (M)	Rate constants $(min)^{-1}$			Standard Deviation
		k_1	k_2	k_3	
0.5	1.30E-03	1.07E-02	1.11E-02	5.90E-09	5.86E-02
1.0	2.59E-03	2.38E-02	2.50E-02	3.80E-03	9.94E-02
2.0	5.19E-03	2.86E-02	2.32E-02	3.87E-03	1.15E-01
4.0	1.04E-02	5.76E-02	3.66E-02	3.81E-03	8.00E-02
5.0	1.30E-02	7.44E-02	3.85E-02	3.43E-03	5.85E-02
6.0	1.56E-02	7.63E-02	3.76E-02	3.70E-03	1.58E-01

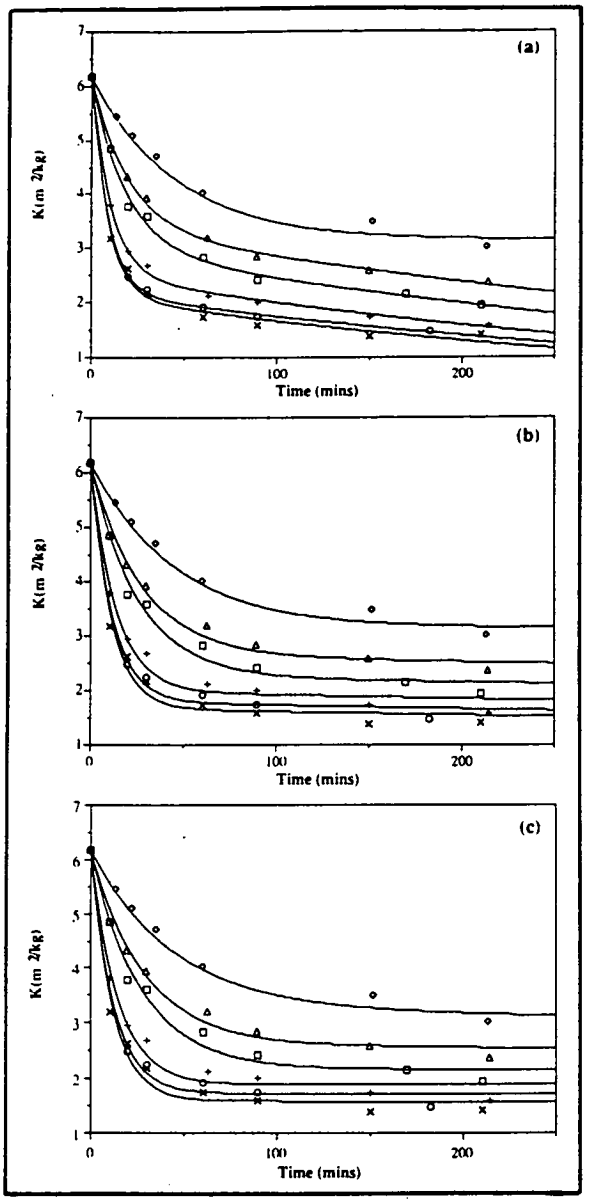

Fig. 4. Variation in absorption coefficient with time for alkaline peroxide bleaching of *Pinus radiata* TMP, fitted to equilibrium model II.
Conditions: pH = 11.0; temperature = 50°C; consistency = 0.3%.
Hydrogen peroxide charge: ◊ = 0.5 g/L, Δ = 1 g/L, □ = 2 g/L, + = 4 g/L, O = 5 g/L, x = 6 g/L.
Solid lines are computer-generated and points are experimentally obtained. Fitting for: (a) $C_{L_0} = 0$, (b) $C_{L_0} = 400$ first solution, (c) $C_{L_0} = 400$ second solution.

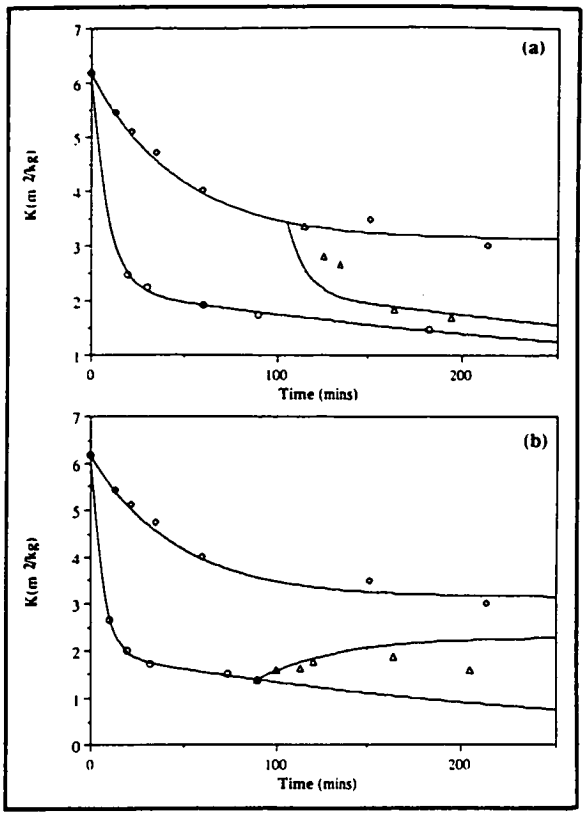

Fig. 5. Computer-generated prediction (solid lines) based on model I ($C_{L_0} = 0$) and observed effects (points) of changing the peroxide concentration during the course of bleaching. Conditions as in Fig. 3.
(a) Increase from 0.5 g/L to 5 g/L after 105 min.
◊ = 0.5 g/L, O = 5 g/L, Δ = 0.5 g/L for 105 min then 5 g/L.
(b) Decreasing from 5 g/L to 0.5 g/L after 90 min.
◊ = 0.5 g/L, O = 5 g/L, Δ = 5 g/L for 90 min then 0.5 g/L.

TABLE II
FITTING RESULTS FOR EQUILIBRIUM KINETIC MODEL I FOR $C_{L_0} = 400$
BLEACHING CONDITIONS: 0.3% CONSISTENCY, 50°C AND pH 11.0

H_2O_2 (g/L)	HO_2^- (M)	Rate constants $(min)^{-1}$			Standard Deviation
		k_1	k_2	k_3	
0.5	1.30E-03	2.17E-02	1.69E-04	1.82E-09	5.86E-02
1.0	2.59E-03	5.04E-02	4.09E-04	1.80E-03	9.94E-02
2.0	5.19E-03	5.32E-02	3.80E-04	2.08E-03	1.15E-01
4.0	1.04E-02	9.51E-02	5.78E-04	2.30E-03	8.00E-02
5.0	1.30E-02	1.13E-01	6.02E-04	2.25E-03	5.85E-02
6.0	1.56E-02	1.14E-01	5.89E-04	2.46E-03	1.58E-01

0.5 g/L to 5 g/L after 105 min, then maintaining the concentration at the higher level. It is apparent that there is a transition in the course of the *K*-time relationship, moving from the 0.5 g/L level towards the 5 g/L level. The course of this transition can be compared with the calculated path which has been computed for both equilibrium models with $C_{L_0} = 0$ by changing the values of the rate constants to correspond to the 5 g/L level after the time corresponding to the transition in peroxide concentration. It can be seen that there is a reasonable correspondence between the observed results and the predicted course of the bleaching process.

The equilibrium models also predict that darkening of the pulp should occur if the peroxide concentration level is reduced at constant pH. This is more difficult to test experimentally as the peroxide concentration cannot be instantaneously reduced without other concurrent changes in the system. A pulp was bleached at a constant peroxide level of 5 g/L and pH 11.0 for 90 min, then isolated by filtration and washed. Subsequently the pulp was introduced into a liquor at pH 11.0 containing 0.5 g/L peroxide. Figures 5b and 6b show that, as a result of this treatment, the pulp underwent darkening and the absorption coefficient in-

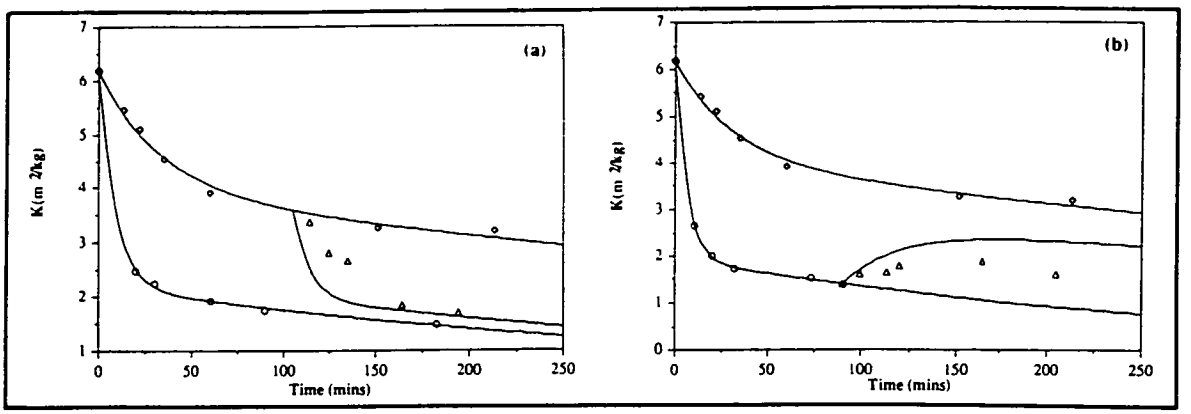

Fig. 6. Computer-generated prediction (solid lines) based on model II ($C_{L_0} = 0$) and observed effects (points) of changing the peroxide concentration during the course of bleaching. Conditions as in Fig. 4. (a) Increase from 0.5 g/L to 5 g/L after 105 min. ◊ = 0.5 g/L, ○ = 5 g/L, Δ = 0.5 g/L for 105 min then 5 g/L. (b) Decreasing from 5 g/L to 0.5 g/L after 90 min. ◊ = 0.5 g/L, ○ = 5 g/L, Δ = 5 g/L for 90 min then 0.5 g/L.

TABLE III
FITTING RESULTS FOR EQUILIBRIUM KINETIC MODEL II FOR $C_{L_0} = 0$
BLEACHING CONDITIONS: 0.3% CONSISTENCY, 50°C AND pH 11.0

H_2O_2 (g/L)	HO_2^- (M)	Rate constants $(min)^{-1}$			Standard Deviation
		k_1	k_2	k_3	
0.5	1.30E-03	1.07E-02	1.11E-02	7.77E-09	5.86E-02
1.0	2.59E-03	2.07E-02	2.88E-02	3.15E-03	9.94E-02
2.0	5.19E-03	2.45E-02	2.71E-02	4.08E-03	1.15E-01
4.0	1.04E-02	5.22E-02	4.04E-02	5.42E-03	8.00E-02
5.0	1.30E-02	6.83E-02	4.19E-02	6.09E-03	5.85E-02
6.0	1.56E-02	6.94E-02	4.13E-02	6.83E-03	1.58E-01

TABLE IV
FITTING RESULTS FOR EQUILIBRIUM KINETIC MODEL II FOR $C_{L_0} = 400$
BLEACHING CONDITIONS: 0.3% CONSISTENCY, 50°C AND pH 11.0

H_2O_2 (g/L)	HO_2^- (M)	Rate constants $(min)^{-1}$			Standard Deviation
		k_1	k_2	k_3	
0.5	1.30E-03	2.07E-10	1.84E-04	2.27E-02	5.86E-02
1.0	2.59E-03	4.96E-08	2.35E-04	3.58E-02	1.77E-01
2.0	5.19E-03	2.70E-07	2.18E-04	3.89E-02	1.96E-01
4.0	1.04E-02	1.23E-07	3.64E-04	7.35E-02	2.01E-01
5.0	1.30E-02	1.17E-06	3.89E-04	8.69E-02	1.68E-01
6.0	1.56E-02	3.60E-07	3.75E-04	9.00E-02	2.30E-01

TABLE V
FITTING RESULTS FOR EQUILIBRIUM KINETIC MODEL II FOR $C_{L_0} = 400$
BLEACHING CONDITIONS: 0.3% CONSISTENCY, 50°C AND pH 11.0

H_2O_2 (g/L)	HO_2^- (M)	Rate constants $(min)^{-1}$			Standard Deviation
		k_1	k_2	k_3	
0.5	1.30E-03	1.99E-03	1.82E-04	2.06E-02	6.35E-02
1.0	2.59E-03	1.65E-02	2.27E-04	1.84E-02	1.84E-01
2.0	5.19E-03	3.46E-02	1.99E-04	2.65E-03	2.07E-01
4.0	1.04E-02	6.77E-02	3.20E-04	1.01E-03	2.32E-01
5.0	1.30E-02	7.27E-02	3.45E-04	8.67E-03	1.95E-01
6.0	1.56E-02	8.44E-02	3.29E-04	5.00E-07	2.51E-01

creased towards the level representing bleaching with a constant concentration of 0.5 g/L peroxide. Again it is possible to calculate a theoretical response to changing the peroxide concentration to a lower level by adjusting the values of rate constants at the time corresponding to the transition in peroxide concentration. Figures 5b and 6b show that the response calculated on the basis of the equilibrium model is somewhat greater than that actually observed.

Similar calculated responses were obtained by using values of rate constants associated with solutions in which $C_{L_0} = 400$ for both increasing and decreasing peroxide concentrations. These experimental results give support to the application of an equilibrium model to peroxide bleaching systems but do not allow us to distinguish readily between models I and II.

REVERSIBILITY OF PEROXIDE BLEACHING

It is well known that peroxide-bleached mechanical pulp can undergo darkening in the presence of alkali [20, 21]. The phenomenon of alkali darkening can occur during industrial bleaching if hydrogen peroxide decomposition is excessive, resulting in low levels of residual peroxide. However it has also been demonstrated that darkening of the pulp can occur when bleached pulps are introduced into liquors containing alkaline hydrogen peroxide [13], even at peroxide concentrations comparable to those used in mills. This has been observed particularly when peroxide decomposition is induced by addition of transition metal ions, such as manganese or copper. Kutney [13] has shown that significant brightness reversion of a bleached groundwood occurred during peroxide decomposition induced by manganese addition, even though most of the peroxide was still present. These experiments suggested that it may be products from decomposition of hydrogen peroxide, particularly radical species such as OH•, which can give rise to chromophore formation during alkaline peroxide bleaching. There has been recent focus of attention on the role of radical species during peroxide bleaching processes [22-24], although it is not yet clear under what circumstances the net effect of radicals is either beneficial or detrimental to brightness development. Studies with model compounds have also shown that formation of a coloured species can be promoted by the presence of metal ions in alkaline peroxide systems [12].

The phenomenon of brightness reversion of bleached mechanical pulps when exposed to light is well known and has recently been reviewed by Heitner and Schmidt [11]. The participation of free radicals has also been implicated in these photochemical processes. Studies have shown that it is possible to darken and bleach mechanical pulp reversibly by the application of radiation of specific wavelengths in the UV and visible regions respectively [25].

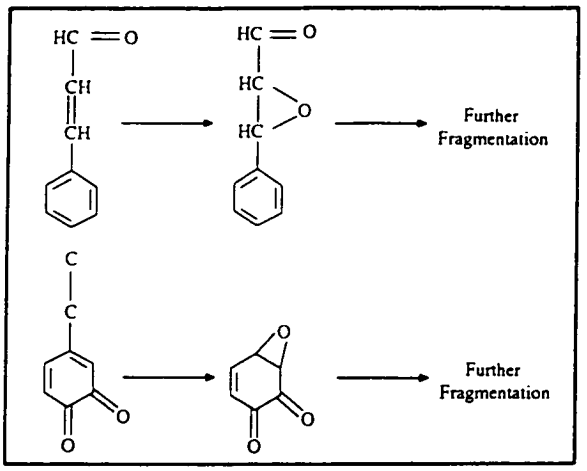

Fig. 7. Reactions of chromophores in alkaline hydrogen peroxide leading to epoxide structures.

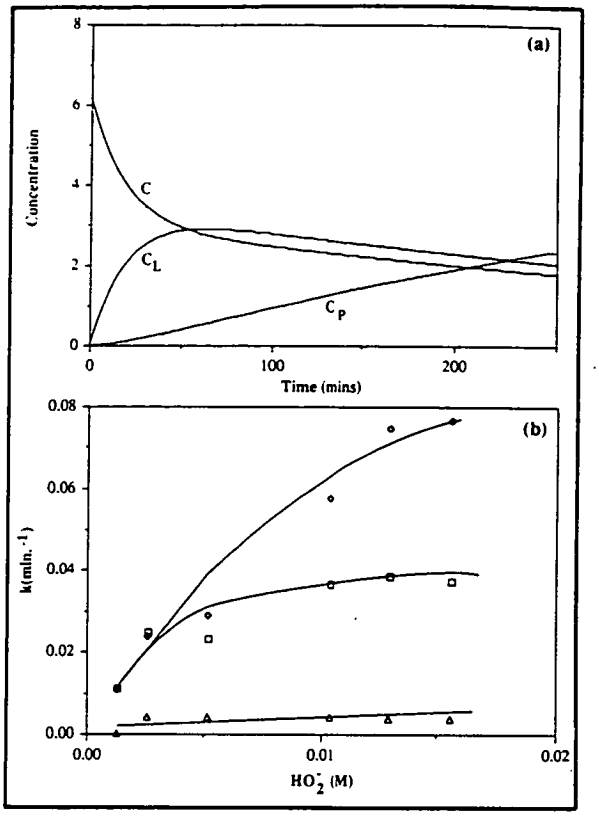

Fig. 8. (a). Calculated concentration profiles for C, C_L and C_P for equilibrium model I ($C_{L_0} = 0$).
(b). Dependence of rate constants k_1, k_2, k_3 (calculated by using equilibrium model I) on the concentration of perhydroxyl anion, HO_2^- for $C_{L_0} = 0$. ◊ : k_1, □ : k_2, Δ : k_3

Recent investigations with diffuse reflectance spectroscopy [26, 27] show that specific absorption bands removed by peroxide bleaching can be restored by exposure to light, which implies a reversibility of these chemical processes.

The nature of reversibility of chemical processes relating chromophores and leucochromophores can be described in the context of the proposed equilibrium model. As already shown, an adequate fitting can be obtained on the assumption that the initial concentration of leucochromophores in the pulp is either very small or very large in comparison with the concentration of chromophores. We can consider the implications of both situations in turn. It is known that there are several types of chemical structure which can be identified with chromophores susceptible to removal by alkaline hydrogen peroxide. The two most common chromophore types are α – β unsaturated carbonyls and *o*- or *p*-quinones [28, 29]. The nature of the leucochromophore structures is less certain.

Case 1 : $C_{L_0} = 0$

These models require that the chromophore species C reacts rapidly and reversibly to produce a structural unit C_L. The chemical structure of C_L must be closely related to that of C for this to occur. If formation of C_L is accompanied by extensive fragmentation, particularly involving the C_9 lignin unit, it is difficult to see how C could be readily reformed. Model compound studies with both α – β unsaturated carbonyl compounds and quinones have been reported. In both cases, the mechanisms proposed for reaction with peroxide [30-32] involve addition of oxygen to the conjugated carbonyl structure, to give an epoxide prior to further reaction involving fragmentation leading ultimately to carboxylic acids (Fig. 7). This mechanism would correspond to model I. It is conceivable that the reaction process to produce the epoxide is reversible, as the structural integrity of the carbon skeleton is maintained. However, further reaction processes involve rupture of C-C bonds and cannot be considered easily reversible. If epoxide structures were to be identified with C_L, it would be necessary for the epoxide to be a stable intermediate with subsequent reaction to oxidized fragments occurring much more slowly. Extensive studies of relative rates of formation of epoxides and further oxidation products have not been reported. However, it has been reported that the epoxide is relatively stable, and has been isolated in some cases [33].

Correlation of C_L with epoxide structures would also necessitate proposing a mechanism whereby the original chromophore can be easily regenerated to give C in the presence of alkaline peroxide. As already discussed, an involvement of free-radical species might be postulated, although we could find no evidence in the literature for conversion of an epoxide to give conjugated carbonyl structures.

Figures 8a and 9a show the calculated concentration-time profiles for C, C_L and C_P corresponding to a constant peroxide concentration of 2.0 g/L for both models. This shows the initial rapid conversion of chromophore to the species C_L, with a slower conversion to the final product C_P. Figures 8b and 9b show the dependence of the three rate constants k_1, k_2 and k_3 on the calculated concentrations of perhydroxyl anion HO_2^-. In both cases, rate constants k_1 and k_2 are an order of magnitude larger than k_3. Thus, the levelling off brightness is essentially controlled by the position of the equilibrium between C and C_L (i.e. the rate constants k_1 and k_2). None of the rate constants is directly proportional to $[HO_2^-]$, which indicates that the steps in this mechanism cannot be elementary reaction processes (i.e. they would involve more than one step).

Case 2: $C_{L_0} = 400$

Both models assume that the initial concentration of leucochromophores is very high compared to that of chromophores. The value of 400 used in the fitting procedures is arbitrary here, as in fact any value such that $C_{L_0} >> C_0$ will produce a satisfactory fitting. The implication of this condition is that the concentration of leucochromophores remains almost constant throughout the course of the bleaching process. In fact, the result is that the rate of chromophore creation can be regarded as almost constant, so that Eqs. (3-7) can be rewritten as :

$$-\frac{dC}{dt} = k_1 C - k'_2 \qquad (11)$$

$$-\frac{dC_L}{dt} = -k_1 C + k'_2 + k'_3 \qquad (12)$$

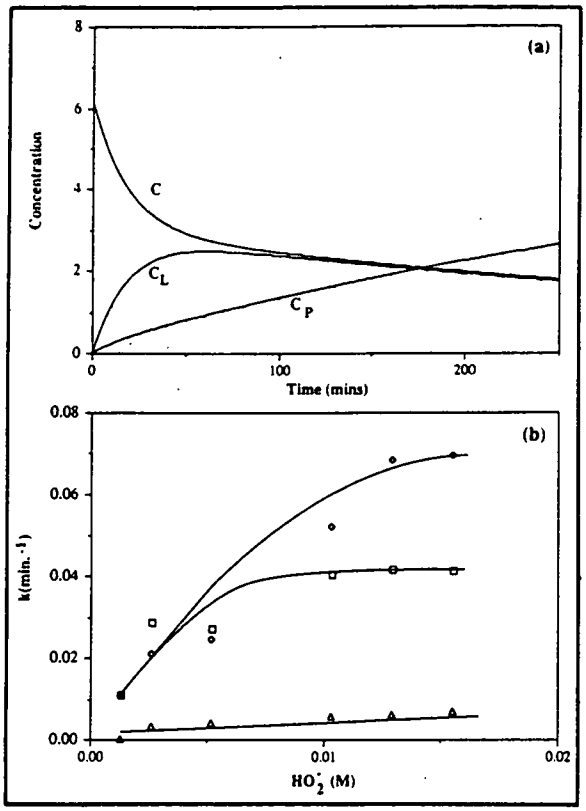

Fig. 9. (a) Calculated concentration profiles for C, C_L and C_P for equilibrium model II (C_{L_0} = 0).
(b) Dependence of rate constants k_1, k_2, k_3 (calculated by using equilibrium model II) on the concentration of perhydroxyl anion, HO_2^- for C_{L_0} = 0. ◊ : k_1, □ : k_2, Δ : k_3

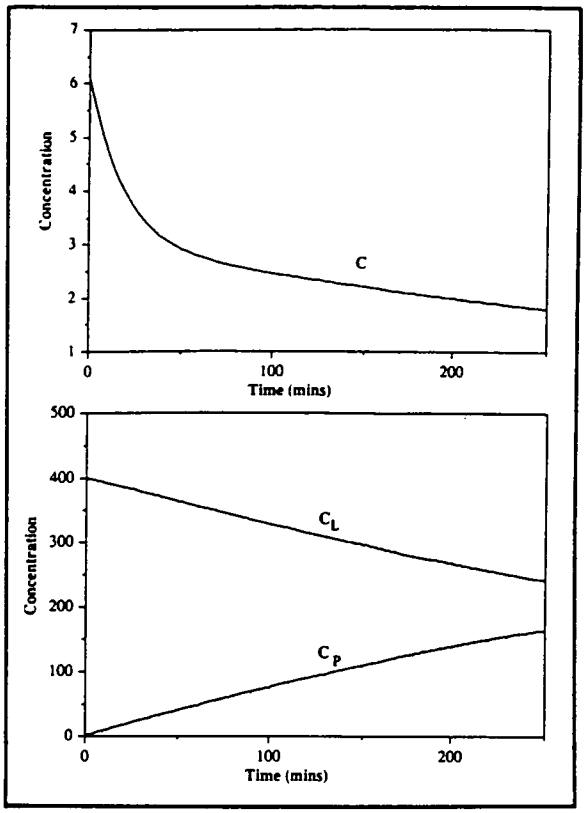

Fig. 10. Calculated concentration profiles for C, C_L and C_P for C_{L_0} = 400 for equilibrium model I.

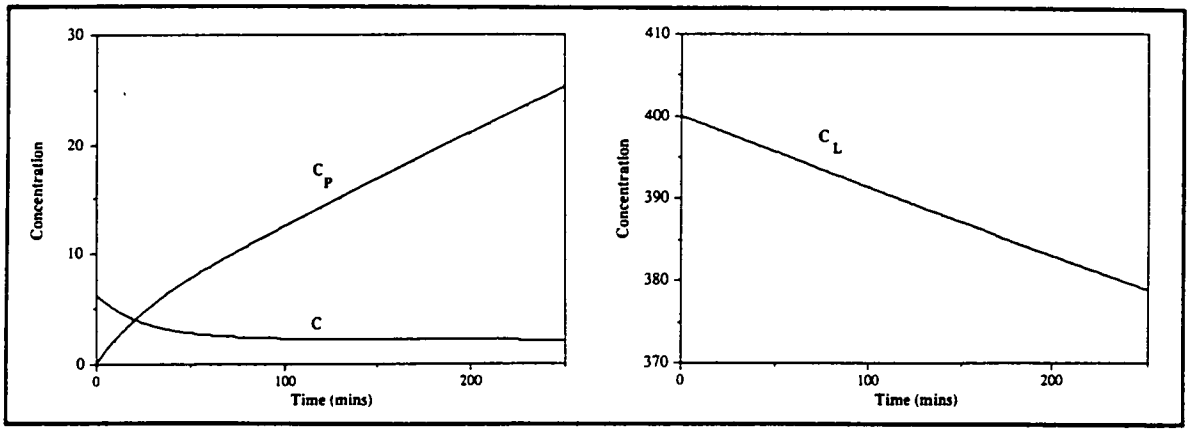

Fig. 11. Calculated concentration profiles for C, C_L and C_P for C_{L_0} = 400 for the first solution of equilibrium model II.

$$\frac{dC_P}{dt} = k'_3 \quad (13)$$

$$-\frac{dC}{dt} = k_1C - k'_2 + k_3C \quad (14)$$

$$-\frac{dC_L}{dt} = k'_2 - k_1C \quad (15)$$

Under this condition k'_2 in Eqs. (11) and (14) represents pseudo zero-order reactions. In chemical terms, this would suggest that chromophores can be created at a constant rate from a large pool of potential sites (or leucochromophores) on the lignin structure. The simplest explanation would be to suggest that, in fact, the lignin structure itself is a large pool of potential chromophores. In comparison, the number of conjugated carbonyl structures (C) is only a few percent of the total C_9 lignin units [29]. The behaviour of the system corresponding to the changes in concentration of C, C_L and C_P with time, as calculated for model I, is shown in Fig. 10.

Interestingly, setting the value of C_L to a high initial value resulted in two possible mathematical solutions for model II, which had similar adequacy of fitting as judged by the values of the standard deviations shown in Tables IV and V. The behaviour of the system corresponding to the changes in concentration of C, C_L and C_P with time for model II is shown in Figs. 11 and 12. In both situations, the lignin structure (or leucochromophores), rather than the chromophores C initially present in the lignin, is the major source of material eventually converted into the final product C_P. However, the two solutions differ in the rela-

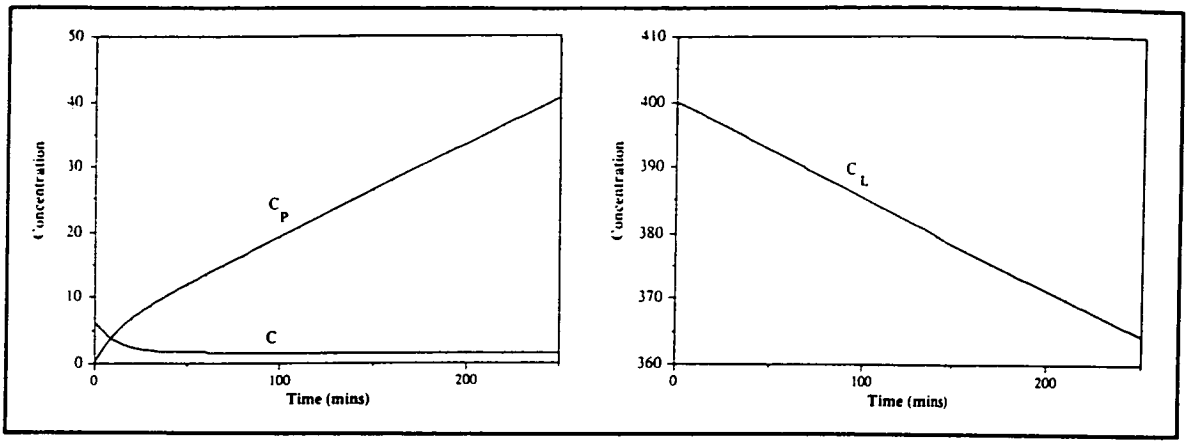

Fig. 12. Calculated concentration profiles for C, C_L and C_P for C_{L_0} = 400 for the second solution of equilibrium model II.

tive magnitude of rate constants. For the first solution, the magnitude of the rate constants is such that $k_1 << k_2 < k_3$. This shows that the equilibrium step could be replaced by an irreversible step, resulting in the mechanism

$$C_L \xrightarrow{k_2} C \xrightarrow{k_3} C_P$$

representing the overall process. For the second solution, the equilibrium process would dominate the overall behaviour, with a slower irreversible step controlled by the rate constant k_3.

CONCLUSIONS

The proposed equilibrium kinetic models for alkaline peroxide bleaching provide an adequate description of the rate of change of chromophore concentration with time under constant conditions of pH and peroxide concentration. The models can also account for observed changes in chromophore content when the peroxide concentration is changed to either higher or lower constant levels. The models allow for the concurrent formation and removal of chromophores in the presence of alkaline peroxide, and can account for darkening reactions which are observed when the peroxide concentration is reduced. Consideration of the available chemical evidence suggests that the leucochromophores can be considered as specific chemical structures which can be reversibly interconverted between chromophores and leucochromophores. Sites on lignin form a large pool of potential sites for formation of these structures.

ACKNOWLEDGEMENTS

Financial support was provided by Australian Newsprint Mills Pty. Ltd., Interox Chemicals Pty. Ltd., and the Australian Research Council. The authors are also indebted to Dr. Michael Whitbeck of Desert Research Institute at Reno, NV, USA, for his skillful assistance in computer programming.

REFERENCES

1. BERGMAN, E.K. and EDWARDS, L.L., "Model Aids Design and Operation of Peroxide CTMP/TMP Bleaching System", *Pulp Paper* 60(6):96 (1986).
2. BRÄUER, P., KAPPEL, J. and RESCH, F., "New Operating Experience in High-Consistency Peroxide Bleaching", TAPPI Pulping Conf., p. 299 (1990).
3. MEYER, K.A., KAPPEL, J. and PETSCHALLER, F., "Criteria for the Selection of Optimum Bleaching Systems for Mechanical Pulp", TAPPI Pulping Conf., p. 291 (1990).
4. MEYRANT, P. and DODSON, M., "High Consistency Bleaching: A Must for High Brightness Targets?", TAPPI Pulping Conf., p. 669 (1989).
5. LUNDQVIST, M., "Kinetics of Hydrogen Peroxide Bleaching of Mechanical Pulp", *Svensk Papperstidn.* 82(1):16 (1979).
6. MOLDENIUS, S. and SJOGREN, B., "Kinetic Models for Hydrogen Peroxide Bleaching of Mechanical Pulps", *J. Wood Chem. Tech.* 2(4):447 (1982).
7. ALLISON, R.W. and GRAHAM, K.L., "Peroxide Bleaching of Mechanical Pulp Fractions from *Radiata pine*", *J. Pulp Paper Sci.* 15(4):J145 (1989).
8. WRIGHT, P. and ABBOT, J., "Kinetic Models for Peroxide Bleaching Under Alkaline Conditions. Part 1: One and Two

REFERENCE: GINTING, Y.A. and ABBOT, J., Testing of Equilibrium Kinetics Models for Peroxide Bleaching of *Pinus radiata* TMP. Journal of Pulp and Paper Science, Vol. 19(3) J143-151 May 1993. Paper offered as a contribution to the Technical Section, Canadian Pulp and Paper Association. Not to be reproduced without permission. Manuscript received January 15, 1992; revised manuscript approved for publication by the Review Panel March 1, 1993.

ABSTRACT: One of our proposed kinetic models for alkaline peroxide bleaching is based on the assumption that an equilibrium is established when the rate of chromophore removal is balanced by the rate of chromophore formation. We have tested this concept by comparing computer simulations with experimental results for the bleaching of *Pinus radiata* thermomechanical pulp (TMP) at pH 11 with peroxide concentrations held constant at levels ranging from 0.5 to 6.0 g/L. The equilibrium model accounts for the observed relationships between absorption coefficient and time under constant conditions, and also explains the response of the pulp when the peroxide concentration is changed. Consideration of the available chemical evidence suggests that the chromophores and leucochromophores can be considered as specific chemical structures which can be reversibly interconverted. Sites on the lignin form a large pool of potential sources for formation of these structures.

RÉSUMÉ: L'un des modèles cinétiques que nous proposons pour le blanchiment au peroxyde alcalin est fondé sur la supposition qu'un équilibre s'établit quand le taux d'élimination des chromophores égale le taux de formation des chromophores. Nous avons mis ce concept à l'essai en comparant des simulations par ordinateur avec des résultats d'expérience provenant du blanchiment de la pâte thermomécanique (PTM) de *Pinus radiata* à un pH de 11 et des concentrations de peroxyde maintenues à des niveaux constants allant de 0,5 à 6,0 g/L. Le modèle d'équilibre rend compte des relations observées entre le coefficient d'absorption et la période de temps sous des conditions constantes, et il explique également le comportement de la pâte quand la concentration de peroxyde est modifiée. La prise en considération de l'évidence chimique disponible suggère que les chromophores et les leucochromophores peuvent être considérés comme structures chimiques spécifiques, lesquelles sont aptes à être interconverties de façon réversible. Des emplacements sur la lignine forment une masse importante de sources potentielles pour la formation de ces structures.

KEYWORDS: PEROXIDE BLEACHING, PINUS RADIATA, THERMOMECHANICAL PULPS, KINETICS, MODELS, EQUILIBRIUM.

Chromophore Models", *J. Wood Chem. Tech.* 11(3):349 (1991).
9. WRIGHT, P., GINTING, Y. and ABBOT, J., "Kinetic Models for Peroxide Bleaching Under Alkaline Conditions. Part 2: Equilibrium Models", *J. Wood Chem. Tech.* 12(1):111 (1992).
10. ABBOT, J. and GINTING, Y., "Development of Kinetic Models for Alkaline Peroxide Bleaching", *J. Pulp Paper Sci.* 18(3):J85 (1992).
11. HEITNER, C. and SCHMIDT, J.A., "Light-Induced Yellowing of Wood-Containing Papers—A Review of Fifty Years of Research", Intl. Symp. Wood Pulp Chem., 1:131 (1991).
12. PERO, R.W. and DENCE, C.W., "The Role of Transition Metals on the Formation of Colour from Methoxyhydroquinone, an Intermediate in the Peroxide Bleaching of TMP", *J. Pulp Paper Sci.* 12(6):J192 (1986).
13. KUTNEY, G.W. and EVANS, T.D., "Peroxide Bleaching of Mechanical Pulps. Part 2: Alkali Darkening—Hydrogen Peroxide Decomposition", *Svensk Papperstidn.* 88(9): R84 (1985).
14. ALLISON, R.W. and GRAHAM, K.L., "Kinetics of Alkali Darkening of TMP from *Radiata pine*", *J. Pulp Paper Sci.* 16(1):J28 (1990).
15. VOGEL, A.I., Quantitative Inorganic Analysis, Longmans, Green and Co., London, p. 425 (1947).
16. SCHMIDT, J.A. and HEITNER, C., "Light-Induced Yellowing of Mechanical Pulp: Effect of Methylation, $NaBH_4$ Reduction and Ascorbic Acid on Chromophore Formation", Intl. Symp. Wood Pulp Chem., 1:263 (1991).
17. ROBINSON, J.V., "A Summary of Reflectance Equations for Application of the Kubelka-Munk Theory to Optical Properties of Paper", *Tappi* 58(10):152 (1975).
18. KUBELKA, P., "New Contributions to the Optics of Intensely Light-Scattering Materials. Part I", *J. Opt. Soc. Am.* 38:448 (1948).
19. CACECI, M.S. and CACHERIS, W.P., "Fitting Curves to Data", *Byte Magazine* 9(5):340 (1984).
20. KUTNEY, G.W. and EVANS, T.D., "Peroxide Bleaching of Mechanical Pulps. Part 1: Alkali Darkening—The Effect of Caustic Soda", *Svensk Papperstidn.* 88(6):R78 (1985).
21. WHITTING, P., PITCHER, J.M. and MANCHESTER, D.F., "Factors Affecting the Use of Chelating Agents to Aid the Brightening of Mechanical Pulps", 70th Ann. Mtg., Tech. Sect., CPPA, Preprints, p. B339 (1984).
22. GIERER, J., JANSBO, K., YANG, E. and YOON, B. H., "On the Participation of Hydroxyl Radicals in Oxygen and Hydrogen Peroxide Bleaching Processes", Intl. Symp. Wood Pulp Chem., 1:93 (1991).
23. SJÖGREN, B., DANIELSON, J., ENGSTRAND, P., GELLERSTEDT, G., ZACHRISON, H., and REITBERGER, T., "The Importance of Radical Reactions for Brightness Increase in Hydrogen Peroxide Bleaching of Mechanical Pulps", TAPPI Conf. Wood. Pulp. Chem., p. 161 (1989).
24. REITBERGER, T., "Chemiluminescence as a Means to Study the Role of Hydroxyl Radicals in Oxidative Processes", *Holzforschung* 42(6):351 (1988).
25. FORSSKAHL, I. and JANSON, J., "Irradiation of Mechanical Pulps with Monochromatic Light at Selected Wavelengths", Intl. Symp. Wood Pulp Chem., 1:255 (1991).
26. MICHELL, A.J., CHIN, C.W.J., and NELSON, P.J., "Bleaching and Yellowing of Eucalypt Chemimechanical Pulps. Diffuse Reflectance Spectra of Oxygen Bleached Pulps", *Appita* 44(5):333 (1991).
27. MICHELL, A. J., NELSON, P. J. and CHIN, C.W.J., "Diffuse Reflectance Spectroscopic Studies of the Bleaching and Yellowing of Eucalyptus Regnans Cold Soda Pulp", *Appita* 42(6):443 (1989).
28. HOLAH, D.G., and HEITNER, C., "The Colour and UV-Visible Absorption Spectra of Mechanical and Ultra-High Yield Pulps Treated with Alkaline Hydrogen Peroxide", TAPPI Intl. Mech. Pulping Conf., p. 177 (1991).
29. LEBO, S.E., LONSKY, W.F.W., McDONOUGH, T.J., MEDVECZ, P.J. and DIMMEL, D.R., "The Occurrence and Light-Induced Formation of Ortho-Quinoid Lignin Structures in White Spruce Refiner Mechanical Pulp", *J. Pulp Paper Sci.* 16(5):J139 (1990).
30. GELLERSTEDT, G., HARDELL, H.L., and LINDFORS, E.L., "The Reactions of Lignin with Alkaline Hydrogen Peroxide. Part IV. Products from the Oxidation of Quinone Model Compounds", *Acta Chem. Scand.* B34:669 (1990).
31. GELLERSTEDT, G. and AGNEMO, R., "The Reactions of Lignin with Alkaline Hydrogen Peroxide. Part III: The Oxidation of Conjugated Carbonyl Structures", *Acta Chem. Scand.* B34:275 (1980).
32. REEVES, R.H. and PEARL, I.A., "Reaction Products Formed Upon the Alkaline Peroxide Oxidation of Lignin-Related Model Compounds", *Tappi* 48(2):121 (1965).
33. PAYNE, G.B., "Epoxidation of Cinnamaldehyde by Alkaline tert-Butyl Hydroperoxide", *J. Org. Chem.* 25(1):275 (1960).